

**CHARACTERIZATION OF THE EZOUSAS AQUIFER IN
SOUTH WEST CYPRUS FOR THE STORAGE AND
RECOVERY OF TREATED SEWAGE EFFLUENT**

By George Christodoulou

**Thesis submitted for the degree of
Doctor of Philosophy
at
Loughborough University**

2016

ABSTRACT

This thesis reports on research from a full-scale demonstration project to recharge a depleted aquifer with treated sewage effluent from the Paphos (Cyprus) wastewater treatment plant. The project artificially recharged the Ezousas river basin, located in the south-western coastal plain of Cyprus, with tertiary treated, disinfected effluent through a network of artificial infiltration ponds.

The aims of the research were to determine the capacity of the aquifer to provide a suitable buffer for the flow from the wastewater without flooding and to measure the changes in reclaimed water quality. The aquifer hydraulics and treatment capacity, including recharge basins, were analysed using field and laboratory measurements.

A geological field survey and modelling was used to assess, both by practice and theory the effectiveness of the Ezousas river aquifer for storage and recovery of the reclaimed water. The aquifer was found to be mainly composed of alluvium with typical hydraulic characteristics. The average porosity was 20% and hydraulic conductivity around 90 m/day, it was concluded the aquifer would be able to accept all the annual output of the treatment plant which was 5 Mm³ /a.

The recharge network consisted of five groups of infiltration basins arranged on both banks of the River Ezousas about 2km upstream of the wastewater treatment plant. Each infiltration basin contained two, four or six recharge ponds, each basin was 2,000m² in area with a depth of 1.5 m. A recharge pattern consisting of alternating weeks of wet-fill and drying cycles was found necessary to maintain the unsaturated zone below the ponds in order to maximise the amount of water that could be recharged whilst optimising water quality.

The hydraulic impact of the artificial recharge and extraction from the field measurements of borehole water levels indicated recharged water down to 15m below the surface. Tracer tests on the groundwater flow, capture zone, residence times and mass balances

of recharged and native waters gave widely varying residence times between 30 days and 5 years, these were attributed to the complex flow patterns found.

Recharged water was sampled using a series of extraction wells located along the downstream river basin, starting at the infiltration ponds and then at stages downstream. Eight production and monitoring wells were tested including control samples up-gradient (upstream) from the ponds, to about 7km down-gradient (downstream).

Water quality was analyzed for the standard wastewater constituents including indicator organisms, organic matter, nutrients N and P and the metals. It was one of the recommendations of the thesis however that attention also be paid to the persistent organics, including the pesticides, biocides, plasticizers and pharma residues.

The chemical data was used to build and validate a solute transport model of the ponds and surrounding area to predict the transport and fate of priority contaminants. In this way, the geo-chemical potential for the retardation, attenuation and chemical or biochemical degradation processes taking place in the unsaturated and saturated zone were assessed. From the results it was concluded that for most analytes, which included metals, nitrate and common salts, the main processes were mixing and dilution by the native ground water. The extracted water was then a mix of waters according to the different residence times and flow of natural groundwater, giving a stable water quality for irrigation. A third reaction involving cation exchange with the local geology was however identified which reduced the concentrations of copper and phosphate beyond what was expected from just mixing.

It was also concluded that denitrification did not occur because of a combination of the high quality of the effluent, the operational cycling of the ponds and the high porosity of the vadose zone. Previous work has found denitrification if the recycled water still contains organic matter, further work was recommended to determine the critical organic concentrations. The renovated water from the Ezousas wastewater reuse Project was able to meet the health and agronomic requirements for unrestricted irrigation.

The risk of flooding with sewage effluent resulting from hydraulic mounding was also investigated to define the growth and decay of the mound. It was possible to report that after more than fifteen years of operation and a total infiltration of 40Mm³, there have been no signs of reduced hydraulic capacity or water quality.

Key words: aquifer, geology, groundwater hydraulics, effluent reuse, effluent recharge, nitrate, phosphate, metals, treated sewage.

ACKNOWLEDGEMENTS

I wish to express my thanks to the Water Development Department (WDD), Cyprus for allowing me to use the data obtained from the monitoring of the Ezousas aquifer that formed the basis for the current study.

Special thanks must go to the former director of WDD, Dr Kyriacos Kyrou for his encouragement and genuine interest throughout the progress of my studies.

Especially I wish to express my sincere gratitude to my supervisors, Professors Andrew Wheatley and Graham Sander for their invaluable advice, continuous guidance and patience during the long period of my research study as well as at the preparation of my actual thesis.

I wish also to give my cordial thanks to Christine Barton and the staff, members of the University for their help throughout my PhD studies.

CONTENTS		Page No.
GENERAL INTRODUCTION AND FORWARD TO THE THESIS		1
CHAPTER 1		
MANAGED AQUIFER RECHARGE (MAR) WITH TREATED WASTEWATER EFFLUENT		5
1.1	Introduction	6
1.2	Soil Aquifer Treatment (SAT)	9
1.3	Engineering Factors that affect the Performance of SAT Systems	13
	1.3.1 Effluent Pre-treatment	13
	1.3.2 Site Characteristics	14
	1.3.3 Operating Conditions	14
1.4	Regulations and Guidelines for Reclaimed Water Used	15
1.5	An Overview of SAT Applications	18
	1.5.1 A European case study	18
	1.5.2 An American case study	19
	1.5.3 An Australian case study	20
	1.5.4 A South African case study	20
	1.5.5 An Israeli case study	21
CHAPTER 2		
SUITABILITY OF THE EZOUSAS AQUIFER FOR THE STORAGE-AND RECOVERY OF TREATED SEWAGE EFFLUENT		
2.1	Introduction	25
2.2	Climate	29
2.3	Geology and Hydrology of the Ezousas River Catchment	
	2.3.1 Regional Geological Setting	30
	2.3.2 Lithology	34
	2.3.3 Bedrock Geology	35

2.3.4	Aquifer Topography	36
2.3.5	Seawater Intrusion	37
2.3.6	Hydrogeological Investigations	39
2.3.7	Storage Capacity Estimates	42
2.4	The Design and Operation of the Recharge Basin System	44
2.5	Aquifer Water Quality	46
2.6	Conclusions	50
 CHAPTER 3		
PAPHOS WWTP - GENERAL DESCRIPTION OF PROCESS		51
3.1	Introduction	52
3.2	Background	56
3.3	The Treatment Process	57
3.3.1	Preliminary Treatment	57
3.3.2	Primary Treatment	58
3.3.3	Secondary Treatment	58
3.3.4	Tertiary Treatment	59
3.3.5	Sludge Treatment	60
3.4	Quality Characteristics and Control of the Treated Effluent	61
3.5	Sampling Procedure	63
3.5.1	Influent	63
3.5.2	Process control	63
3.5.3	Effluent	63
3.6	Data analysis	64
3.6.1	Treatment Parameters	64
3.6.2	Heavy Metals	67

CHAPTER 4	69
THE CHANGES IN NITRATE FROM THE TREATED SEWAGE EFFLUENT	
4.1 Introduction	70
4.2 Objectives	72
4.3 Problems Associated with High Concentration of Nitrates in the Environment	72
4.4 Review of Nitrogen Transformations	73
4.4.1 The Nitrogen Transformation via Natural Attenuation in the Vadose Zone-Overview	
4.4.1.1 Fate and Transport	73
4.4.1.2 Natural Attenuation-The Denitrification Process	74
4.5 Infiltration and Percolation into a Shallow Alluvial Aquifer	77
4.6 The Ezousas Recharge Project	79
4.6.1 The Experimental Site	81
4.7 Experimental Results	
4.7.1 Hydraulic Loading	85
4.7.2 Water Quality Results	87
4.8 Results and Discussion	88
4.9 Conclusions	97
CHAPTER 5	
GEOCHEMICAL CHANGES IN GROUNDWATER FOLLOWING RECHARGING	100
5.1 Introduction	101
5.2 The Aim	103
5.3 Literature Review	103
5.4 The Recharge Water	108
5.5 Methodology: Sampling and Analysis	109

5.6	Results and Discussion	
5.6.1	Major Ion Chemistry and Identification of Hydrogeochemical Processes of Ground Water	111
5.6.2	Geochemical Modelling of Water-Mineral Equilibrium	123
5.6.3	Possible Changes in Physical Characteristics of the Aquifer	129
5.7	Irrigation Use	130
5.8	Overall discussion	131
5.9	Conclusions	132

CHAPTER 6

	FATE OF COPPER AND PHOSPHORUS FROM TREATED EFFLUENT RECHARGE INTO THE AQUIFER	134
6.1	Introduction	135
6.2	Materials and Methods	
6.2.1	Monitoring	137
6.2.2	Groundwater Modelling	138
6.2.3	Laboratory Experiments	145
6.3	Results and Discussion	
6.3.1	Water Quality	145
6.3.2	FEFLOW Results	147
6.3.3	PHREEQC Results	153
6.3.4	Sediment Partition Experiments	153
6.4	Overall Discussion	154
6.5	Conclusions and Recommendations	156

CHAPTER 7

OVERALL SUMMARISING DISCUSSION

	Soil Aquifer Performance	157
	Infiltration Rate Behaviour	158
	Fate of Phosphate and Copper	159

CHAPTER 8	
CONCLUSIONS AND RECOMMENDATIONS	161
REFERENCES	165
APPENDIX 1 - OPTIMUM SOLUTIONS TO WATER TABLE MOUND GROWTH AS A RESULT OF ARTIFICIAL GROUNDWATER RECHARGE	190
APPENDIX 2 - COMPUTER PROGRAMS	249
LIST OF ABBREVIATIONS	i
LIST OF SYMBOLS	ii
LIST OF FIGURES	iii-iv
LIST OF TABLES	v-vi
PUBLISHED WORK	vii

ABBREVIATIONS

AMSL	Above Mean Sea Level
ASCE	American Society of Civil Engineers
ASR	Aquifer Storage and Recharge
BC	Boundary Conditions
BH	Borehole
BNR	Biological Nutrient Removal
BOD	Biochemical Oxygen Demand
COD	Chemical Oxygen Demand
DO	Dissolved Oxygen
DOC	Dissolved Organic Carbon
EC	Electrical Conductivity
EUWFD	European Union Water Framework Directive
FAO	Food and Agriculture Organization (Cyprus)
FM	Formations Geological
GSD	Geological Survey Department (Cyprus)
HRT	Hydraulic Retention Time
ICP	Inductively Coupled Plasma
IWRA	International Water Research Association
MAR	Managed Artificial Recharge
MLSS	Mixed Liquor Suspended Solids
NT	Not Tested
P.E.	Population equivalent
PSTP	Paphos Sewage Treatment Plant
PWWTP	Primary Wastewater Treatment Plants
SAR	Sodium Adsorption Ratio
SCADA	Surveillance Control and Data Acquisition
TDS	Total Dissolved Salts
TOC	Total Organic Carbon

TSS	Total Suspended Solids
UWWTD	Urban Wastewater Treatment Directive
WDD	Water Development Department (Cyprus)
WHO	World Health Organization
WWTP	Wastewater Treatment Plant
XRF	X-Ray Fluorescence
XRD	X –Ray Diffraction
USEPA	United States Environmental Protection Agency
USDA	United States Department of Agriculture

LIST OF SYMBOLS

T	Transmissivity.
k	Hydraulic conductivity
S	Specific Yield.

LIST OF FIGURES

	Page No.
CHAPTER 1	
1.1 Schematic of Soil Aquifer Treatment Systems.	12
1.2 Changes in Nitrogen during Wetting and Drying Cycles	15
CHAPTER 2	
2.1 General area of the Ezousas catchment and Paphos Region.	27
2.2 Geological map of SW Cyprus.	32
2.3 Sieve analysis of near-surface river gravels obtained from five trial pits within the infiltration basins.	35
2.4 Typical borehole lithological profiles of the alluvial aquifer.	36
2.5 Contour map of Ezousas river alluvium aquifer water table, June 2006.	38
2.6 Schematic diagram of the Ezousas Recharge Project.	40
2.7 Hydraulic Conductivity estimates along the Ezousas river alluvial aquifer.	41
2.8 Hydrographs from wells upstream of the Ezousas Recharge Project.	43
2.9 Schematic diagram of an example recharge pond.	45
2.10 Abstraction-Treated effluent recharge.	46
CHAPTER 3	
3.1 Diagram of the Paphos Wastewater Treatment Plant	54
3.2 Sewage treated effluent produced on an annual basis.	55
CHAPTER 4	
4.1 The nitrogen cycle.	77
4.2 Aerial view of the Ezousas Aquifer Recharge Project.	80
4.3 The test setting at pond No.4 (5).	84
4.4 Diagram indicating the water table changes during the test at Basin 5 (Pond 4).	86
4.5 Infiltration efficiency of different wetting cycles.	87
4.6 Nitrate concentrations during the long cycle-test in the raised water table (mound) beneath the infiltration pond (pond's floor elevation = 76.2m (amsl)).	91

4.7	A simplified diagram showing the processes taking place during the long cycle recharge operation.	94
-----	---	----

CHAPTER 5

5.1a.	Piper Diagram – Sampling 23/05/2008.	115
5.1b	Piper Diagram – Sampling 11/03/2009.	115
5.2	Cross-plot of B versus Cl indicating Cl elevated but slightly B increasing.	119
5.3	Chemistry along groundwater flow-path.	120
5.4	(Ca-Mg vs SO ₄ -HCO ₃) scatter diagram showing carbonate dissolution.	121
5.5	Na vs Ca scatter diagram showing increased concentration of Na compared to Ca that indicates reverse ion-exchange.	122
5.6	Nitrate concentration along groundwater flow-path.	123

CHAPTER 6

6.1	Location of the recharge ponds and abstraction wells in the Ezousas catchment.	138
6.2	Calibrated hydraulic conductivity and location of extraction and monitoring wells.	140
6.3a	Abstraction rates (m ³ /d) for the 5 pumping wells.	141
6.3b	Abstraction rates (m ³ /d) for the 4 pumping wells.	142
6.4	Phosphorus concentrations for the native groundwater and the recharged effluent for the period of 25th January 2007 – 19th October 2011.	143
6.5	Copper concentrations for the native groundwater and the recharged effluent for the period of 25th January 2007 – 19th October 2011	144
6.6	Steady state model calibration results (December 2006).	148
6.7	Concentrations of phosphorus for BH3026 the most upstream borehole.	150
6.8	Concentrations of phosphorus in the downstream borehole BH2996.	150
6.9	Concentrations of copper from the upstream borehole BH3026.	151
6.10	Concentrations of copper from the downstream borehole BH2996.	151

LIST OF TABLES

CHAPTER 1		Page No
1.1	Comparison of typical SAT zones.	12
1.2	Quality Parameters and Frequency of Controls of the Reclaimed Water.	17
1.3	Summary of site characteristics, operational and quality parameters for the five sites reviewed.	23
CHAPTER 2		
2.1	Simplified geological succession of South-Western Cyprus.	33
2.2	Aquifer hydraulic parameters.	42
2.3	Aquifer characteristics.	42
2.4	Water quality analysis.	49
CHAPTER 3		
3.1	A list of Wastewater Treatment Plants in Cyprus and their capacities.	56
3.2	Quality Characteristics and Frequency of analysis of the Treated Effluent for Urban Agglomerations- according to "Discharge Permit".	61
3.3	Monthly average concentrations of Treatment Parameters at Inlet and Outlet.	66
CHAPTER 4		
4.1	The cores of the BH3963 at the vicinity of infiltration basin No5, (Pond 4) where the tests were carried out.	82
4.2	Nitrate (NO ₃) and ammonium (NH ₄) concentration in the pond and the percolated water during the long cycle-test (n=14) and the short cycle-test (n=9 and 17 respectively for the ponded and percolated water for 3 consecutive tests).	91
CHAPTER 5		
5.1	Basic water chemistry statistics from about 50 groundwater and treated effluent samples recharged from 2004-2010.	113
5.2	Chemical analysis for major ions and micro-tracers.	114
5.3.	A summary of the charge proportions for the main anions and cations in relation to the three different water types defined for the Ezousas Recharge Project.	118

5.4	Saturation Indices, (SI) for sulphates, carbonates and hydroxides facies in groundwater of the Ezousas Recharge Project.	126
-----	--	-----

CHAPTER 6

6.1	Average heavy metals content and nutrients in Ezousas recharge project for the period 11/2006 up to 10/2011 (n=14 samples).	146
6.2	Mole exchange between the water and the minerals in Ezousas aquifer.	153

PUBLISHED WORK

- (1) Christodoulou, G., Sander, G.C., Wheatley, A.D. Characterization of the Ezousas Aquifer of SW Cyprus for storage-recovery purposes using treated sewage effluent. *Quarterly Journal of Engineering Geology and Hydrogeology* 40(3), 229-240, 2007.
- (2) Christodoulou, G., Dokou, Z., Tzoraki, O., Gaganis, P., Karatzas, G. (2013) Attenuation capacity of a coastal aquifer under managed recharge by reclaimed wastewater: the Ezousas case study. *Proc. SPIE 8795, First International Conference on Remote Sensing and Geoinformation of the Environment (RSCy 2013)*, 879510 (5th August 2013); doi: 10.1117/12.2029178. Published in *SPIE Proceedings Vol 8795*.

GENERAL INTRODUCTION AND FORWARD TO THE THESIS

Most countries depend on groundwater for their water resources and abstraction has increased during recent decades for irrigation, domestic and industrial uses. This has resulted in a progressive and long-term trend of declining water levels and even drying up of some wells. Pressures on ground water use include stricter water-quality standards and the growth in demand (irrigation, industrial and domestic). There is now also the need to adapt to climate change and different water management practices including recycling to meet the increasing demand now needed.

Many developed countries have resorted to desalination but wastewater recycling is more sustainable overall for water management. This thesis reports on the physicochemical impact of wastewater recycling by artificial ground water recharge using tertiary-treated, disinfected municipal wastewater (recycled water). Groundwater recharge is not the only option, but it is an effective and efficient means for restoring the levels of groundwater whilst also offering greater protection to the environment, ecosystems, commercial and social life.

Artificial recharge as a means of retaining sustainable groundwater resources is being increasingly applied around the world to overcome the challenges of climate change and demographic demand. The benefits of artificial recharge include replenishment of depleted aquifers, underground storage of excess surface water and reuse of high quality treated effluents. Current EU treated wastewater standards are based on the concept that urban discharges should not lower natural water quality. Treated wastewaters should therefore be suitable for reuse via aquifers if the hydraulic conditions are right and there are no adverse reactions with the natural geochemistry. This thesis investigates potential generic tools for quantifying these.

Artificial ground water recharge also includes water from other surface sources which is stored in the ground. This process provides filtration within the soil as well as increasing the groundwater resource. Effluents and surface water may contain persistent pollutants and dilution with ground water can improve the quality of the original surface water. The water used for recharge may be excess storm water, river water or recycled water and the recharge technologies used include; surface infiltration, injection wells, artificial ponds and percolation tanks. Selection of the most appropriate system needs to take into consideration factors including topography, soil type, surface and ground water availability and their quality. To prevent both soil and groundwater flooding or contamination and avoid prejudicing any subsequent use, it is important to understand any cross-water interactions and efficacy of the pre-treatment methods.

Artificial recharge of groundwater is an established practice worldwide with a long history of experimentation and there are examples of full-scale recharge projects which have demonstrated the benefits that recycling can bring (examples are included in Section 1). This experience, practical knowledge and the problems and advantages that have occurred from ground water recharge are reviewed in this thesis.

In spite of this experience and a sound knowledge of the basic principles governing groundwater hydrogeology there are few academic studies of the influences on ground water behavior and quality. Many existing applications have been in response to urgent, localized problems and there is no international guidance to aid the geographical expansion. Limitations in both the fundamental understanding of the hydrogeology and/or management of aquifer recharge have been reported. Dillon, (2005) noted that the extent to which managed artificial recharge (MAR) can achieve its potential to provide water supplies will depend upon the confidence in the capabilities and understanding of the catchment and the aquifer system. Dillon (2005) suggested this needed to include; demand, existing water infrastructure, a social and regulatory environment, and skilled personnel (Dillon, 2005).

World-wide water scarcity means that artificial recharge will receive increased emphasis in the future, particularly regarding the treatment and storage of municipal wastewater and other previously thought of as low-quality water for reuse.

This thesis describes a case study of MAR in Cyprus which has the typical Mediterranean water scarcity problems compounded by fluctuating seasonal water demands from agriculture and tourism. There are additional problems in island urban communities when over abstraction of ground water results in sea water ingress into the aquifer. If desalination is rejected as unsustainable then ground water recharge with treated waste water is an alternative but one which carries the risk of irreversible contamination.

In Cyprus about 10% of drinking water needs are met using the artificial recharge of downstream aquifers by water released from dams. Additionally treated wastewaters now need to be used to artificially further recharge the aquifers for subsequent re-abstraction for irrigation purposes. The artificial recharge of coastal aquifers in Cyprus has also been shown to be an effective control against seawater intrusion. Therefore, the use of treated wastewater in Cyprus is expected to increase significantly in coming years.

This research focuses principally on the recharge of unconfined aquifers, the most readily available, affordable and vulnerable source of water in (semi-) arid regions with the recharge rate as the dominant process variable.

The results and analysis included laboratory experiments, controlled field trials with pilot-scale units, field monitoring of full scale systems and analytical and numerical modelling. The aim of the research was to develop a quantitative understanding of performance of treatment and flow on the transport and interactions of pollutants and pathogens in the aquifer. The objectives were to understand the fundamental geochemical and hydraulic impacts of the artificial recharge on water quality. This analysis was used to predict the transport and fate of potential contaminants and the effects of system design, effluent

quality, loading, soil properties and environmental conditions.

The research work presented here was from a seven-year study supported by the Paphos Water Development Department, to explore ways of storing the tertiary treated domestic effluent, from the Paphos treatment plant, using the Ezousas alluvial aquifer both to avoid salt water ingress and enable year-round re-abstraction for irrigation.

The data for the thesis has been compiled part time during full time duties with the Paphos Water Corporation. It has been arranged in a submitted paper format to reflect the schedule of work and papers published during the research. Two of the Sections have been accepted and published as research papers, one has been refereed and edited for resubmission and a forth is in the draft form as presented in the thesis.

CHAPTER 1

MANAGED AQUIFER RECHARGE (MAR) WITH TREATED WASTEWATER EFFLUENT

Chapter Summary

Managed Aquifer Recharge (MAR) is becoming an increasingly attractive water management option for the integrated management of surface water, groundwater and wastewater to allow recycled water resources to supplement limited water supplies.

MAR applications may be grouped into the following broad methods:

- Spreading methods such as infiltration ponds, soil-aquifer treatment (SAT), in which recharge water percolates through the vadose zone into the groundwater.
- Injection wells to force water into an aquifer for later withdrawal and use (e.g. aquifer storage and recovery, (ASR)).

In order to apply MAR it is necessary to set criteria that enables its evaluation, planning, economic assessment and feasibility. Such criteria would include water availability or quantity, water quality and the hydrogeological suitability.

SAT-MAR methods are an important way of addressing water scarcity challenges by reusing water of impaired quality (such as wastewater), as a reliable resource whilst ensuring its safety.

The Groundwater Directive (2006/118/EC) establishes quality criteria that takes account of local characteristics and allows for further improvements to be made based on monitoring data and new scientific knowledge. The National criteria for Cyprus have been set for the use of treated wastewater for irrigation, they are in the form of published guidelines referred to as the Code of Practice for Wastewater Reuse and Sludge Application.

An overview of the SAT systems reviewed for wastewater treatment and reuse are shown in Table 1.3. The summary, based on examples from arid countries, includes information on design, removal efficiencies and pre-and post-treatment options for infiltration basins (Table 1.3).

1.1 Introduction

Managed Aquifer Recharge (MAR) is the purposeful recharge of water to aquifers for subsequent recovery or environmental benefit. The efficiency of MAR systems strongly depends on natural framework conditions for example hydraulic conductivity and ambient groundwater flow but can be further enhanced by adjusted design and operation.

MAR using impaired water sources can be accomplished via riverbank infiltration and surface spreading but for direct aquifer recharge or injection a better water quality is required. For recycled water, surface spreading and direct injection are the most common applications.

Surface spreading typically uses infiltration basins or ponds to enhance the natural percolation of water first into the ground and then into the unconfined aquifers. Surface spreading-infiltration systems require permeable soils (sandy loams, sands, gravels) that have relatively high infiltration rates and that can transmit the applied water without completely saturating the zone above the groundwater.

Surface spreading or infiltration techniques are well established not just to augment water resources but to improve its quality as well. Raw water is introduced into the groundwater through soil percolation under controlled conditions to polish or further treat wastewater. The process, often called soil aquifer treatment (SAT), allows a lower level of wastewater treatment prior to the aquifer recharge, it is also less expensive and has a longer life cycle.

Infiltration basins methods are the most favoured recharge technique because they allow efficient use of space and they require only simple maintenance. Recharge basins are either excavated or enclosed by dykes or levees.

The major operational issue of infiltration systems for artificial recharge of groundwater was reported to be soil clogging caused by to accumulation of suspended solids on the bottom and banks of the infiltration facility as they settle or are strained out onto the soil surface (NRC, 1994). Clogging by biological activity was also noted depending upon the nutrient status and organic composition of the water. The decline in infiltration rate also depends on the basin floor permeability and upon the grain-size. The only feasible method of recovery treatment, developed so far, consists of thoroughly drying the ground under the basin.

Direct Injection techniques use a well or bore that can introduce recharge water into deep confined aquifers but also shallower semi-confined aquifers, in the case of insufficient available area or to enhance soil treatment. For recovery the water is then either pumped from the same well (aquifer storage and recovery – ASR) or from alternative wells with a calculated, defined transport time to aid water quality (aquifer storage, transport and recovery – ASTR). Direct Injection systems require high quality recycled water quality for recharge as well as geochemical compatibility with the aquifer to avoid frequent clogging of injection structures, by biological growths, chemical precipitation or deposition of silt.

A study conducted by The U.S. Environmental Protection Agency (USEPA, 1999) reported on underground injection control (UIC) and noted that treated sewage used for underground injection generally received at least secondary and in many cases tertiary treatment (USEPA, 1999).

The same study noted that secondary treated effluent would contain fecal coliforms and nitrates at concentrations above the maximum recommended contaminant level (MCLs), and both secondary and tertiary treated effluents could exceed the secondary MCLs for chloride, sulfates, and total dissolved solids (TDS). The study also, reported on case

studies where treated sewage effluent recharge wells had contributed to or caused groundwater or surface water contamination.

International experience from different climates and geographies has shown that aquifers can be successfully recharged over long periods without significant clogging if high quality raw water is used and injected into secondary solution features and fractures in rock-aquifer systems (Smith and Pollock, 2010).

The selection of methods for recharge depends on factors, including topography, land availability, soil type, hydrogeological conditions, budget, level of technology and the needs for subsequent recovery of the water. The nature and hydraulic conductivity of the soil or subsoil and the required loading are the major influences over the method used. Suitable subsurface conditions (i.e., slope and/or hydraulic gradient) are essential to ensure that the percolate water can flow away from the site at predictable rates. Irrespective of the method chosen, it is essential to ensure that the pre-treatment of the recharge water is sufficient to prevent soil contamination and enable the resultant groundwater to be suitable for subsequent use.

The studies on artificial recharge techniques are mostly site-specific and descriptive in nature which gives little insight into the key factors involved in leading to the success of aquifer recharge in other locations. Thus, there is need of further academic research and reporting of artificial recharge techniques for variety of conditions (IWMI, 2009).

There are clear economic and sustainability incentives for managed aquifer recharge (MAR) with reclaimed water in water scarce areas. Application of artificial recharge schemes allow groundwater to become a renewable resource, but it also provides a cheaper, faster, and less technologically intensive method of storing water in large quantities. It avoids evaporation associated with surface storage as well as being economically, environmentally and socially more acceptable (Bouwer, 2002). Water resources management as well as wastewater treatment are likely to be improved by well-designed recharge schemes (Wintgens, et al., 2009). Artificial recharge is therefore an

increasingly important strategy during climate change that will help solve the water shortages in a sustainable way.

Managed aquifer recharge is only feasible if the soil and aquifer that can accept a sufficient volume of water at a suitable recharge rate to justify the costs of the project. The major risk is additional limitations may apply in environmentally sensitive areas.

1.2 Soil Aquifer Treatment (SAT)

Additional water treatment within the soil-aquifer treatment (SAT) is anticipated in a managed aquifer recharge (MAR) scheme enabling complementary increases in water availability whilst simultaneously improving its quality.

It was concluded from the literature review, summarized in Table 1.3, that SAT was considered the system of choice for effluent reclamation because it includes inherent natural treatment. SAT schemes also incorporated: storage capacity to buffer seasonal variations of supply and demand, as well as attenuation with natural water, which promotes public acceptance of reuse. It is attractive and reliable in areas where there are suitable conditions, adequate operation, maintenance skills and adequate monitoring of the spreading basins (Idelovitch, 2003).

SAT is a geo-purification system that utilizes physical, chemical and biological processes to improve water quality during infiltration of wastewater effluent through the soil strata. Treatment benefits are achieved both during vertical infiltration of wastewater effluent through the unsaturated zone (vadose zone), during its horizontal movement in the saturated zone and attenuation in the aquifer before it is abstracted again from a recovery well (Weiyang, et al., 2017).

SAT was also defined as three component treatment process by Fox, et al., (1999):

- infiltration through a biologically active infiltration interface (<1m in depth) at the soil/water boundary of the infiltration basin;
- (ii) percolation through the vadose zone below the soil, (3–30m in depth) and
- (iii) storage/transport in the underlying aquifer (6–24 months, >150m horizontally) pending withdrawal at proximate production wells.

The degree to which the processes occur however, depends on a number of conditions that can vary significantly from site to site and from compound to another (NRC, 1994).

The filtration available from SAT means they are able to remove biodegradable organics, suspended solids, bacteria and viruses from wastewater and depending on the loading rates, they can also remove significant amounts of phosphorus, nitrogen and metals. Therefore, properly designed and managed systems can produce a safe, clear, odorless renovated water that can be used for unrestricted irrigation, contact recreation and other purposes (Asano, 2016).

In contrast to advanced treatment with chemicals or membrane filtration SAT does not produce new waste streams, such as the brine solutions from desalination, which require disposal. SAT also provides a two-stage barrier for pathogen removal, making it an attractive process for communities with limited resources. The simplicity and effectiveness of SAT has meant the process has become the most economical reuse alternative for extending potable water supplies, when a suitable aquifer is available. SAT costs are reported to be less than 40 % of those necessary for an equivalent in-plant treatment to achieve the same water quality (NRC, 1994).

The advantages and disadvantages of infiltration basins for groundwater recharge and water reuse can be summarized as below:

The advantages are:

- SAT reclaimed water is from a well, or via surface water source, rather than from a treatment plant and this indirect or natural reuse has greater public acceptance than direct sewage reuse schemes.
- The SAT process is low-cost, simple to operate, robust and a sustainable method of wastewater treatment and reuse.
- SAT offers an aesthetic advantage over conventional sewage treatment works for water recovery by providing additional wetland habitats.
- SAT water quality is safe, clear and taste and odour-free.

The disadvantages are:

- The large areas of land required and distribution system to the basins.
- Suitable hydrogeological conditions are not easily encountered in combination with suitable land for recharge facilities.
- The basins can change the soil and groundwater hydrological properties.
- Constant monitoring of recharging system is required.
- Ground water recharge can raise the potentiometric surface locally which may have an adverse impact on adjacent properties.
- Clogging of the infiltration basin, either from the accumulation of suspended solids in the effluent or from secondary biological growth in the basin, is common and difficult to solve.

The general principles of SAT schemes and the processes involved are summarized in Figure 1.1 and Table 1.1 respectively.

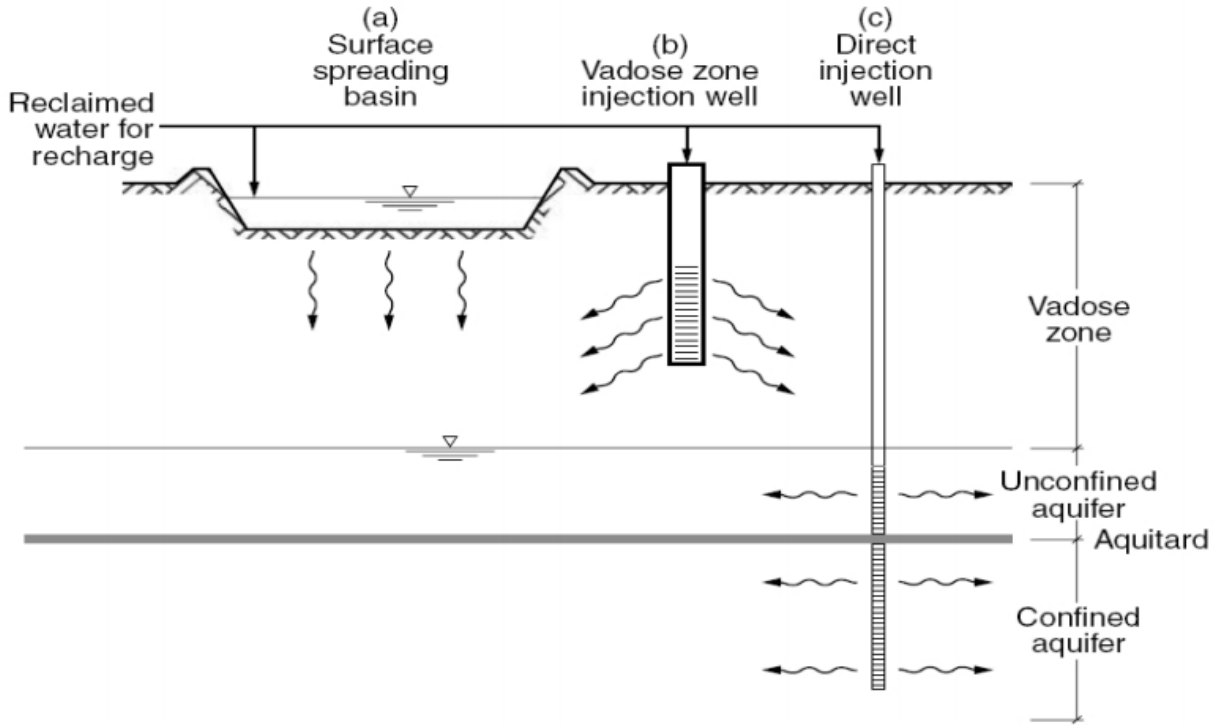


Figure 1.1 Schematic of Soil Aquifer Treatment Systems (Aharoni, et al.,2011)

Table 1.1 Comparison of typical SAT zones (Demoware, 2017)

PROCESS/PARAMETER	INFILTRATION INTERFACE (water-soil)	SOIL-PERCOLATION	GROUNDWATER TRANSPORT
Treatment mechanisms	Filtration, Biodegradation	Biodegradation, Adsorption	Biodegradation, Adsorption, Dilution
Transport	Saturated	Unsaturated	Saturated
Residence time	Minutes	Hours to days	Months to years
Travel distance	Centimeters/inches	3-30 m / 10-100 ft Variable	Variable
Mixing	No	No	Yes (regional G. W.)
Oxygen (O ₂) supply	Recharge water	Unsaturated zone	Regional G. W.
Biodegradable org. carbon availability	Excess	Excess/limiting	Limiting
Redox conditions	Aerobic	Aerobic to anoxic	Anoxic to aerobic

1.3 Engineering Factors that Affect the Performance of SAT Systems

The three main engineering factors that affect the performance of SAT systems are effluent pretreatment, site characteristics and operating conditions (Fox, et al., 2001).

1.3.1 Effluent Pretreatment

The organic content, particularly easily assimilable or BOD and suspended solids of the treated effluent applied to infiltration basins are key factors which affect infiltration rates and are monitored and controlled to be as low as possible. The degree of effluent pretreatment directly impacts on the concentration of these biodegradable components which act as substrates for regrowth in the infiltration basin. This occurs because the highest concentrations of biodegradable matter and oxygen are present measured as COD, BOD and NH_3 and this generates the greatest biological activity at this soil/water interface.

Microbial regrowth and consequent clogging of the infiltration basin is the main limitation of SAT. Houston, et al. (1999) investigated this clogging layer and identified it as mostly a layer of fine sedimentary material which causes a sharp drop in hydraulic head as water infiltrates through this sedimentary zone.

The extent of soil clogging is therefore closely correlated to total suspended solids (TSS), as well as (BOD) and carbon to nitrogen (C:N) ratio. In particular the nutrient load, is an important factor influencing the growth of algae contributing to the clogging layer (Winter and Goetz 2003). The reduction and/ or prevention of clogging, is therefore largely dependent on the quality of the infiltrated water. Bouwer (2002) recommend treating recharge water to “drinking water quality” to reduce the risk of clogging. Thus the quality of the treated effluent applied to infiltration basins is therefore the key factor which potentially controls the whole performance of the SAT system.

1.3.2 Site Characteristics

If infiltration basins are used rather than injection wells, the stratum will be the site characteristic which controls the infiltration rate. This layer is usually the least permeable stratum between the aquifer and the recharge surface. Recharge rates will be controlled by the stratum that has the lowest quotient of permeability (hydraulic conductivity) divided by the stratum thickness, at constant head of water applied. Identifying the controlling stratum is needed to calculate the area of the basins and may entail some sampling, drilling and infiltration testing (USDA, 2010).

The depth, attitude, areal extent and the location and elevation of any outcrops need to be determined.

The aquifers best suited for artificial recharge are those aquifers which absorb and retain water. Theoretically this implies a high vertical hydraulic conductivity while the horizontal conductivity is moderate although these two conditions are not often encountered in nature.

1.3.3 Operating conditions

Generally, recharge facilities are operated (loading schedules) in repeating wet-dry cycles or continuous wet operations (Mays, 1997).

The use of wetting/drying cycles has an important beneficial affect on the microbial growth rate in the subsurface. During wetting, the dissolved oxygen in the infiltrating water becomes exhausted from carbonaceous and nitrogenous oxygen demand and as the soil becomes water saturated, anoxic conditions develop. Reaeration does not occur since this is limited by molecular diffusion through the surface of the basins. Drying overcomes this by allowing air to be drawn back into the vadose zone and aerobic conditions to redevelop. If ammonia is adsorbed during a wetting cycle, the ammonia can be nitrified during a drying cycle resulting in a flush of nitrate during the initial stages of the wetting

cycle. A U.S. Environmental Protection Agency report (U.S. EPA) indicated that 70% of the facilities in U.S. were operated using the wet-dry cycle method (Guihua, et al., 2000). Changes in ammonia and oxygen concentrations, during a wetting and drying cycle are illustrated in Figure 1.2 (LOTT, 2013).

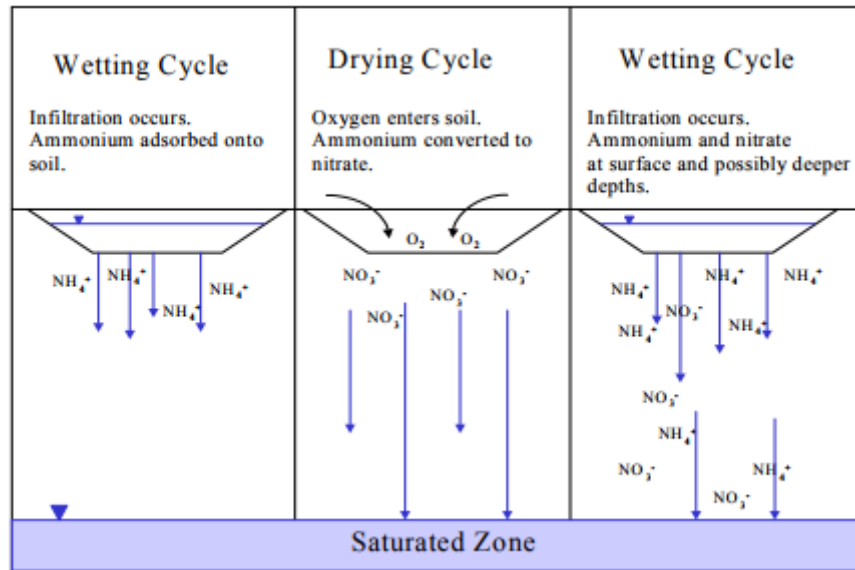


Figure 1.2 Changes in Nitrogen during Wetting and Drying Cycles (LOTT, 2013)

Extending the ponding periods has been shown to accelerate soil clogging, whereas wetting and drying cycles were shown to disrupt the clogging layer. Results from using long-term ponding conditions also demonstrated that the infiltration rate was controlled by precipitation of solids regardless of the native soil media (Beach, et al., 2005).

These were reported to be the main operation factors influencing although weather and other local topographical features have also been shown to influence infiltration rates.

1.4 Regulations and Guidelines for Reclaimed Water Used

The EU Urban Waste Water Treatment Directive (UWWT) (Council Directive 91/271/EEC) and the Integrated Pollution Prevention and Control (IPPC) Directives

amendment to the Directive (2003/35/EC), were incorporated into Cyprus State Laws N.106(I)/2002 concerning 'The Control of the Waters Pollution' and the associated regulations K.D.P. 407/2002, 772/2003 254/2003, KDP269/2005. According to these regulations, the discharge of any polluting effluent, which might cause the pollution of the soil and/or the waters, required a Discharge Permit. These permits are issued by the Minister of Agriculture Natural Resources and Environment on behalf of the Sewerage Boards and the Water Development Department. Permits specify the quality objectives and the disposal conditions of the treated wastewater as well as legally-binding numerical limit values for a range of parameters. In the case where the treated wastewater is intended to be discharged to an aquifer for later reuse the Permit also specifies the maximum permissible concentrations in the reclaimed (abstracted) water (Table 1.2).

Table 1.2 Quality Parameters and Frequency of Controls of the Reclaimed Water

α/α	Parameters	Monitoring frequency	Maximum Permissible
1	Active substances of pesticides (including relevant metabolites, degradation and reaction products ⁽¹⁾)	Every six months during the summer and winter season	0.1 µg /1 0.5 µg /1 (Total) ⁽²⁾
2	Nitrates (NO ₃)		50 mg/1
3	Conductivity		2500 µS/cm
4	Chloride (Cl)		250 mg/1
5	Sulphates (SO ₄)		250 mg/1
6	Trichloroethylene		0.005 mg/1
7	Tetrachloroethylene		0.002 mg/1
8	Arsenic (As)		0.01 mg/1
9	Cadmium (Cd)		0.005 mg/1
10	Lead (Pb)		0.01 mg/1
11	Mercury (Hg)		0.001 mg/1
12	Ammonium (NH ₄)		0.5 mg/1

1. As "pesticides" means plant protection products as defined in article 2 of Directive 91/414/EEC and the biocidal products as defined in article 2 of Directive 98/8/EC.
2. "Total" means the sum of all individual pesticides detected and quantified in the monitoring procedure, including relevant metabolites, degradation products.

1.5 An Overview of SAT applications

SAT has been employed for further treatment and reuse of wastewater effluent in various sites around the world but most published information is descriptive experience of site specific case studies. The review concluded that there were no results which led to appropriate transferable tools, methods, or knowledge transfer to enable replication of this experience at new schemes. A list of all the papers reviewed are included in Table 1.3 and those with data reviewed in more detail by world region as follows.

1.5.1 The European Experience

DEMEAU is a EU-funded scheme to demonstrate projects using novel but promising technologies that tackle emerging pollutants and problems in water and wastewater. The DEMEAU data base includes 270 Managed Aquifer Recharge (MAR) sites of which 200 were still active. River and lake water were the most frequent source of raw water to supplement domestic drinking water supplies. The most frequent MAR recharge method was induced bank filtration.

Treated wastewater effluent, as a raw water source, was part of two other European schemes excluding the Ezousas Project, featured in this thesis. One was at Barcelona where reclaimed water is injected into the Llobregat aquifer via injection wells to counteract seawater intrusion. Pre-treatment of reclaimed water (15,000 m³ /day) included ultrafiltration and reverse osmosis to improve reclaimed water quality before injection (Sprenger, et al, 2017). The project was reverted to stand-by capacity in 2011 due to the running costs of the pretreatment plant.

The other site using reclaimed water is in Torreele/St-Andre (Belgium), where treated wastewater is infiltrated via SAT into sand dunes. The overall scheme produces 2.5×10^6 m³ /annum and uses ultrafiltration following tertiary treatment before infiltration (Vandenbohede, et al. 2013).

1.5.2 The American Experience

SAT, is well established in the United States, where it is also known Rapid Infiltration (RI), (USEPA, 2003). Traditionally the emphasis has been on utilizing land treatment and the soil ecosystem to treat wastewater. There are more than 350 such systems operating in the USA but the potential risks of using SAT for full treatment of wastewaters has led to more stringent standards and extra difficulties in identifying appropriate sites for SAT systems. Most new systems incorporate at least secondary sewage treatment.

Projects in the USA, which have focused on restoration of groundwater levels and underground storage have used surface spreading. An example is the Montebello Forebay groundwater recharge project in Southern California which has been successfully recharging a potable aquifer for more than 50 years using SAT (soil aquifer treatment) *via* spreading basins (Schimmoller, et al., 2015).

Details of an aquifer recharge scheme at Tucson have also been published (Megdal, et al., 2014). The project known as 'Sweetwater Recharge' was introduced to provide sustainable water resource management and avoid the impact of over abstraction. The Tucson facilities utilizes surface spreading as tertiary treatment of wastewater but calculations suggest that most of the water infiltrates into the aquifer is then pumped back out for distribution to supplement other potable water supplies (Megdal, et al., 2014).

Persistent organic pollutants were expected to be an issue for the Tucson scheme and a ten-year study of TOC removal was carried out (Quanrud, et al., 2005). Removals of TOC averaged >90% during percolation through the 37m deep, unconsolidated sediment making up the vadose zone. The majority of removal occurred in the first 1.5 m of soil where removals were attributed to biodegradation. Variations in the duration of wetting/drying periods did not significantly impact organic removal efficiencies (Quanrud, et al., 2005), but it was observed that TOC removal improved during the first 6-12 months of operation following the introduction of recommissioned infiltration basins (Quanrud, et al., 2005).

1.5.3 The Australian Experience

Population growth in Australia combined with the anticipated climate change has led to development into alternative water resources to meet demand. These have included desalination of seawater, stormwater and rainwater harvesting, increased use of groundwater and water recycling. Managed aquifer recharge (MAR) is an important and growing alternative, the largest groundwater recharge project is in Perth. Recycled water is pumped into the underground aquifers to provide drought-proofing of the city's drinking water supply against climate change (Harrington and Cook, 2014).

The first intentional application of SAT in Australia was in Alice Springs where the main operational issue has been the infiltration rate. Experiments from changes to the duration of wet and dry cycles led to the conclusion that the slow infiltration rates were due the underlying soil characteristics. It was found that average infiltration rates varied by an order of magnitude from 0.1 to 1 m/day due to the heterogeneous soil characteristics. Removal of the less permeable sediment in the superficial layers was introduced for future basin rehabilitations but additional ultra-filtration, following the dissolved air flotation plant, doubled infiltration rates in all basins (Barry, et al., 2017).

1.5.4 The Southern Africa Experience

South Africa is also a water-limited country with surface and ground water quality problems, compounded by population growth and rapid social and economic development (Dennis, and Dennis, 2012). For this reason the "National Water Resource Strategy, 2004", recommended MAR to improve water resource management and sustainability (DWAF, 2007).

Artificial recharge, however, had been in use near Cape Town for over 50 years. Known as "The Atlantis Town Water Resource Management Scheme" it used a stormwater collection and recharge to avoid salt water ingress of the aquifer along the arid west coast.

In 1978 it was decided to add treated wastewater from the town of Atlantis to the system and the treated domestic effluent (from maturation ponds) is blended with the lower-salinity urban before being discharged into the main recharge basins.

Blockages to the re-abstraction caused by borehole clogging has been a reoccurring problem. The borehole clogging was attributed to naturally available iron and manganese in the aquifer but the introduction of natural soil bacteria which accumulate iron and manganese may have been encouraged by the increases in dissolved oxygen concentrations due to fluctuating groundwater levels. Borehole design and the pumping regime were also noted as contributing to the problem. The boreholes were rehabilitated between 1999 and 2002 to remove the clogging and reassess the initial yields. There followed a gradual decline in yield as clogging has returned necessitating further rehabilitation in 2015 (Bugan, et al., 2016).

1.5.5 The Israeli Experience

Israel has used artificial recharge of groundwater aquifers (AR) since 1960 using infiltration ponds and recharge wells. For example the Dan Region, has been in operation for 40 years supplying renovated water in the Negev Valley, southern Israel, where it is used for “unrestricted irrigation” (Lakretz, et al., 2017). It has been an essential component in integrating surface and groundwater resources in the arid climate. SAT was deliberately promoted to remove residual contaminants from sewage effluents by filtration and adsorption in the aerated soil zone and by long the long retention times in the aquifer.

The reported challenges to AR that required further research and studies were: the travel and mixing in the aquifer between the recharged and indigenous water and the impact of AR on the quality of the re-abstracted water, including accidental spills. Concerns were also raised about clogging and reduced capacity of both the recharge wells and spreading basins and how to overcome these issues by design and maintenance. How to equitably allocate the costs of AR operations within the National Water Supply System was also

unresolved (Schwarz and Bear, 2016). Two of these research questions are addressed by this thesis, that of mixing and impact on indigenous water qualities.

There are also other examples of basin and surface spreading operations throughout the world, these projects were selected because of their innovative strategies, their long-term use, scale and the availability of data. Table 1.3 provides a summary of the relevant aquifer characteristics and the projects performance.

Project Name; Year started operation	Aquifer Characteristics	Mode and Scale of Operation	Source Water	Water Quality Considerations			Redox conditions	Use
				Native Groundwater	Recharge Water	Reclaimed Water		
Torrelee/St-André case in Flanders, Belgium, 2002. (Magorzo, et al., 2013; Hannappel, et al., 2014; Van Houtte, 2015; Kazner, et al., 2012; Vandenbohede, et al., 2013)	Dune-sand; Thickness: 25-35m- K: 14m/d	Recharge Basin total area: 18,500m ² ; Recharge Load: 6850 m ³ /d (2.5mcm/yr).	Effluent +Runoff; Advance Treatment- Double membrane process: ultrafiltration and reverse osmosis.		pH: 6.62 Total Hardness: < 1 Cond: 31µS/cm Cl: <10 mg/l SO ₄ : <5 mg/l Na: 13 mg/l NO ₃ : 1.7 mg/l NO ₂ : <0.03 mg/l NH ₄ : <0.04 mg/l TP: <0.02 mg/l TOC: - Total coli: Absent	pH: 7.1 – 7.9 Total Hardness: 14.9 Cond: 458 µS/cm Cl: 29.5 mg/l SO ₄ : 30.5 mg/l Na: 17.8 mg/l NO ₃ : 2.0 mg/l NO ₂ : <0.03 mg/l NH ₄ : <0.12 mg/l TP: <0.2 mg/l TOC: 1.6 mg/l Total coli: Absent	Oxic aquifer conditions prevail between the infiltration ponds and the extraction wells.	Sustainable groundwater management. Potable water supply.
Sweetwater Recharge Facilities, AZ, 1980; Tucson USA. (Kmiec, et al., 2005; Bouwer, et al., 2008; LOTT, 2013; Anderson, et al., 1990)	Alluvium Depth: 180m; K: 5.6-29.5m/d; Infiltration: 0.7/day; Depth of GW: 36m;	Eleven Recharge Basins and wetlands-total area: 162000 m ² ; Recharge Load: 8mcm/yr; 5days wet/7days dry - 2 days wet/3 days dry	Secondary (biofilters - activated sludge-chlorination)		TN: 20.6 TKN: 17.6 Nitrate: 2.9 TOC: 20	TN: 14.7 TKN: 8.2 Nitrate: 6.2 TOC: <1	High total oxygen demand maintains anoxic conditions throughout the majority of the wetting/drying cycle.	Irrigation of parks, golf, etc.
Alice Springs, (North Territory), Australia, 2003. (Barry, et al., 2017; Miotliński, et al., 2010)	Alluvium-palaeochannel deposits; K: 4-90m/d; Depth to GW: 18m;	Five Recharge Basins- total area: 38,400 m ² ; HL: 500,000m ³ /yr; Drying intervals: 7- 12 days; Infiltration Rate: 0.1 -1 m/day Max height of the mound: 1.5m	Facultative and maturation lagoons followed by dissolved air flotation (DAF) (until Sep 2013) or dissolved air flotation and filtration (DAFF) and ultraviolet disinfection (from Sept. 2013).	BOD ₅ : - DOC: 1.6 ± 0.5 pH: 7.4 ± 0.2 EC: (µS/cm) 2400 ± 700 Cl: 399 ± 139 SO ₄ : 508 ± 30 Total-N 2.8 ± 2.1 Nitrate-N 2.6 ± 2.0 Ammonium.- N: 0.02 ± 0.01 Phosphate-P: 0.05 ± 0.05	BOD ₅ : 1.1 ± 0.7 DOC: 8.3 ± 1.6 pH: 7.7 ± 0.3 EC: (µS/cm) 1728 ± 143 Cl: 265 ± 28 SO ₄ : 168 ± 68 Total-N: 9.2 ± 4 Nitrate-N: 1.8 ± 1.2 Ammon.-N: 4.9 ± 4.8 Phosphate-P: 0.4 ± 0.2	BOD ₅ : - DOC: 1.9 ± 0.5 pH: 7.4 ± 0.15 EC: (µS/cm) 1940 ± 403 Cl: 304 ± 95 SO ₄ : 248 ± 140 Total-N: 9.3 ± 5.3 Nitrate-N 9.4 ± 3.6 Ammonium-N : <1 Phosphate-P: 0.26 ± 0.27	Redox conditions depends on wetting and drying cycles. Limited (20%) nitrogen removal in the vadose zone.	Irrigation (horticulture and viticulture)

<p>Atlantis, South Africa, 1979. (Kazner, et al., 2012; Bugar, et al., 2016)</p>	<p>Coastal dune sands overlying calcrete and fluvial sand deposits with peat lenses (~45 m thick). Bedrock consisting of shale or granite; Aquifer depth: ~35m</p>	<p>Seven Recharge Basins- total area:28.3ha; 2.3Mm³ /a; Unsaturated depth:1.5m; Infiltration rate: 0.01 – 0.16 m/day 1.50- 2.5mcm/yr (main basin only)</p>	<p>Secondary treatment with nitrification-denitrification following polished in a series of maturation ponds along with stormwater</p>		<p>DOC:9mg/l NO₃-N:3.5-4.5mg/l Ammonium-N:ND Total coliforms: were in the order of 10⁵/100 mL EC: 600 – 950 µS/m; DOC: 8 – 10 mg/L</p>	<p>DOC:4mg/l NO₃-N: virtually disappeared Ammonium-N:ND Total coliforms: 0-100 EC: 600 – 1000 µS/m; DOC: 2 – 7 mg/L</p>	<p>Although the exact redox potentials were not determined, it is evident that reducing conditions prevailed in the subsurface and that denitrification took place.</p>	<p>Augment local groundwater supplies.</p>
<p>Dan Region, (Shafdan) Israel, 1977. (Magorzo, et al., 2013; Goren, et al.,2010; Aharoni,2012)</p>	<p>Sand and Calcareous sandstone; Unsaturated Thickness:15-30m Saturated Thickness:50-80m</p>	<p>Five Infiltration Ponds; Recharge Load:0.2-0.5m/d; 135 -140 (mcm/yr); Wet:1-2 days Dry:2-4days; Unsaturated depth:15-30m</p>	<p>Secondary effluents; pretreatment: coagulation-flocculation, biofiltration and ozonation</p>		<p>TSS:8mg/l BOD₅:8 mg/l COD:40 mg/l DOC:12-18 mg/l TN:20 mg/l NH₄:6 mg/l TP:1-2 mg/l Fe:80 µg/l Mn:25 µg/l F.Coli:1.8E4 T.Coli:5.6E5</p>	<p>TSS:<0.1mg/l BOD₅:<1 mg/l COD:10-20 mg/l DOC:1-2 mg/l TN:5-10 mg/l NH₄:0.1 mg/l TP:<0.02 mg/l Fe:10-100 µg/l Mn:30-500 µg/l F.Coli:0 T.Coli:0</p>	<p>Manganese which is dissolved during the infiltration where the high biological activity in the upper part of the SAT results in oxygen deficiency in the soil, leading to anoxic conditions and consequent manganese dissolution.</p>	<p>Agricultural Irrigation</p>

Table 1.3 Summary of site characteristics, operational and quality parameters for the five MAR reviewed.

CHAPTER 2

SUITABILITY OF THE EZOUSAS AQUIFER FOR THE STORAGE-AND RECOVERY OF TREATED SEWAGE EFFLUENT

Chapter Summary

A hydrogeological characterization of the River Ezousas alluvial aquifer, located in SW Cyprus, was conducted to assess its suitability for groundwater recharge with 5Mm³ annually of chlorinated tertiary treated sewage effluent from the Paphos Municipality Wastewater Treatment Plant. The results presented are from a 3-year field study conducted to establish the regional groundwater characteristics and to define the aquifer hydrology. New drillings at selected locations were made to provide reliable information about the aquifer dimensions and boundaries. Pumping and constant-head permeability tests were used to estimate the key hydraulic properties of the aquifer system. Analysis of this data suggested a storage capacity of 4.2 Mm³. The downstream bedrock of the aquifer, as it approached the sea, was found to be about 40m below sea level, thus indicating the potential for seawater intrusion. A monitoring program consisting of recording piezometric heads and electrical conductivities was used to observe the position of the seawater freshwater interface, this was used to control rates of abstraction and recharge, to maintain a stable interface. The quality of the treated sewage effluent, and of native and abstracted groundwater, was monitored in terms of salinity, heavy metals, persistent organic compounds and indicator bacteria, to ensure the quality of the downstream groundwater used for local irrigation. No specific problems were identified but further work on the persistent organics was recommended.

2.1 Introduction

The water resources in Cyprus are scarce because of the predominantly semi-arid conditions. The sustainable development and management of these water

resources during a period of climate change will play a critical role in, and have a direct bearing on, the economy of the Island. In Cyprus, every effort is made to increase the water availability for both domestic and irrigation purposes. The water policy in the 1960's was traditional and directed the construction of dams and control works to store the water of the seasonal rivers. There are 108 impounding reservoirs with a total maximum capacity of 332Mm³. Data collected by the Water Development Department of Cyprus (WDD) over a 30 year period showed that, on average, 37% of this capacity was filled during the rainy season, which occurs from November to April. This development programme has allowed the capture of almost all the flows from the major rivers and streams across the island. It was realized, however, that to avoid undesirable impacts on the downstream environment, or riparian disputes, regular controlled releases of water would have to be made from these dams. Despite this recognition of the likely long-term problems of over abstraction however, the annual replenishment of the coastal aquifers through the river gravels has now all but ceased.

The total annual water requirements of Cyprus are estimated to be 233Mm³. Historically, agriculture has been the major water user on the island, consuming about 64% of this, 28.4% is used for domestic purposes, 4.7% is used for tourism, with only minor quantities (2.9%) used by industry (WDD, 2016). These quantities exceed the sustainable water supply of the island because groundwater reserves are being replenished at a slower rate than they are used. This is partly due to the absence of any integrated water resources management policy and “the increased frequency and intensity of drought conditions over the last 30 years” (CMS, 2016). Non-conventional water resources, including treated domestic effluents and the desalination of seawater, have had to be increasingly exploited in recent years to relieve these water shortages. Currently 55Mm³ of treated municipal sewage effluent is produced annually, 75.6% is used for irrigation of forage crops and orange orchards, but restricted irrigation such as public amenity areas, golf courses, etc., excluding vegetable and similar crops, 12.4% is used for groundwater recharge (60% of this applies for the Ezousas river aquifer and 40% for the

Kouris river delta), 8.1% discharged into the sea and 3.9% disposed into the dam of Polemidia (WDD, 2016).



Figure 2.1 General area of the Ezousas catchment and Paphos Region

The construction of further sewerage projects for the remaining major towns and the requiring expansion of the existing once the annual production of treated effluent would rise to 85 Mm³ by 2025 (WDD, 2016).

Meanwhile, the prevailing and persisting drought conditions (1996-2000 and 2004-2006) has forced the State to adopt desalination to satisfy the increasing domestic demand. Annual production is currently 75 Mm³ but desalination is considered too expensive and unnecessary for agriculture. It is only used for domestic consumption but this requires a significant subsidy.

The substantial alluvial deposits of Cyprus's rivers constitute the most important aquifers of the island. Their replenishment comes almost entirely through infiltration from seasonal river flows, which normally occur in winter and early spring. These groundwater resources have declined over many years as a result of persistently lower than expected rainfall, and the construction of the impounding reservoirs on most of the major rivers upstream of the alluvial aquifers. The continuous over-pumping from thousands of difficult to supervise boreholes has made the situation worse. It has therefore become paramount to adopt a more sustainable integrated approach to water resources management by reappraisal of both natural and non-conventional water sources.

Research to understand the risks from recycling treated effluent for maintaining consistent water supplies was a major priority in Cyprus. A possible health risk and customer reaction mean that treated sewage effluent can rarely be used directly in public supply (NRC, 1994; NRC, 1998; USEPA, 2004). Indirect use occurs through an "environmental buffer"; that is, a natural water body (river, lake, aquifer) that physically separates the product water from the recycled wastewater. The three perceived benefits of buffers are that they provide (1) an opportunity to further reduce contaminants through natural attenuation processes, (2) a lag time between the wastewater treatment system and use, and (3) the opportunity of the recycled water to blend with natural waters in the environment (NRC, 1998). The efficiency of an aquifer as an environmental buffer depends on the prevailing geological and hydrogeological conditions in the aquifer concerned. The USEPA Guidelines were used to define the geological and hydrogeological characteristics to

determine the total usable storage capacity and the rate of movement of water from the recharge point to the area of extraction. The key aquifer characteristics affecting specific yield; the pattern of pumping; position and allowable fluctuations in the water table; are: aquifer geometry, thickness of the subsurface deposits; depth of groundwater; permeability, transmissivity; hydraulic gradients; structural and lithologic barriers to both vertical and lateral movement of groundwater (USEPA, 2004).

An analysis of soil and groundwater conditions was undertaken to identify favourable areas where treated effluent could be used for artificial recharge. Infiltration basins were proposed to improve the treated effluent water quality. The unsaturated (vadose) zone would act as a natural filter to promote physico-chemical and biological processes for the removal standard pollutants of concern such as suspended solids, organic and inorganic materials, bacteria, and viruses. Flow through the saturated subsurface provides extra seasonal residence times, for additional natural removal of contaminants. Collectively these processes are termed soil aquifer treatment (SAT) and were described in detail by, for example Bouwer (2000) and Fox, et al (2001).

In the case study of the Ezousas River in S.W. Cyprus, its headwaters were dammed in 2005 at Kannaviou, and recharging with treated effluents was an option to sustain the Ezousas aquifer as a downstream regional groundwater resource for crop irrigation in the Paphos coastal plain area. This Section deals with the most downstream section of the Ezousas Valley, where its alluvial fill constitutes an aquifer of regional importance. The location map is shown in Figure 2.1.

2.2 Climate

Climate in the region is Mediterranean with semi-arid periods. The average daily temperature in July and August ranges between 22^oC on the Troodos mountains to 29^oC on the central plain. Likewise, there is a spatial variation in average rainfall depending on altitude. In the Troodos mountain range (peak

height 1950 m) where there is annual snow fall, average precipitation is 1100 mm/year. In the coastal regions including Paphos, the average rainfall is approximately 350 mm/year. November to April is the normal rainy season, during which, rainwater and river flow infiltrate the riverbed to fill the aquifer. Average potential evaporation is 1850 mm/y or roughly five times as high as the precipitation. The aridity index for the south-west of Cyprus, which is based on the ratio between rainfall and potential evaporation, is 0.20. This defines the region as being semi-arid (semi-arid conditions range from 0.2 to 0.5) (Noto, et al., 2013).

2.3 Geology and Hydrology of the Ezousas River Catchment

2.3.1 Regional Geological Setting

The regional geology is largely associated with the ophiolitic structure of the Troodos Massif and is strongly influenced by the regional tectonics and consequent deformations and faults, (Grand, et al., 1993; Swarbrick, 1993; Robertson, et al., 1998). The island was uplifted from the sea mainly in the Pliocene-Pleistocene era. Subsequent periods of intensive rainfall together with the continuing uplift of the Troodos Mountain resulted in the formation of the main southwesterly draining rivers: Ezousas, Xeropotamos, Dhiarizos and Ha-Potami (see Figure 2.1). These rivers have eroded their channels deep into the relatively soft chalk circum-Troodos rocks, (Robertson, 2000; Constantinou, et al., 2002). Therefore, river pathways are often located within deeply entrenched steep-sided valleys, which expand into a wider valley where the bedrock is less resistant to fluvial erosion. The upstream fluvial processes have resulted in the accumulation of large quantities of sediments over the Mesaoria plain and in the river valleys. The same phenomenon occurs at the coastal plains, where the river bedrock lies well below the present sea level; the accumulation of this eroded clastic material has resulted in the formation of the most significant aquifers in the island.

Figure 2.2 shows that, throughout the Ezousas river catchment area, there are a number of different rock outcrops such as pillow lavas of the Troodos Massif and the allochthonous volcanoclastic and sedimentary assemblage of the Mamonia Complex (Triassic- Cretaceous) (Lapierre, et al., 2007). These were found together with chalky limestones and marls of the Lefkara Formation (of Late Maastrichtian to Early Miocene age) and the marly and chalky marls of the Pakhna Formation (of Middle Miocene age), (Eaton and Robertson, 1993). There is a Messinian gypsum outcrop in a location known as the Polemi Basin which is partly exposed along the river's flanks (Robertson, et al. 1995). In the coastal area, the Lefkara and Pakhna chalks are overlain non-uniformly and unconformably by the Athalassa formation of Plio-Pleistocene age, consisting of marl-calcarenite sequences of fluvial sediments (Hadjisravinou and Afrodisis, 1977; Greensmith 1998). The lithology of the river bed has resulted from the fracturing and erosion of these geological formations. A simplified summary of the encountered geology and stratigraphy is presented in Table 2.1.

Catchment area of Ezousa river

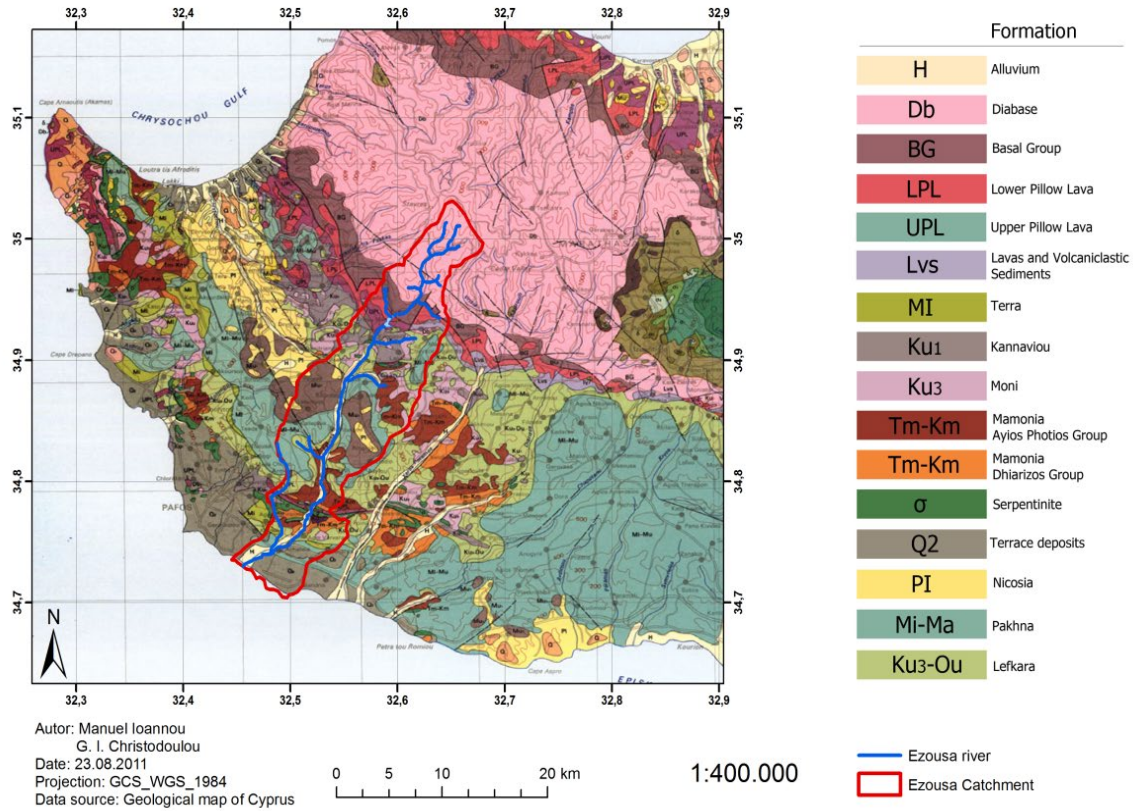


Figure 2.2 Geological map of SW Cyprus (GSD, 2005)

Table 2.1 Simplified geological succession of South-Western Cyprus.

Source: Hadjistavrinou, et al., 1977; Greensmith, 1998; Constantinou, et al., 2002.

Autochthonous Rocks				
Age	Formation, FM	General thickness, m	Typical thickness, m	Lithology
Holocene	Fluvial deposits	0-3	0-3	Fines, sand, and gravels
Pleistocene- Pliocene	Rivers alluvium	6-40	6-40	Gobbles, gravels, sand, silt
	Athalassa FM	0-40	10-15	Calcarenite with marl intercalations
	Nicosia FM	0-800	0-65	Sandy marls with marl intercalations, sandstones
Late Miocene Middle Early	Kalavassos FM	0-150	0-150	Massive or granular gypsum with marls
	Pakchna FM	0-700	0-200	Marls, marly chalks and shales, and siltstones
	Terra FM	0-150	10-20	Reef-limestones
Miocene-Early Maastrichtian	Lefkara Fm	0-800	0-450	White chalks, marls and cherts
Cretaceous	Troodos Pillow Lavas	0 >1500	0 >1500	Lavas
Allochthonous Rocks				
Late Triassic-Middle Cretaceous	Mamonia Complex	Unknown	Unknown	Basalt, serpentinites, melange, sedimentary, metamorphic

2.3.2 Lithology

The depositional sequence was observed at various locations by analysing the borehole logs and from experimental pits excavated at sites selected as the most promising sites for the construction of the recharge basins. The lithological character of the river fill, as found in the pits and demonstrated in analysis grading curves was gravel with some small to medium-size boulders, sand and a minor amount of silt. The results are shown in Figure 2.3. The pit excavations had a limited depth of about 2.5 m and as such captured only the upper layering which was not representative of the full section of the alluvium. The borehole drillings, however, extended through the alluvium and into the bedrock to an average depth of 50m, and provide good detailed lithological data for the river's entire section. A characteristic sample of borehole lithology is illustrated in Figure 2.4 and the locations of the boreholes are shown in Figure 2.5. Although gravels are abundant, fine sediments usually fill the interstices and there are alternating horizontal silty bands with interbedded fine-grained deposits. Clay lenses are encountered throughout the aquifer to varying degrees. The presence of these lenses may be attributed to the erosion of the mélange and clay of the Mamonia Formations.

The upper and middle sections of the Ezousas river length consist of shallow deposits. The most important section, however, is the lower part, which expands along the coastal plain and contained the aquifer under study. The alluvium aquifer of the lower section is 7 km long, and extends laterally about 150-230 m, expanding to 800 m in width at its delta. The maximum thickness of the aquifer is estimated to be 25 - 40 m.

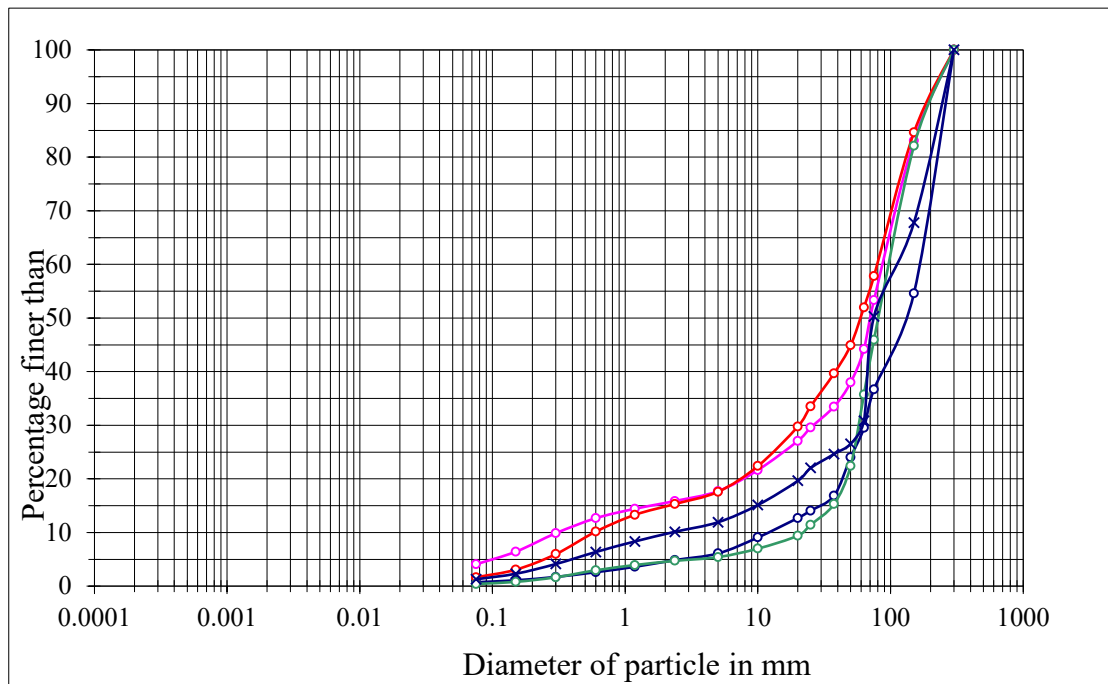


Figure 2.3 Sieve analysis of near-surface river gravels obtained from five trial pits within the infiltration basins.

2.3.3 Bedrock Geology

The bedrock is overlain by fluvial and sedimentary deposits and only occasionally is there an outcrop into the study area. Its geology and topography have been interpreted based on the borehole logs, electrical resistivity soundings (Krambis 1993) and geological maps. Additional borehole logs and lithology, obtained by percussive and auger drillings were available from the Geological Survey Department, Cyprus (GSD, 2005). The interpretation and analysis of these data were used to establish the lateral and longitudinal extent of the gravel aquifer and define the river's bedrock. It was found that alternating marls and marly chinks of the Pakhna Formation characterize most of the downstream section of the river bedrock but further upstream, there is a non-uniform overlay of clay matrix of the Mamonia Group above the Pakhna and Lefkara Formations. Therefore, for the purposes of this study, the bedrock can be treated as the hydraulic base of the clastic aquifer.

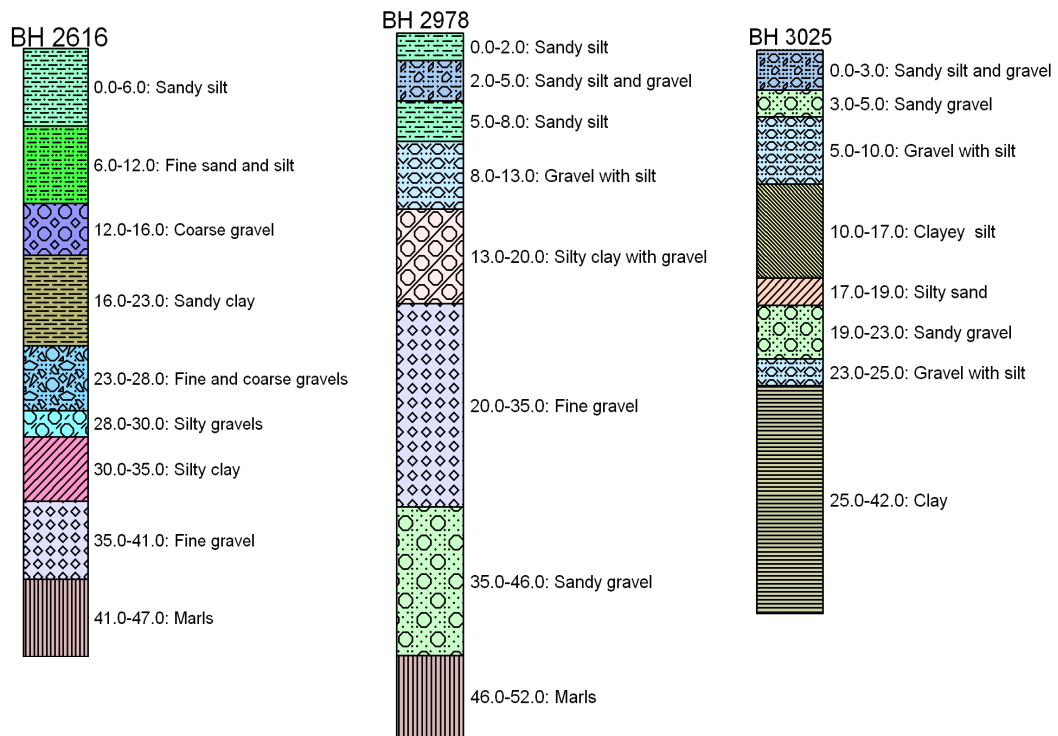


Figure 2.4 Typical borehole lithological profiles of the alluvial aquifer

2.3.4 Aquifer Topography

The alluvial aquifer covers an area of 2.6 km²; with a length of 7 km and variable width between 250 - 300 m. This width expands up to 1.2 km along the river's reach. The depth of the alluvial ranges between 25 and 40 m. The aquifer slopes steadily towards the sea with a gradient of 0.8-1.4%.

The borehole logs indicated that the bedrock lies almost parallel to the river-bed sloping steadily towards the sea with a gradient of 0.8-1.1%. The level ranges from +70m to -40m above mean sea level (a.m.s.l.) and intersects the sea level at 3.2 km inland. Consequently there was the possibility of seawater intrusion which would affect the quality of the groundwater.

2.3.5 Seawater Intrusion

The most important factors that control the seawater intrusion are aquifer type (unconfined, confined, and leaky), hydraulic conductivity, height of groundwater relative to the sea level, distance from the shore and thickness of the aquifer. Drillings along the shoreline were used to indicate that the aquifer bedrock lies, on average, 40m below the mean sea level and that an area of 2.4 km² is prone to potential contamination by seawater. It was concluded therefore recharge-abstraction could be used, to maintain a dynamic balance between seawater and freshwater heads, controlled by observations of the piezometric elevations. The abstraction was to be measured by water meters and controlled by valves installed on the pumping systems. Conductivity and temperature measurements were carried out at 1 m depth intervals within monitoring wells W3829, W2979, W3921 located along the river aquifer close to the sea, as shown in Figure 2.6. The conductivity values measured in all boreholes along the coastal plain ranged between 1200 and 1500 $\mu\text{S cm}^{-1}$, indicating that there was no contamination from the seawater intrusion.

Monitoring the seawater-freshwater interface should therefore ensure that the groundwater basin is protected from seawater intrusion whilst continuing to provide a reliable source of irrigation water for crops in the Paphos region. The groundwater movement was recorded on a water table contour map based on the sea-level datum as shown in Figure 2.5.

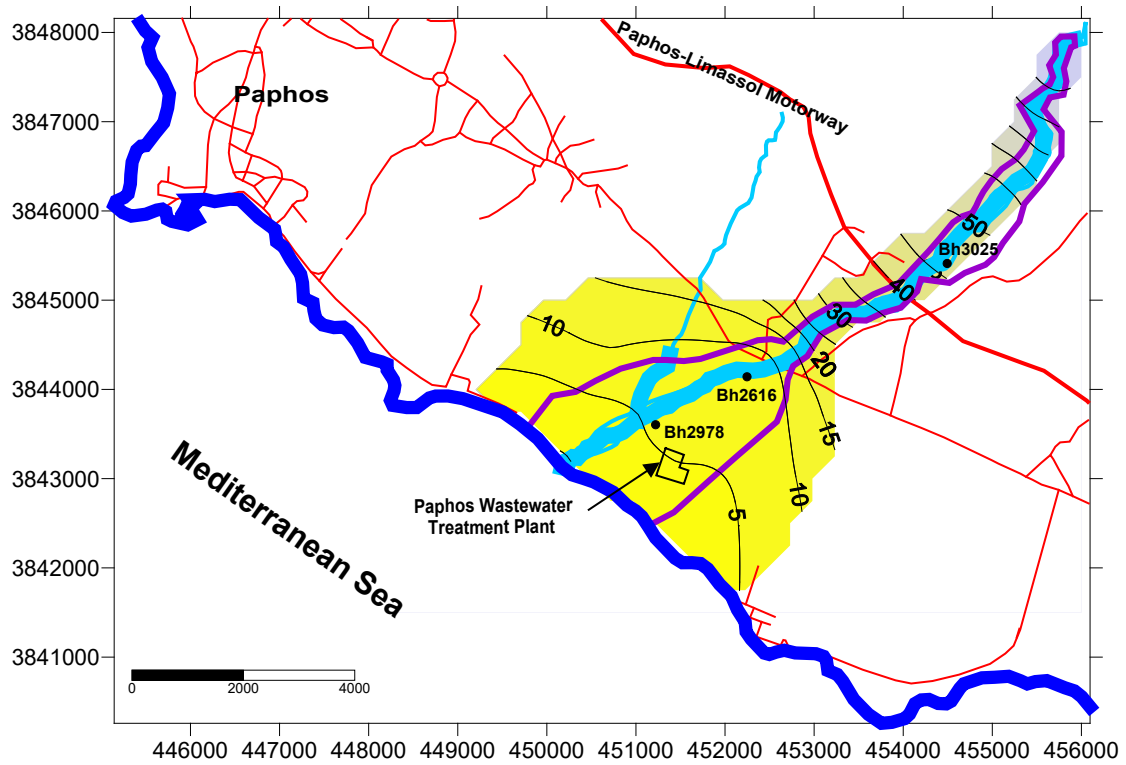


Figure 2.5 Contour map of Ezousas river alluvium aquifer water table, June 2006.

2.3.6 Hydrogeological Investigations

For the most part, the valley fill consisted of interfingering and intermingling layers of sand and gravels of moderate to high permeability with occasional lenses of silty clay and silt. Thus the geology and consolidation indicate an aquifer capable of holding significant amounts of water, although the lenses could significantly impede horizontal flow.

Conventional pumping tests with observation boreholes, single-borehole tests and constant-head permeability tests were conducted throughout the area. New production wells and monitoring piezometers were drilled to supplement data from existing wells. This was done in order to verify the hydraulic conductivity, hydraulic gradient, and flow velocity.

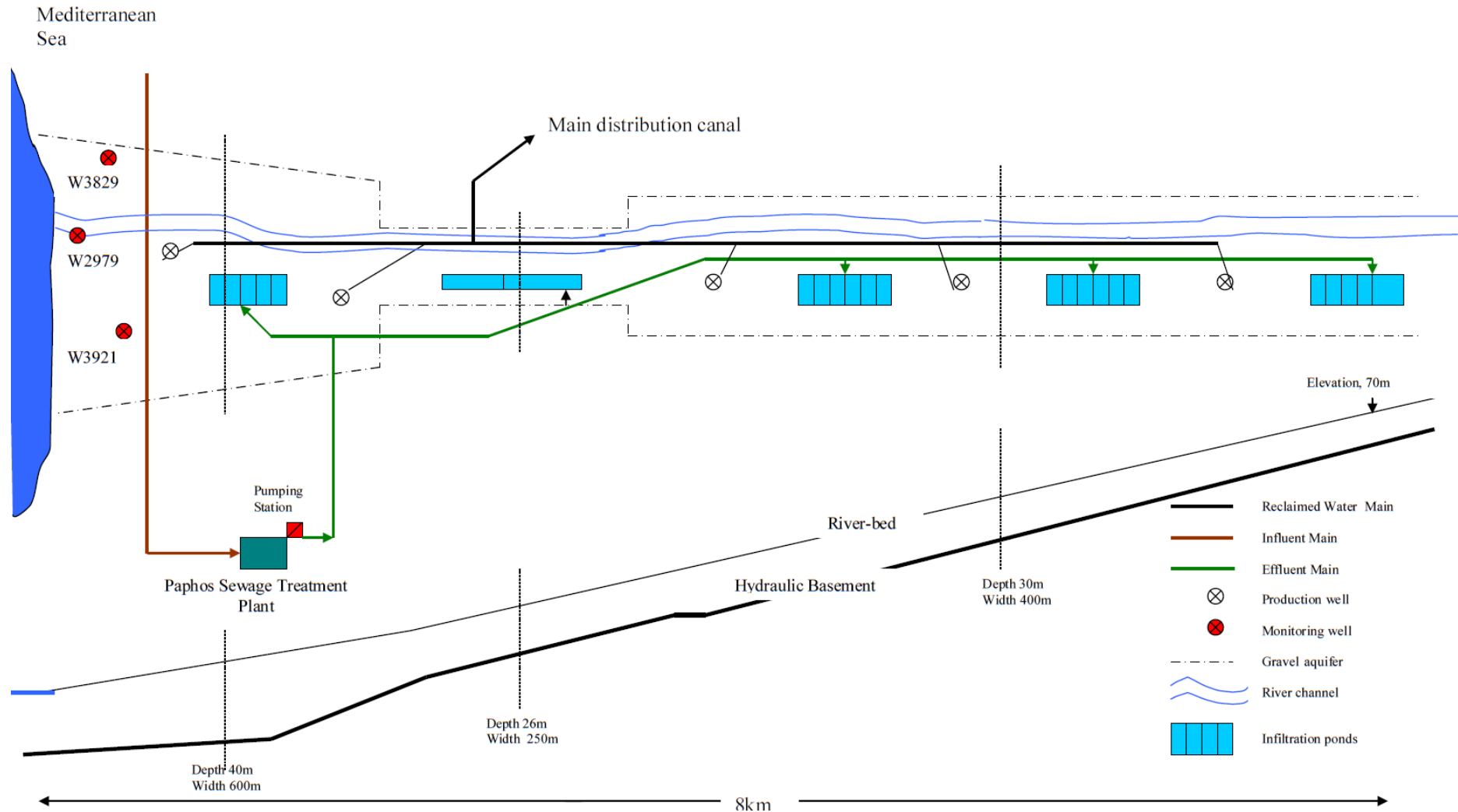


Figure 2.6 Schematic diagram of the Ezousas Recharge Project

Three types of tests were conducted at the project site: a step drawdown test, a constant discharge test, and a recovery test. Drawdown and recovery v. time curves were matched against standard type-curves to obtain estimates of transmissivity (T) and storage (S). The Theis, Cooper-Jacob, and Boulton methods were used to analyse the drawdown test data, the recovery test was analysed using the Theis method. The recovery method gave the best fit to the drawdown v. time-curves and it was found that the permeability ranged from 40 to 160 m/d and the specific yield ranged from 4 to 13% for the eight wells tested. The four constant-head permeability tests provided permeabilities mostly in the range 4 to 60 m/d. The values found for the hydraulic conductivities (K) were, as expected, decreasing towards the sea thus reflecting the flow depositional environment of the river (Figure 2.7). Background knowledge of these deposits in the aquifer material, grain size, and the pumping test data analysis, allowed corroboration of the aquifer's hydraulic properties. These characteristics are presented in Table 2.2 and are the average values obtained from the pumping and constant-head permeability test data.

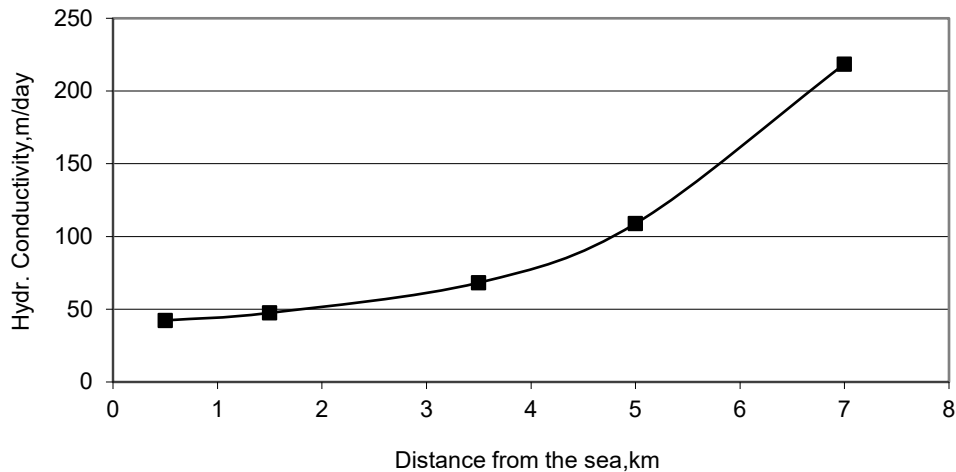


Figure 2.7 Hydraulic Conductivity estimates along the Ezousas river alluvial aquifer.

Table 2.2 Aquifer hydraulic parameters

Transmissivity	Hydraulic conductivity	Specific yield	Porosity
T (m ² /day)	K (m/day)	S _y (%)	n (%)
2400	90	11	20

Table 2.3. Aquifer characteristics

Length	Alluvium area extent	Thickness	Volume of water per meter drop	Effective storage Capacity
(km)	(km ²)	(m)	(m ³)	(Mm ³)
7.8	3.1	25	170000	4.2

2.3.7 Storage Capacity Estimates

Analysis of these geological and stratigraphic features led to the conclusion that the Ezousas river aquifer is structurally and hydrologically a closed, unconfined trough-like basin. It is composed of a single stratification, containing a sedimentary sequence with chalk, marly chalk, and clay bedrock defining its sides. Like all the rivers in Cyprus, the Ezousas has a long dry season. During the rainy season, generally lasting from November to April, the water flow in the river infiltrates through the river bed, filling the underground aquifer. Infiltration is generally greater than the outflow towards the sea, so the water table rises in all areas until the aquifer is full and saturation occurs (zero infiltration) usually at the end of the rainy season, (Figure 2.8).

The study of these piezometric level fluctuations, has allowed estimates to be made of the potential underground reservoir capacity. The assigned geometry of the aquifer, average hydraulic conductivity and an assumed fully saturated condition in May were used in the calculations. The cross-sections and depth of the alluvium was taken from the borehole logs and drillings from the GSD and the WDD, thus the aquifer geometry was defined with some confidence. Darcy's equation, $Q = A.K$ (where K is the hydraulic gradient = dh/dl and A is the vertical cross-section area through which flow occurs), was used with an application of a water balance (i.e. $Q_{in} - Q_{out} = A_{pl}.S_y \Delta h$, where the A_{pl} is the aquifer area in plan, S_y is the specific yield, and Δh is the change in hydraulic head). In this way the effective storage capacity of the aquifer was estimated to be 4.2 M m^3 . The aquifer hydrological characteristics are given in Table 2.2.

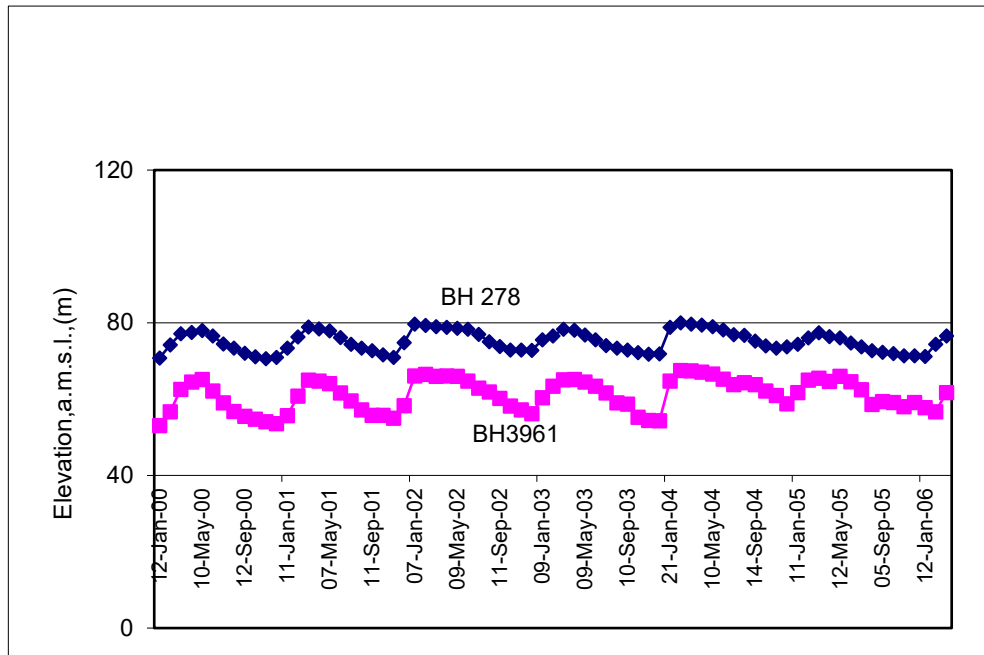


Figure 2.8 Hydrographs from wells upstream of the Ezousas Recharge Project

2.4 The Design and Operation of the Recharge Basin System

The use of abstracted water for drinking purposes requires a large environmental buffer to provide significant lag time between adding the recycled water and its entry into the domestic supply. The Californian regulations are the most widely used (Asano, et al., 2008) and a 6-12 months retention time as an environmental buffer is recommended before reuse as a potable source. The guide also notes the extraction should be no closer than 150m from the point of recharge (NRC, 1998; USEPA, 2004). Therefore the Ezousas aquifer characteristics, in particular its small size and depth, but also the geological heterogeneity including gypsum which dissolves to give a high sulphate content make it unsuitable as a potable source. It was concluded that the recharge system was suitable solely for crop irrigation use.

In general, there are two methods of recharge; the first being through surface percolation (spreading basins) and the second from recharge directly through wells (direct injection). The second has a number of drawbacks which are related to the heterogeneity of the aquifer material. There is also a danger of clogging and contamination of the whole aquifer if there is an undetected accidental spillage into the sewerage system. Thus it was concluded that surface percolation was the most appropriate recharge method. The WDD already had experience of designing infiltration basins to recharge aquifers with raw water from impounding reservoirs (Xeropotamos and Yermasoyia aquifer Iacovides, 1997). Release water has also been used to provide seasonal flows in the Kourris River to recharge and store water the Akrotiri aquifer (WDD, 2005). Recharge with recycled water has never been used in Cyprus before (Nikolaides and Georgiou 1999; SOGESID 2005), and although the process is well documented from applications in other parts of the world, in particular in the USA (Weeks, 2002), it was thought research into and on the local impacts would provide new knowledge to ensure the process was a success.

A pilot demonstration of the design of the proposed infiltration basins was conducted within the alluvium of the Ezousas river bed. Eight trial locations were used with small excavation pits of 2x3x2m. Infiltration rates were found to range between 70 and 120

mm/h. Based on this demonstration the full-scale recharge network consisted of five shallow infiltration basins arranged in series within an area extending 8 km inland from the seashore. Each infiltration basin contained two, four or six recharge ponds, with each pond having a surface area of approximately 2000 m² and a depth of 1.5m. The ponds were constructed with a 1m overflow weir to avoid over topping and embankment erosion. The recharge scheme is outlined schematically in Figures 2.6 and a typical section of a recharge pond is shown in Figure 2.9.

In operation the approach was to maintain an unsaturated zone below the pond so as to avoid clogging the soil matrix and maximize the amount and quality of the water recharged. Soil saturation was measured by adjacent piezometric heads and used to control the wet-dry fill cycle times. This varied from pond to pond but was normally between 5 and 7 days. The ponds are filled from a pressurized 500mm ductile iron main.

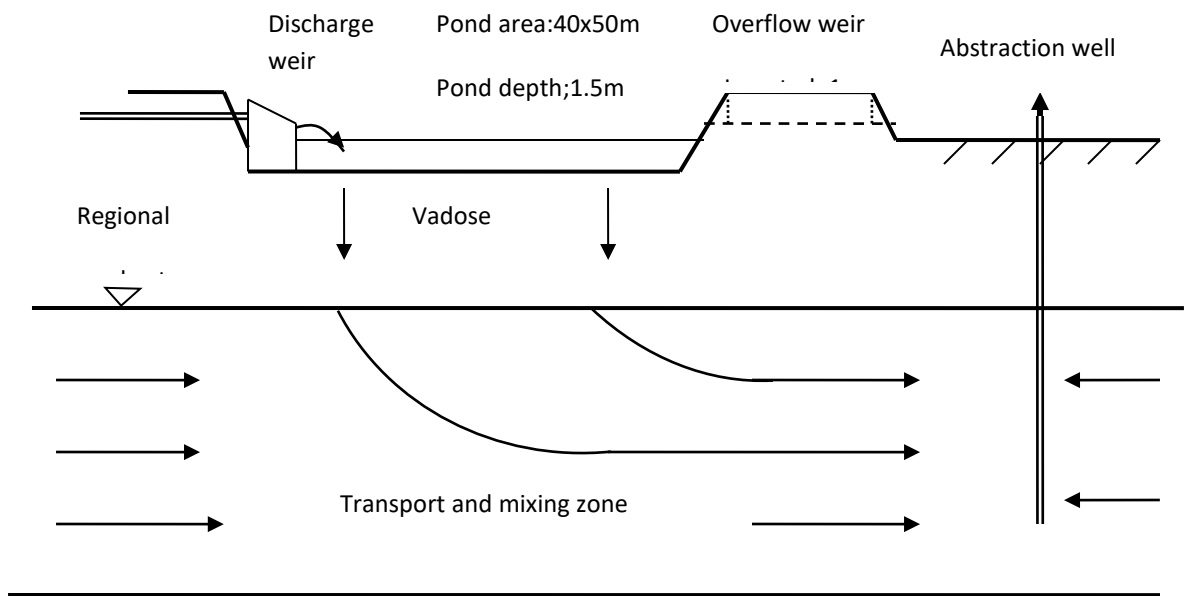


Figure 2.9 Schematic diagram of an example recharge pond

Groundwater abstraction is carried out by pumping from six wells that are located between the infiltration basins. Before going into normal operation, testing was used to corroborate the pilot trial and ensure the integrity of the system. The pumps can be adjusted to changes in demand, within a manometric head of 4 to 78 m above mean sea level (a.m.s.l), thus creating a water storage system. Since the start of the operation in 2004, 32.4 Mm³ of recycled water has been recharged and 34.5Mm³ abstracted; the difference due to the natural recharge into the aquifer, (see Figure 2.10).

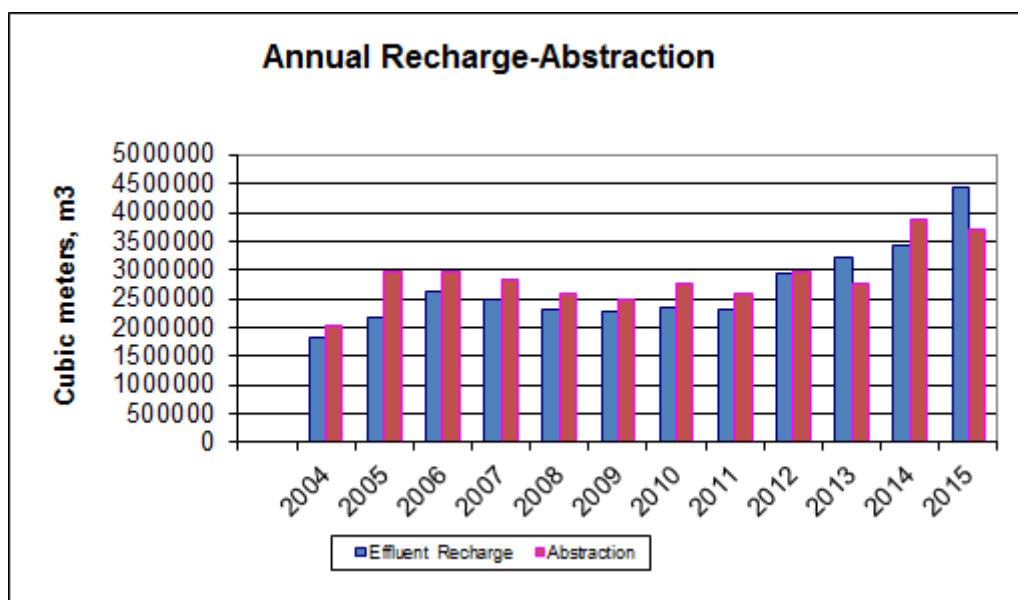


Figure 2.10 Abstraction-Treated effluent recharge.

2.5 Aquifer Water Quality

Chemical analysis of the groundwater quality was used to ensure there were no human or crop health risks. The results were also used to identify if there were any negative impacts on the natural environment. For example, excess concentrations of nitrogen and phosphorus leading to an increase in eutrophication in the near-shore environment (Oude Essink, 2001). It was intended that the recharging of treated effluent near the coast would lead to the formation of a hydraulic barrier to retard both the discharge of fresh groundwater and the ingress of coastal saline water.

The natural Ezousas aquifer is recharged by seasonal surface flows infiltrating down into the aquifer and underground from upstream of the dam. As the surface water percolates through the alluvial material and underlying formations of lavas, marls, chinks, and gypsum it acquires dissolved solids, salinity and a high sulphate content of (around 600 mg/l). It was considered that the mixing of the treated sewage effluent with the native groundwater could give cross chemical reactions. For example, precipitation or increased solubilization of the surrounding aquifer material would increase the concentration of dissolved and suspended solids in the extracted water. The formation of precipitates could also clog the soil-aquifer system limiting flow rates and groundwater capacity. On the other hand, dissolution of soil and aquifer particles could increase local permeability and volume.

Standard analytical methods were used which included monthly: electrical conductivity (Ec), pH, boron and P-total in the recycled water and every 3 months for indicator microbes, heavy metals and persistent organic compounds. Samples were obtained from eight of the infiltration basins, the six abstraction boreholes and an observation borehole upstream of the recharge site, for the native groundwater.

Two of the most important general parameters affecting irrigation water quality are the total dissolved solids (TDS) and the sodium adsorption ratio (SAR). The TDS is also commonly used as a surrogate for the salinity of the water and was more easily measured using the electrical conductivity (EC) method. The SAR of a water sample reflects the proportion of monovalent sodium ions relative to divalent calcium and magnesium ions, $SAR = [C_{Na}] \div [(C_{Ca} + C_{Mg})/2]^{0.5}$. The suitability of irrigation water can be judged by the ratio of EC and SAR based on the system developed for U.S. agriculture, (Todd 1980; Ayers and Westcot 1989). The SAR value of the treated effluent was 3.5, double the 1.8 for the native groundwater and resulted in a mixed water SAR value of 2 for the abstracted water, approximately the mean of the two values. This was an overall improvement of the relative concentrations of univalent and divalent cations according to the USDA

classification. Therefore it was concluded that the abstracted water was suitable for irrigation for all the usual crops that are traditionally grown in the region.

There could be a wide variety of potentially hazardous chemicals and compounds in treated sewage effluent to accumulate and contaminate the aquifer. The Water Framework Directive (2000/60/EC) requires Member States to achieve good chemical status for groundwater and good ecological status in surface waters. Cyprus has set criteria for the protection of its water bodies and for surface recharge through impounding reservoirs and lakes. Limits applicable to heavy metals have been specified (RAA 269/2005, ANON, 2005) which are at or around their detection limits. The concentrations of metals, average results are shown in Table 2.4, are at these low levels and it was concluded do not pose a risk to plants and animals. The Water Framework Directive also specifies a sustainable approach towards river basin management and the restoration of significant water pollution. The concentration of nutrients, especially nitrate and phosphorus are a priority responsible for 50% of WFD water quality failures in Europe (P-total 5 mg/l and 9 mg/l, nitrate in the sewage effluent). Mixing of the effluent with the native water in the aquifer reduced the concentrations to below the WFD recommendations for adverse effect in natural waters. The seawater analysis showed nitrate and phosphorus (P-total) concentrations of 3 mg/L and 0.003 mg/l, respectively.

The international microbial criteria for unrestricted water use quality are based on the absence of indicator organisms including coliforms, *Escherichia coli*, and bacteriophage (USEPA, 2004). The Cyprus microbial criteria specify 15 *Escherichia coli* per 100 ml as the maximum allowed for domestic treated effluent used for unrestricted irrigation (excluding vegetables eaten raw, which require no indicator organisms to be detected RAA269/2005, ANON, 2005). Tests conducted on abstracted groundwater found that there was no *E. coli* in most of the samples analysed. The quality analysis of the native groundwater, the treated wastewater effluent and the abstracted water are summarized and shown in Table 2.4.

Table 2.4 Water quality analysis

	Native Groundwater (n=9)		Tertiary treated effluent (n=13)		Abstracted groundwater (n=32)	
	Average	STDEV	Average	STDEV	Average	STDEV
Biological parameters						
BOD ₅ (mg/l)	3	1.6	6	3.4	3	1.1
COD (mg/l)	6	0.8	17	5.9	6	1.4
Escherichia coli per 100ml	0-2		0-10		0-2	
Toxicity %						
Microtox EC20	TU<1		TU<1		TU<1	
Daphnia EC50	TU<1		TU<1		TU<1	
Algae Eb C50	TU<1		TU<1		TU<1	
Ionics, (mg/l)						
Conductivity (microS/cm)	1730	94.6	1490	37.7	1480	68.6
pH	7.9	0.5	7.5	0.1	7.6	0.3
Total hardness as CaCO ₃	783	147.4	318	32.5	567	62.5
Cl ⁻	118	9.3	233	25.1	149	15.8
SO ₄ ⁼	590	69.8	139	19.1	330	48.1
CO ₃ ⁼	<2		<2		<2	
HCO ₃ ⁻	313	20.2	340	49.1	321	47.6
NO ₃ ⁻	2	1.0	9	3.3	7	5.1
P-Total	0.2	0.3	5	2.4	0.1	0.1
Na ⁺	114	15.1	159	18.5	113	16.0
K ⁺	6	0.6	25	4.0	6	0.5
Ca ⁺⁺	227	18.8	60	5.6	165	19.9
Mg ⁺⁺	52	11.0	61	11.0	37	7.6
Boron,B	0.4	0.1	0.3	0.1	0.2	0.1
Micro-tracers,(µg/l)						
Cadmium, Cd	0.2		<0.02		0.2	
Chromium,Cr	30	0.7	<0.11		13	27.7
Copper, Cu	1	0.6	<0.1		8	114.2
Zinc, Zn	123	86.4	<0.04		70	74.7
Pb	10	0.8	<0.15		3	8.7
Mercury,Hg	0,2		<DL		0.2	
Insecticides Residuals,(µg/l)						
Organochlorines	0.01	0.1	<DL		0.01	
Micro-organic pollutants	<8		<DL		<8	
SAR	1.8		3.5		2	

* Abstracted GW;These are the average values of 8 sampling sources taken on 16/1/2006, 27/4/2006, 3/6/2006,21/9/2006

**TU, Toxicity Unit; TU<1, no toxicity detected

***Micro-organics-43 base/neutral compounds; detection limit 8 µg/l

****DL,Detected Limit

2.6 Conclusions

A hydrogeological investigation was conducted to define the boundaries and hydraulic characteristics of the Ezousas river aquifer in SW Cyprus for recharge with treated sewage effluent. The storage capacity of the aquifer was calculated to be able to accommodate the total annual output of wastewater from the local Paphos Municipal Sewage Treatment Plant (5 Mm³). It was concluded that if the cycle of abstraction and recharge was continuous and steady then this would prevent either seawater encroachment or loss of potentially recyclable water by seepage to the sea. The monitoring programme using piezometers and flow meters was successfully used to measure the fluctuations in position of the seawater- freshwater interface and avoid abstraction of high salinity water for irrigation. The sampling and chemical analysis demonstrated an interaction between the recycled effluent and the natural geological environment. The recharge scheme reduced the naturally high TDS and sulphate in the aquifer which resulted from the solubility of the gypsum and carbonate rocks underlying the river basin. The indicator microbe, toxicity, salinity and heavy metals analysis demonstrated that the mixed abstracted water was suitable for all crops that were traditionally planted within the Paphos irrigation area.

This study has shown that the Ezousas gravel aquifer was suitable for the storage and recycling of the treated sewage effluent. The research has provided useful data to support a practice which had become common in other parts of the world. Aquifer recharge with treated effluent therefore offers an attractive option for improving the reliability and availability, all year round, of an existing groundwater supply. The other benefits included avoiding the expansion of environmentally damaging and costly infrastructure and the permanent contamination of the aquifer by sea water ingress.

CHAPTER 3

PAPHOS WASTE WATER TREATMENT PLANT (WWTP) - GENERAL DESCRIPTION OF PROCESS

CHAPTER SUMMARY

The Paphos wastewater treatment plant (PWWTP) was commissioned in 2003, with a design flow of 8,000 m³/d which was expected to double by 2020. It became apparent, however, that the capacity of the treatment plant had to be increased to cope with more tourism than was anticipated and this was carried out in 2010, to accommodate a flow of 19,500 m³/d.

The plant was designed for domestic wastewater via the sewerage network which included the airport and associated military base and also a substantial input of septic tank wastewater tankered to site.

Treatment consists of the typical process flow train used in Europe. The preliminary treatment is raked, bar screens and grit chambers, followed by primary settlement in two sedimentation basins. Secondary treatment uses activated sludge set up with an anoxic stage, for denitrification and an anaerobic stage with recycle to promote biological phosphorus removal. Final settlement uses four tanks followed by tertiary treatment with sand filters and a final chlorination tank. The design consistently meets the requirements of the European Urban Wastewater Treatment and Bathing Water Directives as flow and pollutant load varies with season and storms.

All the current treated effluent, about 5 Mm³ per annum of tertiary treated wastewater is used for the recharge of the Ezousas alluvial aquifer.

3.1 Introduction

Sewerage treatment for Paphos is managed by a Public Interest Authority, established by a decree from the Council of Ministers. This was constituted as the Sewage Board of Paphos in 1993. The Board's objective was the construction, operation and maintenance of the sanitary sewerage, drainage and sewage treatment system for the Greater Paphos area. The terms of reference included the protection of public health, compliance with EU and international regulations and environmental protection in a cost effective and economic way.

The Paphos wastewater treatment plant (PWWTP) treats domestic, including the seasonal fluctuations from tourist flows, and industrial effluents from the urban and suburban region. The treatment plant is located 10km east of Paphos, at a village called Akhelia and has been in operation since 2003 with the next planned rebuild or extension in 2020.

The designed flows were for a PE of 55,000 expected to be reached in 2010 with a peak flow of 8,000 m³/d., but increases in the population and additional connections, have occurred more rapidly than anticipated. It therefore became apparent that the PWWTP would reach maximum capacity before 2010. As a result the operating capacity which was supposed to be reached in 2020 was reached in 2005. Part of the increase has been due to a greater number tourist arrivals. Extensions were completed in 2010 to accommodate a maximum flow of 19500 m³ /d, with a total BOD₅ load of 9750 kg/d and a further review to be carried out in 2020.

The plant was designed to treat domestic wastewater via the sewerage network and septic tank wastewater tinkered to site. Treatment consists of the typical process flow train used in Europe, shown in Figure 3.1. The preliminary treatment is bar, rack, screens and grit chambers. This is followed by primary settlement in two sedimentation basins. Secondary treatment uses activated sludge, set up with an anoxic stage, for denitrification and an anaerobic stage with recycle to promote biological phosphorus removal. Final

settlement uses four tanks followed by tertiary treatment with sand filters and a final chlorination tank. A diagram showing the treatment plant facilities is shown in Figure 3.1. Figure 3.2 shows the annual total volumes of treated sewage effluent produced, all of which is used for the recharge of the Ezousas alluvial aquifer.

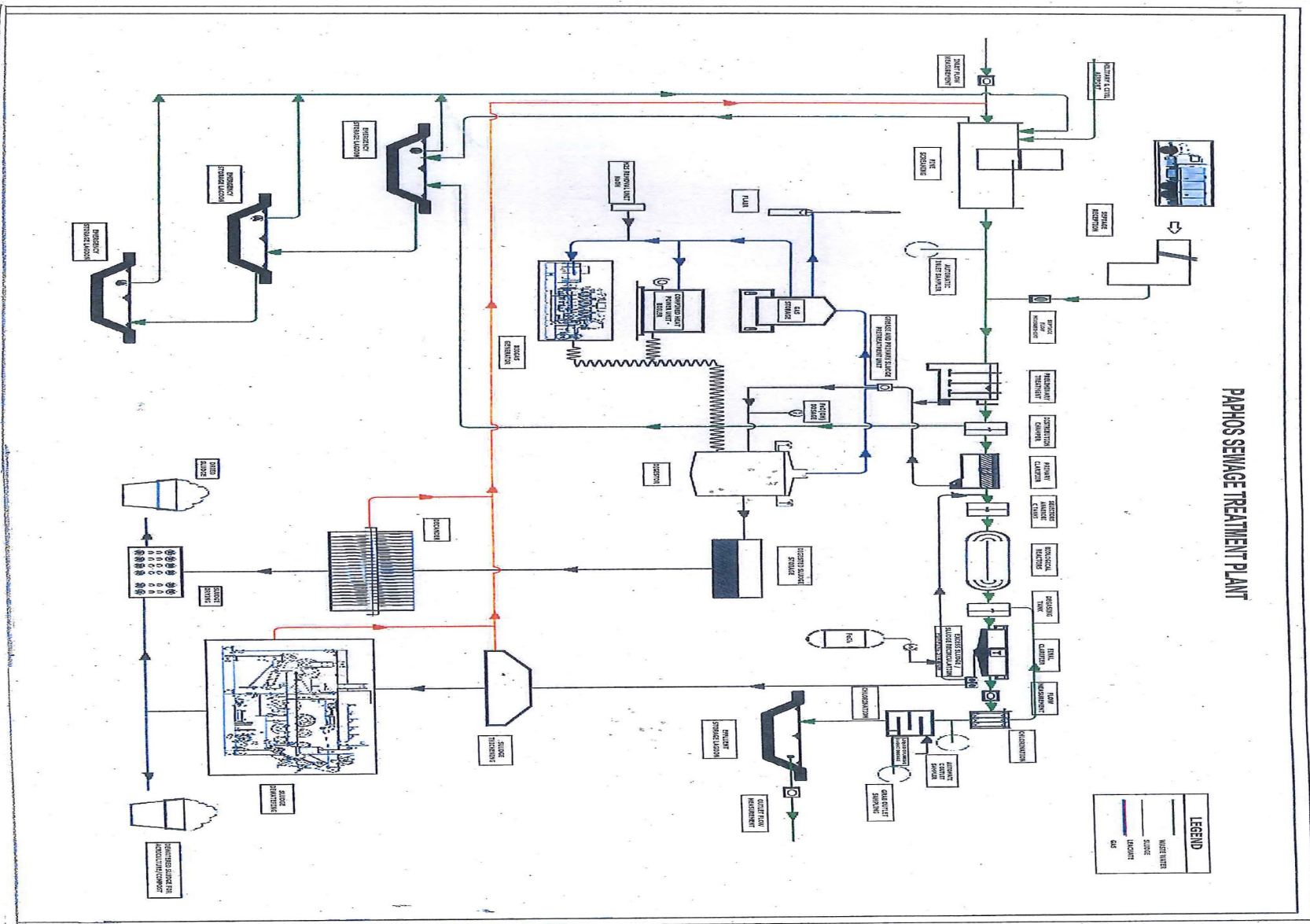


Figure 3.1 Paphos Sewage Treatment Plant

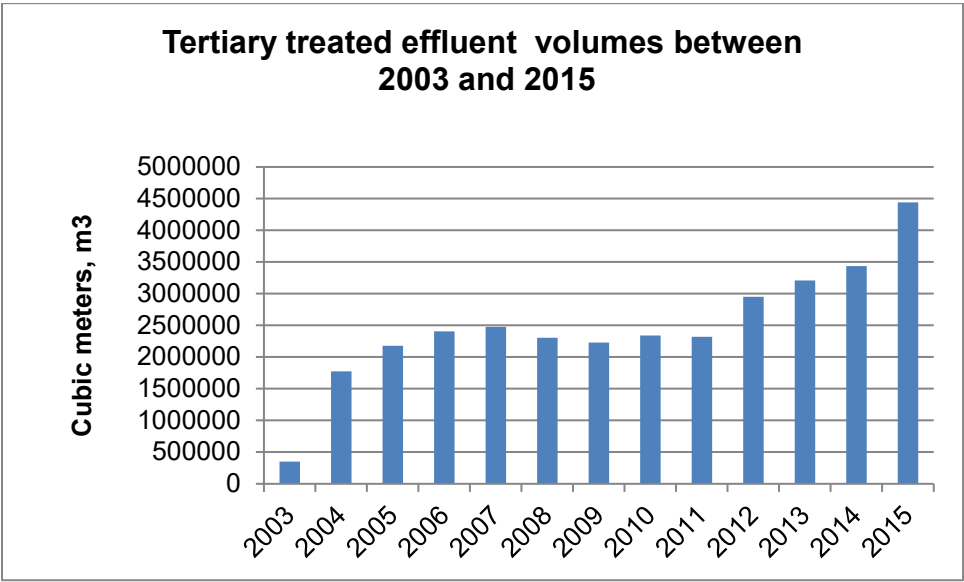


Figure 3.2 Sewage treated effluent produced on an annual basis

3.2 Background

The plant was designed to meet the Urban Waste Water Treatment Directive (UWWTD)91/271/EEC which covers urban wastewater collection and treatment both domestic and industrial and its discharge, according to the natural characteristics of the receiving water. The aim of the UWWTD was to protect and retain environmental quality against the adverse effects of urban wastewaters.

The UWWTD obliges Member States, to install sewerage networks and wastewater treatment plants for communities and municipalities (defined as agglomerations in the Directive) with population equivalents (p.e.) (permanent, seasonal population and tourism) greater than 2,000.

This Directive sets minimum sewage treatment standards to be achieved and includes provision to require advanced wastewater treatment for the removal of nitrogen and phosphorus if the receiving water is in a sensitive area. Sensitive areas include areas susceptible to eutrophication, surface waters intended for the abstraction of drinking water and other waters that require a higher standard of treatment to satisfy the requirements of other Directives. The UWWTD Directive encourages the use of sewage sludge in article 14: with the phrase "Sludge arising from waste water treatment should be re-used whenever appropriate.

As noted, the majority of households in Cyprus are connected to sewerage systems and full implementation of the requirements of the UWWTD was achieved at the end of 2012. The Cyprus Water Development Department (WDD) based on the Integrated Water Management Law, N. 79(I)/2010 has the responsibility of managing the return of treated effluent produced by the wastewater treatment plants (WWTPs) to the environment. This is currently around 55 Mm³/year of tertiary treated effluent (see Section 2.1). The sizes and loads from the PWWTPs of the major towns of the island are cited in Table 3.1.

Table 3.1 A list of Wastewater Treatment Plants in Cyprus and their capacities

Plant	Owner of the Plant	Max. Capacity(m³/day)
Anthoupolis	Nicosia Sewerage Board	13000
Vathia Gonia	Nicosia Sewerage Board	22000
Vathia Gonia	Water Development Department	2.100
Mia Milia	United Nations Development Program, Cyprus	30000
Limassol (Moni)	Sewerage Board of Limassol Amathus	40000
Larnaca	Sewerage Board of Larnaca	18000
Paphos	Sewerage Board of Paphos	19000
Paralimni-Ayia Napa	Sewerage Board of Paralimni- Ayia Napa	21000
Total Capacity 165.600m³/day		

3.3 The Treatment Process

3.3.1 Preliminary Treatment

Preliminary treatment comprises of an inlet chamber, mechanical screening, flow measurement, a septage reception and pretreatment unit, and grease and grit removal prior to- distribution to primary settlement.

The facilities of the septage or tankered in waste unit include a reception area, a storage tank with the possibility for chemical pre-treatment and a pumping station to allow a controlled return to the main flow. The septage pre-treatment unit is located inside a building to avoid odour.

Grit and grease removal is via two parallel, aerated, controlled velocity chambers with their associated mechanical equipment. These grit removal chambers are each 20m long, 5.25m wide and 4.9m deep, and equipped with stainless steel grit and grease removal scrapers. The aeration is from coarse bubble diffusers fed by positive displacement blowers. The grit chambers are underground and housed in a building to avoid environmental impact.

The separated grit passes to a neighbouring building where it is washed prior to storage in a skip for reuse as road fill. Collected grease is stored in two grease pits and intermittently pumped to be mixed with the primary sludge in a pre-treatment sludge storage tank.

A biofilter unit is used for controlling the odour from the air extracted from these preliminary treatment buildings. The biofilter is packed with high density peat granules inoculated with specific bacterial cultures, they are kept irrigated and include under-floor drainage.

3.3.2 Primary Treatment

The flow is subdivided to four primary settlement tanks via a flow distribution chamber. The primary clarifiers include tube settlers (added during the most recent extension to the works) and achieve a 70% reduction in suspended solids and a 40% removal of organic matter in terms of TSS and COD is achieved. The sludge collected from the primary clarifiers is transferred with mono pumps to the primary sludge pre-treatment unit.

3.3.3 Secondary Treatment

The flow of settled sewage is then divided equally between three activated sludge plants. The newer plant (2010), treating 2/3 of the flow, consists of two, parallel, extended aeration, carrousel type, activated sludge. The tanks are designed to induce a circular flow pattern through an anaerobic selector zone, an anoxic/aerobic zone and then a degasification tank. The tanks are 6000 m³ in volume each. Each stream is served by a

separate final clarifier with sludge recirculation pumps (one for each treatment line) and a diverter to the sludge treatment plant for surplus activated sludge. The aeration system for the oxidation ditches consists of fine bubble diffusers and multistage centrifugal blowers with maximum capacity 5.400Nm³/hr each.

The older plant (2003) is a plug flow, rectangular, concrete tank, also divided into two parallel treatment lines. These consist of an initial anaerobic Bio-P zone, followed by a de-nitrification zone, with recycled nitrified mixed liquor, then a combination zone for nitrification/de-nitrification and a final nitrification zone. Each stream is served by a separate clarifier.

There is provision for dosing iron salts (ferric chloride) with feed-back control, if necessary, to achieve the 5mg/l phosphorus concentration required by the UWWTD for coastal discharges.

The secondary treatment plant meets the design criteria anticipated to meet the 95% compliance with the UWWTD. The Biochemical Oxygen Demand (BOD₅) is between 8 to 12 mg/l, COD is 25 to 30 mg/l and Total Suspended Solids (TSS) are 5 to 8 mg/l.

3.3.4 Tertiary Treatment

To meet the standards for unrestricted irrigation, secondary treatment requires supplemental treatment (filtration and/or disinfection). These standards are applicable for agricultural and landscape irrigation, recreational and environmental uses as well as for process water in some industrial applications.

At Paphos secondary effluent is divided between eight concrete built, rapid gravity, sand filters. A further 30 % removal of total suspended solids is achieved and the tertiary effluent has a TSS concentration of 3 to 6 mg/L. and a BOD₅ between 5 to 10 mg/L. The self-contained plant includes automatic back-washing, on rotation and the associated pumps, air compressors, wash water and dirty water storage and controls.

Filtered wastewater is transferred to a chlorination tank with sodium hypochlorite solution (NaOCl) disinfection.

On-line measurement of chlorine residuals in the wastewater is based on the standard commercial units for potable water applications. However, these units are not designed for residual chlorine measurement in wastewater although manufacturers promote this use. The experience at Paphos has indicated care is required in maintaining the on-line equipment. Low chlorine limits are required for effluent discharges because of the residual organic matter which necessitates reliable precise measurement for the control of the chemical dose. The higher residual organic matter also required more frequent cleaning of sample lines, continuous cleaning and flushing was found necessary to achieve accurate results. A long-term pilot study of equipment would now be recommended to perfect the standard system.

3.3.5 Sludge Treatment

Sludge treatment includes separate treatment for the primary and surplus activated sludge (SAS) streams. SAS, together with the settled tertiary sludge from the dirty wash water, is thickened and dewatered by two belt-filter presses.

Primary sludge is anaerobically digested for stabilization followed by dewatering prior to drying. Primary sludge is pre-screened using a stainless steel 6mm aperture size to remove fibrous material. The screenings are compacted before incineration with local domestic refuse. Screened primary sludge is equalized and homogenized in a consolidation tank, equipped with a stainless steel, slow rotating, picket fence scraper. The sludge is then pumped to the digestion plant. Anaerobic digestion is mesophilic plant (approximately 35 degrees) using a digester with volume of 2.500m³. Digester mixing is mechanical using a two impeller agitator, but also includes some mixing by the pumped recirculating heating system using a hot water heat exchanger.

The digester achieves a minimum 45 % destruction of volatile solids and conversion to biogas. The biogas is collected from the dome of the digester and stored and balanced in a double membrane gas storage tank (volume 1.150m³). The biogas is used in a

combined heat and power engine with a generating capacity of 100kW which is fed into the electric grid for the plant. The heat is fed to the heat exchangers for the digester. Excess biogas is burnt in a biogas flare with capacity 200Nm³/h.

The digested sludge is stored and balanced in a sludge storage tank (volume 680m³, sufficient for three days storage) prior to thickening using a decanter centrifuge. The centrifuge has a capacity of 314 kgSS/hr and able to achieve dewatered sludge concentration of 28%.

The combined dewatered sludge (from centrifuges and presses) is dried by solar drying glass house. The total area of the solar drying plant is 3840m², in four individual drying chambers. The solar heat radiation in the greenhouse is circulated by fans and the sludge is also turned on a belt. The turning equipment ensures a uniform thickness and continuous renewal of the surface and breakage of the crust. The climate enables the drying plant to operate all year round using a Programmable Logical Controller to adjust the air circulation by controlled ventilation subject to the humidity to avoid water condensation. The sludge feeding to the plant and the drying process belt speed (from feed-back from the final dry solids content) are also controlled. These controls the solids content of the dried sludge to an average annual dry solids content of 70%.

3.4 Quality Characteristics and Control of the Treated Effluent

Table 3.2 shows the standards required by the Cyprus National Government (defined in the Water Pollution Control Laws(106(I)/2002 to 2009) and the Water Pollution Control Discharge of Urban Waste Water Regulations (No. 772/2003). The Ministry of the Environment regulates Wastewater Discharge through permits to the:

- Urban Sewerage Boards (USB)
- Water Development Department (WDD)

Samples are taken to ensure permit compliance and to control and adjust plant operation.

Table 3.2 Quality Characteristics and Frequency of Controls of the Treated Effluent for Urban Agglomerations- according to “Discharge Permit”

Parameter	Maximum Permitted Concentration	Frequency of Analysis by WDD	Frequency of Analysis by USB
BOD5 (mg/l)	10	4/year	1/15 days
COD (mg/l)	70	4/year	1/15 days
TSS (mg/l)	10	4/year	1/15 days
Conductivity (µS/cm)	2500	4/year	1/15 days
Total Nitrogen (mg/l)	15*	4/year	1/15 days
Total Phosphorus (mg/l)	10**	4/year	1/15 days
Chlorides (mg/l)	250	4/year	1/ month
Fat and oil (mg/l)	5	4/year	1/ month
Zinc (µg/l)	1000***	2/year	2/year
Copper (µg/l)	100	2/year	2/year
Lead (µg/l)	150	2/year	2/year
Cadmium (µg/l)	10	2/year	2/year
Mercury (µg/l)	5	2/year	2/year
Chromium (µg/l)	100	2/year	2/year
Nickel (µg/l)	200	2/year	2/year
Boron (µg/l)	1000	2/year	2/year
Arsenic (µg/l)	10	2/year	2/year
E. Coliforms	5/100 ml	4/year	1/15days
Eggs of intestinal worms	Nothing/l	4/year	4/year
Residual Chlorine (mg/l)	1****	4/year	1/15days
pH	6.5-8.5	4/year	1/15days
Toxicity		1/year	1/year

* For discharge in sensitive areas and into the sea maximum level 10 mg/l

** for discharge in sensitive areas and into the sea maximum level 2 mg/l

*** for discharge into the sea maximum level 100 µg/l

**** for sensitive areas and discharge into the sea 0.5 mg/l

3.5 Sampling Procedure

3.5.1 Influent

A refrigerated composite sampler (ISCO 3710FR) is located just upstream of the flow measuring flume where the samples taken would be well mixed. These composite samples are automatically taken on a flow proportional basis over a 24 hour period twice a week. This sample analysed for the biochemical oxygen demand (BOD) and total suspended solids (TSS) twice a week and for ammonia once a week. Grab influent samples are taken daily from after the grit and flotation tanks but before the primary settlement. This sample is analysed immediately, in an on-site lab. for pH, DO, and temperature. There is also continuous influent temperature measurement recorded by the surveillance, control and data acquisition system (SCADA).

3.5.2 Process Control

For process control grab samples are taken of the mixed liquor in both the anoxic and aerobic basins. The samples are analysed for mixed liquor suspended solids (MLSS) DO and settleability. The DO is measured in each basin with the handheld DO meter at the time of sample collection, the other analysis is carried out at the on-site laboratory. This is typically done two to three times per week but more frequently if adjustments are needed. The water levels of the basins are noted from the SCADA screen. The sample is also used to test for pH, temperature and total and volatile suspended solids.

This solids mass balance is used to assess the quality of the biomass in the system and to determine the wastage rates. Filterability and filtrate turbidity tests are done once a week on MLSS samples. This information is also used to calculate wastage as dry solids and to adjust the DO and redox in the aerated basins and so to adjust the recycle rates from the pumps.

3.5.3 Effluent

Continuous temperature measurements are recorded by the SCADA system for the effluent. It is located in the sampler vault between the chlorination unit and the flow meter.

Effluent samples are taken by a similar flow compensated, automatic, refrigerated, 24 hour composite sample as for the influent (ISCO 3710FR), in this case from the permeate pump room after disinfection. The sample is subdivided and taken to the lab where the pH, DO, and temperature are analyzed immediately. This sample is also used for the biochemical oxygen demand (BOD), total suspended solids (TSS) and an ammonia test twice a week.

Bacteriological samples are collected in a sterile whirlpak bags and analyzed twice a week for Faecal coliforms as indicator organisms.

Samples for metals, arsenic and boron, as shown in Table 3.2 and specified by the Disposal Permission, were collected in a cool-box (4-6⁰C) and immediately transported by the WDD to the State General Laboratory for analysis. The Laboratory is accredited by the Greek State Accreditation Body (ESYD) and the Cyprus Accreditation Body (CYS-CYSAB) for analysis according to international protocols ISO/IEC 17025:2005. Elemental and tracer analysis was carried out by inductively coupled, plasma mass spectrometry (ICP-MS).

3.6 Data Analysis

3.6.1 Treatment Parameters

The parameters that were analysed daily or twice a week (BOD₅, COD, TN, TP, and TSS) were converted to monthly averages and included any supplemental data or samples taken that were recorded in the data base provided by the Sewerage Board of Paphos, (see Table 3.3).

Residual COD is the key measure of the stabilization of the organic materials in the UWWTD and is therefore the most important parameter in treatment process performance. For discharge of treated effluent into the environment the UWWTD specifies a maximum COD 125mg/l the Cyprus Water Pollution Control Laws (106(I)/2002 to 2009) has a discharge limit guideline of 70mg/l. The average data during the study period was

based on 9000m³ of sewage treated, which had an average influent COD of 812.3mg/l and 34.2mg/l after treatment equivalent to a reduction of 95.8%. This is a typical performance from a Biological Nutrient Removal plant and residual organic pollutants similar to background levels in surface waters and therefore has potential for recycle after dilution by the receiving environment.

Equivalent BOD₅ load removal was 98.5% during the study period from an average feed of 522.3 mg/l and effluent of 7.9 mg/l in the final effluent. The UWWTD specifies a discharge limit of 25 mg/l and the Cyprus Department of Environment specifies a discharge level of 10mg/L. BOD₅ is also an important parameter in water pollution control since it indicates the instantaneous level of oxygen demand on the receiving water from easily biodegradable pollutants.

TSS together with COD and BOD is one of the traditional, easy to analyse, indicator parameter of the pollution potential of wastewater. High TSS in the natural water column will cause a reduction in sunlight intensity and reduce primary productivity of algae. This will disturb the aquatic food chain and reduce species diversity. Less light can also affect temperature in the aquatic environment causing temperature stratification and impacting on diversity and productivity. Excess TSS causes an aesthetic nuisance and is likely to represent a significant portion and precipitated reservoir of organic load in the receiving water. Remobilisation of this stored organic matter and subsequent decay can release of nauseating odours.

TSS causes additional problems in recycle and irrigation systems where it can block pipes, sprinklers, pumps and narrow water channels and indirectly in the form of re-growths of algae. TSS can also absorb heavy metals and other micro-pollutants onto their surface and thereby facilitating formation and transport of heavy metal complexes. During the study period the raw wastewater had an average TSS of 326 mg/l and with a 98.26% TSS removal efficiency, an effluent TSS 5.7 mg/l of TSS was discharged. The UWWTD limits discharges to 35mg/l TSS and the local permit a maximum level 10mg/l (Table 3.2).

Extra emphasis on controlling nutrient (N & P) release from municipal wastewater treatment plants has taken place recently. Plant, and therefore algal nutrients, specifically nitrogen and phosphorus causes eutrophication (nutrient enrichment), algal dominance and a reduction in biodiversity an increase TSS as noted above.

The average influent concentration of TN at the treatment plant was 78mg/L and 7mg/l was discharged. In sensitive environments the UWWTD requires a TN of 5mg/L; the Permits (Table 3.2) requires TN concentrations to be less than 10 mg/l to discharging into to the environment.

Total phosphate removal efficiency by the treatment plant, during the study period, was 78% from an intake concentration of 14.5mg/l giving a discharge of 3.2mg/l.

Phosphorus is usually the growth limiting plant nutrient and likely to increase algal growth when above 0.05mg/l.in the receiving water.

Table 3.3 Monthly Average Concentrations of Paphos Wastewater Treatment
Parameters, mg/l except %(n=102)

Parameters	Inlet		Outlet		Removal
	AVER	STDEV	AVER	STDEV	%
pH	7.16	0.11	7.6	0.3	
BOD ₅ (mg/l)	522.31	135.27	7.87	4.78	98.49
COD (mg/l)	812.26	131.43	34.22	15.55	95.79
TSS (mg/l)	325.99	99.56	5.67	2.81	98.26
TN (mg/l)	78.81	17.67	7.04	2.99	91.06
TP (mg/l)	14.51	2.82	3.20	2.88	77.91
FOG (mg/l)	100.7	10.5	<5		

3.6.2 Heavy Metals

Metals are a ubiquitous hazardous pollutant at less than 1 mg/L and of particular concern since metals are accumulative. Heavy metals are therefore included in the main category of environmental pollutants (Azevedo and Azevedo, 2006). The European Union Water Framework Directive and the Clean Water Act in the United States (Ziolko, et al., 2011) seeks to reduce the concentrations of the most toxic metals to the evolving detection limits.

Metals are present in the final effluent, according to solubility and pH, but mostly in the sludge. There are European guidelines for the recycling of sewage sludge to agricultural land complied with the possibility of leaching into the local water course, which might infringe drinking water standards.

It is evident that during primary treatment only metals present in an insoluble form will be removed, but the removal of such forms is strongly influenced by the factors controlling sedimentation. During secondary treatment metals initially present as soluble forms may be removed by association with the settleable biomass: further removal of insoluble

metals also occurs by association with this biomass. Efficient flocculation and settling is critical to the removal of all metal forms during secondary treatment.

The heavy metals defined in the Permission for effluent disposal are: zinc (Zn), copper (Cu), lead (Pb), cadmium (Cd), mercury (Hg), chromium (Cr), nickel (Ni), boron (B) and arsenic (As). The heavy metals (Cd, Hg, Pb,) and arsenic are not needed by organisms for any purpose and are toxic even at relatively small concentrations. Other metals play vital physiological roles (e.g., Zn, Cu, Fe, Mn) as co-factors but are harmful when they exceed optimal concentrations (Singh, et al., 2012).

Excessive heavy metal accumulation impairs either directly or indirectly several biochemical, physiological, and morphological functions in both plants and animals. Excessive metals interferes with crop productivity by bioaccumulation and bio-magnification in the food chain (Asrari, 2014).

Treated effluent concentrations of metals were lower than the EC Directive standards (1998) for discharge into surface water. For example boron was a third of the limit and cadmium was two orders of magnitude lower. The concentrations of the metals considered were in the order B>As>Cu>Ni>Hg >Pb>Zn> Cr. These concentrations of heavy metals were used as indicators that the groundwater of the Ezousas Aquifer, recharged with treated effluent would be safe but continuous monitoring would be necessary both at the treatment plant and in the aquifer.

CHAPTER 4

THE CHANGES IN NITRATE FROM THE TREATED SEWAGE EFFLUENT

Chapter Summary

Treated effluent contains some priority pollutants such as nitrate, phosphate, metals and persistent organics as well as pathogens. There are therefore both environmental and health risks from the recharge of treated effluent to groundwater. This chapter of the thesis discusses the results from the full-scale field demonstration of the Ezousas river alluvial basin and aquifer. The results were specific to nitrate because this contaminant was in the highest the concentration in the treated sewage effluent and a good tracer of redox conditions in the underlying aquifer. Results for nitrate, TOC, dissolved oxygen, redox potential and pH were also included to complement the investigation on how the hydraulic patterns of infiltration and recharge affect the potential for denitrification in the alluvium aquifer.

Nitrate concentrations in the treated effluent ranged from 13-16 mg/L, TOC averaged 7mg/l, the DO was between 7-10mg/l, the pH was < 8 and the redox potential varied from +190 to 350 mV.

The tests demonstrated that the operational modes of the recharge basins affected the infiltration rates and the nitrate concentrations in both the pond water and the aquifer. Long cycles of flooding (45 days) allowed a bio-mat to develop on the floor of the pond which impeded the movement of water and decreased infiltration efficiency whilst generating extra nitrification in the pond. Nitrate concentrations increased to between 19-25 mg/l in the percolating water. On the other hand nitrate concentrations after the short cycle flooding experiments (7days) were unchanged by the pond and decreased to 2.2-

3.7 mg/l in the aquifer. This was attributed to the dilution by the native groundwater, there was no evidence for denitrification. Thus it was concluded that the quality of the treated sewage effluent would deteriorate in the ponds from the potential for algal growth if the retention time was too long. It was also shown that there was dilution of the nitrate in the aquifer and the geochemical conditions did not promote denitrification.

4.1 Introduction

The use of shallow infiltration basins for the replenishment of groundwater supplies from treated wastewater effluents is a common practice in arid and semi-arid regions. Alternating cycles of fill and drainage are used for the recharge to avoid soil saturation and anoxic conditions. The duration of the cycles depends on treated effluent quality and availability but normally filling, draining and drying in the infiltration basins is spread over several days. The water percolates through the vadose zone to an underlying, unconfined aquifer for storage. The water is then available for recovery and reuse through abstraction wells.

The soil–aquifer system acts as a natural filter which improves water quality in a combination of ways the most important are mechanical straining, sedimentation, absorption and bio-transformation. Our present knowledge of vadose zone flow and transport processes limited the ability to predict the effectiveness of these as remediation methods. The interactions between these processes are complex, not fully understood and unpredictable (Taylor, 2003). Mantoglou and Gelhar, (1987) for example, noted the processes were so complex, that the generic models available did not even cover the most basic changes.

Therefore in this thesis, in order to manage groundwater resources, an attempt was made to model and validate these natural systems by field experiments using test wells. Typical model input variables were water input, pressure potential, and temperature. The field experiments were also an opportunity to advance the general understanding flow and transport processes in the vadose zone. The spatial variability of hydraulic properties were used to calibrate both mathematical and physical models.

General agreement was found however that the soil and pond cycle had an important role in controlling the flux and attenuation of nitrate, in particular for example, Harter, et al., (2005) and Schmidt, et al., (2011). Nitrate is a ubiquitous contaminant in shallow aquifers, (Puckett and Cowdery, 2002) and is a cause for concern because of the human health risks (WHO limit value is 50 mg/L as NO_3). NO_3 in surface waters also contributes to eutrophication (EU WFD 2013 limit value is 5 mg/L as N). Consequently, there has been growing interest in processes and conditions that lead to natural attenuation of these contaminants.

The processes that control the movement of water, nitrate and other contaminants through the vadose zone are dependent on the variable, alluvial sedimentary geology. The basic geology underlying the soil and vadose zone was therefore analysed to interpret the monitoring data and assess the adsorption and leaching potential of nutrients and other contaminants into the aquifer.

The geology and hydrogeology of the Ezousas Catchment area and aquifer are described in Chapter 2.

4.2 Objectives

Previous work by Botros, et al., (2012) has provided evidence that even thick vadose zones have limited ability to buffer contaminant transport into the saturated zone. Other research has reported on the fate of a wide range of organic compounds, for example, algal toxins and pathogens during the infiltration of surface water (EC 2001; Langmark, et al., 2004). A previous paper has also reported on changes in redox dynamics in ponded infiltration systems which were shown to cause changes in inorganic chemistry including nitrate (Greskowiak, et al., 2005). The aim of this chapter was therefore to investigate the basic processes that affect the movement of water and contaminants through the vadose zone with special attention to changes in nitrate concentration as the most widespread contaminant in groundwater.

The objectives of this study were:

- To improve our knowledge of the fate of nitrates and other N transformations in soil that could influence their possible transport into groundwater.
- To characterise and understand the transient unsaturated/saturated hydraulics caused by and during the alternate cycles of filling, infiltration or percolation and drying.

4.3 Problems Associated with High Concentration of Nitrates in the Environment

Nitrogen is one of the most common contaminants in groundwater, originating from agriculture and human or animal waste. By the 1950's nitrate/nitrite ingestion through food, feed, and water had been recognized as potentially hazardous for man and livestock. High concentrations of nitrate-nitrogen in drinking waters have been linked to methemoglobinemia in infants thus the tolerance limit in potable water has been set at 10 mg/l as $\text{NO}_3\text{-N}$ (Council Directive 98/83/EC). High dietary nitrate has long been

recognized as one cause of animal health problems, poor growth, abortion and premature death. Excessive levels of nitrate can also be directly harmful to aquatic life and including animals (Kross, et al., 1993; Camargo, et al., 2005).

Thus nitrogen contaminants threaten public and ecosystem health with a serious impact on rivers, wetlands and groundwater quality (USEPA, 1997).

The environmental impacts of nitrogen contamination in groundwater are particularly acute in coastal aquifers, because nitrogen limits the productivity of salt marsh vegetation including phytoplankton and macroalgae in receiving coastal waters. Groundwater nitrogen loads to coastal salt marsh or water body are determined by nitrogen inputs to the aquifer and chemical and microbial process in groundwater, which may attenuate the nitrogen load (DeSimone and Howes, 1998).

4.4 Review of Nitrogen Transformations

4.4.1 Nitrogen Transformations via Natural Attenuation in the Vadose Zone- Overview.

4.4.1.1 Fate and Transport

The rate at which the contaminants move through the vadose zone is controlled by the interaction between the physical characteristics of the area; such as the rainfall, saturation, hydraulic, thermal and vapour gradients. There are also changes from biochemical reactions these include; biodegradation, biotransformation, adsorption, redox and pH (Ward, et al., 2004). Partitioning of the contaminants into the different components of the environment also occurs (i.e. soil, water and air). For the majority of the contaminants, movement through the vadose zone is in the aqueous phase and therefore depends on solubility in the infiltrating water. There are potential interactions

between the contaminants in this infiltration water but the literature and results suggest most changes occurred in the bio-active layer in the pond sediment and in the soil beneath the ponds. The reaction conditions prevailing in the vadose and bio zones differ from those in surface and groundwater (Runnels, 1995), because of air vacuoles, which give a strong oxidizing environment and the large specific surface area available from the soils and sediment for adsorption. For example the sorption of nitrate and the resultant increase in ion-storage in the unsaturated zone is well documented. These excess anions can also associate with cations in a secondary layer or an outersphere complex forming a double layer (Reilly and Baehr, 2006).

4.4.4.2 Natural Attenuation -The Denitrification Process

Nitrogen compounds, in particular, undergo degradation and transformation as a result of chemical and biotic reactions (microbial and plant). These can be important to groundwater quality (Ward, et al., 2004) because of the variable solubility, toxicity and soil adsorption of the different nitrogen compounds. In some cases gases are formed, such as nitrogen and some of the oxides, that escape to atmosphere from ponds, vadose zone or shallow aquifers (Ueda, et al., 1993).

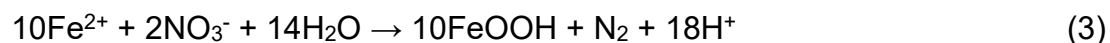
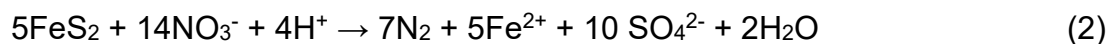
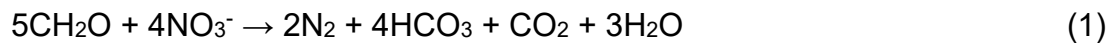
Nitrates are very soluble and as a consequence do not bind to soils and therefore migrate easily into and in the groundwater. Nitrates are stable except at low redox potentials and persist until consumed by plants or other organisms.

Many heterotrophic species of soil bacteria are able to tolerate a wide range of environmental conditions: temperature, pH, salinity, etc. some can also survive adverse conditions by forming spores, which reactivate when conditions improve. Nitrifying bacteria on the other hand are autotrophs which have much lower rates of metabolism

than the heterotrophs, they do not form spores and cannot survive adverse conditions such as the drying out in the infiltration ponds used in this research.

Heterotrophic denitrification can also reverse this autotrophic oxidation but in this case the reduction is to nitrogen gas which is released to the atmosphere. It is also a sequential process of reduction of nitrate (NO_3^-) to nitrite (NO_2^-), nitric oxide (NO), nitrous oxide (N_2O) and dinitrogen (N_2) catalysed by nitrate reductases (Nar or Nap), nitrite reductase (NIR), nitric oxide reductase (NOR) and nitrous oxide reductase (N_2OR), respectively (Morley, et al., 2008).

Nitrate reduction can also be paired to the oxidation of organic matter (Equation 1), pyrite (Equation 2) and iron (Equation 3) under anoxic-anaerobic conditions (Starr and Gillham, 1993; Puckett, et al., 2002; Rivett, et al., 2008).



Biological denitrification has been used to remove nitrogen from aquifers in order to meet the WHO recommended limit in drinking water of 50 mg/L as nitrate. It is reported as a more cost effective treatment than chemical processes such as ion exchange. To promote denitrification in groundwater therefore requires soil bacteria; assimilable organic carbon and anoxic or anaerobic conditions (Korom, 1992; Starr and Gillham, 1993).

All these conditions are seldom combined in the proper proportions in groundwater. This is also true of most recharge projects where aerobic conditions prevail and the easily biodegradable organic carbon has been removed prior to infiltration into the aquifer. Therefore microbial reduction of NO_3 to N_2 for drinking water supplies is often promoted by re-adding easily metabolisable organics such as acetates and alcohols at the treatment plant rather than into the aquifer (Ward, et al., 2004). Most other research into denitrification has concentrated on the fate of nitrate as a fertilizer in the upper soil layers (0-0.45m), (Elmi, et al., 2005). Little research or empirical evidence exists on the spatial distribution of NO_3 in vadose zones and the associated fate and transport of NO_3 between the vadose and the water table (Onsoy, et al., 2005).

Some heterotrophic species can oxidize or reduce nitrogenous compounds directly to nitrites (NO_2), nitrates (NO_3) or other forms of nitrogen (as NO or N_2). Controlled environmental conditions are needed for these anaerobic oxidations of ammonia (e.g. Anammox^R, Bohlke, et al., 2006).

In the absence of an organic nitrogen, many heterotrophs will utilize ammonia as a nutrient and with special conditions ultimately oxidised nitrogen. This is possible in the laboratory or under controlled bioreactor conditions but unlikely naturally in the soil or aquifer.

A typical schematic of the nitrogen cycle is presented in Figure 4.1. These diagrams represent only the natural pathways involved in nitrogen transformations and that the residence time for a nitrogen molecule in any particular state may vary from a few seconds to thousands of years, depending upon its form and the environmental conditions.

NITROGEN REACTIONS IN SOILS

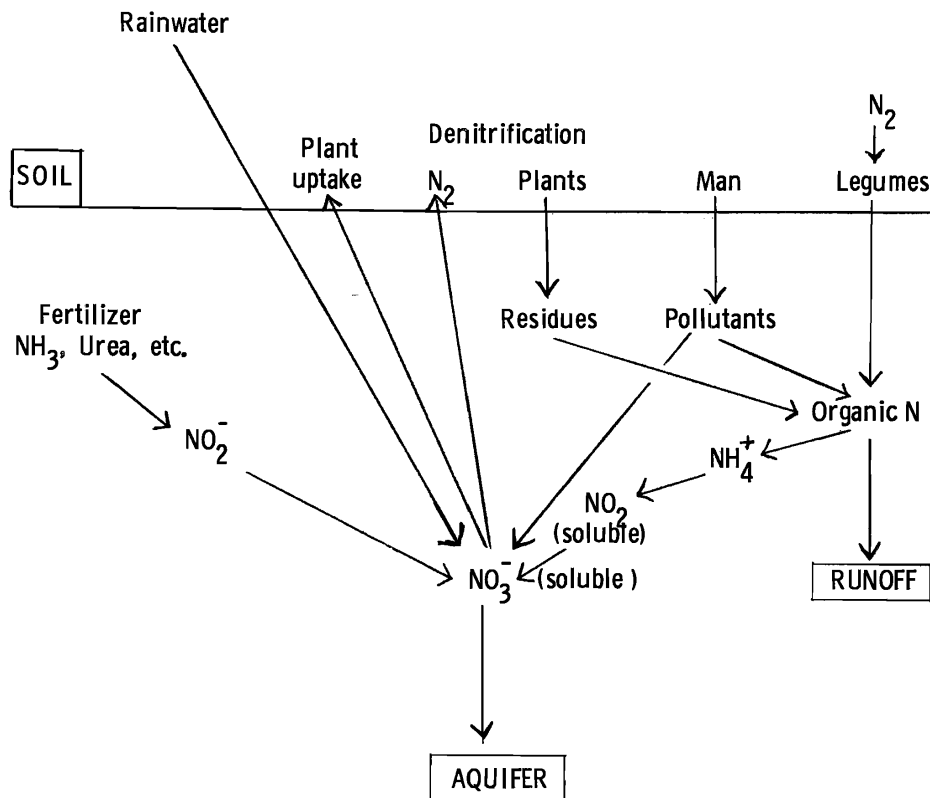


Figure 4. 1 The nitrogen cycle (Keeney,1970)

4.5 Infiltration and Percolation into a Shallow Alluvial Aquifer

The vadose zone is a layer of wet but unsaturated sediments between the ground surface and the water table. Flow in the unsaturated soil of the vadose zone is a more complex transport process than in a saturated aquifer. Water flow in the vadose zone occurs at different spatial and temporal scales depending on the local conditions. Macropores are filled with air, leaving only finer pores to accommodate water movement. The flow of water in fine unsaturated soils is dictated by the difference in matrix water potentials, not gravity. The matrix potential gradient is the difference between the moist soil areas (high matrix potential) and nearby drier areas (low matrix potential) into which the water is therefore

attracted by diffusion and equilibrium (Brady and Weil, 1999). Coarse-textured, sandy soils, after drainage, may be 10 to 20 % water-saturated whereas fine-textured silts or clays may hold as much as 90 % water. Therefore layers of clay lenses or cementing agents will retard drainage, even in otherwise permeable media. Soils that retain extensive water are anoxic or anaerobic. If only part of the void space is filled with water, then chemicals with a significant vapour pressure can move in the gas phase as well as in solution. Thus the water flow rate in the vadose zone is affected by this variable soil resistance which is a nonlinear function of the water content and can vary significantly compared to the saturated zone, where it is likely to be constant.

During inundation or infiltration, because of these difference in pore size, water is likely to penetrate into the soil preferentially at certain locations, through narrow wetting columns. The intervening soil could remain dry and this is commonly observed in practice and referred to as: unstable flow, fingered flow, or preferential flow (Nguyena, et al., 1999). During these unstable flow conditions, water and solutes move through these preferential pathways in the vadose zone at velocities similar to the saturated hydraulic conductivity (Glass, et al., 1988). This flow by-passing and heterogeneity of alluvial aquifers has a profound effect on the transport and amounts of potential harmful contaminants getting into the underlying groundwater (Glass, et al., 1988) as well as affecting the fate and subsequent remediation efforts.

Anisotropic advective flow, dispersion, diffusional transport, contaminant adsorption and other physical/chemical processes are all likely and reported to take place in these complex soil systems (Vance, 1994). Information on sediment texture, homogeneity and depositional characteristics can be used as potential predictors of these hydraulic conductivity variables (Fogg, et al., 1997). Therefore an analysis of the alluvial heterogeneity of the Ezousas river alluvial basin sediments was carried out using borehole logs and field pumping-test data, this was reported as a paper from this thesis (Christodoulou, et al., 2007).

4.6 The Ezousas Recharge Project

The Ezousas Recharge Project was designed to supplement the aquifer with 9000-12000 m³/day of treated sewage effluent from Paphos. The tertiary treated effluent is distributed via a 500 mm pressured main to infiltration ponds about 10 km east of Paphos. The recharge network consists of 23 infiltration ponds organized into groups of between two to six. The infiltration area of each pond is approximately 2000m² and 1.5m deep. Controlled abstraction takes place from the aquifer downstream, thus providing a semi-closed system for the detailed study of the impact on groundwater quality.

The basin sizes and infiltration rate (0.6-0.8 m/day) were designed to provide the wastewater needed to meet the projected abstraction demand in the non-agricultural season, (about 3 Mm³ a year).

Equivalent annual infiltration or "hydraulic loading rates" would be between 60 and 90 m/year, depending on soil, climate conditions, quality of sewage effluent and actual abstraction rates.

The location of the study area and a close up aerial view of the aquifer are shown in Figure 4.2.

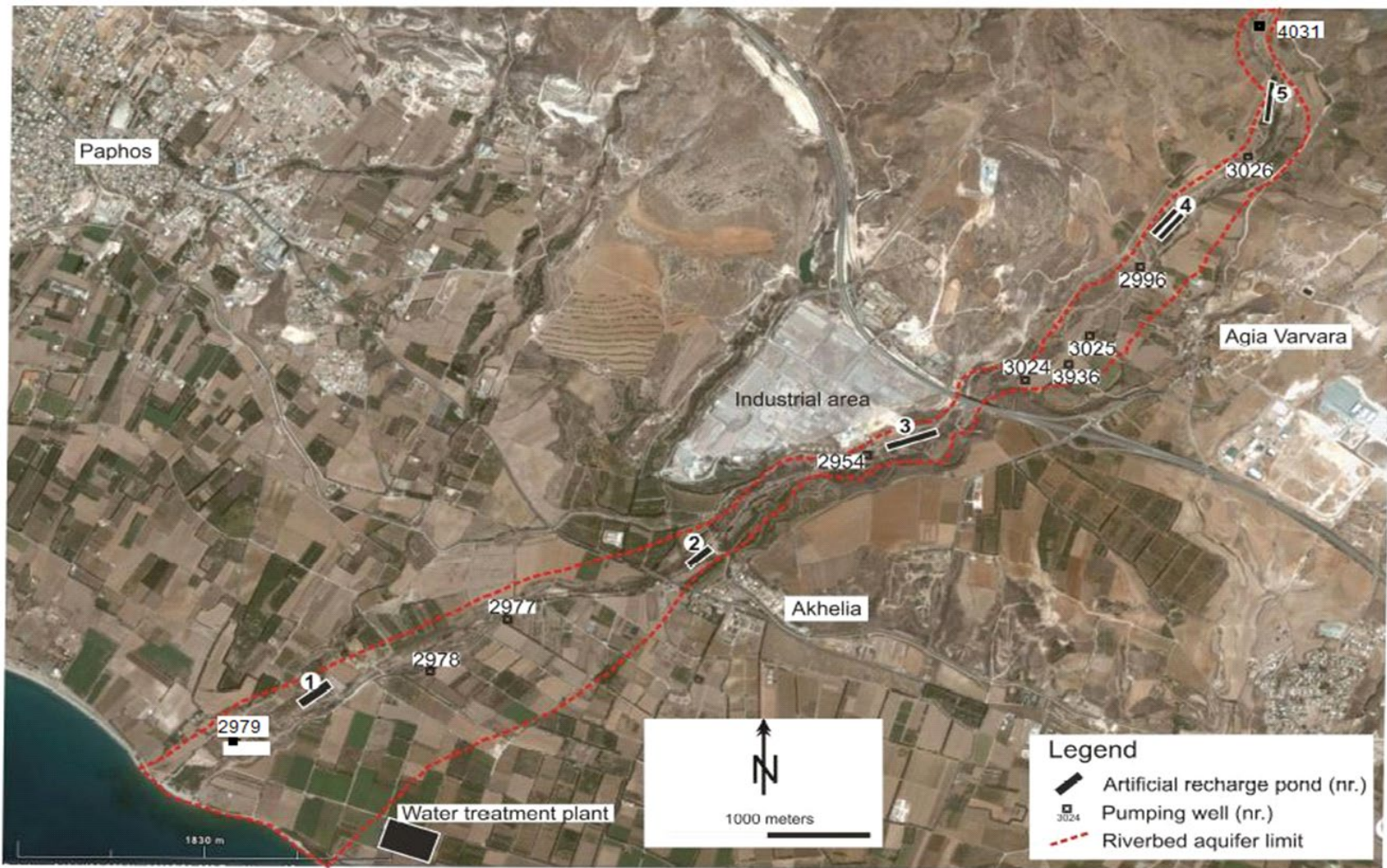


Figure 4.2 Aerial view of the Ezousas Aquifer Recharge Project

4.6.1 The Experimental Site

The applied objectives of the project were:

- Effectively replenish/recharge the local groundwater with treated effluent to reduce the influence of over abstraction on sea water ingress.
- Provide information on the local lithology and stratigraphy.
- Understand the influence of the recharge project on ground water levels and quality by water sampling.

Infiltration basin No 5, pond 4 (the basin location is shown in Figure 4.2) was chosen for research monitoring; since it was the least likely to be affected by agricultural leachate or any uncontrolled recharge/abstraction operations.

The local lithology and stratigraphy was analysed from percussion drilled borehole samples. The subsurface characteristics were found to be heterogeneous layered sediments made up of alternating layers of medium to fine sandy gravel which always contained traces of silt, (Table 4.1). These fine textured silty sand and clay lenses typically have low vertical but relatively high horizontal permeabilities. The flow was dominated by a sequence of these permeable paths which included material that was of two or three orders of magnitude higher in permeability than the bulk soil matrix. Thin layers of permeable paths, such as sand, were found to dominate the flow through several metres of silt or clay and govern overall groundwater flow. These permeable paths promoted lateral spreading of percolated water while horizontal flows followed other preferential paths. Thus, vertical and horizontal hydraulic conductivities varied considerably according to both location and time. This lateral spreading of moisture can also slow down the vertical movement of contaminants within the vadose zone. This type of strata of fine over coarse sediment sequences causes the Richards' affect in which the capillary breaks typically limit the downward migration of water and contaminants while enhancing horizontal flow. Lateral flow generally occurs until the soil-water potential is sufficient to overcome the entry pressure of the coarse underlying layers or some channel or fissure of lower resistance is found (Ward, et al., 2004).

This was as predicted by the literature reviewed in section 4.3, but it was concluded that a complete understanding of these flow paths at this, and most sites, would be practically impossible because of the costs involved in gathering all the necessary data.

Table 4.1 The cores of the BH3963 at the vicinity of infiltration basin No5, (Pond 4) where the tests were carried out (see Figure 4.2).

Depth, (m)	Lithological Description	*Hydraulic conductivity, K (cm/sec)
0 - 1.52	Coarse sandy gravel	$10^{-2} - 1$
1.52 - 7.92	Sandy silt	$10^{-5} - 10^{-3}$
7.92 - 9.14	Sandy silt with coarse gravel	$10^{-3} - 10^{-4}$
9.14 - 12.80	Sandy silty gravel	$10^{-2} - 10^{-3}$
12.80 - 16.46	Coarse gravel with boulders	$10^{-1} - 10$
16.46 - 21.03	Sandy gravel	$10^{-1} - 1$
21.03 - 23.77	Clay (Mamonia)	Practically impermeable
23.77 - 25.30	Serpentinite	?

* The hydraulic conductivity ranges assigned for different soil types based on the USDA (NRCS) National Engineering Handbook, Part 631, and the Code of practice for Foundations, BS 8004:1986.

Piezometers were installed between several of the infiltration ponds to monitor changes in groundwater levels and any mounding that occurred. Water quality monitoring boreholes were also installed, polyvinyl chloride (PVC) tubes, were used to form the well casing which was 110 mm (4 inch) inside diameter. They were screen slotted over the penetrated depth of the aquifer. The wells were protected within a 3m long steel casing which also extended approximately 1.5 m above the ground surface.

This depth was adequate to encompass the full range of changes in water table height expected during recharging of the pond. Monitoring borehole, BH 3963 and two piezometers were positioned adjacent to the test infiltration pond (10m away) to measure any increases in water table. BH 3963 was drilled to a depth of 25 m and passed through the entire 21 m of alluvium and 4m into the bedrock (Table 4.1; Figure 4.2). BH3963 also allowed groundwater sampling from immediately underneath the recharged basin (for monitoring any mounding in water level).

Two other boreholes BH E4, BH E3 were drilled at 30 m and 60 m respectively from the infiltration pond and were used to observe lateral distribution of the infiltration water. The relative positions of the infiltration pond, boreholes and monitoring-piezometers are shown in Figure 4.3 and the water table change in Figure 4.4.



Figure 4.3 The test site pond No.4 basin 5

4.7 Experimental Results

4.7.1 Hydraulic Loading

Tests were carried out with different wet cycle times but using the same one-week dry time. The first test was, one day wet, one week dry; the second test was one week wet-one week dry and the third test was 45 days wet-one week dry. The three tests were carried out between September-October 2008, when there were no surface river flows and minimum groundwater flows draining out of the aquifer, thus the water table was at its lowest level. These conditions were selected for the long wet cycle recharges so that any rise in the mound height would not saturate the test zone and interfere with the data from the experiment.

As previously noted, Pond-E4 was also selected because there were no local abstractions which might have affected the test results. The flooding depth for the first test was aimed to be 0.4 m deep from the base of the pond. The idea was to uniformly cover the area of the infiltration pond as quickly as possible which at the recharge rate of 300 m³/h, was achieved in three hours

The second test, after the week long drying out, used the same filling rate as in the first test but in this case the 0.4m head was maintained for a week by regular additions using a sluice valve. The third test maintained this water level for 45 days; using the same system for topping up.

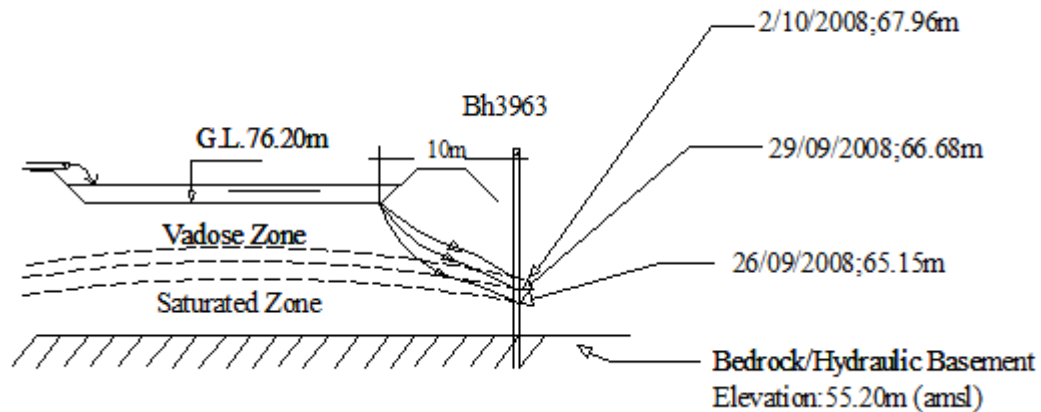


Figure 4.4 Diagram indicating the water table changes during the test at Basin 5 (Pond 4)

During the experiments, the drop-in water level, was recorded every hour from a metering bar installed in the pond. The results of these infiltration measurements, showing the differences between the three pond flooding durations are presented in Figure 4.5.

It was observed, from the third test, that longer flooding encouraged more intensive algae and plant growth which reduced the infiltration rate from the pond. The short wetting cycles (e.g., 1 day wet and 7 days dry experiment), assisted rates of infiltration by reducing plant growth. It was also noticed during the longer wetting tests that careful control of the water depth to 0.4m when filling could help avoid bed compression and a further reduction in hydraulic conductivity.

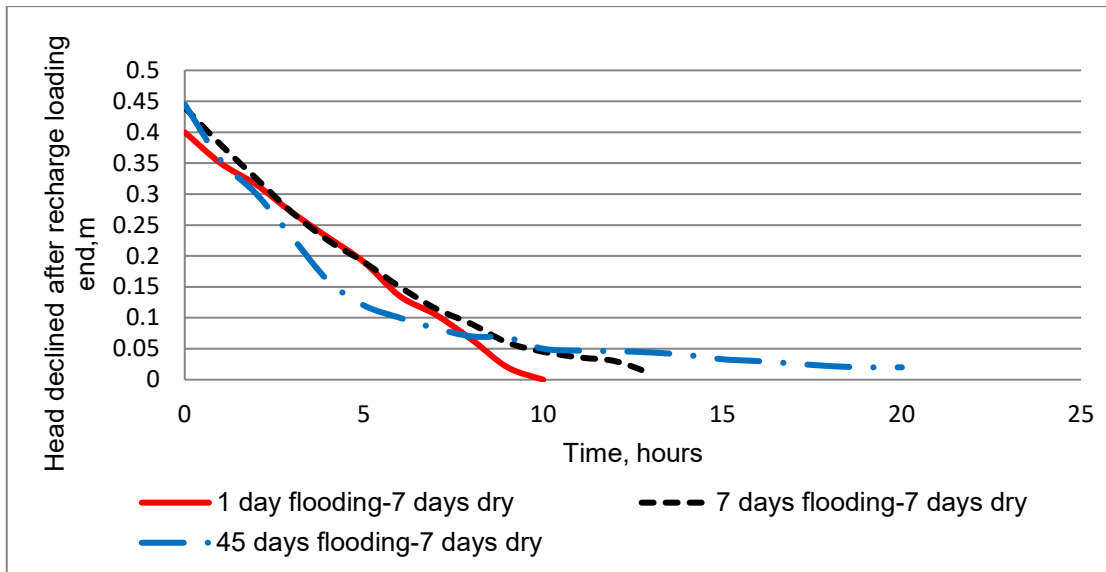


Figure 4.5 Infiltration efficiency of different wetting cycles

4.7.2 Water Quality Results

The recharge infiltration rate was thought likely to affect the efficiency of filtration and adsorption by the soil and therefore the level of treatment achieved in the pond and vadose zone.

Water samples from the pond were taken at 20 to 30 cm below the surface and these were compared with samples from the monitoring boreholes. The samples were analysed immediately on site using USEPA approved test kits (APHA, 2005).

Nitrate ($\text{NO}_3\text{-N}$), ammonia ($\text{NH}_3\text{-N}$), were analysed by a portable data logging colorimeter (HACH DR/890). The Hach DR/890 uses the cadmium reduction and salicylate methods respectively, with UV photometric detection. The kit is certified by the USEPA to be +/- 5% at this range and is well established in the water industry (Danja, 2010). The method is also used by “The State General Laboratory” and the “Aristos Loucaides Lab Ltd.” which are cross laboratory calibration partners to the WDD for water quality analysis; both are accredited by ISO 17025.

Dissolved oxygen (DO) and redox potential (platinum electrodes), were measured with electrochemical sensors (WTW OXI330i/SET), electrical conductivity (EC), pH, air and water temperature were measured with a WTW COND330i/SET. Alkalinity and HCO_3^- were measured using volumetric analysis (Aquamerck 1.11109.0001 titrimetric method), and turbidity by a Micro turbidimeter (Lovibond MicroTPW).

Feecal Coliforms and E. Coli counts together with DOC were analysed less frequently by the registered laboratory (Loucaides Laboratories Ltd). These samples were collected and stored in white, 500ml polyethylene bottles, pre-rinsed with the sample and transported to the laboratory within two hours.

4.8 Results and Discussion

Reduction /Oxidation Potential

The literature review indicated the redox of the environment was a key influence on the speciation and fate of the nitrate recharged into the aquifer from the recycled effluent (Massmann, et al., (2006) presented the example shown of a possible mass balance for the complete oxidation of an organic nitrogen compound to nitrate:



The oxidation and degradation of any residual organic carbon would lead to the reduction of oxygen (O_2), nitrate (NO_3^-), manganese-(Mn IV) and iron-(Fe III) oxides, hydroxides and sulphates SO_4 . Typically this is the sequence of their thermodynamic energy potentials as electron acceptors. These reductions if promoted by an organically enriched effluent would cause undesirable changes in water quality. These could be an increase in ammonia,

a reduction in pH and an increase in calcite, Fe^{2+} and Mn^{2+} . Malodour from the generation of sulphides and amines can also occur. It has also been suggested that the degradation of a number of organic micropollutants, such as pharmaceutical residues, halogenated organic compounds or pesticides require high redox potentials (Massmann, et al., 2006).

In this case study the tertiary treated effluent TOC in the recharge water was low (average 7 mg/l) and the results suggest this was insufficient organic carbon for these reduction processes to occur. Other evidence supporting this conclusion, included the concentrations of dissolved organic carbon (DOC), redox Eh, dissolved oxygen (DO) and ferrous salts as used by Thayalakumaran, et al., (2008).

Dissolved Oxygen

DO results ranged from 7.0-9.5 mg/l (average 7.6 mg/l) demonstrating near saturation conditions. The aquifer is relatively shallow and unconfined and the oxygen saturation would be 9.1 mg/l., the measured DO in the native aquifer was between 6–8.5 mg/l. at a groundwater temperature of around 20°C. Redox measurements, E_h of the flooding and percolated water were between 190-350mV corroborating near oxygen saturated conditions.

Nitrates

The concentration of nitrate in the recycled sewage effluent was between 8-13 mg/l, which was around the EU Drinking Water Directive but within the consented permit level, based on the dilution available. The wastewater treatment plant includes biological nutrient removal (see Chapter 3). Nitrate concentrations in the groundwater (native source) were around 7 mg/L. During the long cycle tests (45 days flooding) there was an increase in nitrate concentrations in the flooding water of 30% compared to that of the fresh effluent (Table 4.2). The percolation water showed even higher concentrations

at between 30-70% more than the flooding water. The results for nitrate and ammonia in both the flooding water and the percolated water are presented in Table 4.2 and Figure 4.5 records the changes in water table beneath the infiltration pond.

Table 4.2 Nitrate (NO₃) and ammonium (NH₄) concentration in the pond and the percolated water during the long cycle-test (n=14) and the short cycle-test (n=9 and 17 respectively for the ponded and percolated water for 3 consecutive tests).

Sampling	Nitrate, NO ₃ (mg/l)		Ammonium, NH ₄ (mg/l)	
	Long Cycle- 45 days	Short Cycle- 7days	Long Cycle- 45 days	Short Cycle- 7days
Ponded water	13-16	5-7.2	<0.01	0.4-0.7
Percolated water	19-25	2.2-3.7	<0.04	2.1-3.4

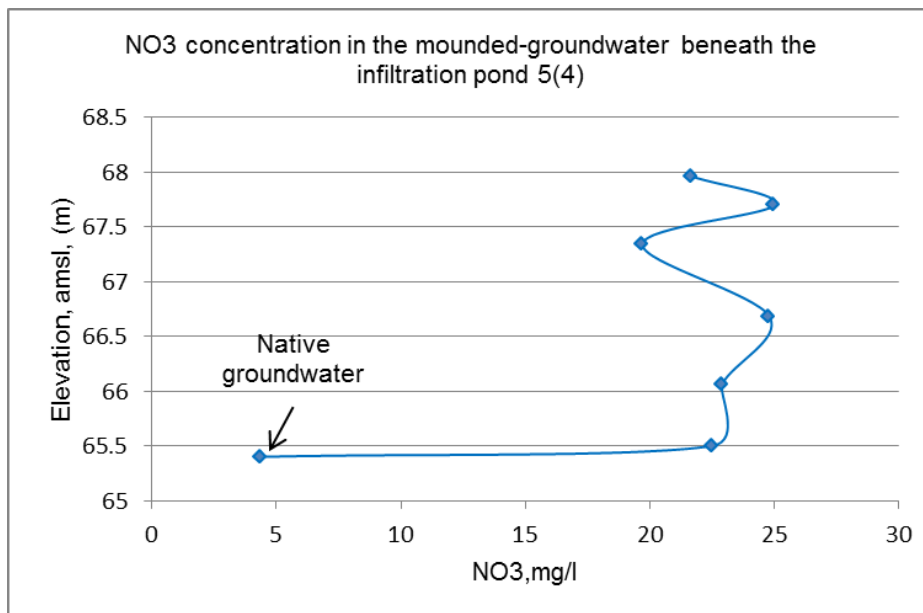


Figure 4.6 Nitrate concentrations during the long cycle-test in the raised water table (mound) beneath the infiltration pond (pond's floor elevation = 76.2m (amsl)).

The short-cycle tests (up to one week of flooding) do not show the increases in NO_3 apparent from the long cycles, there was a decrease in nitrate in the percolated water. The average concentration of nitrate from 9 samples of the pond water was 5.9 mg/l and from 17 samples of percolated water was 3.2 mg/l, the range is shown in Table 4.2.

The sensitivity of nitrate to redox was anticipated from the literature review and denitrification was observed to produce nitrogen bubbles by Puckett and Cowdery, (2002) but this was difficult to observe or measure here. Denitrification should however be accompanied by other redox-active indicators, including DO, iron, manganese and sulphur, as noted (Corstanje and Reddy, 2004).

Denitrifying organisms are able to use either oxygen or nitrate as an electron acceptor depending on the concentration of dissolved oxygen. The sandy gravel sediments of the Ezousas aquifer means very little organic matter in the native water (< 3 mg/L DOC) and low NO_3 (and NO_2) concentrations. Oxygen (O_2) also penetrates into these sediments and can be circulated throughout the deposits by physical processes related to the interaction of currents at the bottom and surface of the sediment. Typically, these sediments will be aerobic with dissolved oxygen (O_2) >2 mg/l., the threshold above which aerobic metabolism is always preferred (Thomasson, et al.,1991). The low nitrate concentrations were coupled with low ferrous iron concentrations. Therefore it was concluded from the high DO concentrations (>7mg/L) and low ferrous concentrations in the groundwater were unsuitable for denitrification or dissimilatory nitrate reduction to ammonium. Similar results from the sub-surface (up to a 2 m depth), at low organic carbon concentrations in well treated effluent have been reported by other researchers (Paramasivam, et al.,1999; Mayer, et al., 2010).

It was not possible to completely exclude the possibility of denitrification in the deeper more confined regions of silty-clayey layers where oxygen levels would

be lower. There are also small confining regions in the aquifer that may result in reduced oxygen concentrations but this was impossible to detect from the experiments conducted. Thus although the low organics in the treated effluent and local environment precludes denitrification in the ground water, there was during the long cycle test an undesirable increase in concentration of nitrate in the flooding and consequently also the percolated water (Figure 4.5).

Soil like organic matter was observed to develop on the bottom of the infiltration basins mainly originating from dead plants and algae which encouraged animal and microbial activity. This material was a mixture of fresh and decomposing biomass at various stages of humification. The anoxic/anaerobic degradation of humic substances containing organic nitrogen would lead to the generation of ammonium in the leachate from deamination, as reported by Koda, et al., (2015). These degradation processes would have released both ammonia and organics from these secondary pond sediments into the recharge water. The organic matter generated in the pond will form nitrates and not ammonium as long as the oxygen is near saturation. In the ponds oxygen concentration was almost saturation (e.g. 8-9 mg/l at 22°C), as previously noted, and it was concluded this new organic matter and its subsequent oxidation was the origin of the increased nitrate concentrations compared to the fresh treated effluent. A simplified demonstration of these processes is shown in Figure 4.7.

This was in contrast to some previous work by Greskowiak (2005) who concluded that NO_3 and Mn-reducing conditions dominate beneath a pond when the soils are water saturated. Greskowiak observed Manganese-, Fe- and SO_4 reduction in a narrow zone directly below the pond and he concluded that this was due to the formation of a clogging layer which caused a decrease in infiltration rate and water saturation. Atmospheric O_2 was then unable to penetrate from the pond into this region leading anaerobic conditions.

Greskowiak (2005) used lower quality effluent and reported greater accumulation of solids at the bottom of the ponds than the results reported here. The ponds used by Greskowiak required cleaning 2-4 times a year to restore infiltration rates but in our case the ponds required no removal of sediment during the 5 years of the experiments. In the long flooding periods however, it was concluded that the algae growth within the ponds increased the total amount of organic matter and it is suggested that this algal productivity was responsible for the increased nitrate in the infiltrating and groundwater in the vicinity of the pond.

In the case of the short cycle recharge, (one day flooding), there was insufficient time for either algae growth or degradation of accumulated solids and the decrease in observed nitrate was attributed to dilution with perched water held in the vadose zone.

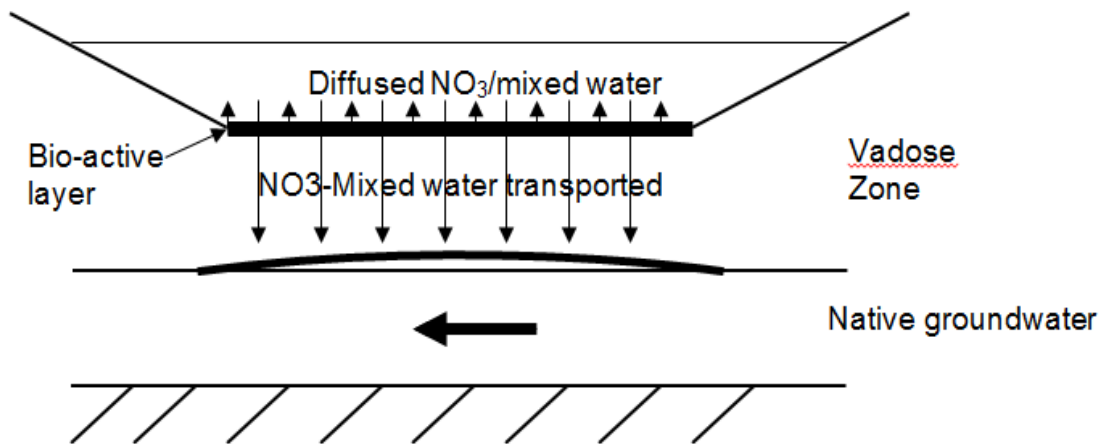


Figure 4.7 Schematic diagram showing the changes in nitrate taking place during the long cycle recharge operation

Ammonium

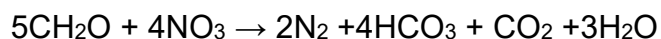
The ammonium concentrations followed a similar pattern. During the long wet cycle experiments the average value for ammonium, in the treated effluent was 0.28mg/l which decreased in the pond water to below the detection limit. Ammonium in the percolated water samples from the adjacent borehole BH 3963, showed values up to 0.56mg/l but in the downstream boreholes further away, ammonia was undetectable.

In the short rotation experiments the recharge effluent water contained 0.04mg/l ammonium and samples of the flooding water, in the pond and adjacent monitoring boreholes showed an average 10 fold increase but as with the long cycle experiments, samples from the downstream boreholes contained no ammonia. It was concluded the increase in ammonia from the short cycle tests was small and insignificant given the changes in hydraulic conditions.

pH and Alkalinity

The pH of the native groundwater was typically neutral (7.5) and the treated effluent averaged 7.9. The water abstracted from the downstream wells averaged 7.7 and it was concluded this was as a result of mixing of the two waters.

Alkalinity can be used as an indicator of biological activity, Bundschuh and Zilberbrand (2011), reported a decrease from more aerobic activity due to the extra dissolved CO₂ produced whereas alkalinity increased during anoxic and anaerobic conditions from both deamination of organics, producing ammonia and bicarbonate generation from denitrification as shown in the equation below.



Bicarbonate (HCO_3) is the major form of alkalinity at neutral pH and concentrations of bicarbonate in all the water samples tested, including the treated water, averaged around 350 mg/l. These relatively high levels act as a buffer via calcite and ammonium carbonate to stabilise pH.

Conductivity

The conductivity of the native water was 1700 $\mu\text{S}/\text{cm}$ greater than the recycled water which was 1500 $\mu\text{S}/\text{cm}$. This was due to the high SO_4 content (600 mg/l) in the native groundwater (see section 2.2.1, Regional Geological Setting). The percolated water below the pond showed a 10-15% decrease in sulphate compared to the fresh effluent, which could have been due to adsorption to the soil, anaerobic reduction or biological uptake. Sokolova and Alekseeva, (2008) reported on the capacity of soil to adsorb sulphates by ion exchange but also noted anion exchange mechanisms in soils were less understood than those for cations.

Suspended Solids

The treated wastewater effluent SS was on average 16 mg/l; but analysis of the pond water showed a wider range and this was attributed to the biological productivity in the ponds. The patterns of SS in the pond water were reflected in the percolated water and the main concern was, therefore, clogging of the infiltration system. The suspended solids generated were usually removed via straining by the soil matrix, and it was concluded that they posed little environmental or health risk.

The turbidity tests conducted showed no statistical differences between the percolated water and the native groundwater. NTU ranged between 1.5 and 1.8 an almost clear water.

E. Coli CFU/100ml

In the recharged effluent E.coli was less 500/100mls but numbers increased in the pond water in line with algal and plant productivity providing additional nutrients. The highest value recorded was 10000/100mls. E. coli counts in the percolated water samples also increased in line with the plant growth in the pond water but were reduced by passing through the soil. E. coli counts sampling wells adjacent to the pond ranged from 100 to 380 CFU/100mls and none were detected in the groundwater abstracted. It is however possible for the bacteria and other pathogens to survive for days and be small enough to pass through the vadose zone. Pathogens may move vertically or horizontally through preferential flow paths and there are many documented cases of bacterial contamination of groundwater via this mechanism (Weiss, et al., 2008). Few studies have examined the efficiency of infiltration practices on the full range of pathogenic indicators (e.g. faecal coliforms, viruses, and other bacteria) and further work is needed.

4.9 Conclusions

It was shown that the nitrate concentrations through the vadose zone was less affected by denitrification than suggested by previous work because of the high quality of the sewage effluent in terms of assimilable carbon and consequent oxic conditions. The drying and rewetting processes did introduce oscillations of soil oxygenation but this was insufficient to generate a similar alternating sequence of aerobic and anoxic microbial activities given the low concentrations of BOD and nitrate in the soil and water column.

The soil pores and the unsaturated conditions in the vadose zone were shown to provide a readily replenished supply of dissolved oxygen to the groundwater, (where the oxygen concentration was limited to approximately 10 mg/l at 20°C, by the average temperature of the shallow groundwater). It was concluded that reaeration was via the superficial, shallow deposits of

sands and gravels in the Ezousas aquifer. These results corroborate previous work which also reports denitrification rates in the unsaturated zone of many aquifers is low except where air exchange is limited by low permeability lithologies or where there are high concentrations of organic wastes or other electron donors, (Buss, et al., 2005).

Some evidence of denitrification was observed in the long cycle recharge with high water contents over long periods. These results did confirm the previous work on stagnant, immobile, water in vadose zones which is often anaerobic and vulnerable to organic matter in the recycled water compared to more dynamic conditions of the short cycles which respond to atmospheric conditions (Kohne, et al., 2006).

The growth of plants and accumulation of debris in the long cycle pond experiments also increased the overall concentration of nitrate in the infiltration water compared to the short cycle recharge, providing further evidence of excess oxygen.

The importance of this finding was that limited denitrification took place even in the stagnant water areas of the vadose zone, suggesting the majority of the nitrate-nitrogen transport occurred through preferential flow paths, where no significant denitrification took place. Preferential flow paths, which are responsible for most of the water and solute transport from the root zone to the water table, quickly flushed nitrate into deeper portions of the vadose zone and the water table, allowing for little or no denitrification.

It was also concluded that this accelerated water flow, transported through preferential routes or from unsaturated water conditions could transport other contaminants from the vadose zone and that these faster travel times would be faster than would be estimated from column experiments or models under

uniform flow conditions. More rapid travel times than expected were noted by Harter (2005) who suggested this would reduce the potential for denitrification and decrease natural attenuation of certain pollutants such as persistent organic pollutants.

Therefore from the results it was possible to recommend that other methods of recharge, such as deep well injection could be investigated if the recharge water quality was high but further work on the impact of persistent pollutants would be needed.

Overall, therefore the quality of the treated water is most important but the variability of controlling factors, such as soil and aquifer geochemistry, makes the generic prediction of the rates of denitrification and transport of pollutants, from the work conducted here difficult. This was also the predominant conclusion in the literature. Korom (1992), in a review of research on denitrification, concluded that, "our current capabilities to predict an aquifer's denitrification characteristics are site specific at best." Debernardi, et al, (2008) suggested that neither single parameters nor vulnerability methods (groundwater occurrence, depth to groundwater table, lithology of aquifer or aquitard (Foster, et al., (2006)); and time of travel, (Zampetti, (1983)) used separately were able to describe the complex phenomena affecting nitrate concentrations in soil, subsoil and groundwater. It can be concluded however, that denitrification rates are commonly low and occur only after or with high concentrations of organic matter or with long residence times or flowpaths in the vadose zone, (Hoffman and Canace, 2001).

CHAPTER 5

GEOCHEMICAL CHANGES IN GROUNDWATER FOLLOWING RECHARGE

Chapter Summary

This Chapter reports on the research of the hydrogeochemical changes in groundwater chemistry following recharge of the Ezousas Aquifer with treated sewage effluent as a Storage and Recovery (ASR) Case study. Groundwater samples were analysed to monitor the variations in water chemistry at different points in the aquifer. These data were used to trace geochemical interactions between the recharge water and natural geology.

It was concluded that the main hydrochemical process affecting the hydrochemical characteristics of the groundwater was simple mixing of the two waters, native groundwater and recharge (recycled, tertiary treated effluent). The results also suggested that there were several other but minor influences on the final water quality including mineral dissolution/precipitation and ion-exchange at specific locations in the aquifer.

The groundwater chemistry was shown to change from one dominated by Ca-SO₄-HCO₃ to Ca-Cl as the most important result of the mixing between the ground and recharge waters. The PHREEQCI equilibrium geochemical model was applied to predict how these different geochemical processes mixing, precipitation and dissolution of the key minerals would be expected to change in the groundwater chemistry. The saturation indices (SI) calculations, from the model, suggested that groundwater would be expected to be saturated with carbonate minerals like calcite (CaCO₃), dolomite [(CaMg(CO₃)₂], aragonite (CaCO₃) and the Fe minerals such as ferrihydrite [Fe(OH)₃], hematite (Fe₂O₃) and goethite (FeOOH). The mixed groundwater following recharge, was predicted and found to have a lower sulphate concentration than the native groundwater which was a gypsum aquifer. This was beneficial to the quality and usability of the recharged groundwater but the salinity was still too high for

all types of crops, even after mixing with native groundwater. It was recommended therefore that it be used with caution and care for irrigation.

5.1 Introduction

Aquifer storage and recovery (ASR) is a type of managed artificial recharge (MAR) and defined as where water is recharged into an aquifer during periods of low demand and then recovered during periods of high demand. The quality of the recharge water available for groundwater replenishment can be used to influence both the operation of the recharge facility and the use to be made of the recovered water.

The ASR recharge water described in this research project was based on the storage of treated wastewater from the Paphos sewage treatment plant in the Ezousas alluvial aquifer. This aim was to ensure water availability during the peak irrigation season. This was predicted to be a more cost-effective and sustainable, alternative water-supply than desalination to help meet agricultural, municipal and recreational needs as well as benefiting ecosystem conservation. The design capacity of the recharge system was 19500 m³ /d, fixed by the size of the pumps used to fill the ponds. This water was re-abstracted downstream for irrigation without any restriction in its application.

A key question for this and any ground water recharge project was the potential influence of water quality as a result of interactions in the unsaturated and saturated zones of the aquifer. When waters with different pH, redox potential and ionic strength are mixed there is instability in the contact zones until equilibrium is achieved. Different recharge pathways were also possible from variations in aquifer geochemistry.

Water chemistry data obtained by sampling groundwater wells and recharged water were entered into the software AqQA (Version 1.1.1) available from RockWare, Inc. and Microsoft Excel (2007) for analysis and plotting using Piper diagrams and bivariate graph analysis. Piper diagrams use ionic percentages in lieu of concentration values and were selected because they simplify screening, sorting and interpretation of large chemical data sets. Furthermore, a Piper diagram can define the patterns of spatial change in the water chemistry in geological units, along a line of section or flow path (Domenico & Schwartz, 1998; Mohammad and Hamed, 2011). Bivariate plots (or scatter plots) show the relative concentrations of two constituents from different samples. These plots were useful for visualizing trends in the data, and for illustrating evolution in ground water chemistry. The water chemistry data were also input into the geochemical modelling program PHREEQCI v.2.17.5.4799 (Parkhurst and Appelo, 2010) to predict aqueous speciation in order to suggest possible chemical reactions in the aquifer and to assess the state of equilibrium between groundwater and minerals present. The results of the geochemical modelling was used to corroborate the role of mixing and the spatial pattern of the aqueous chemistry in the aquifer.

Down-gradient changes in chemistry from the field-scale data and groundwater quality were used to predict the geochemical processes taking place. Reaction kinetics and equilibrium conditions were then inferred from the water-rock interactions observed. Parameters analysed included the affects of residence time on solubility and precipitation as influenced by; carbonate and non-carbonate; redox; cation exchange and salinity reactions in the aquifer.

The literature reviewed indicates every site is unique with respect to lithology and hydrogeology and evidence from one site is not always a prediction of impacts at another site but it was possible to draw general conclusions from the research described in this thesis.

5.2 The Aim

The overall aim was to use the analysis of the controlled, site specific conditions to develop a better fundamental understanding of the complex qualitative and quantitative interactions between ground water and recharge.

The objectives of this section of the research was to investigate the changes in natural minerals in the aquifer as a result of the recharge excluding nitrate which is discussed separately in Chapter 4. The analysis of these changes were then used to assess water re-usability and the possible changes in physical characteristics of the aquifer.

5.3 Literature Review

Hydrochemical Interactions

Examples of water quality changes, during flow through the aquifer and according to geology have been widely reported. Glynn and Plummer (2005) recommended a procedure for the interpretation of the geochemical groundwater processes based on chemical data and model simulations. Possible reactions reported included changes to the carbonate equilibrium, redox and ion exchange. Groundwater geochemistry as a whole, was considered too large a field to review here and only aspects relevant to the interpretation of the results of the recharge have been referred to. This problem is more extensively discussed in Johnson and Bush (1988) and Allen and Matsuo (2002).

Major Geochemical Processes

The most common hydrochemical interactions in groundwater systems resulting from the chemical changes noted above (carbonate equilibria, redox and ion exchange) are: (1) dissolution of aquifer minerals toward a new equilibrium as groundwater moves from recharge to discharge areas; (2)

mixing of groundwater and recharge water and (3) cation exchange between water and aquifer minerals (Johnson and Bush, 1988). These processes may act independently, but more commonly interact with one another (Allen and Matsuo, 2002).

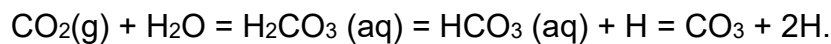
Changes in the Carbonate System Influence on Solubility

The chemical weathering of rock by water erodes minerals solubilising ions (e.g., Na, Ca, SiO₂, and SO₄). This enriches relatively soft upland surface water with total dissolved solids at a rate and to a degree which depends on local conditions. These would include: 1) the relative solubility of the minerals, 2) the temperature and pH of the water, 3) the specific activity and surface area available for ion exchange, and 4) the residence time.

Calcite and dolomite are commonly at equilibrium concentration in groundwater and reactions with these minerals are usually dominant (Chidambaram, et al., 2010). Deutsch (1997) proposed a saturation index (SI), to predict the interactions between strata and groundwater when it was not feasible to collect samples of the solid phase for mineralogy analysis. The SI is defined as the logarithm of the ratio of the ion activity product (IAP) of the ions in solution to the solubility product K for the solid phase ($SI = \log(IAP/K)$). Negative and positive SI values indicate under-saturation and over-saturation, respectively. If the groundwater becomes saturated with respect to a mineral, it will precipitate some of the solute load and on the other hand, if it is unsaturated ($SI < 0$) it will dissolve more mineral into the solution.

In this thesis the chemical equilibrium between minerals and water SI was calculated using the PHREEQC1 geochemical model selecting the constituents input into the model data based on actual groundwater analysis.

The solubility of calcite means that this is usually the dominant source of dissolved calcium in natural waters. It is also one of two sources of dissolved inorganic carbon the other is CO₂ produced from organic decay (Drever 2005). Changes to the carbonate equilibria are usually the dominant influence on water chemistry. The speciation of inorganic carbon depends on a pH controlled interaction between CO₂ (gas), carbonic acid (H₂CO₃), bicarbonate (HCO₃) and carbonate (CO₃), as shown by following equation:

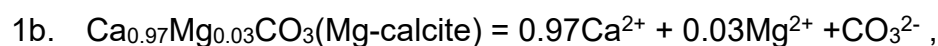


At the pHs commonly encountered in groundwater (6.5-9.1), HCO₃ is the dominant carbonate species present. The lack of CO₂ sources in unadulterated groundwater, means that the carbonate equilibrium is shifted by the consumption of H₂CO₃ by the mineral dissolution reactions (especially calcite (CaCO₃) and dolomite (CaMg(CO₃)₂). The dissolution of these carbonate minerals releases the cat ions and bicarbonate and raises the pH of groundwater.

The carbonate equilibria are controlled by mineral saturation and (or) cation exchange. The important reactions are:



$$\text{Log } K_{25\text{ }^\circ\text{C}} = -8.48$$



$$\text{Log } K_{25\text{ }^\circ\text{C}} = -8.60$$



$$\text{Log } K_{25\text{ }^\circ\text{C}} = -17.09$$



$$\text{Log } K_{25\text{ }^\circ\text{C}} = -4.602$$



$$\text{Log } K_{25^\circ\text{C}} = -8.60$$

Where K is the solubility constant at equilibrium at 25 °C and Ex is the cation-exchange site on the solid phase.

In the absence of other minerals, the concentrations of Ca, Mg and HCO₃ will increase until the groundwater becomes saturated with calcite and dolomite and dissolution ceases.

Cation Exchange

Water, because of its high dielectric constant, is an excellent solvent for most inorganic salts, not just calcium and magnesium (Inglezakis and Loizidou, 2007).

Mixing or change of conditions in the aquifer, such as recharge, promotes ion exchange reactions between the groundwater and the aquifer material, which progressively alters the chemical composition of the water. The ion-exchange process can be conceptualized as the preferential adsorption of one ion with the displacement of another from the surface. This exchange process can be treated as an equilibrium process. The general order of cation exchangeability for the common Group I and II elements in groundwater has been found to be:

Li<Na<K<Rb<Cs and Mg<Ca<Sr<Ba.

The divalent ions are more strongly bonded and tend to replace the monovalent ions (Rashid, et al., 1972). The sequence is reversible however at exceptional concentrations of the monovalent ion (Raju, et al., 1993).

Dispersed clay material within an aquifer releases sodium, in exchange for calcium and generates dissolved sodium bicarbonate. The degree to which the exchange of Ca (and Mg) with Na occurs is dependent on the parameters noted: pH, temperature, the specific surface area and its cation exchange capacity (CEC). CEC varies for different clay minerals e.g. mudstone and zeolites, residence time, partial pressure of CO₂ and the mineral concentrations (Lipson and Stotzky, 1983; Allen and Matsuo, 2002).

The governing equation for the distribution of sodium and calcium on a clay mineral surface will be in the form of:

$$[\text{Ca}_{\text{clay}}] / [\text{Na}_{\text{clay}}]^2 = K ([\text{Ca}] / [\text{Na}]^2)$$

[Ca_{clay}] and [Na_{clay}] refer to the “activities” of calcium and sodium (related to concentrations) on the clay exchange sites; [Ca] and [Na]² refer to the “activities” of calcium and sodium ions in the groundwater and K represents the equilibrium constant.

Simple Mixing

The last of the major process that can influence chemical evolution in groundwater is the degree of mixing and its promotion by effluent recharge. In this thesis, mixing was defined as the simple combining of two waters with different chemical or physical characteristics without reactions. The resulting water composition would then be a hybrid of the two compositions being mixed, with a chemical composition representing a mass balance of the two contributing waters.

There may however be non-linear solubility as a result of variables discussed: salinity, partial pressure of CO₂, temperature, and ionic activity. The activity coefficient of an ion is also not necessarily a linear function of ionic strength

and concentration. Mineral solubility can also be controlled by new reactions and complex formation (thermodynamic potentials) as a result of mixing even if both are saturated. The influence of the carbonate system is typical. For example if two solutions having different CO₂ partial pressure (pCO₂) values are mixed there is a complex redistribution of all the inorganic C- species in the mixture. Often the resulting mixture turns out to be unsaturated with respect to the carbonate minerals because of complex formation. The possibility of these combined influences (reactions and mixing) makes the result of mixing of two waters difficult to predict using any standard models (Herman et al. 1985). In this case study there was the extra complication of reactions and preferential flow paths as the recharge water from the infiltration ponds passed through the vadose zone to gradually mix with the native groundwater. This process may be accelerated in certain zones by the extraction of groundwater (Allen and Matsuo 2002).

5.4 The Recharge Water

The Ezousas Aquifer Storage and Recharge Project (ASR) was conceived in 2003 to store treated effluent from the Paphos Sewage Treatment Plant (PSTP) for potential recycling. It was hypothesised that this would be an alternative, more cost-effective and sustainable raw water-supply. Agricultural, municipal and recreational water demands for the area were increasing whilst avoiding further abstractions from the river basin. Previous work had established that there had been a deterioration in the Ezousas ecosystem as result of the cut-off of its head waters by the construction of the Kannaviou dam.

Currently the PSTP can recharge between 9000-12000 m³/day of treated effluent via 23 infiltration ponds organized in groups of between two and six depending on the local space available. The recycled water is pumped and distributed via 500mm, pressured mains to each infiltration pond. Each infiltration pond is 40x50 m with a minimum depth of 1.5 m which otherwise

follows the irregularities of the ground level. Overflow is at 0.4 m which is the estimated head needed to give a 5-7 day wet/dry cycle. Controlled recharge/abstraction takes place in the lower section of the aquifer, thus providing a semi-closed system for the research and analysis of groundwater quality dynamics.

The infiltration/percolation rate is 0.6-0.80 m/day, so that the infiltration ponds can use all the output from the PSTP and recharge the aquifer through the non-agricultural season. Annual infiltration amounts or hydraulic loading rates (flow per surface area) typically vary from 60 to 90 m/year, depending on soil, climatic conditions, quality of sewage effluent, and abstraction rates.

5.5 Methodology: Sampling and Analysis

Samples were collected quarterly for five years (2005-2009) from selected sampling points in the system:

- Samples of treated effluent were collected from the inlet to the infiltration ponds.
- Representative native ground water was sampled from monitoring well BH4031 (Figure 4.2) which was located approximately 600m up-gradient of the ASR ponds. BH4031 had a 125 mm (6 inch) casing and penetrated all of the alluvium down to the bedrock at 28m.
- Samples of mixed native and recharged water were collected from the production wells BH3026, BH2996, BH3025 and BH2954 which were located along a section, 2 km down-gradient from the infiltration ponds. These were used to study the down-gradient evolution in hydrochemistry and geochemical processes involved. These were expected to be carbonate and non-carbonate reactions; redox processes; cation exchange and salinity as a function of residence time, pH, dissolution and precipitation.

The borehole locations are shown in Figure 4.2.

1 litre or 500 ml polyethylene sample bottles were used for ion analysis and metal analysis respectively. The sampling bottles were thoroughly rinsed 2–3 times using the groundwater to be sampled and care was used to avoid any air being retained in the bottles. Prior to collecting the native water samples, the well was flushed with approximately three casing volumes. Following this flushing period, the discharge was reduced to maintain steady flow for sample collection. Samples from the bore holes were collected after pumping the water for 10 minutes, for the open wells, water samples were collected 30 cm below the water level using a depth sampler.

These samples were immediately stored on ice and in the dark and processed upon arrival at the laboratory, a commercial laboratory and the Cyprus State laboratory were used to ensure analysis within three hours of collection. In either case International Standard methods of analysis were used (APHA, 2005)

Sensitive parameters such as pH, Eh, temperature, conductivity, alkalinity and oxygen content were measured in situ during the sampling with the usual electrochemical probes or field titration. DO, pH, conductivity and temperature were measured using a WTW OXI330i/SET, WTW pH330i/SET and WTW COND330i/SET respectively. Total alkalinity was measured using a Aquamerck 1.11109.0001 field alkalinity test kit. Several but at least triplicate titrations for total alkalinity were done to ensure repeatability. Dissolved nitrate was also measured in the field with a HACH DR890.

The physico-chemical data of water samples from the Ezousas recharge area are summarized in Table 5.1. The analytical precision for the ion measurements was as reported in the standard methods and determined by calculating the ionic balance. The error was generally better than 5%.

The total concentrations of major elements (Na, K, Mg, Ca, Cl, HCO₃, SO₄,) and the trace elements (B, Ba, Fe, Cr, Cu, Mn, and Zn), the nutrients (NO₃, PO₄) and the dissolved oxygen were used for thermodynamic modelling of the inorganic chemical species in the groundwater using the PHREEQCI v.2.1 ion association computer model.

5.6 Results and Discussion

5.6.1 Major Ion Chemistry and Identification of Hydrogeochemical Processes of Ground Water

Water samples were collected quarterly for 5 years from 11 sampling points located along a 8 km longitudinal section of the Ezousas aquifer and analysed for 22 physico-chemical variables. The average and mean values of these data are presented in Table 5.1.

The findings were analysed to answer the following research questions:

- What were the water quality variations when benchmarked against international standards for irrigation and drinking water.
- To understand the interactions of the hydrogeochemical rock characteristics on water quality.
- The degree of saturation with respect to the key minerals expressed as changes to their solubility and or precipitation within the system.

The water chemistry data were analysed by using the software package Rock Ware Aq.QA (version 1.1.1) to provide information about water type, SAR and partial pressure of CO₂ (pCO₂). This program also offers various plotting options. Piper plots were selected because they have been found to be useful for depicting the effects of mixing different water qualities (Cates, et al., 1996), with the results are shown in (Figures 5.1a and 5.1b). Two waters of different

quality (referred to as the end members) are plotted as separate points in each of the three zones of the aquifer (Figures 5.1a and 5.1b). Concentrations should be on a line connecting the two end members (referred to as the mixing line). However, ionic constituents in subsurface groundwater will be subject to the reactions described and will then deviate from the mixing line (Cates, et al., 1996).

The example plot shown in Figure 5.1a and 5.1b, are the major ions from sampling on the 23/05/2008 and 11/03/2009 and are the data shown in Table 5.2. These sampling dates were deliberately selected as representative of the range of hydrologic conditions in the river basin. During the hydrological year, Nov/2007 - Oct/2008, there was a regional drought and nothing drained into the Ezousas river, whereas in the hydrological year, Nov/2008 -Oct/2009, the opposite happened, there was heavy rain and the river flowed throughout the season from December to May.

Table 5.1: Basic water chemistry statistics from about 50 groundwater and treated effluent samples recharged from 2004-2010

Ion, (mg/l)	BH4031			BH3026			BH2996			BH3025			BH2954			BH4029			PWWTR		
	Average	Median	STDEV	Average	Median	STDEV	Average	Median	STDEV	Average	Median	STDEV	Average	Median	STDEV	Average	Median	STDEV	Average	Median	STDEV
Cond. (µS/cm)	1786	1723	161	1623	1570	210	1509	1478	161	1527	1489	166	1471	1448	107	1447	1420	126	1484	1419	200
pH	7.5	7.4	0.2	7.7	7.7	0.3	7.5	7.5	0.2	7.5	7.5	0.2	7.6	7.5	0.3	7.3	7.3	0.3	7.7	7.4	0.7
Total hardn. as CaCO3	798	800	95	620	620	99	505	505	33	542	550	59	544	535	46	554	563	70	291	285	25
Cl-	129	124	12	157	151	21	192	182	42	192	186	35	158	151	25	151	155	28	228	213	42
SO4=	600	608	118	453	459	86	272	266	37	289	277	60	328	335	54	289	304	55	175	171	23
CO3=	0	0	0	1	0	2	0	0	0	0	0	0	0	0	0	0	0	0	3	0	9
HCO3-	321	336	22	288	323	66	332	342	24	316	342	75	302	317	49	354	365	25	311	320	47
NO3-	3	3	1	7	7	3	13	13	5	15	14	5	12	11	3	10	8	6	11	12	3
P- Total	0	0	0	0	0	0	0	0	0	0	0	0	0	0	0	0	0	0	2	2	2
Na+	110	108	8	134	126	17	147	137	25	134	142	25	116	110	20	110	108	20	207	210	12
K+	6	6	0	7	8	1	7	7	2	6	6	1	7	6	1	6	6	1	27	27	5
Ca++	241	242	19	180	180	32	147	147	10	157	157	21	163	166	19	165	170	19	63	64	4
Mg++	50	55	18	41	41	11	33	35	5	37	36	3	36	37	4	34	35	8	32	30	5
Cu	0.014	0.005	0.015	0.010	0.009	0.009	0.012	0.010	0.009	0.002	0.002	0.002	0.006	0.003	0.010	0.014	0.014	0.009	0.014	0.012	0.013
Zn	0.133	0.102	0.102	0.038	0.032	0.024	0.042	0.029	0.039	0.029	0.030	0.014	0.034	0.031	0.019	0.108	0.084	0.080	0.038	0.048	0.022
Pb	0.009	0.007	0.010	0.009	0.009	0.006	0.006	0.002	0.009	0.003	0.002	0.003	0.004	0.001	0.005	0.019	0.018	0.012	0.016	0.016	
Fe	1.889	0.300	2.959	0.729	0.169	1.404	0.766	0.232	1.000	0.182	0.127	0.196	0.199	0.077	0.253	1.796	0.739	2.505	0.260	0.228	0.139
Cr	0.016	0.006	0.018	0.004	0.003	0.003	0.002	0.002	0.001	0.002	0.002	0.001	0.002	0.002	0.001	0.016	0.007	0.029	0.003	0.002	0.002
B	0.515	0.410	0.258	0.392	0.368	0.122	0.321	0.285	0.128	0.363	0.321	0.122	0.279	0.251	0.088	0.312	0.220	0.159	0.395	0.335	0.107
Mn	0.126	0.106	0.095	0.033	0.024	0.023	0.022	0.022	0.020	0.021	0.021	0.027	0.048	0.048		0.227	0.135	0.238	0.066	0.058	0.038
Ba	0.055	0.044	0.033	0.044	0.048	0.016	0.035	0.036	0.021	0.035	0.033	0.022	0.047	0.043	0.022	0.045	0.043	0.023	0.033	0.033	

Table 5.2: Chemical analysis for major ions and micro-tracers

B/h Hydrological No	B/H4031		B/H3026		B/H2996		B/H3025		B/H2954		PSTP		River Flow
	03/11/2008	23/5/2009	03/11/2008	23/5/2009	03/11/2008	23/5/2009	03/11/2008	23/5/2009	03/11/2008	23/5/2009	03/11/2008	23/5/2009	23/5/2009
Conductivity (microS/cm)	1705	2020	1901	1874	1745	1574	1714	1558	1585	1537	1716	1467	1607
pH	7.4	7.5	7.2	7.7	7.2	7.6	7.2	7.5	7.5	7.7	7.3	7.7	7.6
Total hardness as CaCO3	575	885	640	758	465	505	525	480	505	585	323	275	640
Ionics, (mg/l)													
Cl-	124	138	200	160	253	182	231	191	142	182	262	204	93
SO4=	337	681	426	526	211	266	229	240	317	319	142	207	460
CO3=	0	0	0	0	0	0	0	0	0	0	0	0	0
HCO3-	305	290	336	339	345	342	342	345	360	287	366	339	296
NO3-	23	4	13	11	20	13	14	14	11	11	13	14	8
P-Total	0.037	0.6	0.121	0.224	0.305	0.05	0.037	0.014	0.521	0.153	0.517	0.01	0.012
Na+	98	115	166	134	183	143	150	149	146	110	218	218	98
K+	5.8	7.1	7.7	7.9	8.8	6.6	6.9	6.4	9.6	6.3	24.7	33.1	5.8
Ca++	220	246	188	217	154	147	151	139	150	170	67	60	203
Mg++	6	66	41	52	19	33	36	32	32	39	38	30	32
Micro-tracers, (µg/l)													
Copper, Cu	4.75	3.28	1.26	<DL	4.65	2.99	1.72	1.76	2.63	ND	1.43	<DL	1.1
Chromium,Cr	4.27	7.42	1.9	2.07	1.81	1.72	2.16	1.39	1.28	ND	1.44	0.59	<0.16
Zinc, Zn	273.5	33	32	9	38.5	20	49	10	56.5	ND	54	13	64
Boron, B	344.5	714	397	688	352	669	383.5	611	378.5	ND	331.5	519	377.5
Manganese, Mn	162	80	24	<DL	35.5	<DL	39.5	2	47.5	ND	58	33	64
Iron,Fe	300	1980	169	15	412.5	10	554	40	490.5	ND	228	140	337.5
Barium,Ba	58	24	58	20	59	9	63	10	70	ND	32.5	<DL	102
SAR	1.78	1.68	2.86	2.12	3.70	2.77	2.85	2.96	2.82	1.98	5.27	5.74	1.67
LSI	0.41	0.4	0.5	0.62	0.28	0.39	0.25	0.27	0.35	0.48	0.089	0.11	0.46

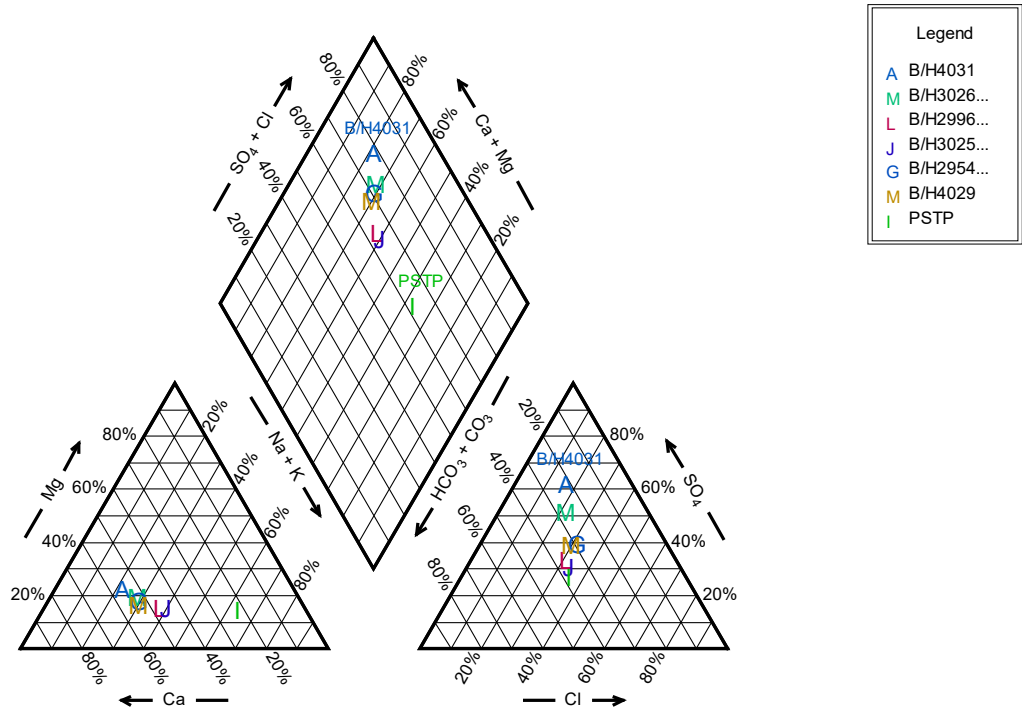


Figure 5.1a. Piper Diagram – Sampling 23/05/2008.

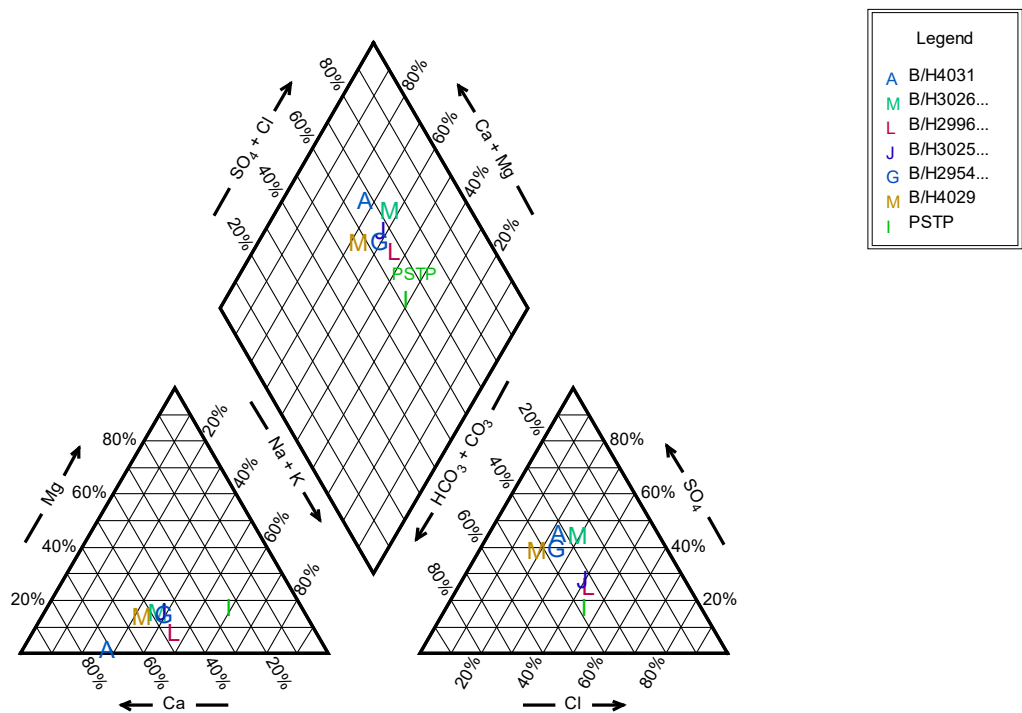


Figure 5.1b. Piper Diagram – Sampling 11/03/2009.

The Ezousas river water originates on the diabase and the pillow lavas of the Troodos mountain Ophiolites (Figure 2.2). Its headwater composition reflects the interaction of water with these rocks and is characterized as Ca-Mg-HCO₃ and Na-HCO₃. It has a low to moderate salinity (TDS 250–450 mg/l) and conductivities ranging between 330-600 μS/cm. Away from the pillow lavas the river flows over various sedimentary rocks composed mainly of clays, gypsum evaporites, chalks and marls. TDS and conductivity are elevated as a consequence to 840mg/l and 1900 μS/cm (range 1716 to 2020 μS/cm) respectively, and the pH becomes slightly alkaline (7.4~7.8). The hardness ranges between 753 ~885 as CaCO₃ and it would therefore be classed as very hard water (EU-DWD, 1998). The water shifts between a Ca-HCO₃ to SO₄-Ca or Ca-SO₄ dominance, depending on the seasonal hydrological conditions.

These are the natural influences on the water quality characteristics of the coastal alluvial aquifer or the native water as sampled from well BH4031 (see Figure 4.2). The anion concentrations were in the sequence SO₄>HCO₃>Cl, and the cation concentrations Ca>Mg>Na. The Ca concentrations were 219~277 mg/l and SO₄ concentrations 540~680 mg/l. the Ca-SO₄ from the gypsum. The water had a high ionic strength ($I=0.3\sim0.4$ where $I=1/2[\sum m_i \times z_i^2]$; m_i is molality; and z_i is the valence of each ion, i).

The tertiary treated effluent (PSTP) composition plot (Figure 5.1) shows Na-Cl as the major ions with a Na concentration of 190~218 mg/l and Cl concentration of 178~330 mg/l. The chloride was >18% meq and sodium >30% meq. The effluent ionic concentration gradient was Na>Ca>Mg: Cl>HCO₃>SO₄.

The conductivity was 1318~1743 μS/cm; and TDS about 1100 mg/l. The hardness as CaCO₃ was in the range 285~328 mg/l that is on average 1/3 of the native groundwater and would be classified as moderate hardness (EU DWD, 1998).

The mixing of the two waters, the native water and the tertiary treated effluent, was most captured at the BH3025 which was located 300m down-gradient of the recharge basin (see Figure 4.2).

The composite sample, BH3025 had a conductivity of 1530 μ S/cm, pH= 7.5; ionic strength I=0.25~0.27; and water hardness as CaCO₃ of 540 mg/l. These are all intermediate between the values of the native water upstream and the treated effluent recharge. Data analysis (values in meq/l) from this well compared to those of the native water indicated a reduction in SO₄ (50.2%), Mg (31.5%), Ca (20.2%), and K (96.7%) and enrichment with Cl (96%), Na (83.3%), HCO₃ (68.2%) and K (27.4%) as would be expected (see Table 5.3).

The Piper mixing plots between the end members in the groundwater and treated effluent predicted the shift from Ca-SO₄ to Ca-Cl as a result of the recharge with saline enriched effluent. The plot shows a shift from Ca-rich to Na-rich water type, which can be explained by an exchange of cations. A cation triangle has been set up which shows the evolution of Na-Cl to Ca-Cl water and then from Ca-Cl to Ca-SO₄ water type. The rapid change from SO₄.Ca- to Na-Cl water type meant that the cation exchange process was due to the recharged treated effluent changing immediately due to the native aquifer water. This pattern suggested that the downstream groundwater chemistry was controlled by simple mixing between the two end members.

Table 5.3. A summary of the charge proportions for the main anions and cations in relation to the three different water types defined for the Ezousas Recharge Project.

Meq/l	Paphos Effluent recharged	BH4031- Native water (N)	BH3025- Mixed zone (M)	(M-N)x100/N
	%	%	%	%
Cl	18.18	8.47	16.60	96.0
SO ₄	13.62	30.93	15.40	-50.2
HCO ₃	17.58	10.35	17.40	68.2
NO ₃	0.71	0.14	0.65	360.4
P	0.01	0.21	0.01	-96.7
Na	29.97	10.89	19.96	83.3
K	2.68	0.40	0.51	27.4
Ca	9.45	26.79	21.38	-20.2
Mg	7.81	11.83	8.10	-31.5

All of the monitoring wells down-gradient of the recharge system show a similar pattern of effect from the treated effluent recharged. The ions fall on the mixing lines of their respective Piper triangles. There was some deviation away of the ideal mixing line in the upper diamond which could be attributed to a solid phase ion exchange mechanism.

Attenuation by dilution can also be assessed by comparing other conservative tracers such as bromide, chloride, sulphate, boron, tritium and conductivity, in the infiltration water compared to receiving groundwater. Plotting these ions,

as for example shown Figure 5.2 for Cl versus B, should show no or minor perturbations as a result of the mixing along the flow path. A small increase in chloride concentration was expected from the chloride in the recharge water but a slightly decreasing boron concentration as a result of dilution from the groundwater.

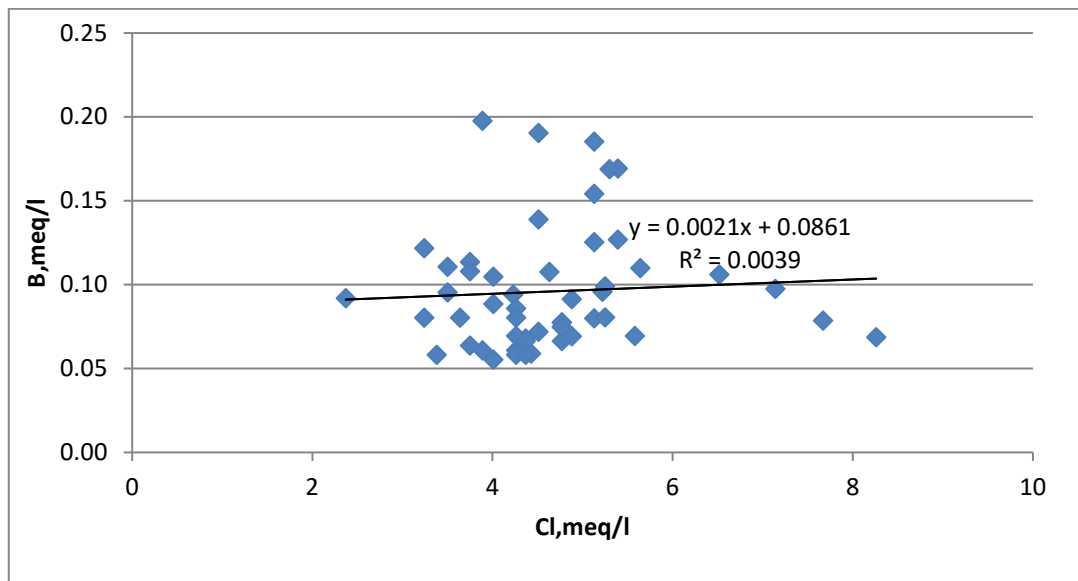


Figure 5.2 Cross-plot of B versus Cl indicating Cl elevated but slightly increasing B

Sulphate content in aquifer groundwater decreases downgradient of the recharge as shown in Figure 5.3 until equilibrium is reached at around 250m downstream. The reduction in sulphate was attributed to dilution by the treated effluent. The slight increase in sulphate concentration within wells BH2954 and BH4039 was attributed to preferential hydraulic pathways for the native water.

For microbial reduction of sulphate to sulphide to occur, a negative redox potential, (Eh of -200 mV and neutral pH, Weiner, 2000) would be required whereas the redox potential in the groundwater was positive and oxidising. The Ezousas aquifer has a DO range from 5 to 8mg/l, and consequently the Eh is 150-250mV and pH is 7.3-8.0. Sulphate reduction could take place in

some limited anaerobic pockets but no sulphide was detected in any of the samples analysed.

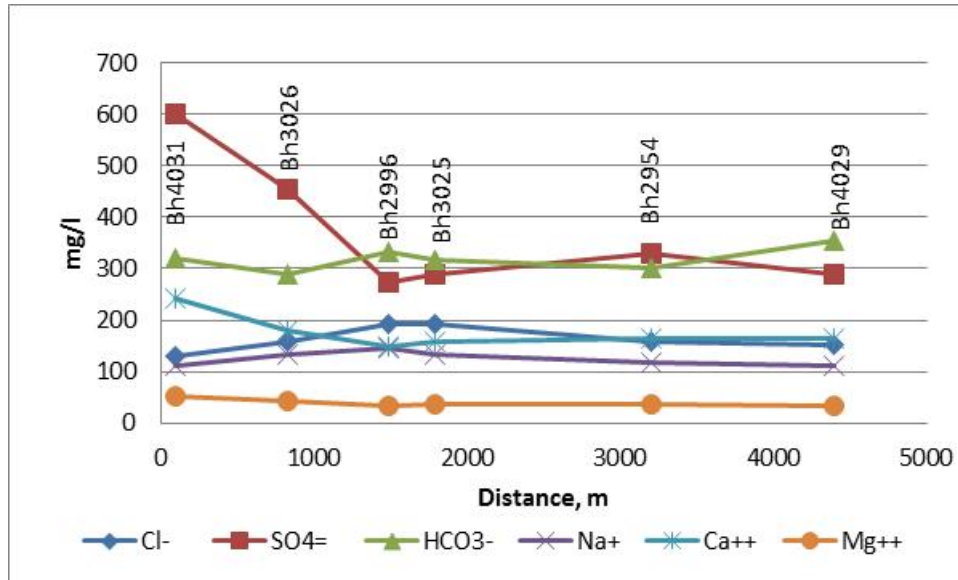


Figure 5.3 Chemistry along groundwater flow-path

Although, the Piper diagrams can identify the major distributions of pairs of ions, they are less useful for comparing several materials at once. Simple X-Y Excel plots were also used to evaluate the ion ratios.

Figure 5.4, shows the important ratio of Ca-Mg versus SO₄-HCO₃ which should be close to unity if the dissolution of calcite, dolomite and gypsum are the dominant reactions in a system (Arehart and Hulston, 1998). In this case, also shown in Figure 5.4, there is the possibility of a deviation at higher concentrations suggesting ion exchange could also be occurring according to the work by Arehart and Hulston, (1998) but this would need more data.

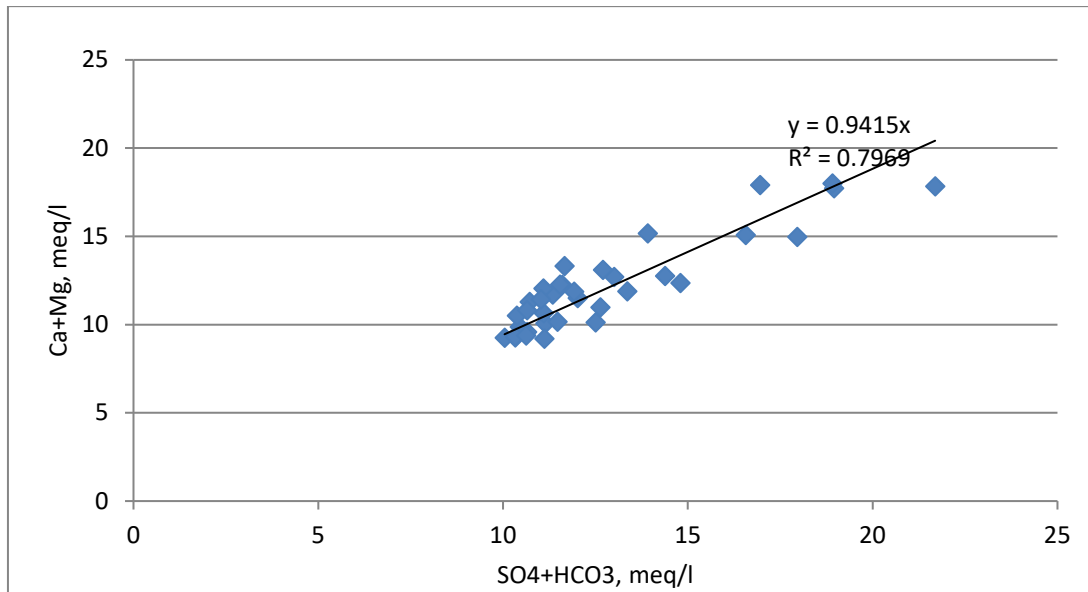
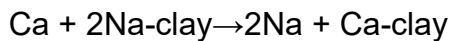


Figure 5.4 (Ca-Mg vs SO₄-HCO₃) scatter diagram showing carbonate dissolution

This corroborates the earlier evidence from the Piper analysis that the attenuation of cations was also affected by some cation-exchange as well as dilution.

Figure 5.5 shows the relationship between Ca and Na and the low Ca/Na ratio has previously been attributed to both ion exchange and/or the precipitation of calcite (Rose and Long, 1989). Rose and Long (1989) suggested that ground water containing calcium ions reacts with clays according to the following equation:



The key minerals, Na, Ca, and Mg will reach equilibrium with the clays (Arehart and Hulston, 1998) but in this case there is evidence that saturation has not been reached and ion exchange was ongoing.

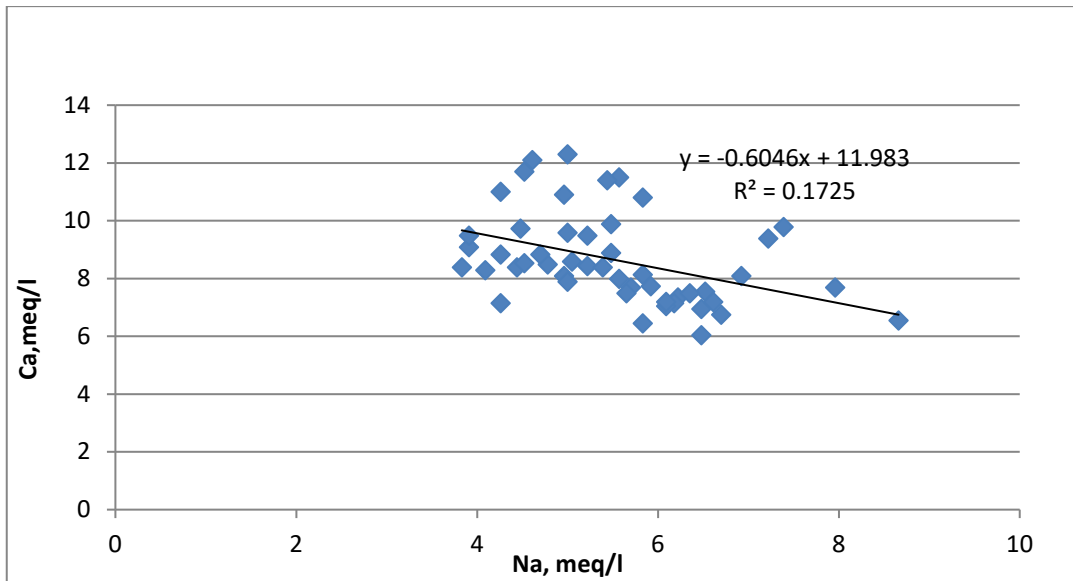


Figure 5.5 Na vs Ca scatter diagram showing increased concentration of Na compared to Ca that indicates reverse ion-exchange.

Nitrate concentration increases down gradient of the infiltration ponds up to the BH3025 (Figure 5.6). This was attributed to the decomposition of 'organic' materials accumulating in the sediment at the bottom of the ponds noted in chapter 4 of the thesis. The operational mode of wet/dry cycles provided excess oxygen for nitrification of organic nitrogen and ammonia in the sediment. The NO_3 passes through the unsaturated zone and enters into the groundwater. Nitrate will be stable in aerobic ground water where there are no organic substrates, such as the Ezousas. It was concluded that the attenuation of nitrate was from simple dilution with the native water.

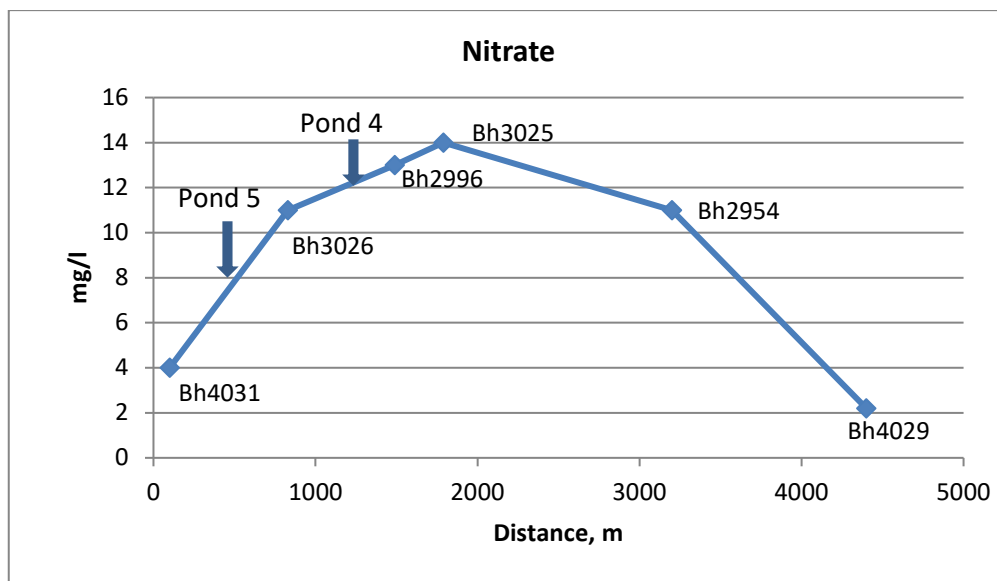


Figure 5.6 Nitrate concentration along groundwater flow-path

Nitrate analysis of water from BH2954 and BH4029, which are located 1100m and 2000m respectively down-gradient from the recharge system, indicate that the groundwater returned in its original proportions (Figure 5.6). Thus, BH 2954 shows $Ca > Na > Mg$: $SO_4 > Cl > HCO_3$ and BH4029 $Ca > Na > Mg$: $SO_4 > HCO_3 > Cl$ which match the native water at the BH4031.

5.6.2 Geochemical Modelling of Water-Mineral Equilibrium

Water quality changes from water-rock interactions and mixing from the recharge scheme were interpreted using the PHREEQC geochemical computer program (Parkhurst and Appel, 2010). The total concentrations of the major elements (Na, K, Mg, Ca, HCO_3 , SO_4 , Cl,), the trace elements (Fe, Mn, Cu, Zn, B and Ba), the nutrients (NO_3 , PO_4) and the dissolved oxygen were thermodynamically modelled. The calculated saturation indices for the different groundwaters with respect to the minerals, ionic strength, partial pressure of CO_2 (pCO_2) and the activity of dominant aqueous species are presented in Table 5.4. The program also predicted the possibility of forming multi-ion complexes as well as the simple ions, (Kania, 2003).

The water samples collected on May 23, 2008 and on March 11, 2009 were chosen for the modelling applications as representative of drought and spate as explained before.

Most of the changes predicted by the model involved the inorganic carbon balance of the water. For example sodium and chloride were present simply as dissolved Na and Cl which constituted 98% the total present. Dissolved inorganic carbon on the other hand is made up of free CO₂, bicarbonate ions (HCO₃) and carbonate ions (CO₃) (which together constitute the carbonate system). Carbon dioxide reacts with water to form carbonic acid, bicarbonate or carbonate depending mainly on pH. The model results confirm that the inorganic carbon present should be as HCO₃ (85-90%) with minor amounts of CO₂ and other carbonates (2.43x10⁻³ moles) as would be expected at the neutral pH. Normally the carbonate system composes the largest proportion of the total dissolved solids (TDS) within alluvial aquifers and usually exerts the major influence on natural water chemistry, regulating pH, alkalinity and hardness thereby affecting water quality.

Aqueous bicarbonate and carbonate are derived almost exclusively from reaction between water containing free CO₂ and the solid phase containing calcium (or magnesium) carbonate. Calcium carbonate, as a single ion, was shown to constitute about 80% of the calcium, followed by CaHCO₃ (15%), CaCO₃ (3%), and CaHPO₄ in minor quantities.

Equilibria in calcite - magnesite - and dolomite - water systems are therefore dependent on the partial pressure of carbon dioxide (Somasundaran, et al., 1985).

Carbon dioxide is obtained from the air or from decomposition of organic matter in the aquifer. Increased partial pressure of CO₂ near the surface of Earth increases the amount of CO₂ dissolved in water, therefore increasing the

solubility of carbonate minerals such as calcite. The $p(\text{CO}_2)$ also gives information on the degree of equilibrium between chemical weathering and atmospheric CO_2 (Gunter, 1998). The solubility of calcite is however, more sensitive to temperature (Gunter, 1998).

Table 5.4 Saturation Indices, (SI) for sulphates, carbonates and hydroxides facies in groundwater of the Ezousas Recharge Project.

Sample No	Date	Anhydrite	Aragonite	Barite	Calcite	CO2	Dolomite	Fe(OH)3	Goethite	Gypsum	Halite	Hematite	Hydroxy-apatite	Jarosite-K	Manganite	Siderite	Zn(OH)2	Ionic Strength	pCO2
BH4031	23/05/2008	-0.82	0.39	0.21	0.54	-2.15	0.79	3.19	8.83	-0.58	-6.43	19.74	3.8	1.54	-5.16	0.24	-3.43	0.415	0.0078
	3/11/2009	-1.05	0.34	0.46	0.49	-2.02	-0.3	2.22	7.93	-0.81	-6.52	17.84	0.08	-1.57	-5.1	-0.47	-2.64	0.298	0.0104
BH3026	23/05/2008	-0.95	0.64	0.08	0.79	-2.27	1.24	1.23	6.94	-0.71	-6.29	15.87	3.4	-5		-2.01	-3.71	0.383	0.0059
	3/11/2009	-1.06	0.07	0.5	0.21	-1.8	0.05	1.53	7.24	-0.83	-6.1	16.47	0.14	-2.76	-6.54	-0.74	-3.95	0.359	0.0173
BH2996	23/05/2008	-1.31	0.44	-0.42	0.59	-2.16	0.81	0.99	6.7	-1.07	-6.19	15.39	0.55	-5.99	-6.45	-2.04	-3.48	0.294	0.0076
	3/11/2009	-1.38	0.04	0.32	0.19	-1.78	-0.24	1.94	7.65	-1.14	-5.94	17.29	1.27	-2.01	-6.34	-0.32	-3.84	0.303	0.0180
BH3025	23/05/2008	-1.37	0.32	-0.4	0.47	-2.06	0.59	1.49	7.2	-1.13	-6.15	16.39	-1.61	-4.28		-1.34	-3.93	0.288	0.0096
	3/11/2009	-1.36	0.03	0.37	0.18	-1.79	0.01	2.07	7.78	-1.13	-6.07	17.55	-1.6	-1.68	-6.29	-0.19	-3.74	0.306	0.0178
BH2954	23/05/2008	-1.19	0.52		0.67	-2.33	0.98			-0.95	-6.31		2.62					0.305	0.0051
	3/11/2009	-1.23	0.36	0.53	0.5	-2.04	0.62	2.57	8.28	-1	-6.29	15.55	3.17	-0.63	-5.37	-0.24	-3.2	0.297	0.0099
PWWTP	23/05/2008	-1.75	0.17		0.32	-2.25	0.62		7.92	-1.51	-5.95	17.83	-2.74	-2.06	-4.95	-1.01	-3.52	0.264	0.0061
	3/11/2009	-1.86	-0.16	-0.05	-0.01	-1.84	0.02	1.91	7.62	-1.63	-5.85	17.23	0.82	-2.23	-5.83	-0.5	-3.52	0.272	0.0156
River flow	3/11/2009	-0.98	0.48	0.78	0.63	-2.23	0.73	2.52	8.23	-0.75	-6.65	18.44	-0.87	-1.03	-4.95	-0.58	-2.96	0.318	0.0065
	Max.	-0.82	0.64	0.53	0.79	-1.78	1.24	3.19	8.83	-0.58	-5.85	19.74	3.8	1.54	-4.95	0.24	-2.64	0.41543	0.0180
	Min.	-1.86	-0.16	-0.42	-0.01	-2.33	-0.3	0.99	6.7	-1.63	-6.52	15.39	-2.74	-5.99	-6.54	-2.04	-3.95	0.26423	0.0051
	Average	-1.3	0.3	0.2	0.4	-2.1	0.5	2.0	7.7	-1.0	-6.2	17.1	0.7	-2.3	-5.7	-0.8	-3.5	0.3	0.0106

The average $p(\text{CO}_2)$ of the Ezousas groundwater was measured as 7×10^{-3} atm. and 1.5×10^{-2} for the selected samples from the 23/5/2008 and 11/03/2009 respectively, these were higher than the $p(\text{CO}_2)$ of the atmosphere ($10^{-3.5}$ atm.).

The $p(\text{CO}_2)$ values (Table 5.4) for the wet year (11/03/09) were double those observed for the drought year (23/5/08), which was attributed to the extra recharge from the flowing water and a rise in the water-table close to the river bed. The water table in a normal year is usually about 8m below ground surface.

In a normal or dry year therefore the native groundwater is unsaturated for carbon dioxide although over-saturated with respect to carbonate species, although in equilibrium with atmospheric CO_2 (Table 5.4). It was concluded that the increasing carbonate was due to Ca concentrations from gypsum dissolution which caused calcite to precipitate. Calcite is one of the most common minerals deposited from water and calcite precipitation is a common process in aquifers. It will precipitate when either Ca or CO_3 is increased, or if the solubility product is reduced. All groundwater samples from the study area showed that the groundwater is super-saturated with calcite, which confirms the model predictions that calcite precipitation is one of the geochemical processes taking place in the alluvial aquifer. Other carbonate species were also supersaturated, including aragonite and dolomite. Siderite was unsaturated except for the native water from BH4031 where the high iron level gives rise to supersaturation.

Sulphate was the next most dominant species in all the groundwater samples. The dissolution and precipitation of gypsum can be expressed by the following chemical reaction:



The solubility expressed as the solubility product is:

$$K_{\text{gyp}} = a_{\text{Ca}} a_{\text{SO}_4} a_{\text{H}_2\text{O}} / a_{\text{CaSO}_4 \cdot 2\text{H}_2\text{O}(\text{s})}$$

Where 'a' indicates the chemical activity of the subscripted species. At 25°C, log K_{gyp} is - 4.58 (PHREEQC database, Parkhurst and Appelo, 2010).

In the case of SO_4 , most was as complexes (75%) 17% with CaSO_4 and 7% including MgSO_4 . Other species like Na_2SO_4 , K_2SO_4 , and FeSO_4 were insignificant contributions to the total concentration. The groundwater was unsaturated with respect to gypsum-anhydrite throughout the aquifer suggesting that the soluble Ca and SO_4 are not limited by mineral equilibrium. Thus it is unlikely that gypsum precipitation caused the observed reduction in predicted SO_4 . Significant sulphide precipitation was not thought possible given the redox conditions noted.

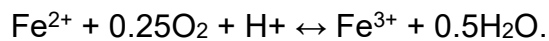
The results of thermodynamic speciation calculations for the aquifer indicate unsaturated values for the anhydrite, halite, Jarosite-K, manganite, siderite and $\text{Zn}(\text{OH})_2$ as well as gypsum in the groundwater. Thus the flowing groundwater should dissolve these minerals if they are present in the aquifer.

On the other hand, aragonite, barite, calcite, dolomite, $\text{Fe}(\text{OH})_3$, goethite, hematite, and hydroxy-apatite show positive saturation index (SI) values and are therefore capable of being precipitated from the groundwater.

Introducing iron content into the calculations, as either Fe^{2+} or Fe^{3+} , suggested the possibility of precipitating goethite, hematite and ferrihydrite from water. The PHREEQC geochemical model predicted near saturation of ferrihydrite and supersaturation of goethite and hematite. An increase in iron oxide precipitation is likely due to the sharp increase in the saturation indices of hematite and goethite in contrast to the decreasing saturation indices of other minerals in the alluvial aquifer (Parkhurst and Appelo, 2010). It was therefore

concluded that precipitation of iron oxides in the Ezousas aquifer were likely from the oxidation of soluble ferrous iron to insoluble ferric iron as a result of the aeration with the recharge water. In addition, the chemical analytes indicate a decrease in the concentrations of both total and dissolved iron further corroborating the conclusion that there was precipitation of hematite and goethite.

This has been reported via the following chemical reaction (Johnson and Bush, 1988; Hem 1989):



The supersaturation with mainly calcite and hematite, as discussed above, signals the precipitation of metals as carbonates which will change the composition of the solids along a flow path.

5.6.3 Possible Changes in Physical Characteristics of the Aquifer

The aquifer reactions discussed above suggest changes in the aquifer permeability could be occurring. The dissolution of aquifer rocks will increase the porosity and permeability of the aquifer, which could be the basis for the development of preferential conduits, whereas precipitation of new minerals has the potential for decreasing porosity and permeability. This latter process is more likely for compact or consolidated formations from fractures. The Ezousas aquifer is unconsolidated sedimentary alluvium, composed mainly of loose sands, gravels, alluvial grains, clayey sand, sandy clays and clays. This constitutes a porous and continuous medium and it was concluded that the precipitation within the aquifer would have a small and long-term effect on permeability. It was also possible to conclude that infiltration rates from the recharge ponds into the aquifer would be more affected by plant growth and organic precipitation within the ponds.

5.7 Irrigation Use

The proportion of Na to Ca and Mg has an important effect on the quality of irrigation water. The Gapon equation (White, 2006) shows that the proportion of exchangeable Na to exchangeable Ca and Mg ions is determined by the Gapon coefficient $K_{Na-Ca-Mg}$ and the molar concentration of (Na): $(Ca+Mg)^{1/2}$ in the water (White, 2006). In practice when concentrations are expressed in mmols /L, of recharge water the SAR is written as:

$$SAR = [Na^+] / \{([Ca^{2+}] + [Mg^{2+}]) / 2\}^{1/2}$$

The groundwater quality as irrigation water was compared with the literature based on electrical conductance and sodium absorption ratio (Burger and Celkova, 2003). This indicated that mixed groundwater was not ideal for irrigation because of the elevated salinity. In some areas, irrigation may require careful records and management to prevent build-up of crop-damaging salts in the soil. Calculated values of SAR are cited in Table 5.2.

Other irrigation water indicators were improved for example the native water has high sulphate concentrations (600 mg/l) which has been a problem, especially for citrus growing in the Ezousas area. Its dilution with recharge water has reduced the level to 300 mg/l and improved irrigation water quality.

Boron occurs in relatively low concentrations (average 0.4 mg/L) in both native ground water and after mixing with the treated effluent. Boron in irrigation water above 0.5 mg/L may be toxic to plants.

The chemical analysis data also provided warnings of potential problems, from scaling and corrosion to irrigation equipment (detailed in Section 6.2). Assessments based on the Langelier Saturation Index (LSI); an index widely used to indicate the potential for scale formation and accumulation from pH as

the master variable (Roberge, 2007). The calculation of the LSI confirmed the risk, but as with the sulphate and boron, the recycled water LSI (< 0.1) reduced the LSI and the mixed water LSI was 0.25 (Table 5.2).

5.8 Overall Discussion

It has been evident from the analysis of the potential geochemical changes that ground water quality would be expected to be different as a result of the recharge with treated effluent. The major change noted was on gypsum as the most soluble and the mineral at the highest concentrations in the native groundwater. The high level of Ca activity in gypsum-water systems would be expected to lead to precipitation of calcium carbonates and the iron salts; (goethite, hematite, magnetite and siderite). This was also predicted from the modelling calculations (PHREEQCI). This supersaturation, oxidizing conditions and precipitation of iron (oxides and hydroxides) are expected to contribute to corrosion and clogging of the abstraction, distribution systems and pumping facilities. Field observations and a simple test with sulphuric acid on bore scale showed that the deposits were superficially calcium precipitation.

It was possible to conclude however that, in general, reclaimed waters, when used for recharge, did not contain sufficient inorganics to cause concern. The recharged effluent should equilibrate with the local geochemical conditions without problems to the hydraulic properties of the aquifer. This conclusion was based on both the literature (Section 5.3) and the results from Section 5.6. The only recycled waters noted in the literature as likely to cause problems were those with unusually elevated salts, for example from industrial processing or desalination (Lefebvre and Moletta, 2006).

5.9 Conclusions

It was concluded that the main hydrochemical processes, following recharging ground water with treated sewage effluent were simple mixing, cation exchange and ion exchange between Ca (and Mg) and Na (and K). Geochemical mass balance modelling confirmed that the main chemistry of the groundwater was controlled by the calcium-ion.

The results of conductivity and dissolved ions analysis (including modelling) suggested the recharged water reacted with the native geochemistry to change the mineral equilibrium. The results showed precipitation, dissolution, sorption and desorption and ion-exchange (with gypsum, calcite and dolomite Section 5.6). Water composition, therefore, deviated from simple conservative mixing of the treated effluent recharge and native groundwater.

The native groundwater samples suggest that the solubility of gypsum caused high concentrations of Ca and SO₄. Super-saturation of groundwater samples with respect to calcite and dolomite are frequently reported in the literature as a result of the relatively high solubility of gypsum (Elgettafi, et al., 2012). Despite this and the fact that sulphate was the dominant ion in the groundwater, super-saturation did not occur in this case because of the kinetic competition from the other dissolved minerals. Variations in residence time would be expected to lead to different degrees of equilibrium between groundwater and the carbonate rock.

In this case it was concluded that the depletion of sulphate down gradient of the recharge ponds, was due to dilution with the recharge water. Redox potential and effluent quality were too high for microbial reduction. Iron and related inorganics could be removed by precipitation or as a consequence of changes in their redox state in a well aerated shallow aquifer like the Ezousas.

Most reclaimed domestic waters, would not be expected to contain sufficient inorganics to cause hydraulic, corrosion or salt toxicity problems. There was literature however noted in Section 5.5 that indicated limited reverse ion exchange reactions between sodium and calcium could take place in chloride dominated water types.

CHAPTER 6

FATE OF COPPER AND PHOSPHATE FROM TREATED EFFLUENT RECHARGE INTO THE AQUIFER

Chapter Summary

Managed Aquifer Recharge (MAR), as noted, is an attractive water management option, especially in semi-arid areas. Nevertheless, there are few reported field studies on the fate and transport of either potentially hazardous substances such as the heavy metals and persistent organics or priority pollutants such as the nutrients within the recharged aquifer. The aim of this project was to study the hydrological conditions of the coastal Ezousas aquifer and study its ability to attenuate pollutants from the treated effluent from the Paphos Wastewater Treatment Plant which was recharged into the aquifer through artificial ponds along the riverbed. The Ezousas riverbed is a locally important aquifer and the mixed native and recharged groundwater is abstracted for irrigation from downstream wells. The hydrological conditions of the river and aquifer were already modified by the construction of the Kannaviou dam in 2005. This has reduced the natural recharge of the Ezousas aquifer and allowed saltwater intrusion in the coastal region.

A three-dimensional finite element model of the area was constructed using the FEFLOW software program to simulate the groundwater flow and the transport of phosphorus and copper in the subsurface from the recharge process. The EU Water Framework Directive (EU, 2000) has suggested 75% of European waters are polluted by excess phosphorus. Copper was chosen as a tracer because of its relatively high concentration in domestic sewage and complex chemistry and solubility. The model was calibrated using hydraulic head and chemical data from

2002-2011. The groundwater model was coupled with a geochemical model PHREEQC to evaluate changes in water quality attributable to the mixing of the natural and reclaimed water. Inverse modeling calculations were used to determine reactions and phase changes in three marker pollutants phosphorus, nitrate (discussed in Chapter 4) and copper.

6.1 Introduction

Managed Aquifer Recharge (MAR) has become an important option in semi-arid areas to replenish raw water resources and buffer seasonal variation in water supply and demand. The alternative desalination is unsustainable in most countries. In coastal regions groundwater recharge with wastewater has also become a method of avoiding seawater intrusion. There are some detailed descriptions in the literature, for instance, the Tel Aviv re-use project (1.5 million inhabitants), injects 95 Mm³/year of treated sewage effluent into the coastal aquifer (Lazarova, et al., 2001). It was calculated that there was an attenuation and retention time of two months within the aquifer before re abstraction for agriculture. There are also EU precedents, for example Sabadell city in Spain where 6.9 Mm³/year are recovered from an otherwise dry River Ripoll for agriculture following infiltration with secondary sewage effluent into the aquifer. There was also an Italian case study reported by Lazarova, et al, (2001) from the city of Nardo where 4.4 Mm³/year were recovered following direct injection into a confined and fractured aquifer via a sinkhole. MAR is an attractive method of storing and to improve reclaimed wastewater quality in terms of traditional parameters for example salinity and bacterial counts but more work is needed on the newly emergent risks such as the priority substances according to Directive 2008/105EU. Data on the fate of metals and pharmaceutical or personal care products discharged into an aquifer are very rare (Kuster, et al., 2010; Teijon, et al., 2010). It is likely that metals such as Cd, Hg, Ni and Pb present in wastewater will be attenuated within the aquifer. Teijon et al., (2010) published results from Depurbaix Barcelona. The analysis included Ni, which was reduced by half in the aquifer

although unusually high at 28.2 mg/L in the tertiary treated effluent. On the other hand Kuster, et al., (2010) for instance reported non polar materials were not reduced. The research tracked the common pesticide Diuron, the injected wastewater contained 30.7 ng/L, and the abstracted groundwater about 24.6 ng/L.

Factors affecting the concentration of wastewater pollutants during infiltration and in the groundwater, include soil properties, dilution, hydraulic conditions and the organic and microbial load in the injected water. Different aquifer matrices are also likely to have variable abilities to retard, sorb or deactivate priority substances. Thus, the aim of this project was to study and develop effective models and methodologies to judge the capacity of soils and aquifers to attenuate pollutants. The Paphos, Ezousas Recharge Project was used as a case study to construct a three-dimensional finite element model of the riverbed aquifer. FEFLOW software was used to simulate the groundwater flow conditions and the transport of pollutants in the aquifer emanating from the recharge process.

The groundwater model was coupled with the geochemical model PHREEQC to evaluate transport processes and predict chemical concentrations. The model was calibrated using hydraulic head and validated by chemical data from a monitoring network over the thesis time period of 2007-2011. The validation included laboratory studies to evaluate the effect of aquifer matrix characteristics on the partitioning and phase coefficients. The reactive transport model was based on mass balance equations adapted by field and laboratory measurements to include any new reactions identified.

6.2 Materials and Methods

6.2.1 Monitoring

The impact of the recycled wastewater on groundwater composition was measured by samples from boreholes in different parts of the aquifer (8 wells see also section 3; and Figures 6.1 and 6.2). Natural groundwater upstream of the recharge (well (B/H4031) was sampled as a control (Figures 6.1 and 6.2). Groundwater and reclaimed wastewater were collected three times per year during 11/2006 – 10/2011 for the standard sanitary parameters (APHA, 2005). Organic carbon was measured by BOD₅, and COD; bacteriological quality by total coliforms, *Escherichia coli* and bacteriophages. Physicochemical measurements were pH, conductivity and total hardness. The major anions analysed were Cl⁻, SO₄⁻², HCO₃⁻, F⁻, NO₃⁻, NO₂⁻ and the cations Na⁺, K⁺, Ca²⁺, Mg²⁺, NH₄⁺. Phosphorus was analysed and expressed as total phosphorus (TP). Other metals and metalloid analysed were As, Ni, Cd, Cr, Cu, Zn, Pb, Hg, Co, V, Fe, Se, B, Ba. Anion and cation analyses were performed by the Cyprus State Chemical Laboratory in Nicosia, using ion-exchange chromatography and inductively coupled plasma-mass spectrometry, respectively according to the international standard methods (APHA, 2005). In addition, toxicity tests were carried out (MTX EC₂₀, MTX EC₅₀, *Daphnia* EC₅₀). Indicator pesticide and insecticide residues were also measured in the samples used for the toxicity tests.

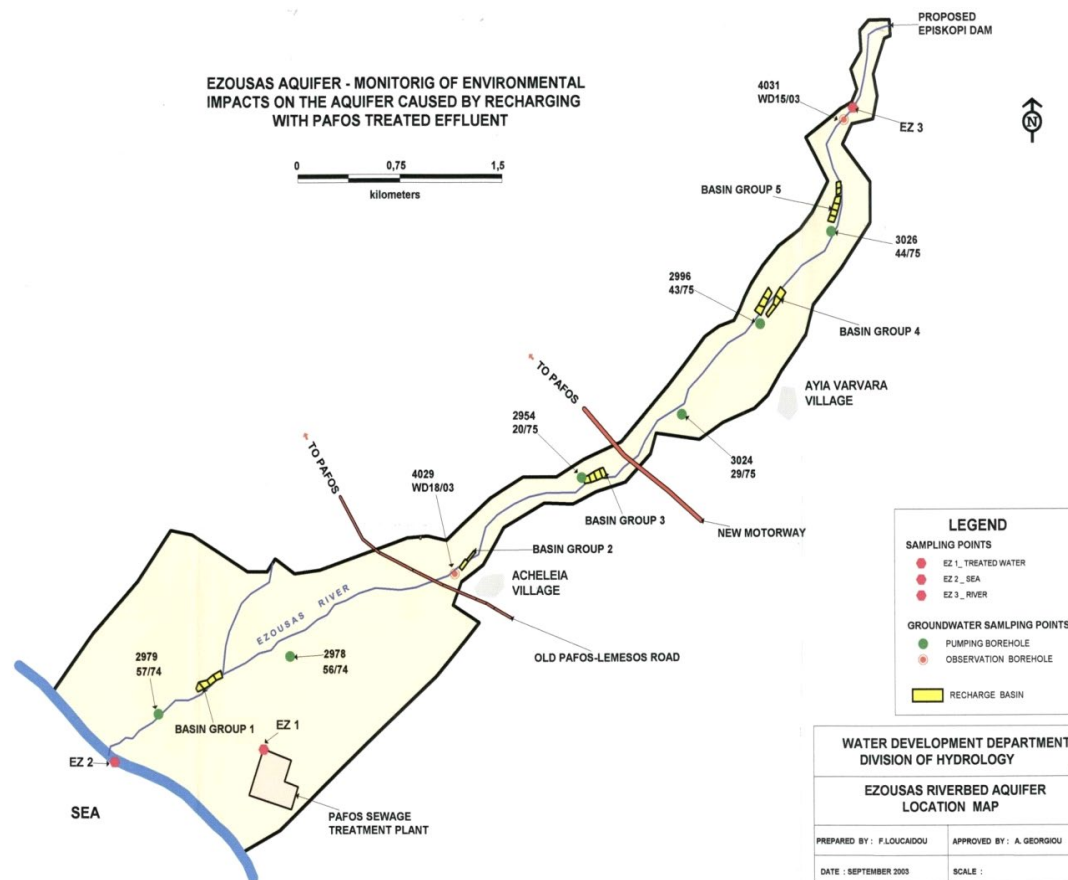


Figure 6.1: Location of the recharge ponds and abstraction wells in the Ezousas catchment

6.2.2 Groundwater Modelling

FEFLOW Model Setup

FEFLOW is a commercial finite element, subsurface flow and transport simulation system and there was an existing version of the Ezousas validated with data from 2002-2007, prepared by Milnes, (2007). It was extended for this work to include data up to the end of 2011 and by the addition of a contaminant transport function.

The horizontal discretization of the unconfined aquifer was implemented using a triangular finite element mesh consisting of 7738 nodes and 6354 elements. The vertical discretization of the model area was based on vertical cross sections created from the bore-hole data. The conceptual model was based on an unconfined aquifer that was about 40 m deep at the downstream end and 10 m deep at the upstream extremity. It was discretized in 2 layers: a superficial layer of 1m thick that followed the topography of the area to allow definition of rainfall infiltration, riverbed and artificial recharge and a lower aquifer layer of variable thickness that followed the underlying bedrock morphology.

The hydraulic conductivity of the model was based on the 2006/7 measurements at the start of the project and was modified during the project to take into account and re-calibrate with the new measurements. The final hydraulic conductivities used are shown in Figure 6.2 together with the location of the monitoring, abstraction pumping wells and the 5 sets of artificial recharging ponds.

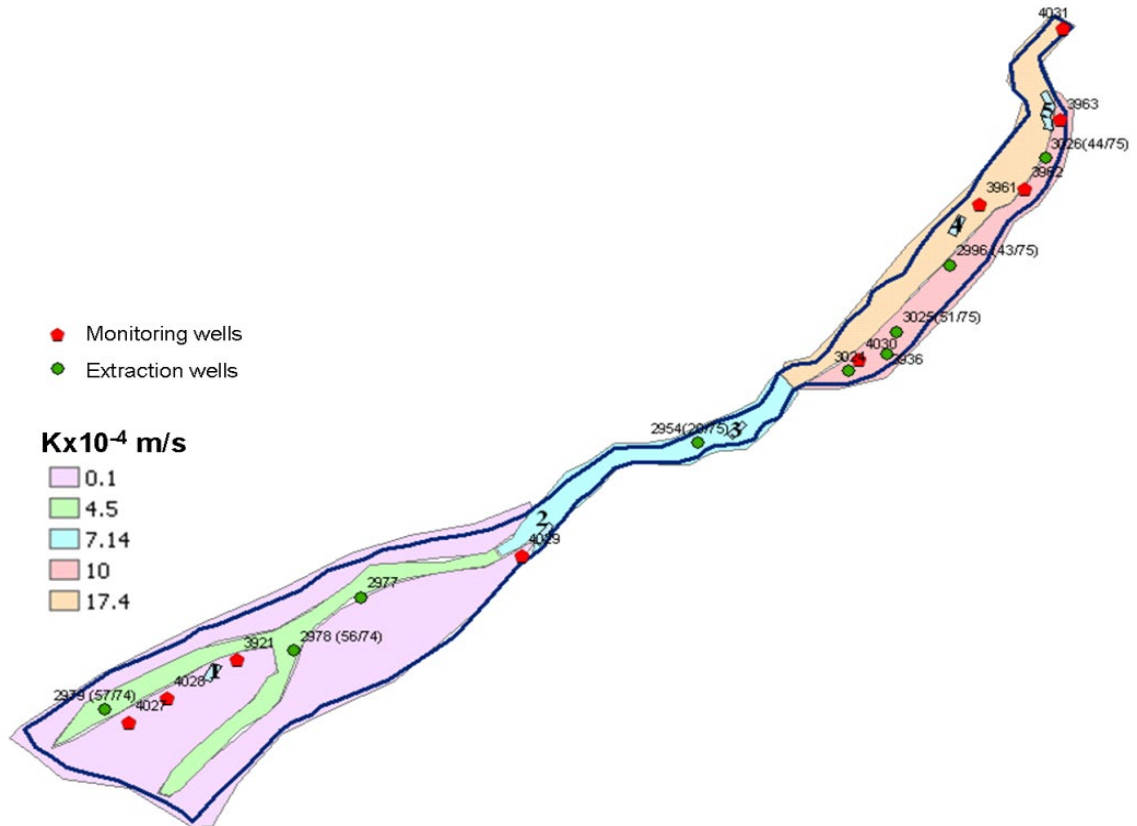


Figure 6.2 Calibrated hydraulic conductivity and location of extraction and monitoring wells

The Flow Model

The main types of boundary conditions (BC) applied in the model were as follows: 1) A first type BC (constant head of 0 masl) on the coastline boundary, 2) A first type BC (constant head of 77.1 masl) on the upstream boundary to simulate ambient flow (estimated at approximately at $5 \times 10^5 \text{ m}^3/\text{yr}$), 3) A first type BC (decreasing constant head over a length of 500 m, varying between 77.1 and 72.7 masl) to simulate river infiltration (estimated at approximately at $2 \times 10^6 \text{ m}^3/\text{yr}$ before and $5 \times 10^5 \text{ m}^3/\text{yr}$ after the construction of the Kannaviou dam). 4) A first type BC (time varying constant head) on the 5 artificial ponds to simulate artificial recharge, as observed by nearby wells. This type of boundary condition was chosen because the precise amounts of effluent recharged in the ponds was not available. 5) A well BC (flux in m^3/d) to simulate the pumping occurring from the extraction wells. Rain infiltration was assigned as a uniform value on the top layer according to

meteorological data from a nearby station. Boundary cases 2 and 3 were linked to a constraint that water may only infiltrate into the system.

The model was divided into three time periods: 1) October 2002 – December 2003 (0-456 days). This period corresponds to the steady state simulation of the model during which no artificial recharge occurred. The coastline, ambient flow and river infiltration BCs are active at this time. 2) January 2004 – July 2005 (456-1002 days). This was the period when the artificial recharge started and the ambient flow and river infiltration BCs are still active. 3) July 2005 – December 2011 (1002-3375 days). At the beginning of this period the Kanaviou dam was built thus the ambient flow and river infiltration BCs were turned off while artificial recharge and pumping continued.

The information regarding the daily extraction rates from the 9 extraction wells that were introduced in the model were available from January 2004 – December 2011 and are shown in Figure 6.3a (upstream) and 6.3b(downstream).

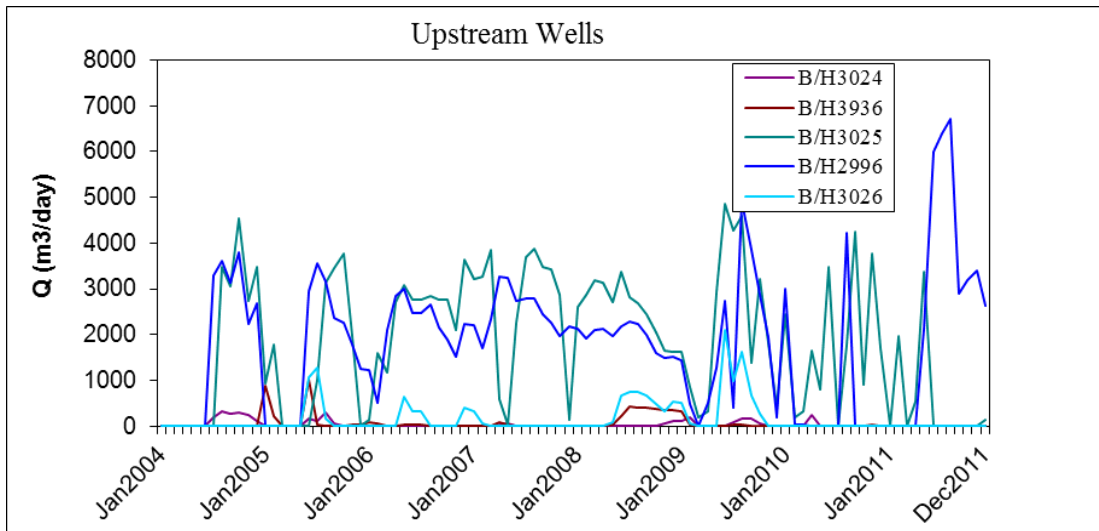


Figure 6.3a Abstraction rates (m^3/d) for the 5 upstream pumping wells.

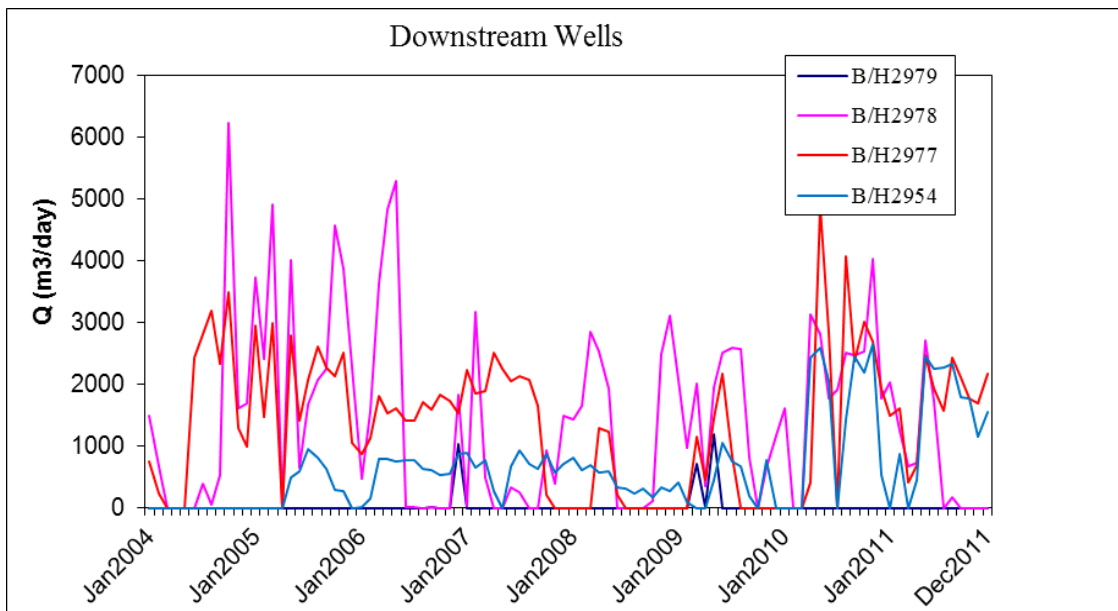


Figure 6.3b Abstraction rates (m³/d) for the 4 downstream pumping wells

The transport Model

The subsurface transport of phosphorus and copper from the recharge were also studied using the FEFLOW model. The available measurements for the native groundwater (at well BH4031) and the recharged effluent (at the five ponds) for the period of 25th January 2007 – 19th October 2011 were used as a time dependent constant concentration boundary conditions (Figure 6.3a, 6.3b). Figure 6.4 shows the native groundwater phosphorus concentrations are low and a peak in phosphorus in the reclaimed wastewater in May 2007. This was attributed to a problem with the biological phosphorus removal at the wastewater plant which required most of the rest of the year to recover as the enhanced biological P removing population was re-established. Figure 6.5 shows a high concentration of copper was observed in 2007-2008 for both native groundwater and reclaimed wastewater that was not easily explained. It was possible that the ground water was contaminated from agricultural applications of animal waste (copper is used as a prophylactic in animal rearing) which then also got into the drinking water via

the water supply but this is speculative. The concentrations remained low for the rest of the monitoring period.

In order to account for the natural (background) groundwater concentrations of phosphorus and copper, the native groundwater measurements taken at well BH4031 (Figure 6.2) were set as boundary conditions. These were duplicated at various locations over the entire study area due to a lack of additional measurements but also on the assumption that the background concentrations did not vary significantly over the aquifer.

The model was calibrated in order to match the observed phosphorus and copper concentrations in the downstream stream monitoring wells BH3026 and BH2996. These wells were selected since most of the wastewater (about 75%) is recharged in ponds 4 and 5 adjacent to these wells (Figure 6.2).

The sorption isotherms used in the model for the phosphorus and copper were determined by sorption experiments and are described in the next sub section. The porosity was estimated at 0.3 and the longitudinal and transverse dispersivities were determined (after the process of calibration) at 20m and 2m, respectively.

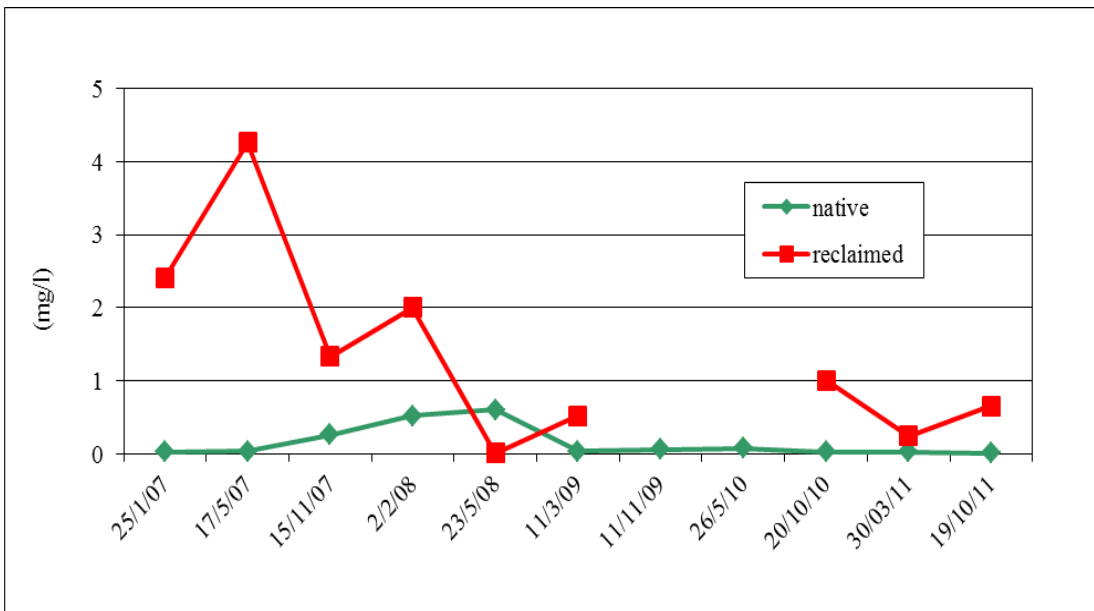


Figure 6.4 Phosphorus concentrations for the native groundwater and the recharged effluent for the period of 25th January 2007 – 19th October 2011

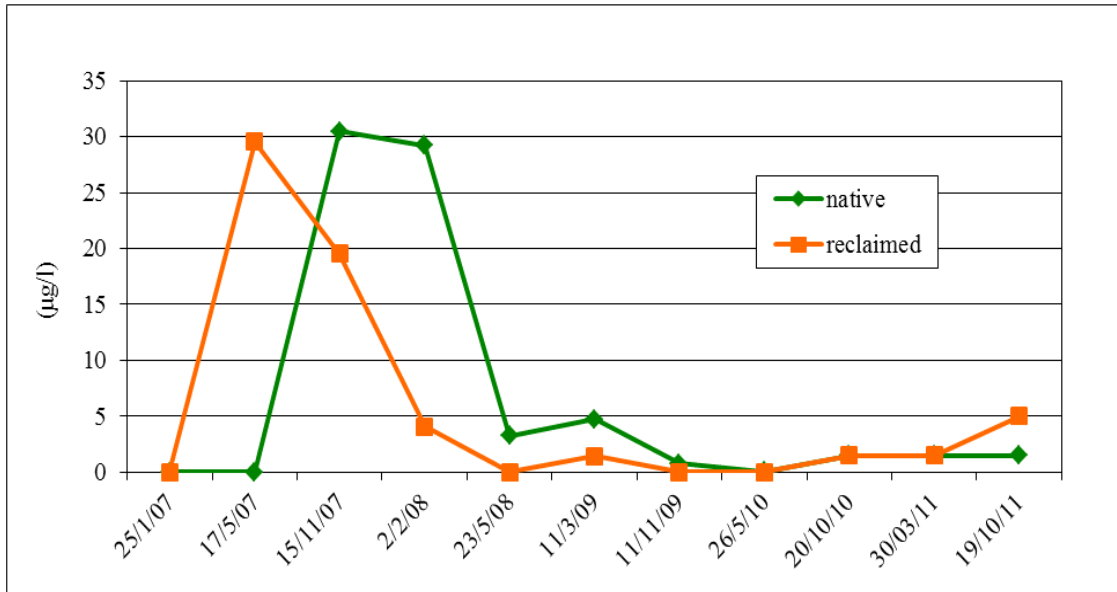


Figure 6.5 Copper concentrations for the native groundwater and the recharged effluent for the period of 25th January 2007 – 19th October 2011

PHREEQC Model Setup

PHREEQC is a freely available geochemical modeling program (Parkhurst and Appelo 2010; Wong, et al., 2012), was used to simulate the combinations, proportions and amounts of minerals from their end-members. The end members (initial solutions) modelled were the amended groundwater, from the well B/H3026 (downstream of recharge basin group 5, Figure 6.2) and the reclaimed wastewater from the basins. The model was also able to predict changes in gas partial pressures, phase and mole transfers that result from the differences in composition of two mixing waters. An uncertainty limit is specified by the user for each component. Inverse modeling was performed for this case study to understand the contribution of reclaimed water to groundwater characteristics for different rainfall patterns. The composition/proportions of groundwater during dry and transition to

wet periods could impact on the quality of the water for irrigation. These changes and evolution between wet to dry period were studied using samples taken from 25/01/2007 (wet) and 20/10/2010 (dry) as previously noted.

6.2.3 Laboratory Experiments

To understand the role of sediments in the mixed groundwater quality (adsorption, leaching and precipitation) laboratory partition experiments were carried out using sediment samples. These sediment samples were taken from different depths (0.3m, 1.0m and 3.0m) in and below the infiltration ponds in Basin 5 (Figure 6.2,) and compared with upstream natural sediment as a reference. Sediment samples were analysed for basic metals (XRF), trace metals (ICP) and minerals (XRD). Batch kinetic or rate of chemical change experiments were also used to assess the capacity of sediments to both release or adsorb phosphorus and copper.

6.3 Results and Discussion

6.3.1 Water Quality

Table 6.1 shows the average nutrients and selected metal concentrations of reclaimed water, native groundwater and resulting mixed groundwater. Key results are phosphate adsorption, an increase in nitrate and dilution of the native metals by the recharge water, although it was concluded that the copper results were biased by the high standard deviations caused by the unusual results in 2007/8 (Figure 6.5). It was assumed that phosphorus must be absorbed since the reduction from the reclaimed water from 1.3 mg/L to 0.1 mg/L, in the abstracted groundwater, was greater than can be explained by the dilution effect noted in the other parameters.

Thus the metals including iron are mostly geogenic in origin and diluted by the recharge water. For nitrate the dilution effect was the other way around to the metals with the lower level in the native groundwater (4.9 mg/L) than the recharge and abstracted groundwater 12.1 mg/L. (Table 6.1). The results for iron, in common with many of the metals (Table 6.1), shows a 50% reduction which could however be linked to the precipitation of phosphate as well simple dilution and this was explored by the modeling in Section 6.3.

Table 6.1 Average heavy metals content and nutrients in Ezousas recharge project for the period 11/2006 up to 10/2011 (n=14 samples)

	Mixed Groundwater		Native Groundwater		Reclaimed Water	
Heavy metal Concentration in µg/L						
	Average	Standard Deviation	Average	Standard Deviation	Average	Standard Deviation
Cadmium, Cd	0.1	0.2	0.1	0.2	0.1	0.1
Copper, Cu	12.8	20.2	6.3	11.1	7.1	10.3
Chromium, Cr	4.9	5.8	11.6	15.0	2.5	2.0
Zinc, Zn	61.0	36.3	103.1	102.5	27.8	20.5
Lead, Pb	6.6	7.4	7.1	8.1	4.8	5.7
Cobalt, Co	1.6	1.0	1.6	2.0	0.4	0.3
Vanadium, V	10.0	3.8	14.5	12.3	2.7	0.2
Arsenic, As	1.3	0.8	0.8	0.8	1.0	0.9
Nickel, Ni	8.4	3.4	13.7	14.8	7.8	8.0
Beryllium, Be	N.D.	-	0.1	0.1	0.03	0.0
Selenium, Se	0.8	1.3	2.3	2.3	4.6	2.3
Mercury, Hg	0.3	0.5	0.2	0.0	0.2	0.0
Boron, B	219.0	189.9	347.5	322.6	315.8	138.9

Manganese, Mn	111.2	75.8	85.9	90.5	58.7	28.4
Iron, Fe	526.5	652.3	1242.0	2412.0	176.3	130.5
Barium, Ba	31.2	17.4	48.6	26.7	18.3	14.7
Nutrients Concentration in mg/L						
NO ₃	12.1	2.9	4.9	5.6	13.9	7.6
PO ₄	0.102	0.1	0.135	0.2	1.289	1.3

6.3.2 FEFLOW results

Flow Results

The FEFLOW flow model used was assembled by Milnes (2007). Adjustments were made to include the more recent results and the new calibration data. The results for the original steady state model and the actual water depths are shown in Figure 6.6.

The most important water balance components are the pumping wells (80% of system outflow) and the upstream riverbed infiltration (about 65% of groundwater recharge). The upstream riverbed infiltration recharge and ambient flow are the main sources of aquifer recharge.

The results for the transient period are similar to those in Figure 6.6 (and not shown for brevity) with the difference that in the downstream area there is a more prominent drawdown. This is due to both increased extraction rates and the construction of the Kannaviou dam which diminished the main recharge sources of the aquifer (upstream riverbed infiltration and ambient flow). The resulting lowering of the hydraulic head levels in the Ezousa aquifer has led to saltwater intrusion in the coastal area. The results obtained indicated that artificial recharge

may compensate for the lack of upstream recharge but the location of the recharge (space and time) and abstraction rates would affect the success of the project in avoiding a water deficit.

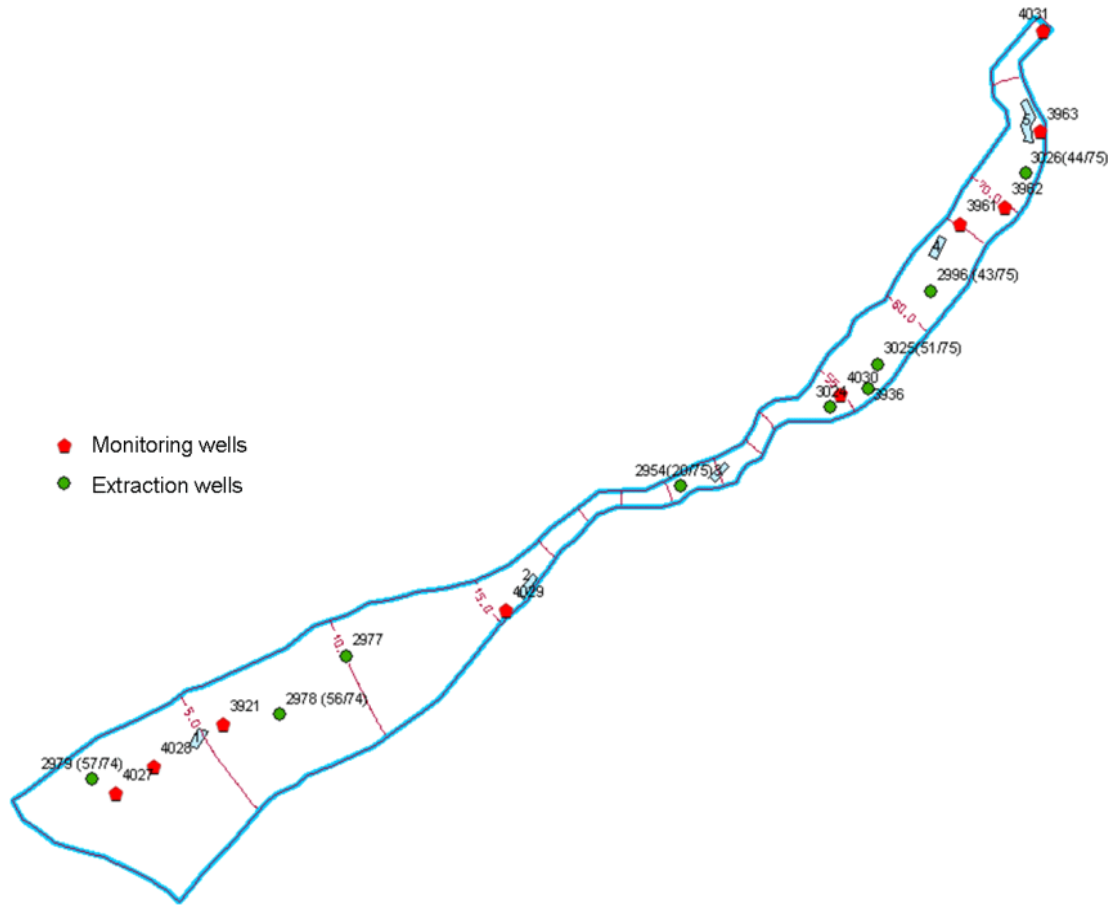


Figure 6.6 Steady state model calibration results (December 2006).

Mass Transport Results

The model suggested that the aquifer recharge proportions from each pond was 54.1% from Pond 5, 22.4 % from Pond 4 but Pond 3 contributed almost no wastewater. The proportions for the two downstream infiltration ponds were 8.5% (Pond 1) and 14.5% (Pond 2).

The model results for the evolution of phosphorus concentrations are shown from BH3026, downstream of Pond 5 the most upstream pond (54 % of recharge), in

Figure 6.6 and below Pond 4, 22% of the recharge, in Figures 6.7 BH2996. The results are in good agreement with the observed values for the downstream well BH2996 but less well for the upstream BH3096 particularly for the period 23/5/08-26/5/10. This was attributed to two factors firstly the concentrations in the native groundwater at this most upstream point were very low and at the analytical detection limit and secondly there was insufficient data for the actual wastewater for that period which would have also influenced the accuracy for BH2996.

For the copper results, the explanation for the deviation between measured and modeled values in both wells was thought to be different. The peak in copper concentration in the wastewater was in May 2007, as previously noted and shown in Figure 6.5 was picked up by the model, Figures 6.9 and 6.10, especially in the downstream well BH2996 as shown in Figure 6.10 and 11. The observed decline in copper however was more rapid than the model predicted for either well (Figures 6.9 and 6.10). This was attributed to the fact that the actual rate of reduction was quicker than the response time of the model. As was the case with the phosphate, the last measured values were at the detection limit ($<5 \mu\text{g/l}$.) but are plotted on the graph as $5 \mu\text{g/l}$.

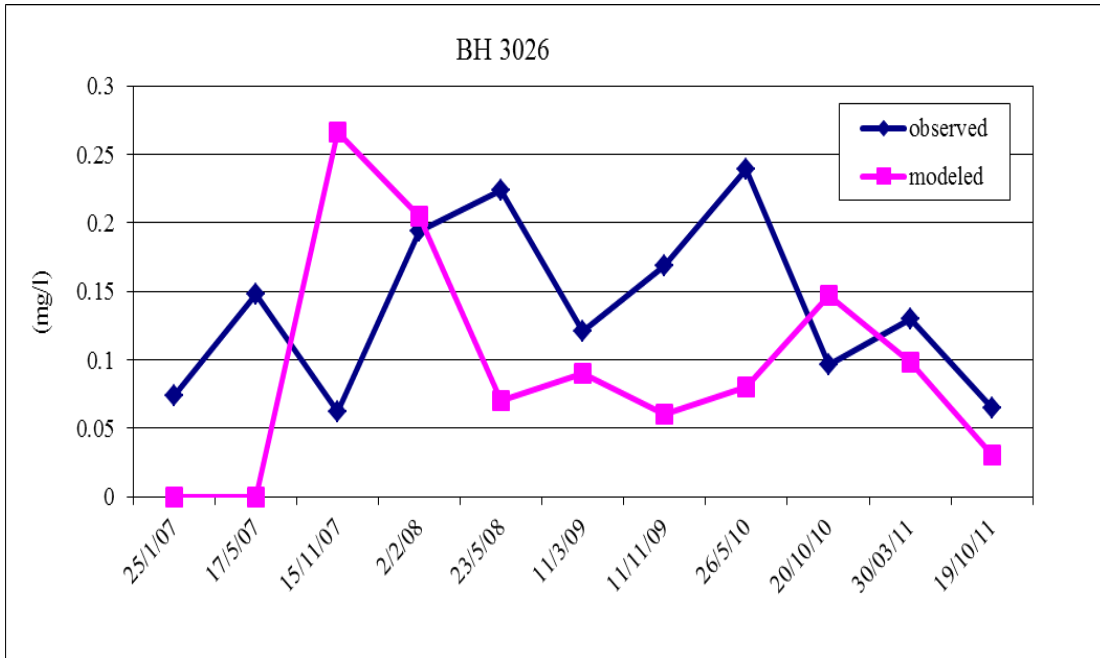


Figure 6.7 Concentrations of phosphorus for BH3026 the most upstream borehole

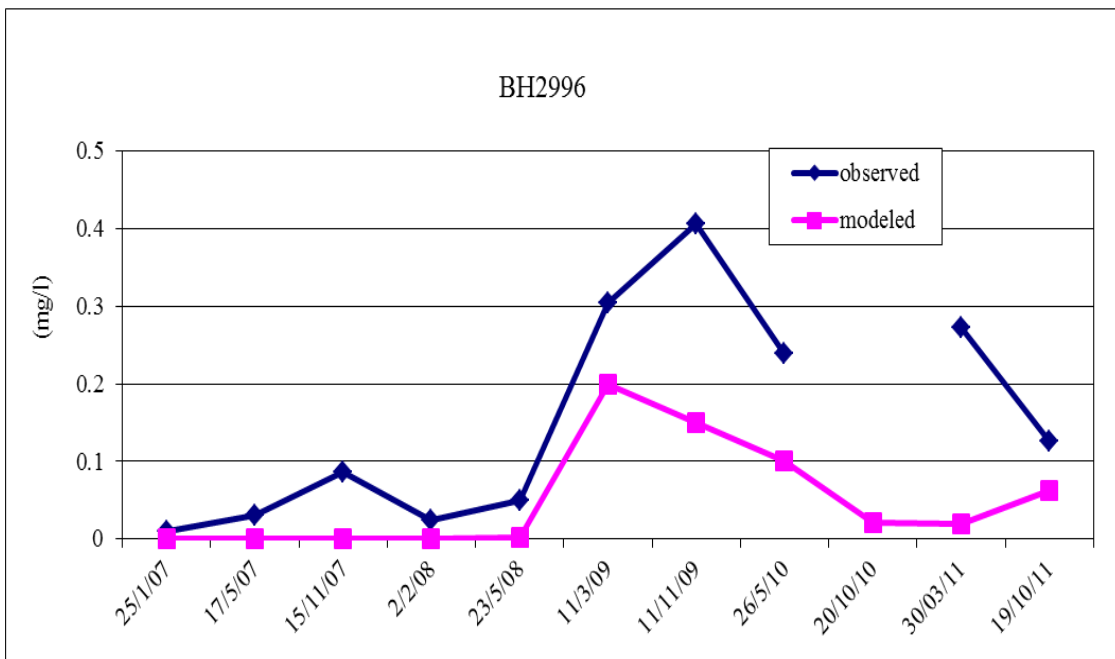


Figure 6.8 Concentrations of phosphorus in the downstream borehole BH2996

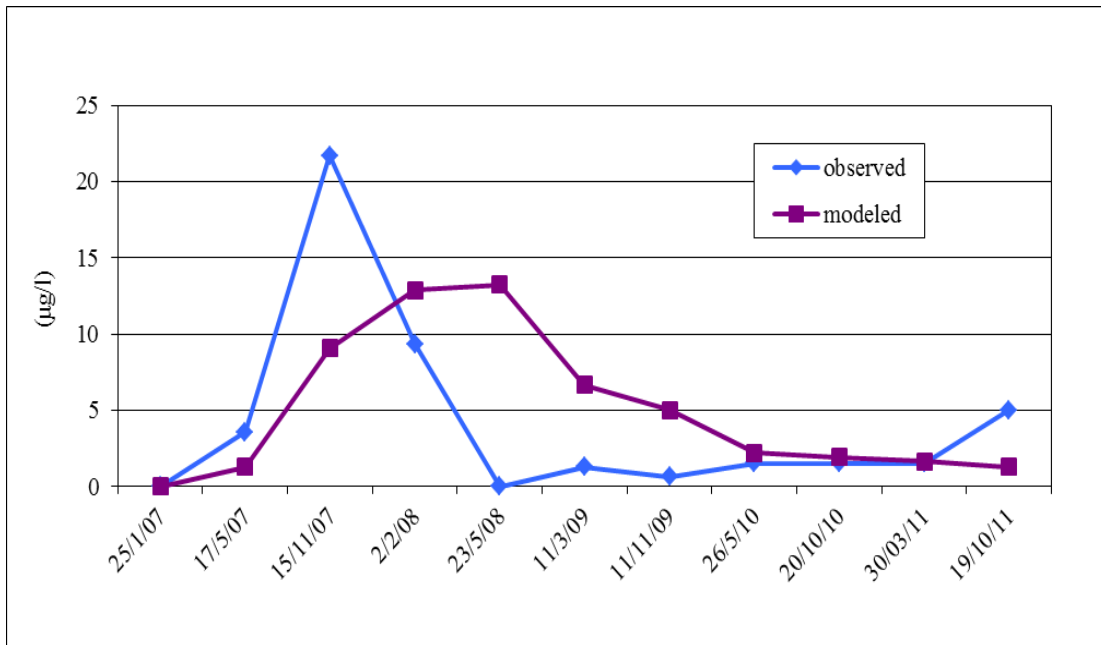


Figure 6.9 Concentrations of copper from the upstream borehole BH3026

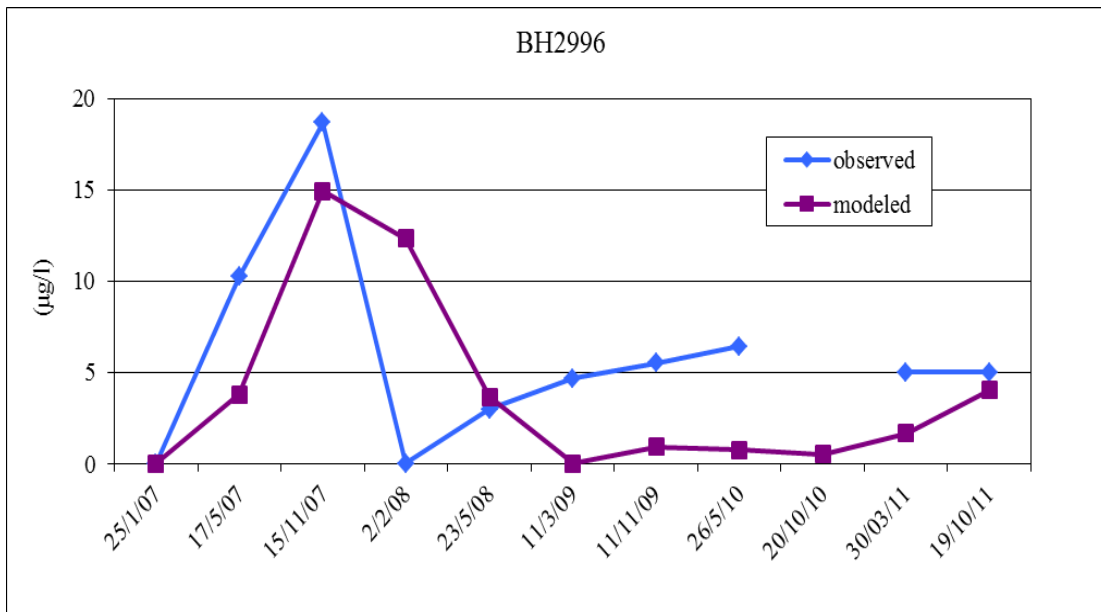


Figure 6.10 Concentrations of copper from the downstream borehole BH2996

6.3.3 PHREEQC Results

The results of the XRD analysis (Table 6.2) indicated the minerals were mainly silicates and carbonates (calcite (30-44%), quartz (19-36%), montmorillonite (0-3%), labradorite (22-26%) and clinocllore (8-9%). The XRF analysis indicated a similar predominance of silica SiO₂ (51%) and calcite (27.5%) in the sediments with iron as ferrous (5.5%), Mg (3.6%) and Na (2.7%) oxides. The analysis of the phase changes, expressed in moles transferred between the mineral and the water are shown in Table 6.2. The greatest transfers occur from the hematite and goethites which corroborates the ICP data shown in Table 6.1.

The mixed water from the study of the dry and wet period is shown in Table 6.2. PHREEQC modelling indicated that the upper part of Ezousas aquifer was recharged during the wet periods by 97-100% groundwater and 0-3% reclaimed water. In dry periods the groundwater was still mainly groundwater (mainly reservoir leakage 95%) but with a greater contribution from reclaimed water (5%).

6.3.4 Sediment Partition Experiments

Sediment sorption isotherms were conducted of 20°C and the 3m depth, phosphorus results, are representative. At low P concentration (4-5 mg/L P-PO₄) the isotherm is linear and the K_d was calculated to be 2.82 ml/gr at pH 7.8. At <4 mg/L P concentrations, P leaching was observed with poor reproducibility in the experimental results. Re-mobilization of P from especially anaerobic sediments is the basis of the BPR at the treatment plant and widely reported (for example Wu, et.,2015; Sharpley, et al., 2013).

Table 6.2: Mole exchange between the water and the minerals in Ezousas aquifer.

	Ca	Mg	Na	C(4)	Cl	S(6)	N(5)	pH	P
	mg/l	mg/l	mg/l	mg/l	mg/l	mg/l	mg/l		mg/l
Wet period - 25/01/2007									
Native groundwater	242	59	106	336	133	594	2.03	7.7	0.023
Recharged groundwater	198	49	126	342	151	459	2	7.4	0.074
Reclaimed wastewater	64	30	190	320	204	171	1.58	7.9	2.4
Phase	Ca-Montmorillonite	Quartz	Calcite	Goethite	Gibbsite	Gypsum	Hematite	Halite	Apalite
Mole transfer	-2.87E-03	1.05E-02	6.76E-04	1.15E+01	6.68E-03	-5.76E-04	-5.75E+00	8.93E-04	
Dry period - 20/10/2010									
Native groundwater	241	59.2	105	347.7	116	661	0.7	7.2	0.024
Recharged groundwater	215	49.7	94.5	347.7	121	576	1.8	7	0.096
Reclaimed wastewater	63.5	31.6	188	375.2	185	156	2	7.4	1.007
Phase	Ca-Montmorillonite	Quartz	Calcite	Goethite	Gibbsite	Gypsum	Hematite	Halite	
Mole transfer	ND	ND	0.000203	-68.83	ND	-0.00827	28.33	-0.00388	

6.4 Overall Discussion

Flow model results showed that a lowering of the water table levels of the Ezousa aquifer had occurred and it was concluded this was due to increased extraction rates combined with the construction of the Kannaviou dam. The analysis has suggested that artificial recharge can compensate for some of the reduction in upstream recharge but that the extractions would need monitoring to avoid

continued decline in the water table and further saltwater intrusion in the coastal area (Figure 6.6). The results have shown that the artificial recharge with treated sewage effluent improves water quality in terms metals, metalloids and sulphate without causing an unacceptable increase in nitrate, chloride or phosphate. Increases in the volumes of artificial recharge can be recommended as a method of reducing the impact of stricter controls on the abstractions or further releases from the Kannoviou reservoir.

The analysis showed the concentration of phosphate in the groundwater could be increased via wastewater inputs although the results were close to the detection limits and complicated by biochemical changes during the infiltration process. Both adsorption of and re-release of phosphate by sediment samples (basin five only tested) were demonstrated under laboratory conditions, depending on the initial phosphorus concentrations. Low phosphorus concentrations in the anaerobic sediment leading to release, as had been previously reported in the literature.

The experiments also demonstrated the aquifer sediment adsorbed copper strongly with estimated distribution coefficients (16.90-18.77 ml/gr). The calculated partition coefficient (K_d) value of copper adsorption from the column experiments was found to be dependent on input copper concentration and also the phosphate concentrations. An increase of phosphate led to an increase in copper adsorption, previous research has reported similar adsorption/desorption behavior. Saha and Badruzzaman, (2014), found copper adsorption in sandy soils varied with other factors as would be expected including pH, ionic strength and concentration of organic matter. Jalali and Moharrami, (2007), also reported similar K_d values (2.5-30.7 ml/gr) of copper absorption in ten calcareous soils of Northern Iran, copper showed the highest sorption of all the examined soils and metals tested examined. The formation of ferrous minerals such as hematite and goethite need further study because these minerals can act as precursors for clogging of the aquifer.

6.5 Conclusions and Recommendations

The FEFLOW model confirmed the field data that the increased extraction and reduction in River flow caused the Kannaviou dam, had lowered the water levels of the Ezousas aquifer sufficiently to allow saltwater intrusion at the coast (Figure 6.6). The model results also suggested the artificial recharge could only compensate for about 5% of the loss of upstream recharge.

The sorption experiments demonstrated mineral phosphate and copper sorption or precipitation and the sediment partitioning coefficients for phosphorus and copper were estimated at 2.82 ml/gr and 16.9-18.8 ml/gr respectively at pH 7.8. These experiments also showed re-release of P from the sediments when the P concentration was < 4mg/L.

The contaminant transport model (PHREEQC) also successfully captured the general trends in phosphorus and copper relatively well but with varying accuracy.

Copper, was mainly geogenic, in origin and the adsorption process (laboratory experiments) has shown that it is adsorbed onto the sediment matrix in important quantities.

Copper dissolution and precipitation processes were shown to be complex and would be expected to depend on various alluvial soil parameters such as; pH, salinity and concentration of organic matter. Therefore, it is suggested that the geogenic enrichment and aquifer spatial heterogeneity be taken into consideration when designing a monitoring network for MAR systems.

CHAPTER 7

OVERALL SUMMARISING DISCUSSION

Soil Aquifer Treatment Performance

Some key operating conditions were identified during the research for this thesis that would be required to ensure successful long term (10 years) recharge performance. Practical problems which were found and corroborated by the previous literature reviewed were:

- 1) The hydraulic conductivity of the infiltrative surface zone was easily affected by fines either natural or compaction, produced during installation and startup; a) clogging was dependent on the hydraulic loading rate and/or quality of raw water used for recharging; b) soil depth and profile provided treatment - depending on effluent loading rate and quality. Previous work had suggested a minimum depth of unsaturated aerobic soil was needed for oxidative treatment to occur. The research here indicated there was unsaturated flow through the soil profile with long travel times so there was sufficient time for typical aerobic, heterotrophic and autotrophic activity to remove pollutants (e.g., BOD, NH_4^+ , Faecal coliforms); if subsurface conditions are conducive to biotreatment (e.g., neutral pH, normal temperatures and no biotoxins). In our particular case study the tertiary treated effluent with biological nutrient removal (BNR) led to well oxygenated conditions and the results showed little subsequent treatment in the vadose zone; c) there was sufficient soil grain surface area for sorption processes); although there was evidence for a greater effect on, for example P removal, from precipitation as iron salts.
- 2) This study in common with previous work indicated that the physical heterogeneity of the deep vadose zones may have limited effects on the

concentrations of conservative contaminants such as copper or sodium chloride applied through artificial recharge with treated effluent. Changes were mainly due to dilution from the native groundwater.

Infiltration Rate Behavior

The literature suggested continuous use of soil treatment from months to years which included sewage effluent solids, as measured by total suspended solids and biochemical oxygen demand can contribute to pore filling of the infiltrative surface noted in Point 1 and loss of infiltration capacity (Bouma, 1975; Siegrist *et al.* 2004; Beach *et al.* 2005; Beal Van Cuyk *et al.* 2005; Lowe and Siegrist, 2008).

With long term operation, the native soil capacity to infiltrate wastewater effluent will decline due to clogging phenomena depending on effluent quality and drying. The decline in infiltration capacity during operation was often characterized as a 3-phase process (shown Figure 4.5). The infiltration ponds were shown to be vulnerable to biomat formation and pore-filling, caused by the primary growth of algae and aquatic plants, at and near the location where effluent entered the soil network (effects II and III in Figure 4.7).

Denitrification

The treated effluent used for groundwater recharge will be a source of elevated nutrient concentrations, this was the case even for well treated effluents compliant with the EUWFD. Thus there is a need to understand the local conditions under which the quality of managed recharge is used. It was commonly thought and previous research has shown that the vadose zone would act as a limited buffer zone where nitrate would be attenuated by denitrification before reaching groundwater. Denitrification, (microbial reduction of NO_3^- to N_2) in groundwater aquifers is an important process and method for NO_3^- removal containing or to

which reactive reducing substrates such as organic (organic C or sulfide S) have been added. Other studies have indicated that removal of NO_3^- from shallow groundwaters by biological assimilation may also be occurring near the water table (Greskowiak, 2005).

The current study suggested alternatives, with results indicating that non-uniform, heterogeneous flow with low-resistance flow paths in the vadose zone could occur and increase the amount of nitrate leaching through the vadose zone and entering the groundwater (Ünlü, et al., 1990; Harter and Yeh, 1996; Simunek, et al., 2003; Baran, et al., 2007).

Secondly in this case study the dissolved oxygen of the tertiary treated effluent was too high for anoxic denitrification to occur, nitrate concentrations increased in the ponds as a result of the algal and plant growth.

Fate of Phosphate and Copper

The continuous operation of groundwater recharge with effluents has been suggested as likely to increase metals in the soil and accumulate to levels that may be undesirable for crop growth. Much previous work has been with effluents which included wastewater from traditional industries but most of these have closed or improved and heavy metals in treated effluents within the EU will be low. The results from this work confirms this, with the heavy metals in the native groundwater higher than the reclaimed water, the metals were therefore mostly geogenic. A focus was made on copper in this work because of it is common and has complex solubility behavior. It was found that the Ezousas sediments exhibited strong copper adsorption and copper concentrations were always below maximum limits for irrigation use.

Total phosphorus (including particulate P) was also strongly absorbed and attenuated into the aquifer matrix the average concentration of the reclaimed water was 1.29 mg/L and the abstracted groundwater 0.10 mg/L. lower than can be explained by simple dilution. The P analysis used did not separate the phases of the P and this would be useful in future monitoring.

CHAPTER 8

CONCLUSION AND RECOMMENDATIONS

CHAPTER 1

The Ezousas aquifer recharge project reported on in this thesis was shown to be able to replenish, the otherwise depleted groundwater, without prejudicing water quality. Managed Aquifer Recharge has been demonstrated to be a useful element for integrated water resource management. Reuse of treated wastewater via groundwater recharge was found to have been trialed in other arid regions of the world with similar success. Therefore, it was concluded that groundwater replenishment with treated wastewater will be an important contribution to climate resilient, water resources especially in the Mediterranean climatic region where power for desalination is limited. It was also concluded that most locations could benefit from groundwater recharge to help to conserve surface water resources, improve groundwater quality and minimize evaporative losses, while increasing the volume of groundwater available for use.

The results indicated however that local hydrogeology conditions and water quality (see also conclusions from Chapter 2 and 3) would need to be investigated and confirmed as adequate prior to and during recharge projects.

CHAPTER 2

It was concluded from the fundamental analysis of the hydrological properties (hydraulic conductivity, transmissivity, porosity) of the Ezousas aquifer that it would be suitable for the recharge project. The analysis of the alluvium hydrogeology indicated there was sufficient capacity to accommodate and store the total annual output of the Paphos wastewater treatment plant with no adverse effects on water quality, on the contrary the results suggested there were several benefits. The advantages found were; a) increasing the seasonal availability of irrigation water, b) buffering against salt water ingress up the coastal aquifer c) a reduction in

corrosivity from the naturally high gypsum sulphate and d) reduced natural phytotoxins (boron and metals) by dilution of the native groundwater. It was also possible to conclude that there was no pathogenic risk from the treated sewage effluent although Paphos includes chlorine disinfection as part of the tertiary treatment and this could generate a risk from chlorinated by-products, there was also a small increase in the salt from the recharged effluent. Thus further work in this area of residues from treatment is needed but overall it was concluded that there was greater scope worldwide for ground water recharge using well treated sewage effluent.

CHAPTER 3

Chapter 3 reported on the design of the Paphos wastewater treatment plant which was found to be the standard European process train to achieve background environmental levels of; organic carbon, solids, nitrogen, phosphorus and indicator organisms as specified in the Urban Wastewater Treatment and Water Frame Work directives. The Paphos treatment includes chlorination as noted in the Conclusion to chapter 2 and a further analysis of the risk vs benefits of this was recommended. Persistent chemical residues in treated sewage effluents (pesticides, biocides, pharma residues and metals) have been reported as causing potential problems in receiving waters and it is recommended that this requires further work in groundwater recharge research.

CHAPTER 4

The method of recharge was found to influence water quality, in this case the use of ponds stimulated plant growth and increased organic productivity. Total nitrogen was increased in the system by these algae, plants and higher organisms growing in the pond generated ecosystem. The residual organic content in the tertiary treated municipal effluent was too low to provide a substrate for heterotrophic growth, oxygen depletion or denitrification in either the ponds or vadose zone. Denitrification did occur in discrete pockets within the pond sediments and soil and

could be affected by the operational cycle. Periodic drying by operating in a wet and dry cycle enabled aeration and oxidation of the sediments and accumulations of anoxic and anaerobic organic matter was avoided and denitrification prevented. Two cycles were tested (4 and 7 days) only the longer drying time enabled a full recovery of infiltration rates, suggesting more research could generate a standard pond design guide which would be useful.

The hydraulic analysis using recharge wells to avoid the productivity and insect activity, in the ponds. Further work however is needed to understand potential changes in water quality from less aeration from the well injection.

The results indicated that the number and design of the wells would and could be adjusted using modified basic theory to overcome subterranean mounding.

CHAPTER 5 AND 6

In this project the main influence on nitrate concentration in ground water following recharge was the dilution with native groundwater and its nitrate concentrations. It was concluded that similar results would be obtained when EU standard municipal effluent were used. Further investigations would be needed for other grades of effluents and levels of treatment, if meeting the WHO nitrate standard depended on treatment by the soil or vadose.

The analysis of the other priority pollutants selected, namely metals and phosphate in the recharged effluent, did show reductions. Copper and phosphate were adsorbed as well as dilution and from both the equilibrium calculations and the modeling it was possible to conclude this was through an ion exchange mechanism with the calcium and iron naturally present in the aquifer clays. Calcium and iron and their analogues are the most common mineral ions and it was concluded this mechanism will be reproducible in all aquifers, but this needs further confirmation

especially in aquifers where the alkalinity balance is different as a consequence of changes in the inorganic carbon speciation.

Once ion exchange had been accounted for then the fate of all the monitored materials demonstrated a final concentration dependent on dilution by the groundwater. It was concluded the results demonstrated that there was simple, rapid and complete mixing in the aquifer and it is suggested that this conclusion would also be transferable to most other catchments. The distance between recharge and re-abstraction in this case study was 5-7km and shorter retention times than used here is unlikely but new work on more complex aquifers or with perched zones are likely to produce different results.

There was validation of the hydraulic and water quality models used, (FEFLOW and PHREEQC), which showed good agreement with the field data and it was concluded that these models would be useful to predict flow and water quality available for abstraction. It was also suggested that they could be more widely used by practicing engineers as a catchment management tool.

REFERENCES

Aharoni, A., 2012. Effluent Reuse Projects in Israel for Agricultural Irrigation. Workshop on Wastewater treatment and effluent reuse Shafdan, 9-12 July 2012. file:///C:/Users/User/Downloads/mekorot%20wastewater%20treatment%20and%20reclamation.pdf

Aharoni, A., Guttman, J., Cikurel, H., and Sharma, S. K., 2011. SWITCH – Sustainable water management in the city of the future: Guidelines for design and operation and maintenance of SAT (and hybrid SAT) system. Mekorot and UNESCO–IHE, D 3.2.1.f - i.

Allen, D.M., and Matsuo, G.P., 2002. Results of the Groundwater Geochemistry Study on Hornby Island. Available from:

www.islandstrust.bc.ca/poi/pdf/itpoitasrptgrndwtrfinalapr2002.pdf

Anderson, T.W., G.W. Freethey, and Patrick Tucci, 1990, Geohydrology and Water Resources of Alluvial Basins in South-Central Arizona and Parts of Adjacent States: United States Geological Survey Open-File Report.

ANON, 2005. Regulative Administrative Act, RAA, 269/2005. Protection of the Water Resources. Official Gazette of the Republic of Cyprus, 4000.

APHA, 2005. Standard Methods for the Examination of Water and Wastewater, 21th edition. American Public Health Association, Washington, D.C.

Arehart, G.B., and Hulston, J. R., 1998. Water-rock interaction: In proceedings of the 9th International Symposium on Water-Rock Interaction -- WRI-9, Taupo, New Zealand, March-April 1998. Rotterdam, A.A. Balkema.

Asano, T., 2016. Artificial Recharge of Groundwater. Elsevier.
ISBN:1483163202.

Asrari, E., 2014. Heavy Metal Contamination of Water and Soil: Analysis, Assessment, and Remediation Strategies. Apple Academic Press, CRC Press, SBN 10: 177188004X / ISBN 13: 9781771880046

Ayers, R.S., and Westcot, D.W., 1989. FAO irrigation and drainage paper, 29 Rev.1, Food and Agriculture Organization of the United Nations, Rome.

Azevedo, J.A., Azevedo, R.A., 2006. Heavy metals and oxidative stress: where do we go from here? Commun. Biometry Crop Sci. 1 (2), 135-138.

Baran, N., Lepiller, M., and Mouvet, C., 2007. Hydrodynamic and geochemical constraints on pesticide concentrations in the groundwater of an agricultural catchment (Brevilles, France). Environmental Pollution 148, 729-738.

Barry, K.E., Vanderzal, J.L., Miotlinski, K., Dillon, P.J., 2017. Assessing the Impact of Recycled Water Quality and Clogging on Infiltration Rates at A Pioneering Soil Aquifer Treatment (SAT) Site in Alice Springs, Northern Territory (NT), Australia. Water 2017, 9(3), 179; doi:[10.3390/w9030179](https://doi.org/10.3390/w9030179)

Beach, D.N.H., McCray, J., Lowe, K. S., Siegrist, R. L., 2005. Temporal changes in hydraulic conductivity of sand porous media biofilters during wastewater

infiltration due to biomat formation. *Journal of Hydrology*, Volume 311, Issue 1-4, p. 230-243.

Beal, C., Gardner, E., Menzies, N., 2005. Process, performance and pollution potential: a review of septic tank-soil absorption systems. *Australian Journal of Soil Research*.

Bohlke, J. K., Smith, R. L., and Miller, D.N., 2006. Ammonium transport and reaction in contaminated groundwater: Application of isotope tracers and isotope fractionation studies. *Water Resources Research*, 42(5), 1-19.

Botros, F. E., Yuksel, S. O., Ginn, T R., and Harter, T., 2012. Richards equation-based modeling to estimate flow and nitrate transport in a deep alluvial vadoze zone. *Vadoze Zone Journal*. 11(4), 1-16. Available from <http://groundwater.ucdavis.edu/files/152104.pdf>

Bouma, J. 1975. Unsaturated flow during soil treatment o septic tank effluent. *J. Am. Soc. Civ. Eng.* 01(E6): 967-983.

Bouwer, H.,2000. Integrated Water Management Emerging Issues and Challenges. *Agricultural Water Management*, 45, 217-228.

Bouwer, H., 2002. Artificial recharge of groundwater: hydrogeology and engineering. *Hydrogeology Journal* 10(1), 121-142.

Bouwer, H., Pyne, R.D.G., Brown, J., Germain, St. D., Morris, T.M., Brown, C.J., and Rycus, M.J., 2008. Design, operation and maintenance of sustainable underground storage facilities. AWWARF Report. Denver, USA.

Brady, N.C., and R.R. Weil., 1999. *The Nature and Properties of Soils*. Upper Saddle River, New Jersey, Prentice Hall.

Bugan, R. D.H., Nebojsa, J. Israel, S; Tredoux, G., Bettina, G., Steyn, M; Allpass, D., Bishop, R., Marinus, V., 2016. Four decades of water recycling in Atlantis (Western Cape, South Africa): Past, present and future. URI: <http://www.ajol.info/index.php/wsa/article/view/146982>

Bundschuh, J., and Zilberbrand, M., 2011. *Geochemical modeling of groundwater, vadoze zone and geothermal systems*. Boca Raton, CRC Press.

Burger, F., and Čelková, A., 2003. Salinity and sodicity hazard in water flow processes in the soil. *PLANT SOIL ENVIRON.*, 49, (7): 314–320

Buss, S.R., Herbert, A.W., Morgan, S.F., Thornton, S.F., and Smith, J.W.N., 2005. A review of ammonium attenuation in soil and groundwater. *Quarterly Journal of Engineering Geology and Hydrogeology*, 37(4), 347-359.

Camargo, J.A., Alonso, A., Salamanca, A., 2005. Nitrate Toxicity to Aquatic Animals: A Review With New Data for Freshwater Invertebrates. *Chemosphere*. 58. 1255-67.

Cates, D.A., Knox, R.C., and Sabatini, D.A., 1996. The impact of ion exchange processes on subsurface brine transport as observed on Piper diagrams. *Ground Water*, 34(3), 532-544.

Chidambaram, S., Ramanathan, Al., Shivanna, K., and James, R. A., 2010. Trends in Water Research: Hydrochemical And Hydrological Perspectives. New Delhi, International Publishing House Ltd.

Christodoulou, G., Sander, G.C., and Wheatley, A.D., 2007. Characterization of the Ezousas aquifer of SW Cyprus for storage-recovery purposes using treated sewage effluent. Quarterly Journal of Engineering Geology and Hydrogeology, 40(3), 229-240.

CMC, (Cyprus Meteorological Service),2016. Meteorological Reports. http://www.moa.gov.cy/moa/MS/MS.nsf/DMLclimet_reports_en/DMLclimet_reports_en?opendocument.

Constantinou, G., Pangides, I., Xenofontos, K., Afrodisis, S., Michaelides, P., and Krambis, S., 2002. Cyprus Geology: Geological Survey Department. Nicosia, Bulletin No10.

Corstanje, R., and Reddy, K. R., 2004. Response of Biogeochemical Indicators to a Drawdown and Subsequent Reflood. Journal of Environmental Quality, 33(6), 2357-2366.

Debernardi, L., De Luca, D. A., and Lasagna, M., 2008. Correlation between nitrate concentration in groundwater and parameters affecting aquifer intrinsic vulnerability Environmental Geology, 55(3) 539-558.

DEMOWARE, 2017. Deliverable D1.4 Pretreatment requirements and design guidelines for SAT technologies, and two SAT case studies.

Dennis, I., and Dennis, R., 2012. Climate change vulnerability index for South African aquifers. ISSN 1816-7950 (On-line) = Water SA Vol. 38 No. 3 International Conference on Groundwater Special Edition 2012.

[https://dspace.nwu.ac.za/bitstream/handle/10394/17510/Water%20SA-2012-38\(3\)-417.pdf?sequence=1](https://dspace.nwu.ac.za/bitstream/handle/10394/17510/Water%20SA-2012-38(3)-417.pdf?sequence=1)

Dillon, P., 2005. Future management of aquifer recharge. Hydrogeology Journal, Volume 13, Issue 1, pp.313-316.

Desimone, L. A., and Howes, B. L., 1998. Nitrogen transport and transformations in a shallow aquifer receiving wastewater discharge: A mass balance approach. Publication: Water Resources Research, Volume 34, Issue 2, pp. 271-285.

Domenico, P., and Schwartz, F., 1998. Physical and Chemical Hydrology. New York, John Wiley & Sons Inc.

DWAF (Department of Water Affairs and Forestry), 2007. Artificial recharge strategy.

Version 1.3.

<http://www.dwaf.gov.za/Documents/Other/Water%20Resources/ARStrategyforSAJun07SecA.pdf>

Eaton, S., and Robertson, A. H. F., 1993. The Miocene Pakhna Formation, Southern Cyprus and its relationship to the Neogene tectonic evolution of the Eastern Mediterranean. Sedimentary Geology, 86(3), 273-296.

Elgettafi, M., Elmandour, A., Himi, M., Casas, A., and Elhaouadi, B., 2012. Messinian salinity crisis impact on the groundwater quality in Kert aquifer NE

Morocco: Hydrochemical and statistical approaches. International Journal of Water Resources and Environmental Engineering Vol. 4(11), pp. 339-351. Available online at <http://www.academicjournals.org/IJWREE> DOI: 10.5897/IJWREE12.002 ISSN 1991-637X ©2012 Academic Journals

Elmi, A.A., Astatkie, T., Madramootoo, C., Gordon, R., and Burton, D., 2005. Assessment of denitrification gaseous end-product in the soil profile under low water table management practices using repeated measures analysis. Journal of Environmental Quality 34(2), 446-454.

European Communities, 2001. Artificial recharge of groundwater. EC project ENV4-CT95-0071. ISBN 92-894-0186-9.

European Union-DWD, 1998. EU Drinking Water Directive, Council Directive 1998/83/EC.

European Union-WFD, 2000. Water Framework Directive, Council Directive 2000/60/EC.

Fogg, G.E., Noyes, C.D., and Steven F. Carle, S.F., 1997. Geologically based model of heterogeneous hydraulic conductivity in an alluvial setting. Hydrogeology Journal 6 (1), 131-143.

Foster, S., Tuinhof, A., and Garduno, H., 2006. Groundwater Development in Sub-Saharan Africa: A Strategic Overview of Key Issues and Major Needs. World Bank GWP Associate Program. Sustainable Groundwater Management: Concepts and Tools. Case Profile Collection No. 15.

Fox, P., Nellor, M., Arnold, B., Lansey, K., Bassett, R., Gerba, C., Amy, G., Yanko, W., Baird, R., Reinhard, M., Houston, S., and Drewes, J., 1999. Implications of Soil Aquifer Treatment for Sustainable Water Reuse on

Groundwater Quality.WRPMD'99: Preparing for the 21st Century. Proceedings of the 26th Annual Water Resources Planning and Management Conference, Tempe, Arizona, June 6-9, 1999. Tempe, Arizona, United States. American Society of Civil Engineers.

Fox, P., Houston, S., Westerhoff, P., 2001. Soil aquifer treatment for sustainable water reuse. AWWA Research Foundation and American Water Works Association. Research Foundation: Denver, CO, USA. ISBN, 1583211330, 9781583211335.

Glass, R.J., Steenhuis, T.S., Parlange, J.Y., 1988. Wetting front instability as a rapid and far-reaching hydrologic processes in the vadoze zone. *Journal of Containment Hydrology*, 3(2), 207–226.

Glynn, P.D., and Plummer, L.N., 2005. Geochemistry and the understanding of groundwater systems. *Hydrogeology Journal*, 13(1), 263-287.

Goren, O., Lazar, B., Burg, A.and Gavrieli, I., 2010. Water-rock interactions during recharge of effluents into a calcareous sandstone aquifer. *Water-Rock Interaction - Proceedings of the 13th International Conference on Water-Rock Interaction, WRI-13*. 249-252.

Grand, H., Lapierre, H., Mascle, G. H., Ohnenstetter, M., & Angelier, J., 1993. Superimposed tectonics of the Cyprus ophiolitic massifs. *Tectonics*, 12(1), 93-102.

Greensmith, T., 1998. Southern Cyprus. *The Geologist's Association Guide No 50*. London, Geologist's Association.

Greskowiak, J., Prommer, H., Massmann, G., Gunnar, C.D., Nützmann, G., and Pekdeger, A., 2005. The impact of variably saturated conditions on

hydrogeochemical changes during artificial recharge of groundwater. *Applied Geochemistry*, 20(7), 1409-1426.

GSD (Geological Survey Department), 2005. *Geology and Hydrogeology of the Paphos Region-Internal Reports*;

Gunter, F., 1998. *Principles and Applications of Geochemistry* (2nd ed.). Upper Saddle River, New Jersey, Prentice-Hall.

Guihua, L., Zongwu, T., Larry, W., Mays, Fox, P., 2000. New Methodology for Optimal Operation of Soil Aquifer Treatment Systems. *Water Resources Management*, Volume 14, Issue 1, pp 13–33 (2000)
<https://doi.org/10.1023/A:100813070>

Hadjisravinou, Y., and Afrodisis, S., 1977. *Geology and Hydrogeology of the Paphos Region*. Geological Survey Department. Nicosia, Ministry of Agriculture and Natural Resources, Cyprus.

Hannappel, S., Scheibler, F., Huber, A., Sprenger, C., 2014. Characterization of European managed aquifer recharge (MAR) sites - Analysis, Demonstration of promising technologies to address emerging pollutants in water and waste water (DEMEAU).

file:///E:/Chapter%201/M11_1%20catalogue%20of%20european%20MAR%20applications_plus_appendix.pdf

Harrington, N. and Cook, P., 2014. *Groundwater in Australia*, National Centre for Groundwater Research and Training, Australia.

Harter, T., Onsoy, Y. S., Heeren, K., Denton, M., Weissmann, G., Hopmans, J. W., Horwath, W. R., 2005. Deep vadoze zone hydrology demonstrates fate of nitrate in eastern San Joaquin Valley. *California Agriculture J.*, 59(2), 125-132.

Harter, T., Yeh, T. C., 1996. Stochastic analysis of solute transport in heterogeneous, variably saturated soils. *Water Resources Research*, 32(6), 1585-1595. DOI: 10.1029/96WR00502

Hem, J.D., 1989. Study and interpretation of the chemical characteristics of natural water. *Water Supply Paper 2254*, 3rd edition. Washington D.C., U.S. Geological Survey. Available from:
<http://pubs.usgs.gov/wsp/wsp2254/pdf/intro.pdf>

Herman, J.S., Back, W., & Pomar, L., 1985. Geochemistry of groundwater in the mixing zone along the east coast of Mallorca, Spain. *Karst Water Resources*, 161, 467-479.

Hoffman, J.L., and Canace, R.J., 2001. *Technical Guidance: A Recharge-Based Nitrate-Dilution Model for New Jersey*. New Jersey Geological Survey, Technical Guidance. Trenton, New Jersey.

Houston, S.L., Duryea, P.D., Hong, R., 1999. Infiltration considerations for groundwater recharge with waste effluent. *J. Irrig. Drain. Eng.* 125, 264–272.

Idelovitch, E., 2003. SAT (Soil Aquifer Treatment)—The long term performance of the Dan Region reclamation project. Washington, DC: The World Bank Water Week.

<http://siteresources.worldbank.org/EXTWAT/Resources/4602122-1213366294492/5106220-1213366309673/15.2SoilAquiferTreatment-Israel-E.pdf>

Inglezakis, V.J., and Loizidou, M.D., 2007. Ion exchange of some heavy metal ions from polar organic solvents into zeolite. *Desalination* 211(1), 238–248. Available from: <http://www.desline.com/articoli/8583.pdf>

IWMI, (International Water Management Institute), 2009. Strategic Analyses of the National River Linking Project (NRLP) of India Series 5. Proceedings of the Second National Workshop on Strategic Issues in Indian Irrigation, New Delhi, India, 8-9 April 2009. <http://publications.iwmi.org/pdf/H042682.pdf>

Jalali M, Moharrami S. Competitive adsorption of trace elements in calcareous soils of western Iran. *Geoderma* 2007; 140: 156-163.

Johnson, R.H., and Bush, P. W., 1988. Summary of the Hydrology of the Floridan Aquifer System in Florida and in Parts of Georgia, South Carolina, and Alabama. Professional Paper 1403-A. Washington D.C., U.S. Geological Survey.

Kania, J., 2003. Geochemical interpretation of thermal fluids from low-temperature wells in Stykkishólmur, W-Iceland and Pырzyce, NW-Poland. Reports of the United Nations University Geothermal Training Programme, No13. Reykjavik, Iceland.

Kazner, C., Wintgens, T., Dillon, P., 2012. Water Reclamation Technologies for Safe Managed Aquifer Recharge. IWA. ISBN: 9781843393443.

Keeney, D.1970. Nitrates in plants and waters.*J. Milk Food Technol.* 33, 425–432.

Kmiec, J. P., Thomure, T. M., & Tucson Water. 2005. Sweetwater recharge facilities: serving Tucson for 20 years. Tucson.

Koda, E., Osinski, P., Sieczka, A., Wychowaniak, D., 2015. Areal Distribution of Ammonium Contamination of Soil-Water Environment in the Vicinity of Old Municipal Landfill Site with Vertical Barrier. *Water*, 7: 2656–2672.

Kohne, S., Simunek, J., Kohne, M., Lennartz, B., 2006. Simulating simultaneous nitrification and denitrification in mobile and immobile soil water regions of the vadoze zone. *Geophysical Research Abstracts*, Vol. 8, 04443.

Korom, S.F.,1992. Natural denitrification in the saturated zone: A review, *Water Resource Research.*, 28(6) 1657-1668.

Krambis, S., 1993. Electrical sounding resistivity survey in Paphos Coastal Plain. File Data. Geological Survey Department, Nicosia. Cyprus.

Kross, B.C., Hallberg, G.R., Bruner, D.R., Cherryholmes, K., and Johnson, J.K.,1993. The nitrate contamination of private well water in Iowa.*American Journal of Public Health* 83(2), 270–2.

Kuster, M., Diaz-Cruz, S., Rosell, M., Lopez de Alda, M., Barcelo, D., 2010. Fate of selected pesticides, estrogens, progestogens and volatile organic compounds during artificial aquifer recharge using surface waters. *Chemosphere*, 79(8), 880-886.

Lakretz, A., Mamane, H., Cikurel, H., Avisar, D., Gelman, E., Zucker, I., 2017. The Role of Soil Aquifer Treatment (SAT) for Effective Removal of Organic Matter, Trace Organic Compounds and Microorganisms from Secondary Effluents Pre-treated by Ozone, *Ozone: Science & Engineering*, DOI: 10.1080/01919512.2017.1346465.

Lapierre, H., Bosch, D., Narros, A., Mascle, G. H., Tardy, M., & Demant, A., 2007. The Mamonia Complex (SW Cyprus) revisited: remnant of Late Triassic intra-oceanic volcanism along the Tethyan southwestern passive margin. *Geological Magazine* 144(1), 1-19.

Langmark, J., Storey, M. V., Ashbolt, N. J., Stenström, T. A., 2004. Artificial groundwater treatment: biofilm activity and organic carbon removal performance. *Water Res.*, 38(3), 740-748.

Lazarova, V., Levine, B., Sack, J., et al 2001. Role of water reuse for enhancing integrated water management in Europe and Mediterranean countries. *Water Science and Technology*, 43(10), 25-33.

Lefebvre, O., and Moletta, R., 2006. Treatment of organic pollution in industrial saline wastewater: a literature review. *Water Res.* 40(20):3671-82.

Lipson, S.M., Stotzky, G., 1983. Adsorption of reovirus to clay minerals: effects of cation-exchange capacity, cation saturation, and surface area. *Appl Environ Microbiol.* 46(3), 673-82.

LOTT Clean Water Alliance, 2013. Reclaimed Water Infiltration Study. Technical Memorandum - "Case Study Summary".

LOTT Clean Water Alliance, 2013. Reclaimed Water Infiltration Study Technical Memorandum - "State of the Science".

Lowe, K.S., and Siegrist, R.L., 2008. Controlled Field Experiment for Performance Evaluation of Septic Tank Effluent Treatment during Soil Infiltration. *J. Environ. Eng.*, 134(2):93-101.

Magorzo, C., Hernandez, M., Bernat, X., 2013. Integrated Urban Water Management and Investigation of New Resources for Regions under Water Stress D5.1.5.b Identification of control parameters in water catchment and conservation systems under high flow events (subsurface accumulation). <http://www.prepared-fp7.eu/viewer/file.aspx?FileInfoID=306>

Mantoglou, A., and Gelhar, L.W., (1987). Stochastic modeling of large-scale transient unsaturated flow. *Water Resources Research*, 23(1), 37–46.

Massmann, G., Greskowiak, J., Dünnebier, U., Zuehlke, S., Knappe A., and Pekdeger, A., 2006. The impact of variable temperatures on the redox conditions and the behaviour of pharmaceutical residues during artificial recharge. *Journal of Hydrology*, 328(1-2), 141-156.

Mayer, P.M., Groffman, P.M., Striz, E.A., Kaushal, S.S., 2010. Nitrogen dynamics at the groundwater-surface water interface of a degraded urban stream. *Journal of Environmental Quality*, 39(3), 810-23.

Mays, L., 1997. *Optimal control of hydrosystems*. Taylor & Francis Group, ISBN 10: 0824798309/ ISBN 13: 9780824798307.

Megdal, S. B., Dillon, P., and Seasholes, K., 2014. Water Banks: Using Managed Aquifer Recharge to Meet Water Policy Objectives. *Water (Switzerland)*, 6, 1500–1514.

<http://doi.org/10.3390/w6061500>

Milnes, E., 2007. Simulation of groundwater flow conditions in the Ezousa river bed aquifer. Technical Report WDD-Paphos, 1-49.

Miotlinski, K., Barry, K., Dillon, P., Breton, M., 2010. Alice Springs SAT Project Hydrological and Water Quality Monitoring Report 2008-2009. CSIRO: Water for a Healthy Country National Research Flagship. Available from: https://www.researchgate.net/publication/265635038_Alice_Springs_SAT_Project_Hydrological_and_Water_Quality_Monitoring_Report_2008-2009 [accessed Dec 03 2017].

Mohammad R. Al-Agha, Hamed A. El-Nakhal, 2011. Hydrochemical facies of groundwater in the Gaza Strip, Palestine. *Hydrological Sciences Journal*. Available from: <http://www.informaworld.com/smpp/title~content=t911751996>.

Morley, N., Baggs, E.M., Dörsch, P., and Bakken, L., 2008. Production of NO, N₂O and N₂ by extracted soil bacteria, regulation by NO₂⁻ and O₂ concentrations. *Microbiology Ecology*, 65(1) 102–112.

Nicolaidis, P., and Georgiou, A., 1999. An assessment of the environmental impact in the Akrotiri aquifer by using treated effluent for groundwater recharge. In proceedings. Hydrogeological Conference; “Water Resources Management”. Bulletin 9, 115-132, Nicosia, Cyprus.

Nguyena, H.V., Niebera, J.L., Ritsemab, C.J., Dekkerb, L.W., Steenhuisc, T.S., 1999. Modeling gravity driven unstable flow in a water repellent soil. *Journal of Hydrology*, 215(1), 202–214.

Noto, M.T., Vega, T., Lopez, A., Francesco Viola, F., 2013. Strategic master plans for small and large med islands. MEDIWAT Sustainable management of environmental issues related to water stress in Mediterranean islands 2G-MED09-262.

NRC (National Research Council), 1994. Issues in Potable Water Reuse. National Research Council. Washington D.C., National Academy Press.

NRC (National Research Council), 1998. Nutrient Requirements of Swine. Tenth Revised Edition. National Academic Press, Washington, D.C. 20418 USA.

Onsoy, Y.S., Harter, T., Gin, T. R., and Horwath, W.R., 2005. Spatial variability and transport of nitrate in a deep alluvial vadoze zone. *Vadose Journal* 4(1), 41-54.

Oude Essink, G.P., 2001. Improving fresh groundwater supply – problems and solutions. *Ocean and Coastal Management*, 44(5), 429-449.

Paramasivam, S., Alva, A. K., Prakash, O., and Cui, S. L., 1999. Denitrification in the vadoze zone and in surficial groundwater of a sandy entisol with citrus production. *Plant and Soil*, 208(2), 307-319.

Parkhurst, D.L., and Appelo, C.A.J., 2010. User's Guide to PHREEQC (Version 2)-A Computer Program for Speciation, Batch-Reaction, One-Dimensional Transport, and Inverse Geochemical Calculations. Washington D.C. U.S. Geological Survey, Water Resources Investigation Report, 99-4259.

Puckett, L.J., and Cowdery, T.K., 2002. Transport and fate of nitrate in a glacial outwash aquifer in relation to groundwater age, land use practices and redox processes. *Journal of Environmental Quality*, 31(3), 782-796.

Puckett, L.J., Cowdery, T.K., McMahon, P.B., Tornes, L.H., and Stoner, J.D., 2002. Using chemical, hydrologic, and age-dating analysis to delineate redox processes and flow paths in the riparian zone of a glacial outwash aquifer-stream system. *Water Resources Research*. Available from:
https://water.usgs.gov/nawqa/nutrients/pubs/wrr_v38/wrr_v38.html

Quanrud, D.M., Drewes, J., Milczarek, M., Conroy, O., Ela, W.P., Lanse, K.E., and Arnold, R.G., 2005. Soil Aquifer Treatment: A Sustainable Process For Organics Removal. Paper presented at the 12th Biennial Symposium on Groundwater Recharge, Tucson, AZ, June 8-10, 2005.
file:///C:/Users/User/Downloads/2005Quanrudetal12thGWrecharge%20(1).pdf

Raju, R. T., Jemno, K., and Wada, S.I., 1993. Unsaturated flow in an evaporative regime and *cation exchange* in soils. In: *Proceedings of the Yokohama*

Symposium, July 1993. International Association of Hydrological sciences Publ. no. 212.

Rashid, A. K, Ferrell, R.E., and Billings, G.K., 1972. The Genesis of Selected Hydrochemical Facies in Baton Rouge, Louisiana, Ground Waters. *Ground Water*, 10(4), 14-20.

Reilly, T.J., and Baehr, A.L., 2006. Methodology to evaluate the effect of sorption in the unsaturated zone on the storage of nitrate and other ions and their transport across the water table, southern New Jersey: US Geological Survey Scientific Investigations Report 2006-5074.

Rivett, M.O., Buss, S.R., Morgan, P., Smith, J.W.N., Bemment, C.D., 2008. Nitrate attenuation in groundwater: a review of biogeochemical controlling processes. *Water Research*, 42(16), 4215-4232.

Roberge, P.R., 2007. *Corrosion Inspection and Monitoring*. John Wiley & Sons, ISBN

0470099755, 9780470099759.

Robertson, A. H. F., 2000. Tectonic Evolution of Cyprus. In: *Proceedings of the Third International Conference on the Geology of the Eastern Mediterranean*, Nicosia, (1998). Cyprus Geological Survey Department, Nicosia-Cyprus, pp11–44.

Robertson, A. H. F., Eaton, S., Follows, E. J., and Payne, A. S., 1995. Depositional processes and basin analysis of Messinian evaporates in Cyprus. *Terra Nova* 7(2), 233-253.

Robertson, A. H. F., Emeis, K-C., Richter, C., and Camerlenghi, A., (eds) 1998. 1998. In: Proceedings of the Ocean Drilling Program, Scientific Results, 160. Ocean Drilling Program, College Station, TX.

Rose, S., and Long A., 1989. Dissolved inorganic carbon in the Tuecon Basin Aquifer. *Ground Water*, 27(1), 43-49.

Runnels, D.D., 1995. Basic contaminant fate and transport processes in the vadose zone- Inorganics. Handbook of Vadoze zone Characterization and Monitoring. L.G. Wilson, L.G. Everett, and S.J. Cullen, Geraghty & Miller Environmental Science and Engineering Series.

Saha, P.K., and Badruzzaman, A.B.M.,2014. An experimental investigation of sorption of copper on sandy soil by laboratory batch and column experiments. *International Journal of Environment and Waste Management*; 13(2): 160-178.

Schmidt, C.M., Fisher, A.T., Racz, A.J., Lockwood, B.S., and Los Huertos, M., 2011. Linking denitrification and infiltration rates during managed groundwater recharge. *Environmental Science and Technology*, 45(22), 9634-9640.

Schimmoller, L. J., Kealy, M. J., and Foster, S. K., 2015. Triple bottom line costs for multiple potable reuse treatment schemes. *Environmental Science: Water Research Technology*, 1(5), 644-658. doi:10.1039/c5ew00044k

Schwarz, J., and Bear, J., 2016. Artificial Recharge of Groundwater in Israel. <https://recharge.iah.org/files/2016/08/Israel-Schwarz-and-Bear-Israel-10apr16.pdf>

Sharpley, A., Jarvie, H.P., Buda, A., May, L., Spears, B., and Kleinman, P., 2013. Phosphorus Legacy: Overcoming the Effects of Past Management Practices to Mitigate Future Water Quality Impairment. *J. Environ. Qual.* 42:1308–1326

Siegrist, R.L., McCray, J.E., Lowe, K.S., 2004. Wastewater Infiltration into Soil and the Effects of Infiltrative Surface. *Architecture. Small Flows Journal*, 5(1):29-39.

Simunek, J., Kohne, J. M., Kodesova, R., and Sejna, M., (2008). Simulating nonequilibrium movement of water, solutes and particles using HYDRUS-a review of recent applications. *Soil Water Res.* v. 3(Spec. Iss. 1), S42–S51.

Singh, R., Gautam, N., Mishra, A., Gupta, R., 2011. Heavy metals and living systems: An overview. *Indian Journal of Pharmacology* 43(3):246-53

Smith, A. J. and Pollock, D. W., 2010. Artificial recharge potential of the Perth region superficial aquifer: Lake Preston to Moore River. CSIRO: Water for a Healthy Country National Research Flagship.

SOGESID, 2005. Local Water Supply, Sanitation and Sewage—Cyprus. Societa Gestione Impianti Idricil, Internal report for the Water Development Department, Nicosia, Cyprus.

Sokolova, T.A., and Alekseeva, S.A., 2008. Adsorption of sulfate ions by soils (A Review) *Eurasian Soil Sc.* Volume 41,2, pp 140–148.
<https://doi.org/10.1134/S106422930802004X>

Somasundaran, P., Amankonah, J.O., and Ananthapadmabhan, K.P., 1985. Mineral-Solution Equilibria In Sparingly Soluble Mineral Systems. *Colloids and Surfaces*, 15 309-333.

Sprenger, C., Hartog, N., Hernández, M., Vilanova, E., Grützmacher, G., Scheibler, F., Hannappe, S., 2017. Inventory of managed aquifer recharge sites in Europe: historical development, current situation and perspectives. *Springer, Hydrogeol J.* DOI 10.1007/s10040-017-1554-8

Starr, R.C., and Gillham, R.W., 1993. Denitrification and organic carbon availability in two aquifers. *Groundwater*, 31 (6), 934–947.

Swarbrick, R.E., 1993. Sinistral strike-slip and transpressional tectonics in an ancient oceanic setting: the Mamonia complex, southwest Cyprus. *Journal of the Geological Society*, 150(2), 381–392.

Taylor, J.R., 2003. Evaluating groundwater nitrates from on-lot septic systems, a guidance model for land planning in Pennsylvania. Penn State Great Valley, School of Graduate Professional Studies: Malvern, Pennsylvania.

Teijon, G., Candela, L., Tamoh, K., Molina-Díaz, A., Fernández-Alba, A.R., 2010. Occurrence of emerging contaminants, priority substances (2008/105/CE) and heavy metals in treated wastewater and groundwater at Depurbaix facility (Barcelona, Spain). *Science of the Total Environment* 408(17), 3584-3595.

Thayalakumaran, T., Bristow, K. L., Charlesworth, P.B., and Fass, T., 2008. Geochemical conditions in groundwater systems: Implications for the attenuation of agricultural nitrate. *Agricultural Water Management*, 95(2), 103-115.

Thomasson, A.J., Bouma, J., Leith, H., 1991. Soil and Groundwater Research Report. II. Nitrate in Soils. EUR13501 Luxembourg Office for Official Publications of the European Communities.

Todd, D.K., 1980. Groundwater hydrology. 2nd Ed. Chichester, John Wiley.

Ueda, S., Ogura, N., and Yoshinari, T., 1993. Accumulation of nitrous oxide in aerobic groundwaters. *Water Research*, 27(12), 1787-1792.

Ünlü, K., Nielsen, D.R., Biggar, J.W., Morkoc, F., 1990. Statistical parameters characterizing the spatial variability of selected soil hydraulic properties. *Soil Science Society of America Journal - SSSAJ*. 54.
10.2136/sssaj1990.03615995005400060005x.

USDA, NRCS, 2010. Part 631 National Engineering Handbook, Ground Water, vol. 33, No. 6. US EPA, 1999. U.S. Environmental Protection Agency, Office of Ground Water (4601). Report to Congress: Class V Underground Injection Control Study. Volume 7, Sewage Treatment Effluent Wells. <http://www.water-research.net/Waterlibrary/Injectwell/injectionsewage7.pdf>

USEPA. Exposure Factors Handbook (1997, Final Report). U.S. Environmental Protection Agency, Washington, DC, EPA/600/P-95/002F a-c, 1997.

USEPA, 1999. The Class V Underground Injection Control Study, Volume 21, Aquifer Recharge and Aquifer Storage and Recovery Wells. Office of Ground Water and Drinking Water, EPA/816-R-99-014u.

USEPA, 2003. Wastewater Technology Fact Sheet Rapid Infiltration Land Treatment. https://www3.epa.gov/npdes/pubs/final_rapidinfiltration.pdf).

USEPA, 2004. Guidelines for Water Reuse, EPA/625/R-04/108, Washington D.C.

Vance, D.B., 1994. Anisotropic flow in heterogeneous granular media: analysis of complex systems. National Environmental Journal, 4(5), 24-25.

Vandenbohede, A., Warllis, I., Van Houtte, E., Van Ranst, E., 2013. Hydrogeochemical transport modeling of the infiltration of tertiary treated wastewater in a dune area, Belgium. Hydrogeol J. V 21(6).

Van Houtte, E., 2015. Water reuse for aquifer recharge 'the Torreele/St-André project'. Technical Workshop "Water reuse in agricultural irrigation and aquifer recharge – Towards minimum quality requirements at EU level". Brussels, June 25th & 26th, 2015.

Ward, A.L., Gee, G.W., Zhang, Z.F., and Keller, J.M., 2004. Vadoze zone contaminant Fate-and-Transport Analysis for the 216-B-26 Trench. Pacific Northwest National Laboratory, PNNL-14907. Richland, WA99352.

WDD, (Water Development Department), 2005. Annual Report, Nicosia.

WDD, (Water Development Department), 2016. Symposium "Reuse of treated effluent in Cyprus", Limassol, 11/05/2016.
[http://www.cyprus.gov.cy/moa/wdd/Wdd.nsf/All/5B994CCD737A6940C2258160003D7255/\\$file/1_limassol.pdf](http://www.cyprus.gov.cy/moa/wdd/Wdd.nsf/All/5B994CCD737A6940C2258160003D7255/$file/1_limassol.pdf)

Weeks, E.P., USGS, US Geological Survey, Office of Ground- water, 2002. Artificial Recharge Workshop Proceedings. Sacramento, California. US Geological Survey. Open-File Report 02-89, 5–12. Available from: <http://water.usgs.gov/ogw/pubs.html>.

Weiner, E.R., 2000. Applications of environmental chemistry: A practical guide for environmental professionals. Boca Raton, Lewis. Available from: Chemical. Mem.Ir/Part,Showattachment/Id,99/Lang,Fa/. Retrieved 10th January 2011.

Weiss, P.T., LeFevre, G., and Gulliver, J.S., 2008. Contamination of Soil and Groundwater Due to Stormwater Infiltration Practices. In: SAFL Project Report 515, June 2008. Available from: <http://purl.umn.edu/115341>.

Weiyang, P., Yunwu, X., Quanzhong, H., and Guanhua, H., 2017. Removal of Nitrogen and COD from Reclaimed Water during Long-Term Simulated Soil Aquifer Treatment System under Different Hydraulic Conditions. *Water* 2017, 9, 786; doi:10.3390/w9100786 www.mdpi.com/journal/water).

White, R.E., 2006. Principles and practice of soil science: the soil as a natural resource. 1st Ed. Oxford, Blackwell.

Winter, K.J., and Goetz, D., 2003. The impact of sewage composition on the soil clogging phenomena of vertical flow constructed wetlands. *Water Science & Technology*, 48(5), 9–14.

Wintgens, T., Hochstrat, R., Kazner, C., Jeffrey, P., Jefferson, B., Melin, T., 2009. Managed Aquifer Recharge as a component of sustainable water strategies. https://circabc.europa.eu/sd/a/049c2aba-fe3e-481a-95f3-d956be4e52e4/RECLAIM_WATER_Policy_Brief_Final.pdf

Wong, C.I., Mahler, B.J., Musgrove, M., Banner, J.L., 2012. Changes in sources and storage in a karst aquifer during a transition from drought to wet conditions. *Journal of Hydrology*, 468, 159-172.

Wu, Z., Wang, S., He, M., Zhang, L., Jiao, L., 2015. Element remobilization, Binternal P-loading, and sediment-P reactivity researched by DGT (diffusive gradients in thin films) technique.

Environ Sci Pollut Res 22(20):16173–16183. doi:10.1007/s11356-015-4736-8

Zampetti, M., 1983. Information and data on the quantity and quality of water sub-divisions in the European Community . Pollution of groundwater from compounds chlorinated organisms of industrial origin.

Ziolko, D., Martin, O.V., Scrimshaw M.D., Lester, J.N., 2011. An evaluation of metal removal during wastewater treatment: the potential to achieve more stringent final effluent standards. *Critical Reviews in Environmental Science and Technology*, V. 41,(8) 733-769.

APPENDIX 1

OPTIMUM SOLUTIONS TO WATER TABLE MOUND GROWTH AS A RESULT OF ARTIFICIAL GROUNDWATER RECHARGE

ABSTRACT

This study presents analytical solutions to the mound growth problem. The literature review has covered the development of aquifer mound growth theory whose origins were from the application of heat transfer equations. The literature review suggested that using the Laplace partial differential equation (PDE) of groundwater flow was the most appropriate technique.

Following on from this conclusion, a first principles solution of the linear PDE is presented; applied to confined aquifers with the well functions evaluated by two methods. Firstly, the Simpson's Rule Method (SRM) was used with a specified accuracy and secondly a Direct Integration Method (DIM), following evaluation of the Euler constant to ten decimal places using SRM. Cylindrical co-ordinates with radial symmetry were then used to reflect the actual site conditions. These were of a 4m diameter, 9m deep percolation pit used for these effluent recharge experiments. The infiltration well met the initial water table level of the aquifer whose thickness was estimated to be 10 m. The results of the two methods were shown to coincide over a range heads and time at the fixed radius.

For unconfined aquifers the literature review reported that the PDE becomes non-linear and needed to be linearized for a solution to be possible. The Hantush linearization method was identified by the literature as the most common method of overcoming this.

Hantush linearization solutions were derived from first principles and the solution adopted in this work was to linearise the PDE by enlarging the aquifer thickness by replacing the non-linearity variable $\bar{h}_A = H_A + h_{KOKOS}$ where the constant $h_{KOKOS} = \lambda(t)h(r_{MIN}, t)$ was proportional to the maximum head at the percolation pit radius. The calculations demonstrated that a change in the variable proportionality constant noted above was needed ($\lambda(t)$ to be 0.5) for the Hantush linearization to work.

The observed field results presented for mound heads $h(r, t)$ with respect to time at the fixed radius are identical to those obtained by this modification to the Hantush linearization where the $\lambda(t)$ constant was taken as 0.5, that is $\bar{h}_H = H_A + 0.5h_{MAX}$.

Therefore, it was concluded that the results, based on the normal Hantush linearization constant, although widely used by hydrologists, were neither optimum nor unique, as there was no theoretical basis, physical or hydraulic to substantiate his assumed linearization. This study also, therefore, examines the properties of the proportionality factor derived from this research $\lambda(t)$ using the *Recharge-Voids*

Volume relationship. This makes the radius square to the time ratio, $\frac{r_{CRIT}^2}{t_{CRIT}} = \frac{Q}{\pi S \bar{h}_A}$

constant and as a consequence when this is substituted into the well function it renders time invariant as shown in Eq.29. The corresponding critical head h_{CRIT} at this particular radius and time was also then time invariant; which represents a plane, h_{CRIT} above the initial water table. This plane then represents the saturated depth of the aquifer a relationship which is maintained up to $r \rightarrow \infty$.

Optimum values of $\lambda(t)$ at given times t using the ratio of the critical height to the maximum mound height at the percolation pit radius, $\lambda(t) = \frac{h_{CRIT}}{h(r_{MIN}, t)}$ were then examined in this study. The optimized $h(r, t)$ results, thus obtained, are higher than those of Hantush, which was also supported by experimental data found in the literature (Marino, 1967; Korkmaz, 2012).

1. INTRODUCTION

This study analyses the problem of transient groundwater mounding for the Ezousas case study of an unconfined aquifer recharged from a constant head in a cylindrical percolation pit. This has led to a proposed alternative general solution for mound growth in unconfined aquifers subject to recharge. The solution was based on the introduction of a critical depth to give a time optimum linearization constant which unlike the original Hantush method is not restricted to being a constant 0.5.

2. LITERATURE REVIEW

2.1 The Hydraulics of Recharge

Recharge of unconfined and confined aquifers is usually achieved by employing spreading basins, percolation pits and by well injection.

In a recharge basin the water after infiltration moves downward, under the influence of gravity and horizontally due to water head differences. The driving force which causes the water to move laterally away from the subsurface can be predicted by Darcy's Law, with several assumptions (collectively known as the Dupuit-Forcheimer assumptions): (1) vertical flow below the drain field is ignored; (2) all flow in the aquifer is horizontal and laminar; and (3) horizontal flow is uniformly distributed with depth. These assumptions are closely approximated when the water slope is small, usually $<0.01\%$ (Todd,1980; Marino and Luthin,1982). This involves solution of the Laplace equation subject to appropriate boundary and initial conditions.

When the infiltrating water reaches the groundwater table, then a water mound will begin to build up. The formation, shape and evolution of the groundwater mound, beneath the artificial recharge basin are important to maintaining continued recharge. Excess mound growth will lead to overland flow with the usual range of flooding problems (Bansal and Das, 2010). In the case that the recharge scheme relies on the soil treatment, then there may be additional problems from the contamination of native surface and ground water (Bouwer, 2002).

The shape and growth of the mound depend on the infiltration rate, size of the basin and the hydraulic properties of the aquifer. Hydraulic conductivity is the most important but this presents difficulties since it cannot be measured accurately (Todd, 1961; Ferguson, 1990; Aish, 2010). Critical site factors noted as affecting head differentials are: whether the recharge rates are continuous or intermittent, the various hydraulic conductivity values of the soils underlying the drain-field area, the depth of the vadose zone and aquifer, the basin shape, depth and area.

Previous work has suggested that the recharge water mound is defined by its shape or height, radius, and its duration. These can also be used as indicators of the hydraulic properties of the soil and underlying strata and thus important to engineering questions concerning the storage available in the aquifer and rate of infiltration.

The bell like mounding shape is nonlinear and therefore complex. Solutions are obtained by the linearization of the simplified partial differential equations governing groundwater. Although water mounding is a transient process, it may reach a quasi steady state when the rate of infiltration is equalized by the rate of recharge to the groundwater table (Bouwer et al, 1999).

Various models have been used to describe the mounding shape: nonlinear potential theory; the Dupuit-Forchheimer approximation; the linearized Dupuit-Forchheimer approximation; and linear potential theory (Kacimo,1997). Even though computing algorithms (e.g. the finite difference method) and models are effective in predicting complex non-steady groundwater systems, simpler analytical solutions would be more accessible and widely used. Validation of these numerical models are also required and computing power and time may not always be available. The basic equations are not easy to use and require appropriate assumptions. For instance, the linearization term, in the most common equations used, the Hantush's solution (1967) needs to be approximated by the aquifer thickness which results in less precision than those obtained by the true effective thickness (Guo, 2001 and 2003).

For an infinite aquifer, the ground-water mound profile has been obtained in the form of Theis and Hantush partial differential equation 5. The well function has been tabulated for a certain range of arguments. However, to use this table, double interpolation is necessary, which increases the error and a tabular solution cannot be used for analytical purposes. Thus, there is an incentive to find a more useful and less computationally demanding algebraic approximations of the definite integral (Swamee and Ojha,1997).

The research reported here also suggests adjustments to the basic equations could provide a better fundamental insight into the processes. This is the general view in the literature for example; Bouwer (1962), Glover (1964), Marino (1967), Singh (1976), Morel-Seytoux et al (1989), Zomorodi (1991), Finnemore (1993) have published modified and simplified methods to give approximate solutions to mound growth.

2.2 Mathematical Solutions

Investigations on the development of mounded phreatic surface under different conditions have been carried out by many researchers.

The first to deal with transient flow in aquifers were the well-known Theis equations published by the USGS in 1935 (Howden, N., and Mather, J., 2012). These introduced analytical solutions to determine the drawdown adjacent to pumping wells from confined, non-leaky aquifers (Batu, 1998). The analogy between heat flow from a long, straight wire to groundwater flow to a well was used to develop solutions. As an interesting historical aside, it was reported that Theis corresponded with a mathematician, Clarence Lubin at the University of Cincinnati in 1934 regarding the problem of radial flow given a plate of constant thickness and a uniform initial temperature. Lubin responded with the line source equation derived from Carslaw and Jaeger (reported by Napolitan, 2010). Transposing the variables from heat conduction to groundwater flow, Theis wrote the familiar seminal paper that revolutionized groundwater analysis (Napolitan, 2010).

Once Theis and later Jacob (1940) had shown the analogy between groundwater and heat flow, further research has been published to solve the appropriate boundary values and solutions to describe various schemes for flow development (Bredehoeft, 2002).

The standard aquifer equations assumed $h=aW(u)$, where h is the mound high, a is a constant and $W(u)$ is the Theis well function. The solution for h was given by the standard Euler equation in the form of a series (reported by Wang et al. 2004). This solution corresponded to flow in a confined aquifer and the values obtained would be higher for unconfined aquifers. Refinement and adjustments to the

mound height were made for unconfined aquifers to take into account the other contributing factors. This allowed h to be approximated for unconfined aquifers too. These later versions of the Theis equations are in widespread use of the by the groundwater community (Wang et al, 2004).

Mathematical equations for rising and falling ground water mounds by artificial recharge were given specifically by Baumann (1952). The Baumann solutions were based on the heat flow analog model (Schiff and Dyer, 1964). Baumann considered a two-dimensional condition, where the length of spreading area was much greater than the width. He showed that for certain conditions the Boussinesq (1877) equation for unsteady groundwater flow reduces to an analog of the heat flow and at steady flow, reduces to the Dupuit (1948) equation. Marmion (1962), using similar principles, derives equations for various stratigraphic conditions and shapes of mounds obtained from the equations developed by Baumann (1952) and Glover (1961). Glover applied the method suggested by Baumann (solutions to the linearised Boussinesq equation) to predict the formation of groundwater mounds beneath the artificial recharge basins from constant replenishment (Bansall and Das, 2010). The shapes were obtained in a two-dimensional model representing a vertical section in an unconfined aquifer. All of these earlier expressions by Baumann (1952) and Glover (1961) were based on the assumption that the mounding was less than 2% of the initial depth of saturation and this limits their usefulness because larger and potentially more critical mounds form most readily in shallow saturated zones (Finnemore, 1995). Todd (1961) assumed an axisymmetric cylindrical model with horizontal flow and simply used the Dupuit equation to give the change of height with radius. The optimum radius of the influence in terms of the recharge was approximately stated and his relationship did not include time.

The importance of geometric variables; such as size of recharge basin, depth to ground water, and thickness of the aquifer have also been considered. One of the most important factors noted was the ability to include variable recharge rates. These were investigated by Bouwer (1962) who presented an equation to predict rise and fall of the mound below the centre of either a rectangular or round recharge basin. In this case he used the analogy with an electrical resistance network to establish equations for the analysis of rising, falling, and stable groundwater mounds. The solutions were based on the Laplace equation and the analogy between Darcy's and Ohm's law. The solutions were two-dimensional or radial flow under the recharge and required simplifying assumptions. Bouwer concluded that graphical solutions and curve fitting were necessary for accurate results.

One of the best known analytical solutions for predicting groundwater mound development was presented by Hantush (1967). The Hantush method has most recently been reviewed by Poeter et al (2005) and Thompson et al (2007). Hantush solved the linearized form of the saturated, radial, groundwater flow equation and applied it to mound formation beneath rectangular and circular infiltration basins. The solution was for a transient mound with a constant rate of infiltration, and required inputs of saturated hydraulic conductivity, storage capacity and initial saturated thickness. Marinos (1967) verified the validity of the Hantush's linearization method by comparing the analytical results with those obtained from the Shaw model was found that when the rate of percolation (RR) $\leq 0.2K$ and $h-h_o \leq 0.5h_o$, the maximum deviation between the two solutions was 6%. Even for $h-h_o \geq 20h_o$, the maximum deviation was 12.2%. Finnemore (1995) and Sunada et al (1983) found the Hantush solutions (1967) to be the most accurate and amenable to numerical integration (reported by Carleton, 2010).

Brutsaert and Ibrahim (1966), Murray and Johnson (1977) and Rao and Sarma (1980), have all shown that the Hantush's method of linearization would be more widely applicable compared to the Baumann's method. It was also demonstrated by Rai and Singh (1996) that the Hantush analytical results agreed reasonably well with their experimental data. Rao and Sharma (1981) were one of the groups which demonstrated the utility of Hantush's mound function in representing groundwater mounds. Rao and Sharma (1981) also compared the Hantush analytical solutions with those of the two-dimensional 2D- linearised Boussinesq equation. These were applied to predict the evolution of a groundwater mound under rectangular recharge basins with constant discharge.

Rai and Singh (1981, 1993) presented similar analytical solutions to that of Hantush (1967) and in a number of articles they derive solutions that include a variety of different boundary conditions (for example, with Manglik and others, 1997, 2000, 2003). The aquifer was assumed to be lying between an impermeable boundary and an open surface reservoir or having invariant water level at an elevation equal to the height of the initial water table. Localized recharge was applied from a fixed width strip with the recharge rate exponentially decreasing with time from an initial upper to a lower value and which thereafter remained constant.

Manglik and Rai (2000) also developed analytical solutions to model water table fluctuations in an isotropic unconfined aquifer in response to time varying recharge from multiple rectangular basins. This solution incorporated prescribed head boundary conditions and approximated well when used in conjunction with small dimension rectangular recharge basins. In a following article, with a similar assumed isotropic aquifer, Manglik et al, (2004) developed analytical solutions, with prescribed zero flux boundary conditions, to describe water table heights with time, according to recharge rate from any number of pumped recharge basins.

Dagan (1967) applied first-order theory to compare with the Hantush predictions of water table elevations when aquifer thickness was significantly less than the characteristic horizontal length of the recharge basin. Dagan (1967) also derived additional compact closed formulas for mound elevations of infinitely deep aquifers, thus validating the Hantush for both shallow and deep aquifers. It has been argued by Zlotnik and Ledder, (1993) however that the most common practical case is when aquifer thickness is similar to the source size and this was not covered by either Dagan (1967) or Hantush (1967).

Zomorodi (1991) used field data, from the Ghazvin Plain in Iran, to refine a simpler numerical model for groundwater mounding. Zomorodi (1991) found, as was noted previously, that there was a decline in the rate of recharge and solutions based on an assumed constant rate of recharge that did not predict the recession of the mound. Incorporating an effect from a unsaturated zone and declining rate of recharge improved the reliability compared to previous methods.

The Zomorodi (1991) methods were used to simulate the shape of a groundwater mound beneath hypothetical infiltration basins by Sunada et al (1983) which suggested these were inaccurate without numerical integration. Sunada et al (1983) and Warner et al (1989), therefore, developed computer programs to solve the Hantush equation for both steady (continuous) or transient recharge with user-specified input variables; these were transmissivity, basin size, and recharge rate. These computer programs are no longer readily available and do not run on some personal computers (for example, they will not run on computers using a 64-bit processor Carleton (2010).

Hantush's solution for a rectangular source has also been adapted to predict contaminant transport from stormwater infiltration basins during the soil treatment of wastewater (Poeter et al, 2005). The solution assumes a homogeneous and isotropic aquifer, bounded by a horizontal water table with overlying mounding.

It has been concluded from the literature review, that because of its accuracy and wide spread use, the Hantush method is the most extensively used model to calculate the time-varying heights of groundwater mounds on and near horizontal saturated zones. The Hantush method however remains inconvenient requiring function evaluations and two-dimensional interpolation between tabulated values, which must be performed iteratively.

Finnemore (1995) produced a FORTRAN computer program to perform these necessary iterations and sub-routines to evaluate the long and complex equations. These equations avoid the need for interpolation or other approximation procedures and they provide more accurate solutions for all conditions. Comparison of the results from the computer program with results from the original approximation procedures has indicated the areas which were unreliable in the original Hantush procedures. Zomorodi (2005) provided a simplified method for solving the Hantush equations, but both approaches are only suitable for steady-state conditions.

For all of the analytical solutions reviewed, it was assumed that flow away from the recharge basin was horizontal and into an isotropic homogeneous aquifer and the change in height of the water table was not large (generally less than one-half the aquifer thickness).

These solutions, incorporating simple boundary conditions to the governing differential groundwater equations, can be used for specific groundwater interactions when various stresses are applied to the aquifer.

On the other hand commercial programs such as MODFLOW, using finite difference methods and HYDRUS, with finite element solutions, are available nowadays. These enable the handling of more complex boundary conditions and multiple types of interactions compared to the original analytical equations. These comparisons have been investigated in this study of the thesis.

3. AIMS AND OBJECTIVES

The aim of this work was to develop analytical solutions to predict mound height build up that could be easily used by field engineers and hydrogeologists. A physical basis has been sought for any assumptions required for the solution of linear and non-linear partial differential equations used to represent the flow in confined and unconfined aquifers.

As a result for confined aquifers the well function has been evaluated using the Simpson's rule method with specified errors which has been compared with a direct integration procedure following evaluation of the Euler's constant.

This approach was extended to unconfined aquifers by introducing a new linearization constant \bar{h}_A , to the nonlinear partial differential equation governing the flow. This was in the form $\bar{h}_A = H_A + \lambda(t)h_{MAX}$. Where H_A is the aquifer depth to the initial water table, $\lambda(t)$ a time dependent constant and h_{MAX} was the maximum mound height at the percolation pit radius.

For this purposes the value of $\lambda(t)$ for a physically optimum solution was explored and proposed.

The approach to the statement of the problem is summarized in Figures 1, 2 and 3.

4. FIELDWORK

4.1 Introduction

The Ezousas Recharge Project was designed to recharge between 9000-12000m³ /day of chlorinated, tertiary treated effluent from the Paphos wastewater treatment plant. The plant consists of two parallel streams of activated sludge (one oxidation ditch and one conventional both incorporating biological nutrient removal stages).

The artificial recharge is through a number of infiltration basins, 7km from the coastal reach upstream of the Ezousas alluvial river basin (Fig 6.1). The continued expansion of the Paphos sewerage scheme, and because of the limited land available, the Cyprus Water Development Department, decided to investigate alternative designs for groundwater recharge, in order to utilize the extra effluent available. This study describes the research work on vertical, rectangular or circular pits penetrating deep into the vadose zone as percolation wells.

The percolation pit concept was therefore numerically analysed in the second part of this study to increase the understanding of the overall impact of the infiltration scheme.

4.2 Materials and Methodology

4.2.1 Experimental setup

In order to determine the bed characteristics and best locations along the River basin a test borehole was drilled into the alluvium, this was a 225mm diameter, 30m deep well made with a rotary drilling machine. The materials obtained at different core depths are shown in Table 1.

Table 1. Geological characteristics of the sample cores at different depths.

Subsoil thickness, m	Material description
0 - 5.5	gravel and brown clay
5.5 - 8.8	gravel with silty brown sand
8.8 - 13.4	fine to coarse grey sand and gravel
13.4 - 20.4	very coarse gravel with medium to coarse sand
20.4 - 35.1	very coarse gravel, small boulders with coarse sand

A full scale, cylindrical demonstration pit, 2 m in diameter and 9 m deep, was also later drilled and backfilled with cobbles and gravels to prevent collapse. The tertiary treated effluent was introduced via a 250 mm pipe into the pit at a depth of 1.5 m.

The trial recharge experiment was conducted for 450 days to fill the aquifer and monitor the response in terms of the mound growth and dissipation. The permeability of the underlying strata was determined with a constant head penetration test and was found to be 4.8 m/day. During the test a steady state recharge rate of 500 m³/day was applied. The experiments took place between

May 2008 and August 2009 and controls on abstraction were imposed in order to limit any interference to the test.

The head changes in the percolation pit, during the test period, were monitored by means of a standpipe piezometer fitted with an electronic water level sensor. These measurements were used to track changes in water depth as the recharging test progressed and to compare with the mathematical solutions described in the next study.

4.2.2 Experimental Results

The water table in the percolation pit was recorded every thirty days and shown in Table 2.

Table 2. Experimentally measured mound heights results 2008/2009.

Days	Mound height in m at the percolation pit
10	5,52
30	6,63
60	7,15
90	7,51
120	7,49
150	7,40
180	7,54
210	7,83
240	8,01
270	8,35
300	8,48
330	8,61
360	8,52
390	8,50
420	8,36
450	8,31

5. GROUNDWATER FLOW ANALYSES

5.1 Mathematical Solutions of Groundwater Recharge

As mentioned in the literature review the shape and analytical solution of the growth of the mound due to localized recharge is both complex and difficult mathematics for hydrologists and engineers to understand. One of the common approaches used and reviewed is Simpson's rule (referred to in p.212, 213, 214) which uses linear partial differential equations (PDE) for flow in confined aquifers.

The Hantush approach, referred to in p.221,222, is also an established solution for the nonlinear PDE of flow and was also examined for this research. This solution, however, was shown by the literature review to depend on intuitive assumptions whose physical or analytical basis was not as well justified as the Simpson approach. It was therefore concluded, from the review, that there were possibilities to simplify the solutions and application of these classic aquifer equations. This study of the research sets out to develop and presents potentially more practical methods to apply these differential equations to the well function. The concept developed depends on defining critical depth to produce an optimum solution to the nonlinear PDE based on physical and hydraulic criteria.

5.3 Confined Aquifers

5.2.1 Model Description

Confined aquifers are water-bearing formations with both an impervious base, (mostly bedrock) and overlaying formations. Thus artificial recharge of a confined aquifer is only possible if the confining and overlaying materials are artificially penetrated.

Figure 1 shows a model confined aquifer horizontally extending towards infinity. It has been assumed that a well fully penetrates the aquifer and recharge is maintained at a constant rate. Transient flow is driven by the recharge rate into the aquifer. The piezometric head of the aquifer takes the form of a function primarily of radius and time which are governed by Eq. 3 and the corresponding solution by Eq. 7.

The model's notation is as below:

h = pressure head with reference the top of the aquifer, m

h_H = pressure head with reference the bottom of the aquifer, m

H_A = aquifer thickness, m

h_{MAX} = pressure head at the percolation pit radius with reference to the top of the aquifer, m

Q_R = recharge, m³/day

r = distance from the centre of the percolation pit, m

t = time elapsed since initiation of recharge, days

S = aquifer storage coefficient (dimensionless)

K_R = aquifer hydraulic conductivity, m/day

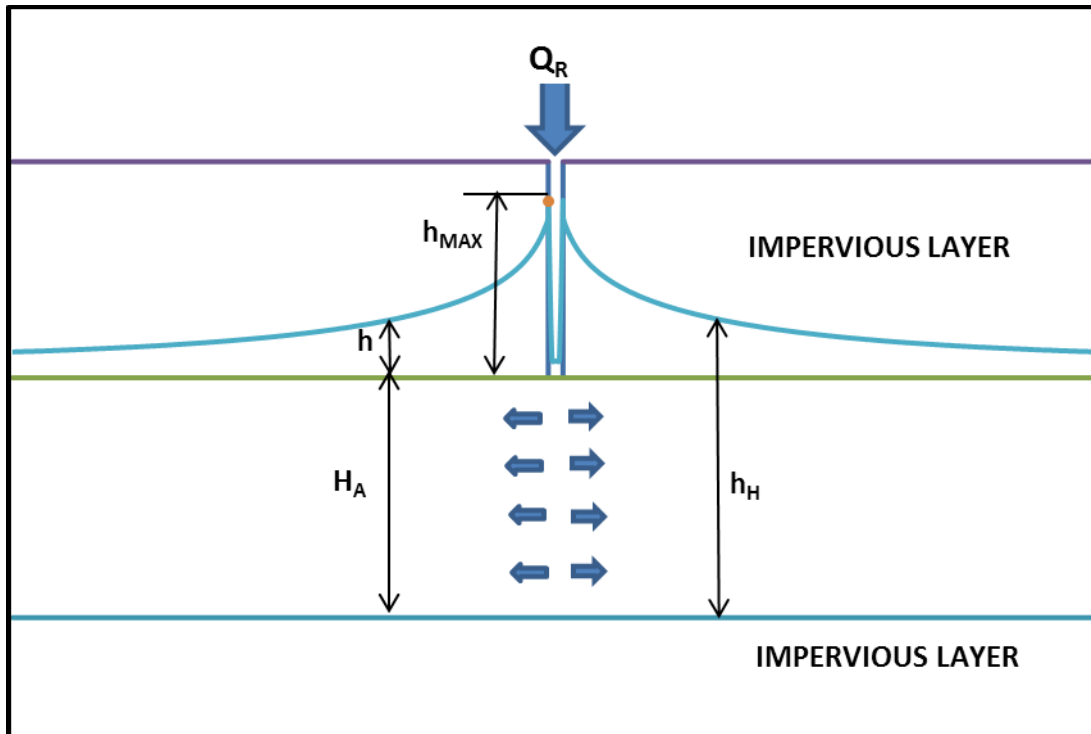


Figure 1. Recharge well in confined aquifer

5.2.2 Solution to the Radial Flow Linear PDE

This study of the thesis:

- Derives the solution to the linear PDE for radial flow for confined aquifers.
- Evaluates the well function, using the Simpson's Rule Method (SRM) after setting the accuracy required to achieve a solution.
- Obtains, by the direct integration method (DIM), a series solution to the well function, after evaluating the Euler's constant using the SRM.
- The flow in porous media is governed by the three dimensional Cartesian coordinates.

The linear Partial Differential Equation (PDE) is:

$$K_x \frac{\partial^2 h}{\partial x^2} + K_y \frac{\partial^2 h}{\partial y^2} + K_z \frac{\partial^2 h}{\partial z^2} = \left(\frac{S}{H_A}\right) \frac{\partial h}{\partial t} \quad (1)$$

where K_x, K_y and K_z are the hydraulic conductivities in each of the co-ordinate directions, S is the aquifer storage coefficient and H_A the thickness of the aquifer.

The above general PDE can be written in cylindrical co-ordinates r, θ, z when the symmetry in the θ direction is assumed and the hydraulic conductivity K_R in r direction is set to constant, the PDE then becomes:

$$\frac{K_R}{r} \frac{\partial}{\partial r} \left(r \frac{\partial h}{\partial r} \right) + K_z \frac{\partial^2 h}{\partial z^2} = \left(\frac{S}{H_A}\right) \frac{\partial h}{\partial t} \quad (2)$$

The term $K_z \frac{\partial^2 h}{\partial z^2}$ is negligible (Dupuit assumption for horizontal flow) the above PDE can be simplified to the Theis radial flow, linear partial differential equation.

$$\frac{1}{r} \frac{\partial}{\partial r} \left(r \frac{\partial h}{\partial r} \right) = \left(\frac{S}{H_A K_R}\right) \frac{\partial h}{\partial t} \quad (3)$$

The solution, from first principles, is given below:

Adopting new variable $u = \frac{S}{4H_A K_R} \left(\frac{r^2}{t}\right)$

From which the first derivatives of u with respect to r and t become

$$\frac{\partial u}{\partial r} = \left(\frac{S}{4H_A K_R}\right) \frac{2r}{t} = \frac{2u}{r} \quad \text{and} \quad \frac{\partial u}{\partial t} = -\left(\frac{S}{4H_A K_R}\right) \frac{r^2}{t^2} = -\frac{u}{t}$$

Hence the left hand side of the PDE can be changed to:

$$\frac{1}{r} \frac{\partial}{\partial r} \left(r \frac{\partial h}{\partial r} \right) = \frac{1}{r} \frac{\partial}{\partial u} \left(\frac{r \partial h}{\partial u} \frac{\partial u}{\partial r} \right) \frac{\partial u}{\partial r} = \left(\frac{4u}{r^2}\right) \frac{\partial}{\partial u} \left(\frac{u \partial h}{\partial u} \right)$$

$$= \frac{4u}{r^2} \left(\frac{\partial h}{\partial u} + u \frac{\partial}{\partial u} \left(\frac{\partial h}{\partial u} \right) \right) \quad (4)$$

and the right hand side of the PDE can also modified to:

$$\left(\frac{S}{H_A K_R} \right) \frac{\partial h}{\partial t} = - \left(\frac{S}{H_A K_R} \right) \left(\frac{u}{t} \right) \frac{\partial h}{\partial u} \quad (5)$$

Therefore:

$$\frac{4u}{r^2} \left(\frac{\partial h}{\partial u} + u \frac{\partial}{\partial u} \left(\frac{\partial h}{\partial u} \right) \right) = - \left(\frac{S}{H_A K_R} \right) \left(\frac{u}{t} \right) \frac{\partial h}{\partial u}$$

$$\left(\frac{\partial h}{\partial u} + u \frac{\partial}{\partial u} \left(\frac{\partial h}{\partial u} \right) \right) = - \left(\frac{S}{4H_A K_R} \right) \left(\frac{r^2}{t} \right) \frac{\partial h}{\partial u}$$

$$\frac{\partial h}{\partial u} + u \frac{\partial}{\partial u} \left(\frac{\partial h}{\partial u} \right) = -u \frac{\partial h}{\partial u}$$

$$\frac{d}{du} \left(\frac{dh}{du} \right) = - \left(\frac{1+u}{u} \right) \frac{dh}{du}$$

by setting $z = \frac{dh}{du}$ then $\frac{dz}{z} = - \left(1 + \frac{1}{u} \right) . du$

and hence

$$\ln(z) = A - \ln(u) - u. \text{ Therefore } z = e^A \left(\frac{e^{-u}}{u} \right) \text{ and hence } h = e^A \int \frac{e^{-u}}{u} du$$

where e^A is the limit for $\lim_{r \rightarrow 0} (uz)$. By using Darcy:

$$r \frac{\partial h}{\partial r} = \frac{Q_R}{2\pi H_A K_R} \text{ and } r \frac{\partial h}{\partial r} = r \frac{\partial u}{\partial r} z = 2uz$$

Therefore $e^A = \frac{Q_R}{4\pi H_A K_R}$ and the solution is given by

$$h(r,t) = \frac{Q_R}{4\pi H_A K_R} \int_{u_1 = \frac{r^2}{4H_A K_R t}}^{\infty} \frac{e^{-u}}{u} du \quad (6)$$

or in the Theis notation as

$$h(r,t) = \frac{Q_R}{4\pi H_A K_R} W(u_1) \quad (7)$$

where u_1 is the lower integration limit of the integral of Eq.6.

5.2.3 Well Function Evaluation by the Simpson's rule method (SRM)

The well function was evaluated from first principles using Simpson's Rule Method

by finding the area under the function $f(u) = \left(\frac{e^{-u}}{u} \right)$ of the well function

$W(u_1) = \int_{u_1}^{\infty} \frac{e^{-u}}{u} .du$ by assigning suitable step size (ST) and number of steps n . The

Simpson' Rule expression is then given by:

$$S_{2n} = \frac{(ST)}{3} [f(u_1) + 4f(u_2) + 2f(u_3) + 4f(u_4) \dots + \dots 2f(u_{n-2}) + 4f(u_{n-1}) + f(u_n)] \quad (8)$$

The evaluation was achieved by finding the area under the function $f(u) = \left(\frac{e^{-u}}{u}\right)$ by the writing and use of a visual basic subroutine referred to as **KOKOS_SRM** developed for this thesis.

5.2.4 Error Stipulation in the KOKOS_SRM

The integration, however, of the analytic function $f(u) = \left(\frac{e^{-u}}{u}\right)$ by this thesis specific SRM will inevitably be subject to numerical errors and the magnitude of these errors depends on:

- The step size, **ST**, which was directly related to the fact that Simpson's rule summation Eq.8 was only exact for algebraic functions of three orders; the truncation error(E_0) was equal to

$$(E_0) \leq \frac{n(ST)^5 f^{IV}(u)}{90} \quad (9)$$

where **n & ST** the step size and number of steps was chosen respectively

$f^{IV}(u)$ is the forth differential coefficient of the analytic function $f(u) = \left(\frac{e^{-u}}{u}\right)$

which was equal to $f^{iv}(u) = \left(\frac{e^{-u}}{u}\right)\left(1 + \frac{4}{u} + \frac{12}{u^2} + \frac{24}{u^3} + \frac{24}{u^4}\right)$

where u took the value of the lower integration limit; this was made in order to maximize the value of $f^{iv}(u)$, and hence the error E_0 .

- The relationship between the **n & ST** was also examined, since in this instance the upper integration limit was infinity and an additional error existed due to the terminal part present in Eq.12; thus as **n** increases **ST** could decrease and vice versa; the aim being to make the lower integration limit α_m of the terminal part $\int_{\alpha_m=\beta_{m-1}}^{\infty} \frac{e^{-u}}{u} du$ of

Eq.12 (10)

as large as possible thus reducing its effect on the error estimation.

Thus the well function, error estimation was carried out by splitting the region of u into a number of **m** parts, keeping the step size **ST & n** the same for all parts as follows;

$$W(u_1) = \left(\frac{4\pi H_A K_R}{Q_R}\right)h(r,t) =$$

$$= \int_{\alpha_1=u_1}^{\beta_1=u_1+2n.s} \frac{e^{-u}}{u} du + E_1 + \int_{\alpha_2=\beta_1}^{\beta_2=2u_1+4n.s} \frac{e^{-u}}{u} du + E_2 + \dots + \int_{\alpha_p=\beta_{p-1}}^{\beta_p} \frac{e^{-u}}{u} du + E_p + \dots + \int_{\alpha_m=\beta_{m-1}}^{\infty} \frac{e^{-u}}{u} du \quad (11)$$

It can be seen that under constant **ST & n** condition for all parts the ratio of the error in successive parts was given by $\frac{E_p}{E_{p-1}} = \frac{f^{V^4}(pu_1 + 2ns)}{f^{V^4}((p-1)u_1 + 2ns)}$; thus the total

error is given by

$$Er = E_1 + E_2 + \dots + E_p + \dots + E_p + \int_{\alpha_m=\beta_{m-1}}^{\infty} \frac{e^{-u}}{u} du \quad (12)$$

The project visual basic subroutine **KOKOS_SRM**, had the facility to assign an acceptable error **Er** and the number of steps **n** in the SRM which in turn evaluated the step size **ST** in order to maintain the solution within the specified error. The total error that was present in an evaluated $h(r,t)$ head for the values of **Er** and **n**,(and for all the programs) was set at $Er=0.00001$ and $n=1000000$ respectively, values were also recorded.

The thesis subroutine **KOKOS_SRM** evaluated the head ordinates $h(r,t)$ for any value of r and t , that was required.

It should be noted that the Theis head in confined aquifers is equal to the following function $h = \Phi(r,t,Q_R,H_A,K_R,S)$.

The thesis program **KOKOS_SRM** was able to evaluate the head h , see Fig.1, for any one variable chosen, keeping the other variables constant, while at the same time ensuring the accuracy was equal to the values set.

5.2.5 Well Function Evaluation by the Direct Integration Method (DIM)

In order to compare calculated outputs the well function using the direct integration method was also evaluated as shown below:

Expand e^{-u} , and divide by u each term and integrate to obtain Eq.14.

$$W(u_1) = \int_{u_1}^{\infty} \frac{e^{-u}}{u} \cdot du = \int_{u_1}^{\infty} \left[\frac{1 - \frac{u}{1!} + \frac{u^2}{2!} - \frac{u^3}{3!} + \dots + \frac{u^{n+1}}{(n+1)!}}{u} \right] du$$

$$\begin{aligned}
&= \int_{u_1}^{\infty} \left\{ \frac{1}{u} - 1 + \frac{u}{2!} - \frac{u^2}{3!} + \dots - \frac{u^{n-1}}{n!} + \dots \right\} du \\
&= \left[\ln(u) + \sum_1^n (-1)^n \left(\frac{u^n}{n.n!} \right) \right]_{u_1}^{\infty} \tag{13}
\end{aligned}$$

The summation term above was split into two parts from u_1 to 1 and from 1 to infinity.

$$\begin{aligned}
&= \left[\ln(u) + \sum_1^n (-1)^n \left(\frac{u^n}{n.n!} \right) \right]_{u_1}^1 + \left[\sum_1^n (-1)^n \left(\frac{u^n}{n.n!} \right) \right]_1^{\infty} \\
&= \left\{ \ln(1) + \sum_1^n (-1)^n \left(\frac{1}{n.n!} \right) \right\} - \left\{ \ln(u_1) + \sum_1^n (-1)^n \left(\frac{u_1^n}{n.n!} \right) \right\} + W(1) \\
W(u_1) &= \text{CONSTANT} - \left\{ \ln(u_1) + \sum_1^n (-1)^n \left(\frac{u_1^n}{n.n!} \right) \right\} \tag{14}
\end{aligned}$$

where the constant is given as below:

$$\text{CONSTANT} = \ln(1) + \sum_1^n (-1)^n \left(\frac{1^n}{n.n!} \right) + W(1) \tag{15}$$

The above constant is the well known *Euler Constant*, the evaluation of which was achieved by the use of a similar subroutine as was developed for the **SRM** method but in this case referred to as program **KOKOS_EULER ERM**.

- The first term of the constant is zero.
- The second is the summation of the series $\sum_1^n (-1)^n \left(\frac{u^n}{n.n!} \right)$; which was carried out by using the recurrence relationship $A_{n+1} = -A_n \frac{n.u}{(n+1)^2}$ (16)
- The third term is the well function $W(u_1)$

The above well function constant was evaluated using the **KOKOS_ERM**. sub-routine noted previously. A result to twelve decimal places was achieved confirming the effectiveness of the available error control in the **KOKOS_ERM**. program.

Once the Euler constant had been evaluated then a comparison was made between the two methods SRM and DIM which gave identical results thus supporting the accuracy of the simpler SRM.

5.3 Unconfined Aquifers

5.3.1 Model Description

In contrast to confined aquifers, in unconfined aquifers, the recharge process water passes through the soil above the water table. Thus the effective water table height can be changed to include a mound shape. As noted this is a function of radius and time which is governed by Eq. 17 and its corresponding solutions by Eq.20 and 23. A definition diagram is presented in Figure 2. with the notation as follows:

h = mound height, m

H_A = initial depth of the aquifer m

H_{AE} = equivalent aquifer depth= $H_{AE}=H_A+h_{CRIT}$, m

h_H =Hantush mound height, m

$\lambda(t)$ = coefficient in linearization assumption, dimensionless

h_{MAX} = maximum mound height at the percolation pit, m

Q_R = recharge, m³/day

r = distance from the centre of the percolation pit, m

t = time elapsed since initiation of recharge, days

S = aquifer storage coefficient (dimensionless)

K_R = aquifer hydraulic conductivity, m/day

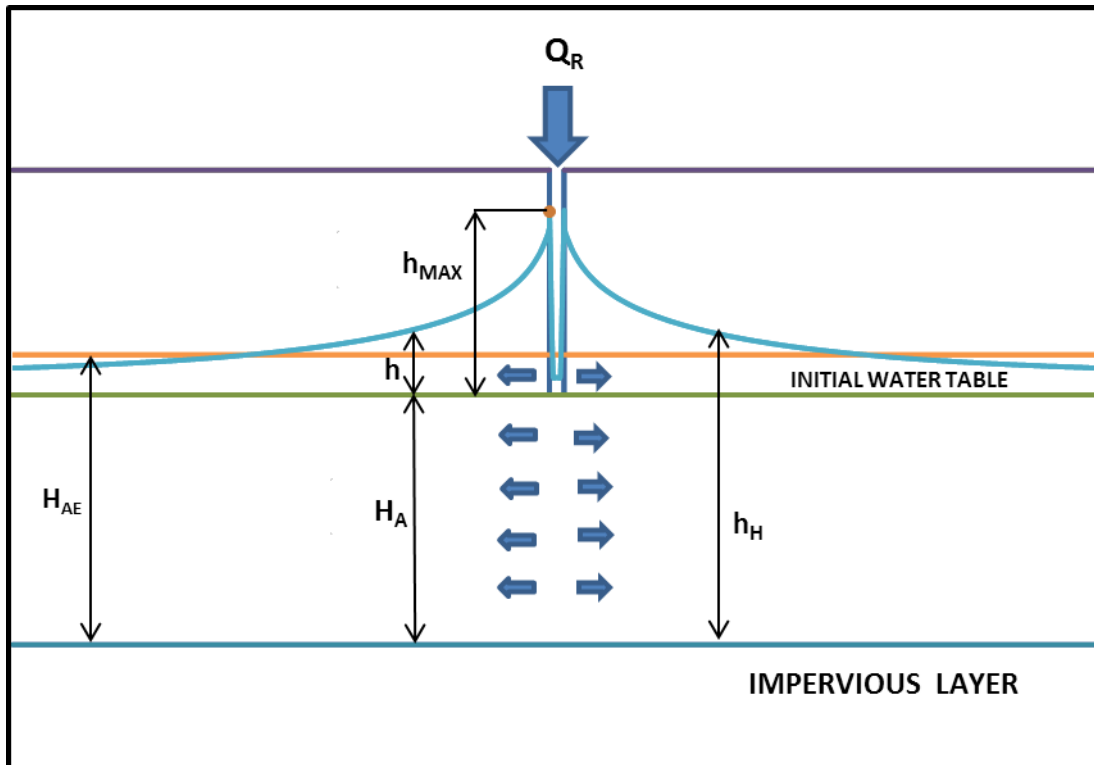


Figure 2. Recharge well in unconfined aquifer

The study describes the steps used to resolving these equations by:

- Linearizing the governing nonlinear PDE of radial flow for unconfined

Aquifers. This was done by setting to a constant the variable flow depth h_H , see Fig.2 in the PDE, at the outset, as $\bar{h}_A = H_A + \lambda(t)h_{MAXKOKOS}$ while keeping the recharge Q_R and the other variables constant.

- Derives the Hantush linearization, from first principles and solves the non-linear PDE using Hantush linearization assumption, $\bar{h}_H = H_A + 0.5h_{MAXHANTUSH}$
- Derives the optimum values of the $\lambda(t)$ -factor, using basic physical and hydraulic considerations.

5.3.2 Governing Non-Linear PDE of Flow

The absence of the confining impervious layer and formation of a mound shape results in nonlinear flow governing PDE which become:

$$\frac{1}{r} \frac{\partial}{\partial r} \left(r h_H \frac{\partial h_H}{\partial r} \right) = \left(\frac{S}{K_R} \right) \frac{\partial h_H}{\partial t} \quad (17)$$

or since $h_H = H_A + h$

$$\frac{1}{r} \frac{\partial}{\partial r} \left(r (H_A + h) \frac{\partial h}{\partial r} \right) = \left(\frac{S}{K_R} \right) \frac{\partial h}{\partial t} \quad (18)$$

Thus the depth flowpath h_H (see Fig. 2) is now variable, unlike the constant flow path thickness (H_A) that characterized the confined case. It is argued in this thesis that, since direct solutions to the nonlinear PDE of unconfined aquifers are impossible, mound growth height can only be obtained by utilizing approximations,

but these need to have been justified hydraulically and physically. These approximations of nonlinear PDE of the flow and variable water table terms h_H and can be achieved by using a Darcy variable for the recharge flow

$$Q_R = 2\pi K_R (rh_H) \frac{\partial h_H}{\partial r}$$

5.3.3 Linearization Used

The approach suggested in this thesis was to determine the equivalent constant aquifer thickness by evaluating the $h_{MAXKOKOS}$ at $r = r_{MIN}$. The variable h_H is replaced with an equivalent constant $\bar{h}_A = H_A + \lambda(t)h_{MAXKOKOS}$ where $0 \leq \lambda(t) \leq 1$; which in effect means the aquifer is assigned a new and constant equivalent thickness

$H_A + \lambda(t)h_{MAXKOKOS}$; thus Eq.18 can be express as:

$$\frac{1}{r} \frac{\partial}{\partial r} \left(r \frac{\partial h}{\partial r} \right) = \left(\frac{S}{K_R (H_A + \lambda(t)h_{MAXKOKOS})} \right) \frac{\partial h}{\partial t} \quad (19)$$

and the solution for $h(r_{min}, t)$ is

$$h(r_{MIN}, t) = \left(\frac{Q_R}{4\pi K_R (H_A + \lambda(t)h_{MAXKOKOS})} \right) W \left(\frac{S \left(\frac{r^2}{t} \right)}{4K_R (H_A + \lambda(t)h_{MAXKOKOS})} \right) \quad (20)$$

where $h_{MAXKOKOS} = h(r_{MIN}, t)$, and hence after a few iterations, $h_{MAXKOKOS}$ for any given

value of $\lambda(t)$ can be determined.

The solution of the Eq.20 for $h(r_{min}, t)$ which should be equal to $h_{MAXKOKOS}$ was achieved by the following iterative procedure:

- Set the value of $\lambda(t)$ (note that the linearization assumption is $0 \leq \lambda(t) \leq 1$)
- Set $h_{MAXKOKOS}=0$ and obtain $h(r_{min}, t)_1$
- Set $h_{MAXKOKOS}=h(r_{min}, t)_1$ and obtain afresh $h(r_{min}, t)_2$
- Continue this process until $h(r_{min}, t)_n = h_{MAXKOKOS}$.

Another program subroutine **KOKOS_NONLINEAR** was produced to deal with this task.

5.3.4 The Hantush Linearization

The aim of the traditional Hantush approach is also to determine the equivalent constant aquifer thickness by evaluating the $h_{MAXHANTUSH}$ at $r = r_{MIN}$. In the Hantush method the head variable h_H , in Eq.17, is measured from the base of the aquifer and is replaced by the transformation $z = h_H^2 + C$; the derivative

$\frac{\partial h_H}{\partial z} = \frac{1}{2h_H}$ is then substituted into the governing nonlinear PDE Eq.17

and after the manipulation shown below. Equation, Eq.21, is obtained.

$$\frac{1}{r} \frac{\partial}{\partial r} \left(r \frac{\partial z}{\partial r} \frac{\partial h_H}{\partial z} \right) = \left(\frac{S}{K_R} \right) \frac{\partial z}{\partial t} \frac{\partial h_H}{\partial z}$$

$$\frac{1}{r} \frac{\partial}{\partial r} \left(r h_H \frac{\partial z}{\partial r} \frac{1}{2h_H} \right) = \frac{\partial z}{\partial t} \frac{1}{2h_H}$$

which becomes

$$\frac{1}{r} \frac{\partial}{\partial r} \left(r \frac{\partial z}{\partial r} \right) = \left(\frac{S}{h_H K_R} \right) \frac{\partial z}{\partial t} \quad (21)$$

- For the first boundary condition at $r \Rightarrow \infty$ where $h \Rightarrow 0$:

Hantush sets $z = 0$ in order to make $C = H_A^2$ and also to satisfy infinity condition.

- The second boundary condition is set at $r = r_{MIN}$ where $h = h_{MAXHANTUSH}$.

It is suggested here, that there is no physical meaning to $z(r_{MIN}, t)$ and Hantush at this stage of the solution stated his *linearization constant condition* as:

$$\bar{h}_H = \frac{(h_{HMAXHANTUSH} + H_A)}{2} = (H_A + 0.5h_{MAXHANTUSH}) \quad (22)$$

which in fact meant that he actually decided to set the required equivalent constant aquifer thickness as $(H_A + 0.5h_{MAXHANTUSH})$; which is for a particular case. In this new approach, suggested in this thesis, this is when $\lambda(t) = 0.5$, for the constant equivalent aquifer thickness.

Therefore, $h_{MAXHANTUSH}$ can be evaluated using Eq.20 or Eq.23

$$h(r_{MIN}, t) = \frac{Q_R}{4\pi K_R (H_A + 0.5h_{MAXHANTUSH})} W \left(\frac{S(r_{MIN}^2 / t)}{4K_R (H_A + 0.5h_{MAXHANTUSH})} \right). \quad (23)$$

and after a few iterations the actual value of $h_{MAXHANTUSH}$ is found.

Hantush specified the transformation for $z(r_{MIN}, t)$ as below

$$z(r_{MIN}, t) = (h_{MAXHANT} + H_A)^2 - H_A^2 = 2h_{MAXHANT} (H_A + 0.5h_{MAXHANT}). \quad (24)$$

In order to obtain the $z(r_{MIN}, t)$ solution shown below

$$z(r_{MIN}, t) = \left(\frac{Q_R}{2\pi K_R} \right) W \left(\frac{S \left(\frac{r_{MIN}^2}{t} \right)}{4K_R (H_A + 0.5h_{MAXHANTUSH})} \right) \quad (25)$$

and using his z-transformation to reevaluate

$$h_{MAXHANTUSH} = \sqrt{z(r_{MIN}, t) + H_A^2} - H_A \quad (26)$$

$$(h_{MAXHANTUSH} + H_A)^2 = z(r_{MIN}, t) + H_A^2$$

$$2h_{MAXHANTUSH} (H_A + 0.5h_{MAXHANTUSH}) = z(r_{MIN}, t)$$

which leads, as expected, to same expression as Eq.23

$$h_{MAXHANTUSH} = \left(\frac{Q_R}{4\pi K_R (H_A + 0.5h_{MAXHANTUSH})} \right) W \left(\frac{S \left(\frac{r_{MIN}^2}{t} \right)}{4K_R (H_A + 0.5h_{MAXHANTUSH})} \right) \quad (27)$$

Once $h_{MAXHANTUSH}$ is obtained the equivalent aquifer thickness \bar{h}_H is given as

$$\bar{h}_H = H_A + 0.5h_{MAXHANTUSH}$$

and therefore from this point onwards the solution proceeds in exactly the same way as the linearization approach proposed in this thesis. The equality of the

answers of the values of $h_{MAXHANTUSH}$ and $h_{MAXKOKOS}$ was also confirmed by the numerical evaluations from the subroutines **KOKOS_NONLINEAR** and **KOKOS_HANTUSH**.

Comparison of the Hantush and this alternative approach suggested here, indicates that the Hantush method has mathematical circularity; with z-substitution and as a result does not lead to an independent linearization method. This however, needs confirmation by further research.

5.3.5 Optimization Solution

It is evident from the above discussion that the value of $\lambda(t)$ is an important factor in the correct evaluation of the mound height. Therefore, the next stage to the development of a new method was to explore a possible physical or hydraulic reason to assign an optimum value for $\lambda(t)$.

A definition diagram is presented in Figure 3. The notations are as follows:

h = head, m

H_A = aquifer thickness, m

h_H =Hantush mound height

h_{MAX} = head at the percolation pit radius, m

h_{CRIT} = the critical depth, a time independent constant, m

Q_R = recharge, m³/day

r = distance from the centre of the percolation pit, m

t = time elapsed since initiation of recharge, days

S = aquifer storage coefficient (dimensionless)

K_R = aquifer hydraulic conductivity, m/day

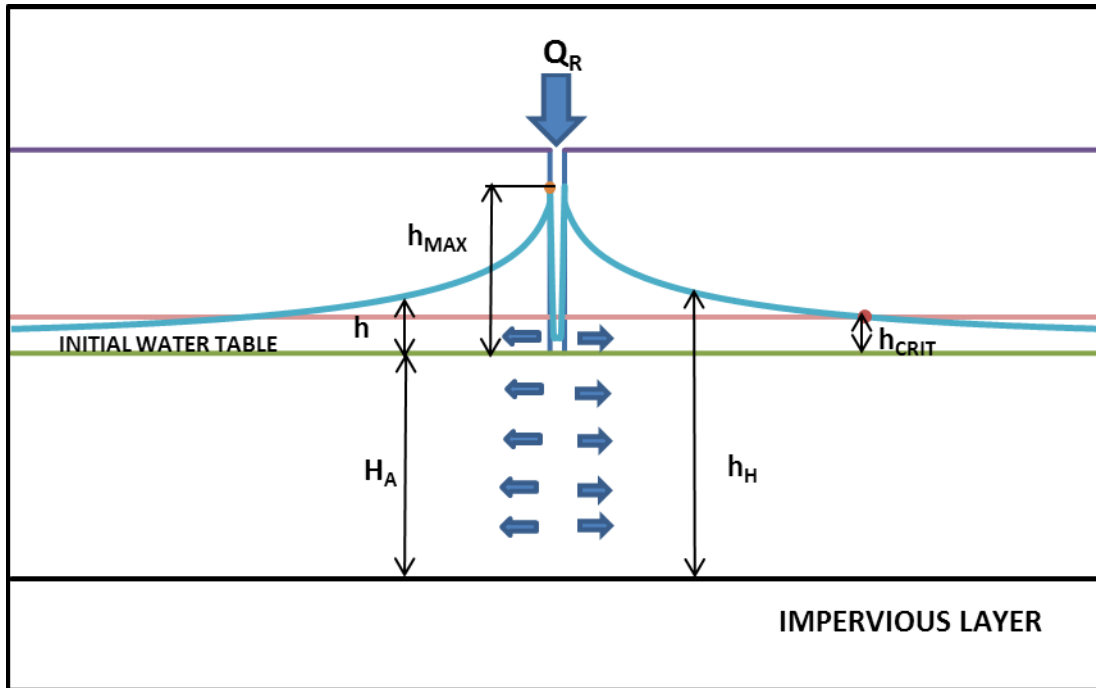


Figure 3. Recharge well in unconfined aquifer and the Critical Depth

5.3.6 Definition of Critical Depth

The position of the flow water front, after t -days, in an unconfined aquifer subject to constant recharge is given by the *Recharge-Voids Volume* relationship which is

$$Qt_{CRIT} = S\pi\bar{h}_A r_{CRIT}^2 \quad (28)$$

Where $\bar{h}_A = H_A + h_{CRIT}$

h_{CRIT} being water front height above the initial water table at a radius r and time t

that obey the condition $\frac{r^2_{CRIT}}{t_{CRIT}} \square \frac{Q_R}{S\pi(\bar{h}_A)}$

The well function, when the above expression is substituted in it, becomes

$$W\left(\frac{Q_R}{4\pi K_R(\bar{h}_A)^2}\right)$$

$$\text{Hence } h_{CRIT} = \frac{Q_R}{4\pi K_R(\bar{h}_A)} W\left(\frac{Q_R}{4\pi K_R(\bar{h}_A)^2}\right) \quad (29)$$

h_{CRIT} was evaluated by the subroutine **KOKOS_OPTIMUM_LAMDA** by using the iterations. It should also be noted that the critical depth is a time invariant constant, since the well function becomes constant due to the above equation (Eq.29).

5.3.7 Procedure for Optimized Solutions using the Linear PDE

To help solve the PDE, the properties of the critical depth in conjunction with

Subroutine **KOROS_SRM_LINEAR** was used and applied to the thesis evaluation.

This exploited the fact that the critical depth is a time invariant constant for the flow and thus making the aquifer equivalent depth for all t equal to

$$H_{AE} = H_A + h_{CRIT}$$

hence

$$h(r,t) = \frac{Q_R}{4\pi K_R(H_{AE})} W\left(\frac{S}{4K_R(H_{AE})} \left(\frac{r^2}{t}\right)\right) \quad (30)$$

5.3.8 Evaluation of the Optimum $\lambda(t)$

The relationship of the optimum factor $\lambda(t)$ is governed by

$$\lambda(t) = \frac{h_{CRIT}}{h(r_{MIN}, t)} \quad (31)$$

and

$$h(r_{MIN}, t) = \frac{Q_R}{4\pi K_R (H_A + \lambda(t) h_{MAX})} W\left[\frac{S}{4K_R (H_A + \lambda(t) h_{MAX})} \frac{(r_{MIN})^2}{t}\right] \quad (32)$$

By using the thesis subroutine **KOKOS_OPTIMUM_LAMDA** the optimum values of $\lambda(t)$ vs time were obtained as shown in Figure 6.

Once an optimum value of $\lambda(t)$ for a specific time had been determined it was introduced into the thesis subroutine **KOKOS_NONLINEAR** using the equation below to evaluate the optimum mound heights

$$h(r, t) = \frac{Q_R}{4\pi K_R (H_A + \lambda_{OPT}(t) h_{MAX})} W\left(\frac{S}{4K_R (H_A + \lambda_{OPT}(t) h_{MAX})} \left(\frac{r^2}{t}\right)\right) \quad (33)$$

5.3.9 Variation of the Aquifer Parameters of T and S

From the experimental results in combination with the selected optimum mound heights

$h(r, t)$ of Eq. 33, an estimate of the ratio $\frac{\Delta h(r, t)}{h(r, t)} = \frac{h_{EXPERIMENT}}{h(r, t)_{OPTIMUM}} - 1$ is possible.

$$h(r, t) = \left(\frac{Q_R}{4\pi}\right) \left(\frac{1}{T}\right) W\left[\left(\frac{S}{T}\right) \left(\frac{r^2}{4t}\right)\right]$$

where $T = K_R \times H_{AE}$ and Q_R constant.

Taking logs and differentiating Eq. 34 was obtained

$$\ln(h(r,t)) = \ln\left(\frac{Q_R}{4\pi}\right) - \ln(T) + \ln(W)$$

$$\frac{\Delta h(r,t)}{h(r,t)} = -\frac{\Delta T}{T} + \frac{\Delta W}{W} \quad (34)$$

$$\text{where } \frac{\Delta W}{W} = 1 - \frac{W(u + \Delta u)}{W(u)} = 1 - \frac{W\left[\left(\frac{S(1 + \frac{\Delta S}{S})}{T(1 + \frac{\Delta T}{T})}\right)\left(\frac{r^2}{4t}\right)\right]}{W\left[\left(\frac{S}{T}\right)\left(\frac{r^2}{4t}\right)\right]} \quad (35)$$

Note that when:

1. $\frac{\Delta T}{T} > 0$ and $\frac{\Delta S}{S} > 0$ then $\frac{\Delta W}{W} < 0$ and $\frac{\Delta h(r,t)}{h(r,t)} < 0$
2. $\frac{\Delta T}{T} < 0$ and $\frac{\Delta S}{S} < 0$ then $\frac{\Delta W}{W} > 0$ and $\frac{\Delta h(r,t)}{h(r,t)} > 0$

$\frac{\Delta h(r,t)}{h(r,t)}$ can be estimated from the available experimental data.

where $\Delta h(r,t) = h(r,t)_{EXPERIMENT} - h(r,t)_{OPTIMUM} > 0$ and hence $\frac{\Delta h(r,t)}{h(r,t)} > 0$

therefore, the condition 2 above holds.

- If $\frac{\Delta T}{T} = 0$ then $\frac{\Delta W}{W} = \frac{\Delta h(r,t)}{h(r,t)} = \frac{W_0 - W_1}{W_0}$ and hence by trial and error the maximum value of S was estimated at $S^*(1+0.08)=0.216$.
- If $\frac{\Delta S}{S} = 0$ then for $\frac{\Delta T}{T} = -\alpha_T$, $\frac{\Delta W}{W} = \alpha_W$ such that $-\alpha_T + \alpha_W = \frac{\Delta h(r,t)}{h(r,t)}$; it is noted that the value $-\alpha_T$ is dominant in relation to α_W ; by trial and error the minimum value of T was estimated at $T^*(1-0.093)=0.907T$
- From $T = H_A K_R$ the respective errors are given by $\frac{\Delta T}{T} = \frac{\Delta H_A}{H_A} + \frac{\Delta K_R}{K_R}$ if the error for the aquifer depth was set at $\frac{\Delta H_A}{H_A} = \pm 0.1$, then the value of K_R could be as little as $K_R(1-0.193) = 4.035$.

6. DISCUSSION OF RESULTS AND SOLUTIONS

The mounding problem has been shown to be complex with solutions depending on the physical and analytical approximations used. As a result a number of solutions were investigated both using linear and nonlinear partial differential equations describing flow to determine which gave the most realistic solutions. The results are summarized in the following graphs from the subroutines described and developed in Visual Basic programs these are detailed in Appendix 2.

The linear partial differential Eq. 3 and its solution Eq. 6 were used to provide a comparison between the results from **KOKOS_SRM_LINEAR** which used a Simpson's Rule Solution and **KOKOS_DIM_LINEAR** which used the Direct Integration Method and these are presented in Figure 4.

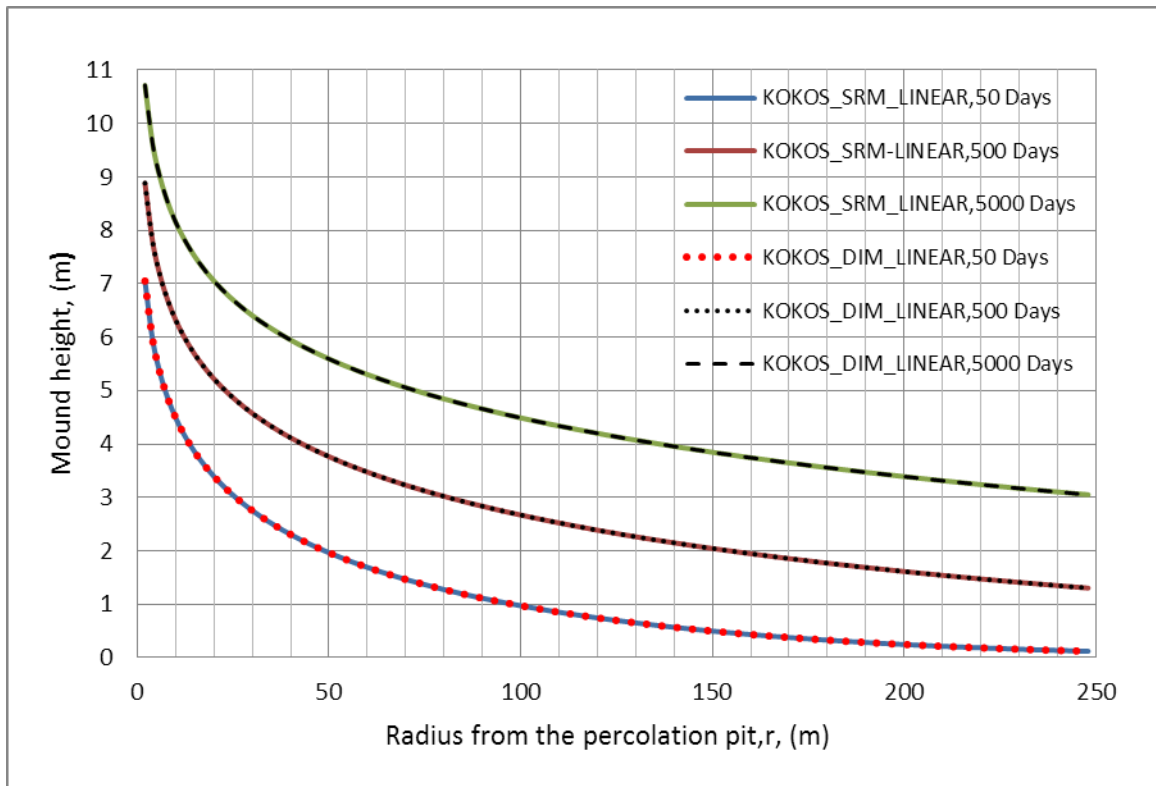


Figure 4. Comparison of mound height vs radius, KOKOS_SRM_LINEAR and KOKOS_DIM_LINEAR for $Q_R=500$, $K_R=5$, $H_A=10$, $S=0.2$

A comparison between the nonlinear solution, Eq. 19 & 20 developed for the thesis and the Hantush approach, Eq. 21 & 25, was carried out by using subroutines **KOKOS_NONLINEAR** and **KOKOS_HANTUSH** and these are shown in Figure 5.

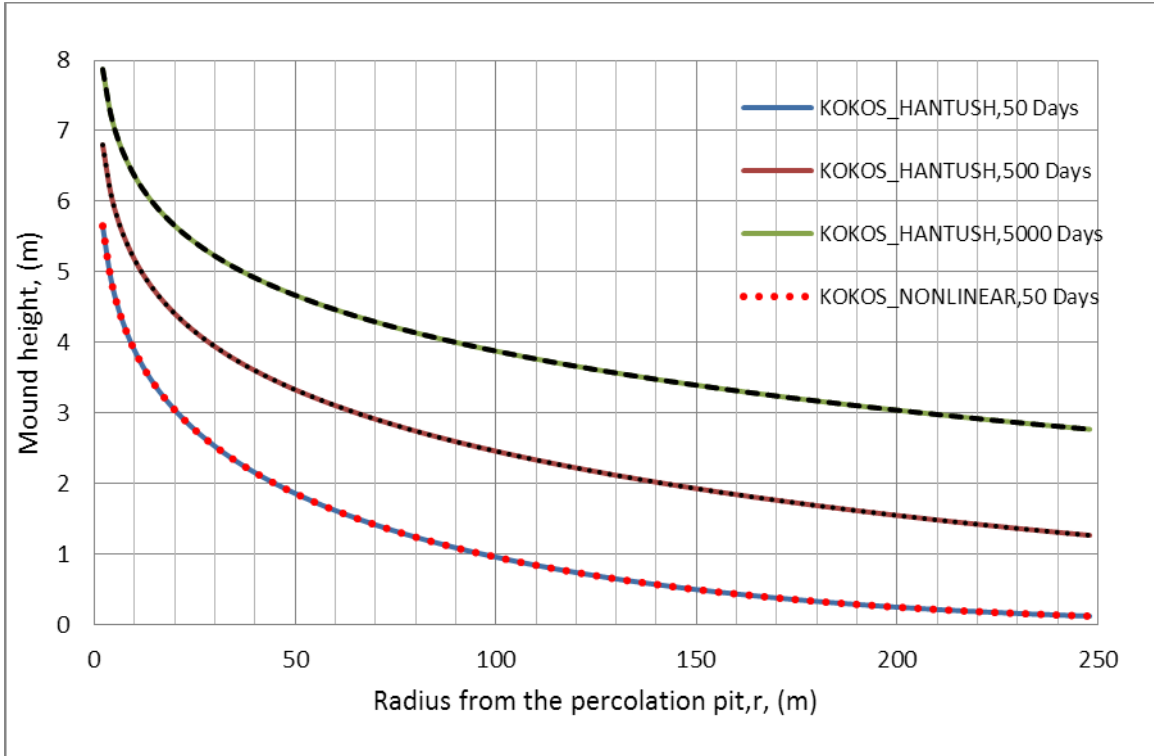


Figure 5. Comparison of mound height vs radius, KOKOS_NONLINEAR, $\lambda(t)=0.5$, and KOKOS_HANTUSH Constant=0.5; for $Q_R=500$, $K_R=5$, $H_A=10$, $S=0.2$

Figure 6 shows the predicted position of the water front in the aquifer with the passage of time whereby $\frac{r_{CRIT}^2}{t_{CRIT}} = \frac{Q_R}{\pi S(H_A + \lambda(t)h(r_{MIN},t))}$ is constant.

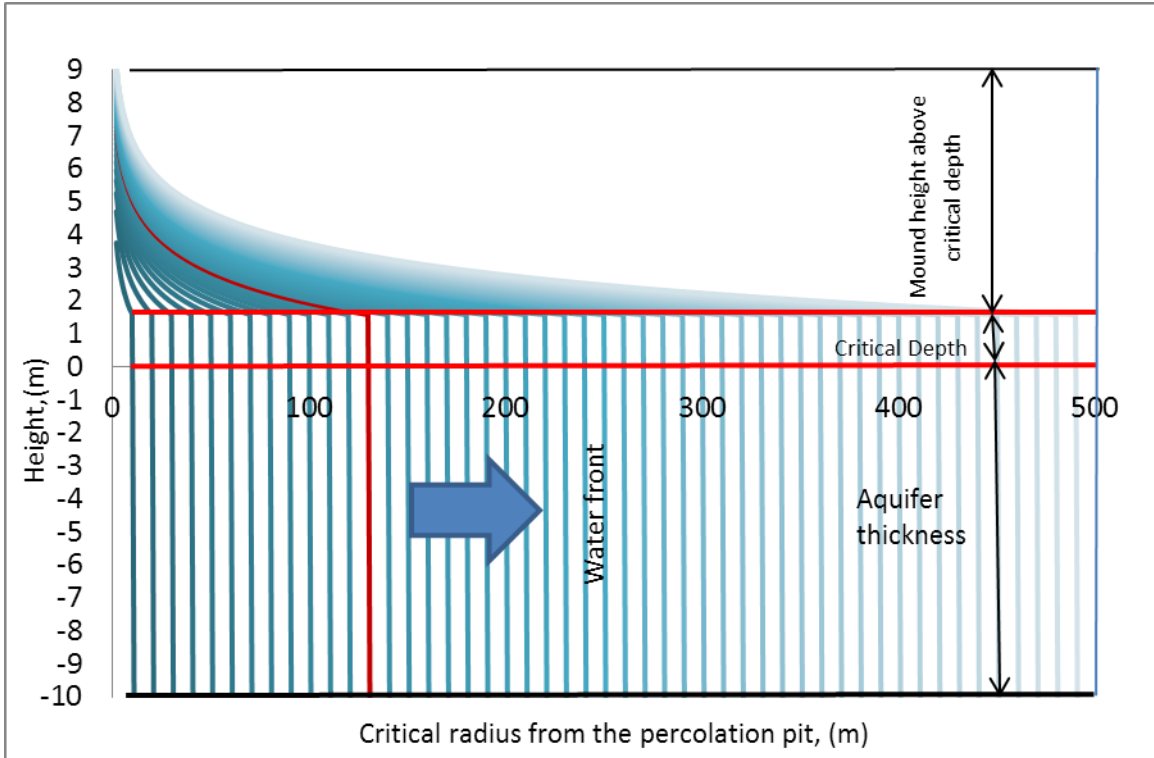


Figure 6. Aquifer height increase due to recharge water front expansion

Figure 7 represents the optimum plot of $\lambda(t)$ based on the Eq. 31 & 32, using the subroutine **KOKOS_OPTIMUM_LAMDA** from which the optimum values of $\lambda(t)$ were obtained and placed into the **KOKOS_NONLINEAR** subroutine to derive the optimum solution for the mound problem at a specified time.

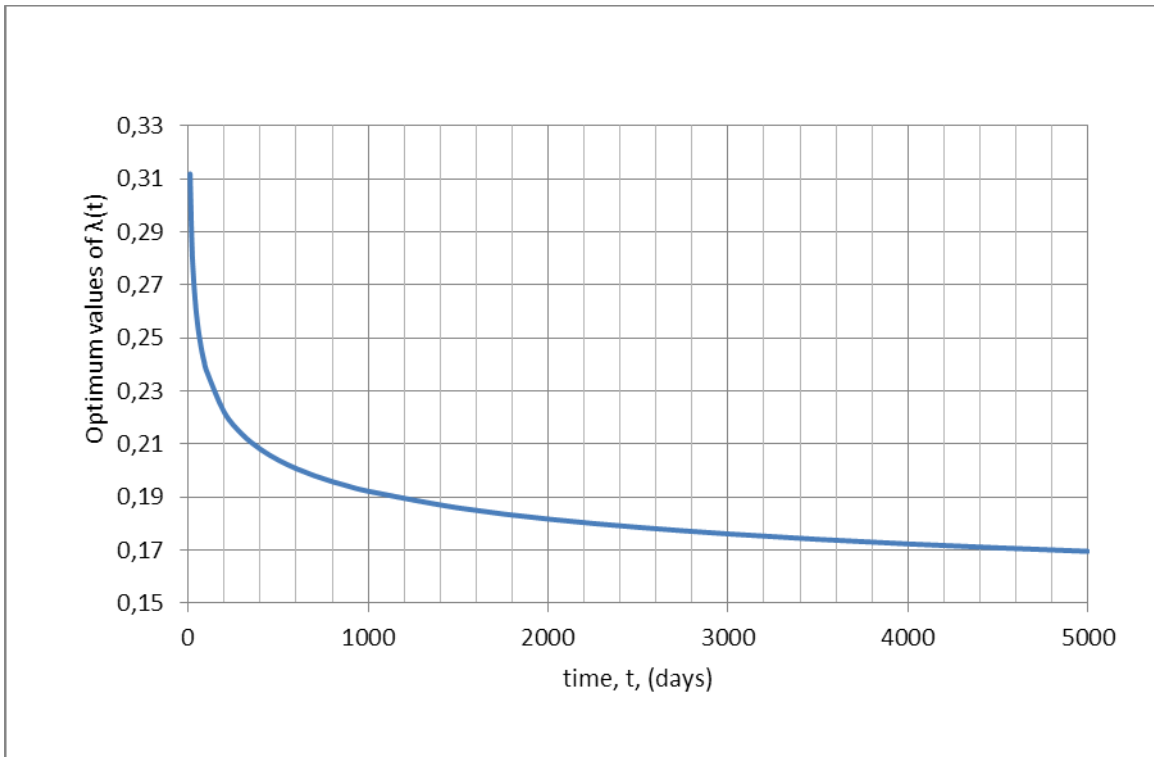


Figure 7. Optimized linearization constant $\lambda_{OPT} = (\lambda(t))$ using the thesis KOKOS_OPTIMUM_LAMDA for $r=2$, and $t=50, 500, 5000$ days

The plot in Figure 8 shows a comparison between the nonlinear and linear optimum solutions derived from the thesis method together with the classic Hantush nonlinear solution. The percentage difference between the three solutions are shown in Figure 9.

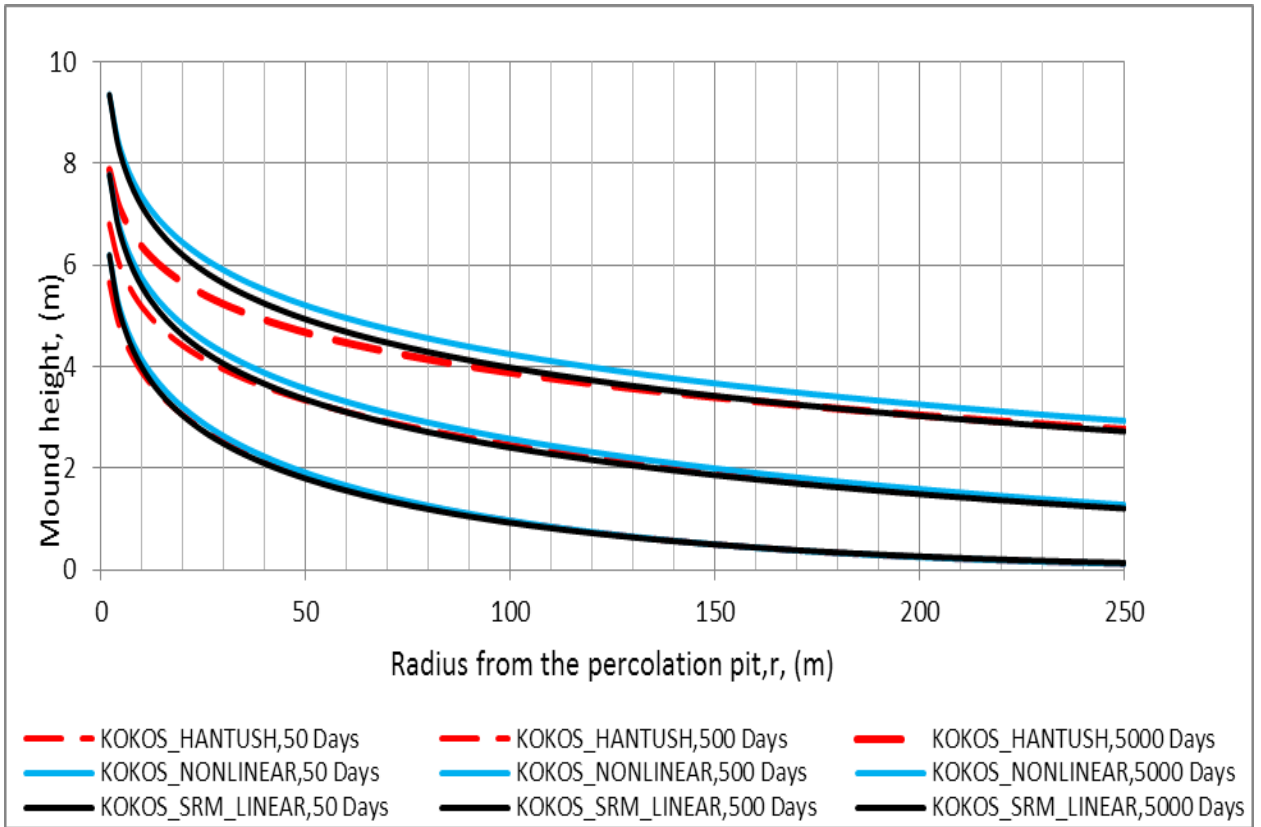


Figure 8. Comparison of mound heights KOKOS_OPTIMUM_NONLINEAR with values of optimum $\lambda(t)$; KOKOS_SRM_LINEAR with $H_{AE}=H_A+h_{CRIT}$ and KOKOS_HANTUSH with Constant=0.5; for $Q_R=500$, $K_R=5$, $H_A=10$, $S=0.2$

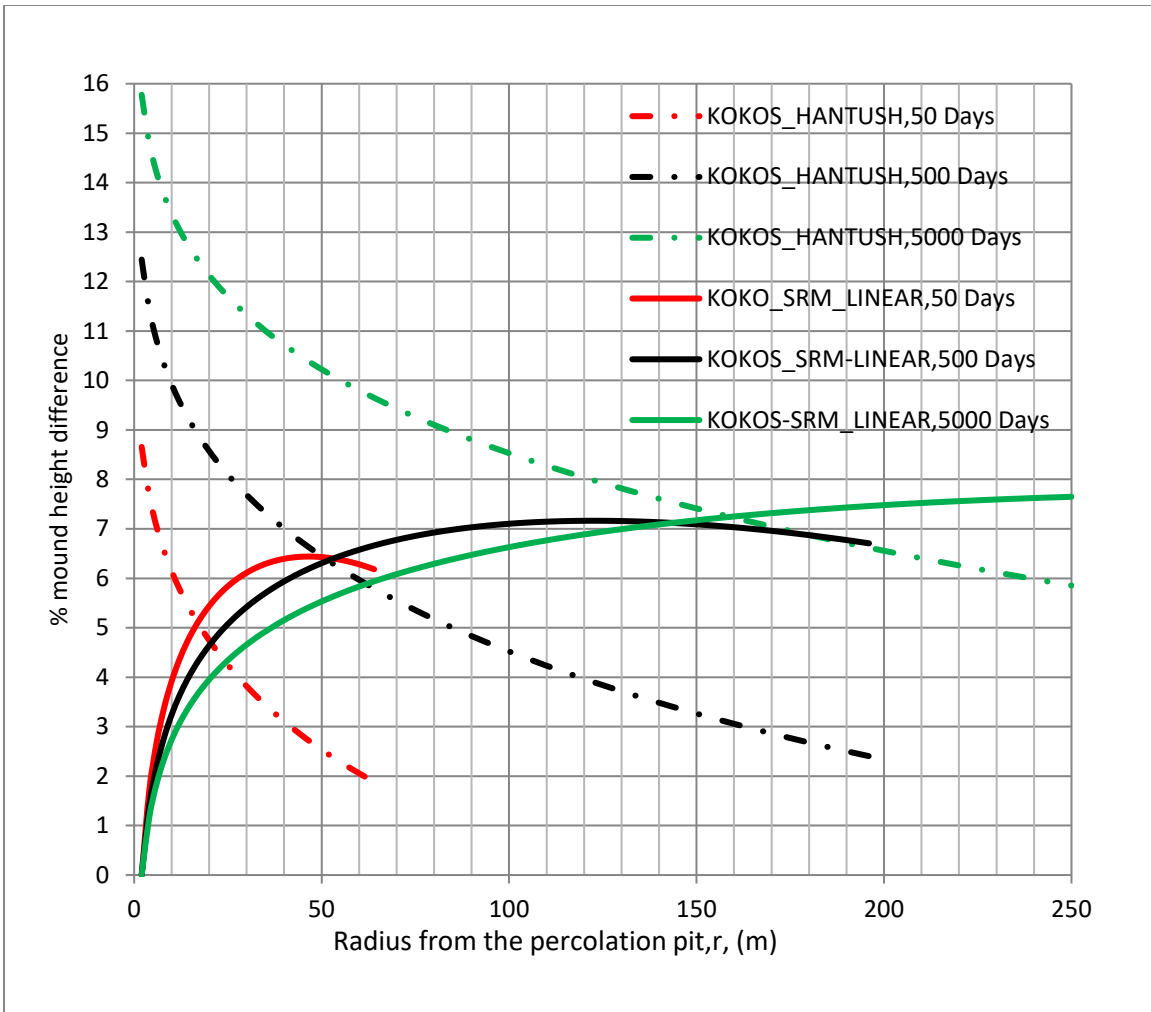


Figure 9. Percentage (%) difference from KOKOS_NONLINEAR with optimum $\lambda(t)$ and KOKOS_HANTUSH Constant=0.5 and KOKOS_SRM_LINEAR with $H_{AE}=H_A+h_{CRIT}$

The experimental results from the field test well are shown in Figure 10 together with the Hantush and the thesis nonlinear optimum solutions.

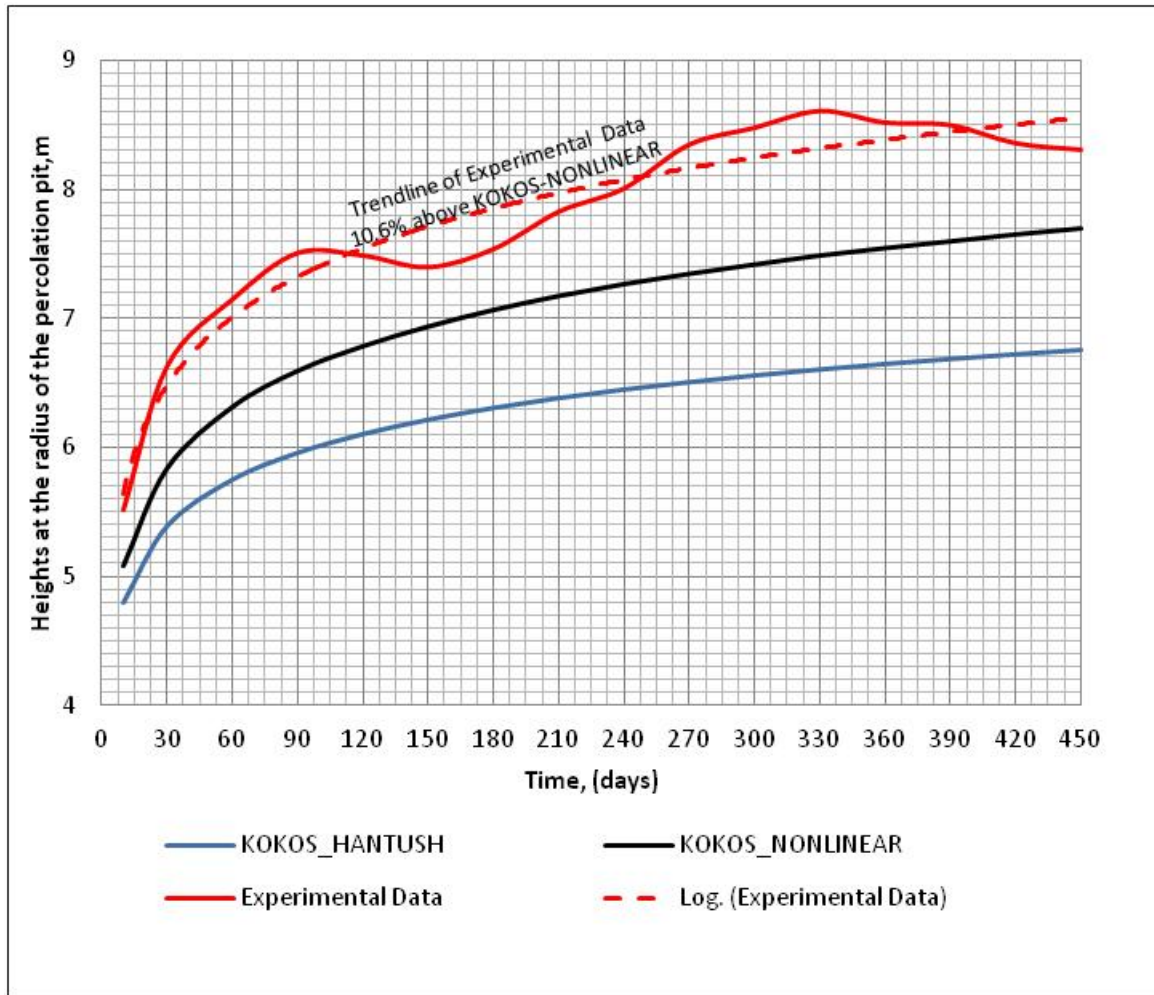


Figure 10. Comparison of Experimental Data with KOKOS_HANTUSH with Constant=0.5 and KOKOS_NONLINEAR optimum $\lambda(t)$

7. OVERALL DISCUSSION

The objective of this study was to conclude whether the conventional low rate percolation ponds could be replaced by more land efficient percolation wells to introduce recharge water direct into the aquifer to avoid mounding and subsequent flooding.

An experimental test well was built to provide experimental data from these direct recharge experiments and to validate the solutions to the classical equations governing flow in aquifers. The well was 9 m deep (4 m diameter) to connect directly with the original aquifer water table, estimated to be 10 m thick. The well was used with a constant recharge rate of 500 m³/day.

A new sub routine program was developed to predict and understand the impact on water table height and mounding. The technique was validated with these field measurements and compared to the classical governing equations derived from the literature review. The aquifer storage coefficient and hydraulic conductivity were estimated at 0.2 and 5 m³/day respectively.

From this work it was concluded that recharging at constant rate via specially constructed percolation pits that direct the recharge water into the aquifer's initial water table is ideal for preventing saturation of the infiltration zone.

The analytical work described in this study of this thesis developed the classical, commonly used, partial differential equations governing the flow in confined and unconfined aquifers used for estimating the resulting mound growth. These traditional and well known analytical solutions were originally proposed by Theis and Hantush. They were developed using the now commonly available Visual Basic solution methods used and generally are familiar to engineers and hydrologists. The process used also sought to provide optimum solutions based on the local physical and hydraulic characteristics of the infiltration arrangements. It is suggested this is a new advancement compared to the traditional Hantush method which uses an assumed linearization constant to ensure that solutions to the equations are possible.

For this new proposed software routine and for mathematical solutions to be possible a number of assumptions were found to be necessary. For the confined aquifers these assumptions were:

- The aquifer should be horizontal and of infinite extent in all directions around the percolation pit recharge entry.
- The aquifer is enclosed by two impervious layers at the top and bottom but at a constant distance apart and through which the recharge water flows uniformly with the depth.
- The soil between the impervious layers is saturated and has constant porosity and hydraulic conductivity.
- The flow is assumed to be purely horizontal since the second derivative of the head $\frac{\partial^2 h}{\partial z^2}$ relative to the saturated depth z is neglected.
- The recharge is continuous and constant and is applied only through the percolation pit entry direct into the aquifer simulating a line source entry into the aquifer.
- As soon as the recharge starts, the water flow front is assumed to have reached the radius at infinity; *this assumption has to be imposed despite however unrealistic it sounds*. The family of curves, $h = \Phi(Q_R, K_R H_A, S, r, t)$, representing the mound heights versus the radius from the percolation pit, were used to show an infinite extent in order to satisfy the condition at infinity where at $r=\infty$, $h=0$. The two solutions to the linear PDE governing the confined aquifers were tested in this study of the thesis:
- The first is based on the Simpson's Rule Method (SRM), which it was believed was being put forward for the first time; the method was enhanced by a function to specify the accuracy.

- The second was based on a Direct Integration Method (DIM) of the well function integral. This required an initial evaluation of the Euler constant of integration by using the SRM.

The results, were shown in Figure 4, comparing the mound heights obtained from the different methods (SRM and the DIM) they were found to be coincident, which corroborated and supported the accuracy of the new method but also all the methodologies tried.

The proposed analytical method was then considered for the case of an unconfined aquifer. The Ezousas aquifer, in this case study was unconfined below pervious soils and alluvial gravels.

Thus the recharge water inevitably also enters the soil region above the aquifer's original water table despite the well and rises above it, to a height h of a similar shape to that of the head in the confined aquifer case; in other words the flow path is changed from H_A of the confined case to $h_H = H_A + h$ in the unconfined case; this change renders the governing PDE to nonlinear, for which a direct solution is not possible.

As for the confined case, a solution has been proposed which linearizes the PDE by assuming that $\bar{h}_A = H_A + \lambda(t)h(r_{MIN}, t)$, where $\lambda(t)$ is a time depended constant. The Hantush linearization in contrast was given as $\bar{h}_H = H_A + 0.5h(r_{MIN}, t)$, where the constant 0.5 is iteratively or intuitively chosen but does not have an underpinning hydraulic or physical justification.

The results, for the mound heights obtained from the Hantush assumption compared with the proposed assumption (where $\lambda(t)$ was set to 0.5) were presented in Figure 5 and found to be coincident.

The family of curves produced to give the mound heights $h = \Phi(Q_R, K_R H_A, S, r, t)$ with respect to the radius from the percolation pit, keeping the Q_R , K_R , H_A , and S constant were assumed, as was the case for the confined aquifer, to have an infinite extent in order to satisfy the condition that at $r=\infty$, *and* h which was required to be equal to zero. This condition however is also idealized; since at any instant of time t the water flow front in the aquifer can only reach a uniquely specified critical radius, r_{CRIT} from the percolation pit (see Figure 6). This radius is related to volume of water that is capable of being stored in the soil medium and the duration of flow; therefore, there exists a real physical hydraulic relationship between the above squared radius and time.

The derived solutions were found it to be *constant*; this ratio is given by

$$\frac{r_{CRIT}^2}{t_{CRIT}} = \frac{Q_R}{\pi S (H_A + \lambda(t) h(r_{MIN}, t))};$$

This ratio is towards the lower integration limit of the well function integrals; therefore, the value of the mound heights at all points that obey this ratio are the same height.

The term critical height was used and given by:

$$h_{CRIT} = \frac{Q_R}{4\pi K_R (H_A + h_{CRIT})} W\left(\frac{Q_R}{4\pi K_R (H_A + h_{CRIT})^2}\right) \text{ where, } h_{CRIT} = \lambda(t) h(r_{MIN}, t) \text{ is a time}$$

invariant constant, and $\lambda(t)$ is a time dependent constant.

Once the nature of the critical height and the factor $\lambda(t)$ have been found, the value of $\lambda(t)$ with time was established and was presented in Figure 7.

Using the optimum $\lambda(t)$ corresponding to a time t the mound heights at that time are found by the subroutine developed **KOKOS_NONLINEAR**.

In addition a solution for the mound heights was obtained by the use of the **KOKOS_SRM_LINEAR** by changing the aquifer thickness from H_A to its equivalent

$$H_{AE} = H_A + h_{CRIT}.$$

The Hantush and the two thesis solutions were coincident and shown in Figure 8.

8. CONCLUSIONS

It was concluded that the traditional Simpson's Rule, with specified accuracy provided a practical means of evaluating the well function integral and was demonstrated to be a useful tool for the prediction of mound problems.

The concept of critical depth, h_{CRIT} , was introduced based on fundamental hydraulic characteristics and this provided the opportunity to propose two new solutions to the mound problem:

1. A solution by using the linear PDE with an equivalent aquifer thickness equal to $H_A + h_{CRIT}$ instead of H_A .
 2. A solution by using the nonlinear PDE whereby a general linearization expression, which has underpinning principles based on well radius and soil saturation for the solution using as a linearization constant $\bar{h}_A = H_A + \lambda(t)h_{MAX}$
- In contrast to the classical Hantush linearization expression of

$\bar{h}_H = H_A + 0.5h_{MAX}$; where the coefficient of 0.5 was introduced to make quadratic substitution solvable.

The proposed linearization coefficient, $\lambda(t)$, has as an optimum value that corresponds to the ratio of critical thickness divided by the maximum mound height at the percolation pit radius, $\lambda(t) = h_{CRIT}/h_{MAX}$; and its values were presented in Figure 6.

It was concluded and worth noting that the solutions using the linear PDE lies between the two nonlinear PDE solutions. The Hantush results were consistently smaller than the method proposed in this thesis for nonlinear PDE solution. The differences at 50 days were between 2 to 8.7% at 500 days, 12.5% to 2.5% and 15.8% to 7.7% at 5000 days for a radius between 2 to 250 m (see Fig. 9). This corroborated previously published data which also suggested the Hantush results to be smaller than experiment by 3% to 6% (Marino 1967; Korkmaz 2012).

Thus it was concluded that the Hantush method was likely to under estimate mound height by around 5% at these recharge durations and radii used in the experiments described.

There are discrepancies of around 10% between the experimental results (presented in Fig. 10) for the mound heights versus time compared to the thesis derived optimum solutions. It is suggested these are a result of variations in local aquifer characteristics but this needs to be confirmed by further research.

REFERENCES

Aish, A.M, 2010. Solution of groundwater mound resulting from proposed artificial recharge of treated sewage effluent case study-Gaza wastewater treatment plant Palestine. *Geologia Croatica* 63/1 67–73.

C:\Users\C\AppData\Local\Microsoft\Windows\Temporary Internet Files\Content.IE5\PX06HXJW\OJS_file.pdf

Bansal, R. and Das, S., 2010. Analytical Study of Water Table Fluctuation in Unconfined Aquifers due to Varying Bed Slopes and Spatial Location of the Recharge Basin. *J. Hydrol. Eng.*, 15(11), 909–917. doi: 10.1061/(ASCE)HE.1943-5584.0000267

Batu, V., 1998. *Aquifer Hydraulics: A Comprehensive Guide to Hydrogeologic Data Analysis*. John Wiley & Son. ISBN: 0-471-18502-7.

Baumann, P., 1952. Groundwater movement controlled through spreading. *Amer. Soc. Civil Engrs.* Vol.117, pp1024-1074.

Bouwer, H., 1962. Analyzing Groundwater Mound by Resistance Network. *ASCE Journal of Irrigation and Drainage Engineering*, 88(IR3):15-36.

Bouwer, H., 2002. Artificial recharge of groundwater: hydrogeology and engineering. *Hydrogeol. J.V.* 10, pp121–142.

Bouwer, H, Back, J.T., and Oliver, J.M., 1999. Predicting infiltration and ground-water mounds for artificial recharge. *ASCE J. of Hydrologic Engineering*, Vol 4, (4), October, pp 350-357.

Bredehoeft, J.D., 2002. The water budget myth revisited: Why hydrogeologists model. *Ground Water* Vol.40, (4),pp 340-345.

Brutsaert, W., and Ibrahim, H. A., 1966. On the first and second linearization of the Boussinesq equation. *Geophysical Journal of the Royal Astronomical Society*, Vol.11(5) pp 549–554. doi: 10.1111/j.1365-246X.1966.tb03166.x

Carleton, G.B., 2010. Simulation of Groundwater Mounding Beneath Hypothetical Stormwater Infiltration Basins. Scientific Investigations Report 2010–5102. U.S. Geological Survey, Reston, Virginia: 2010

Dagan, G.,1967. Linearized solutions of free-surface groundwater flow with uniform recharge. *J. Geophys. Res.*, Vol.72(4), pp1183– 1193.

Ferguson, Bruce K., 1990. "Role of the Long-term Water Balance in Management of Storm Water Infiltration," *Journal of Environmental Management*, Vol 30, pp 221-233.

Finnemore, E. J., 1993. Estimation of Ground-Water Mounding Beneath Septic Drain Fields. *Groundwater*, 31(6), 884–889.

Finnemore, E.J., 1995. A program to calculate ground-water mound heights: *Ground Water*, Vol. 33, (1), pp. 139–143.

Glover, R. E., (1961). Mathematical derivations as pertain to groundwater recharge. Mimeographed report, Agricultural Research Service, U. S. Dept. Agriculture, Ft. Collins, Colo: 81.

Glover, R.E., 1964, Ground-water movement: U.S. Bureau of Reclamation Engineering Monograph. Series, no. 31. http://www.usbr.gov/pmts/hydraulics_lab/pubs/EM/EM31.pdf

Guo, James C.Y., 2001. "Design of Circular Infiltration Basin Under Water Mounding Effects," *ASCE J. of Water Resources Planning and Management*, Vol 127, No.1, Jan/Feb.

Guo, James C.Y., 2003. "Design of Infiltrating Basin by Soil Storage and Conveyance Capacities," IWRA International J. of Water, Vol 28, No. 4, December.

Hantush, M. S., 1967. Growth and decay of groundwater mounds in response to uniform percolation. *Water Resources Research*, 3: 227-234.

Howden, N., Mather, J., 2012: History of hydrogeology. CRC Press, ISBN 9780415630627 - CAT# K15478

Jacob, C.E., 1940. On the flow of water in an elastic artesian aquifer. *Transactions of American Geophysical Union*, Volume 21, Issue 2, p. 574-586.

Kacimo, A. R., 1997. Dynamics of groundwater mounds: analytical solutions and integral characteristics. *Hydrological Sciences-Journal-des Sciences Hydrologiques*, 42(3) June 1997.

Korkmaz, S., 2012. Formation of Unsteady Groundwater Mounds under Constant Recharge: Application to a Stormwater Dispersion Trench. BALWOIS 2012-5th Conference on Water, Climate and Environment. Macedonia.

Manglik, A., Rai S.N., (2000). Modeling of water table fluctuations in response to time-varying recharge and withdrawal. *Water Resources Management* 14(5):339–347.

Manglik, A., Rai SN, Singh, V.S., 2004. Modelling of aquifer response to time varying recharge and pumping from multiple basins and wells. *Journal of Hydrology*, 292:23–29

Marino, M. A., 1967. Hele-Shaw model study of the growth and decay of groundwater ridges. *Journal of Geophysics Research* 72: 1195-1205.

Marino, M. A., & Luthin, J.N., 1982. Seepage and Groundwater. Elsevier Scientific Publishing company. ISBN 13: 978-0-444-41975-0.

Marmion, K. R., 1962. Hydraulics of artificial recharge in nonhomogeneous formations. Hydraulic Lab., Univ. of California, Berkeley. Water Resources Center Contrib. no. 48, Pp 88.

Morel-Seytoux, H.J., Miracapillo, C., and Abdulrazzak, M.J., 1989. Distribution of aquifer recharge from a circular spreading basin under transient operations. Groundwater Management: Quantity and Quality (Proceedings of the Benidorm Symposium, October 1989). IAHS Publ. no. 188, 1989.

Murray, W. A. and Johnson, R. L., 1977. Modeling of Unconfined Ground-Water Systems. Ground Water. Vol. 15 (4), pp 306–312. doi: 10.1111/j.1745-6584.1977.tb03176.x

Napolitan, M., 2010. Formation Thermal Conductivity Testing of the Ledger Formation in Lancaster County Pennsylvania.

http://www.taylorgeoservices.com/papers/Michael_Napolitan_Capstone_FCT_Paper.pdf

Poeter, E., McCray, J., Thyne, G. and Siegrist, R., 2005. Guidance for Evaluation of Potential Groundwater Mounding Associated with Cluster and High-Density Wastewater Soil Absorption Systems. Project No. WU-HT-02-45. Prepared for the National Decentralized Water Resources Capacity Development Project, Washington University, St. Louis, MO, by the International Groundwater Modeling Center, Colorado School of Mines, Golden, CO. This report is available online at www.ndwrcdp.org.

Rai, S.N., and Singh, R.N., 1981. A mathematical model of water-table fluctuation in a semi-infinite aquifer induced by localised transient recharge: Water Resources Research. Vol. 17, p. 1028–1032.

Rai, S.N. and Singh R.N., 1993. Evolution of the phreatic surface in a fenic aquifer due to transient recharge. Paper presented at International conference on /hydrology and Water Resources, Dec. 20-22, 1993 New Delhi.

Rai, S.N. and Singh R.N., 1996. Analytical modeling of unconfined flow induced by time varying recharge. Proc. Indian Natn.Sci. Acad.,62, A, No.4, pp.253-292.

Rao, N.H., and Sarma, P.B.S., 1980. Growth of Ground-Water Mound in Response to Recharge. Ground Water.Vol. 18(6), 587-595. doi: 10.1111/j.1745-6584.1980.tb03653.x

Rao, N.H., and Sarma, P.B.S., 1981, Ground-water recharge from rectangular areas: Ground Water, v. 19, no. 3, p. 270–274.

Schiff, L., and Dyer, K.L., 1964. Some physical and chemical considerations in artificial ground-water recharge. International Assoc. Sci. Hydrology Pub., vol. 64, 347-358.

Sunada, D.K., Warner, J.W., and Molden, D.J., 1983, Artificial groundwater recharge, San Luis Valley, Colorado: Fort Collins, Colo., Colorado Water Resources Research Institute, Colorado State University, Research Project Technical Completion Report, Project no. A-050-Colo,
http://digitool.library.colostate.edu///exlibris/dtl/d3_1/apache_media/L2V4bGlicmlzL2R0bC9kM18xL2FwYWNoZV9tZWRpYS8xMjE1MQ==.pdf

Swamee, P. K., and Ojha, C. S. P., 1997. “Groundwater mound equation for rectangular recharge area.” J. Irrig. Drain. Eng., 123(3), 215–217.

Thompson, A., Nimmer, M., and Misra, D., 2007. Groundwater mounding and contaminant transport beneath stormwater infiltration basins (Wisconsin groundwater management practice monitoring project, [DNR-189]).

Wisconsin Department of Natural Resources, 2007 URL to cite for this work:
<http://digital.library.wisc.edu/1711.dl/EcoNatRes.ThompsonGroundwater>

Todd, D. K., 1961. The distribution of ground water beneath artificial recharge areas: Internat. Assoc. Sci. Hydrology Pub. 56, p. 254-262.

Todd, D. K., 1980. Groundwater hydrology. 2nd Ed. John Wiley & Sons.

Wang, X. S., Chen, C. X., and Jiao J. J., 2004. Modified Theis equation by considering the bending effect of the confining unit. Advances in Water Resources 27 (2004) 981–990. Elsevier

Warner, J. M., Molden, D., Chehata, M. & Sunada, D. K., 1989. Mathematical analysis of artificial recharge from basins. Wat. Resour. Bull. 25(2), 401-41.

Zlotnik, V. A. and Glenn, L., 1993. Groundwater Velocity in an Unconfined Aquifer With Rectangular Areal Recharge. Papers in the Earth and Atmospheric Sciences. Paper 160. <http://digitalcommons.unl.edu/geosciencefacpub/160>
Water Resources Research, Vol. 29, No. 8, pp 827-2834

Zomorodi, K., 1991. Evaluation of the Response of Water Table to a Variable Recharge Rate. Journal of Hydrological Sciences, 36(1):67-78.

Zomorodi, K., 2005. Simplified solutions for groundwater mounding under stormwater infiltration facilities: Proceedings of the American Water Resources Association 2005 annual Water Resources Conference, November 7–10, 2005, Seattle, Washington.

APPENDIX 2

COMPUTER PROGRAMS

SUBROUTINE, 1. KOKOS_SRM_LINEAR

```
Sub KOKOS_SRM_LINEAR()

Sheets("KOKOSSRMLINEAR").Activate

10  QR = 500:
    HA = 10: HN = 10
    KR = 5:
    S = 0.2:
    RMIN = 2
    RMAX = 250
    '*****
    n = 1000000:
    Er = 0.0001
    '*****
    XMAX = 10

    TIM = 10

    '*****
      'OUTPUT DATA HEADINGS
    '*****
15  Cells(1, 3).Value = "No.DAYS": Cells(2, 3).Value = (TIM)
    Cells(1, 6).Value = "No. STEPS": Cells(2, 6).Value = n
    Cells(1, 7).Value = "ERROR": Cells(2, 7).Value = Er
    Cells(1, 4).Value = "ITER.ACC"
    Cells(1, 2).Value = "h(r,t)"
    Cells(1, 1).Value = "RADIUS"
20  Cells(1, 5).Value = "STEP SIZE"
    '*****
    RR = 2
    '*****
30  ' THE R RADIUS LOOP
    '*****
    For R = RMIN To RMAX Step 2

40      HO = QR / (4 * 3.14 * HA * KR)
        '*****
        'EVALUATES THE STEP ST FOR THE SET ACCURACY Er
        '*****
50      ALFA = S * R ^ 2 / (4 * HA * KR * TIM):
        F41 = (Exp(-ALFA) / ALFA)
        F42 = (1 + (4 / ALFA) + (12 / ALFA ^ 2) + (24 / ALFA ^ 3) + (24 / ALFA ^ 4))
        F4ALFA = F41 * F42
```

```

F42 = (1 + (4 / ALFA) + (12 / ALFA ^ 2) + (24 / ALFA ^ 3) + (24 / ALFA ^ 4))
F4ALFA = F41 * F42
60      ST = (90 * Er / (F4ALFA * n)) ^ 0.2

'*****
' THE ZZ ACCURACY LOOP
' ZZ IS THE NUMBER OF PARTS THE WELL FUNCTION INTEGRAL NEEDS
' TO AUTOMATICALLY SPLIT INTO TO ENSURE THE SET ACCURACY
'*****

'ESTABLISHES THE CUMULATIVE ERROR AND MOUNT HEIGHT THAT COMES
'FROM THE SUCCESSIVE INTEGRATION OF THE PARTS OF THE WELL FUNCTION
'EVALUATION OF THE HMAX CORRESPONDING TO AQUIFER THICKNESS HA
'*****

70      ZZ = 1

      SA = 0
82      BETA = ALFA + 2 * n * ST
      ORD = 0:
      u0 = ST
      U1 = ALFA
      U2 = BETA
      FIRST = Exp(-(U1)) / (U1)
      LAST = Exp(-(U2)) / (U2)

      For J = 2 To (2 * n - 2) Step 2:
          EV = 4 * Exp(-(U1 + ST * (J - 1))) / (U1 + ST * (J - 1))
          OD = 2 * Exp(-((U1 + ST) + ST * (J - 1))) / ((U1 + ST) + ST * (J - 1))
          ORD = ORD + (EV + OD)
      Next J

      AREA = (FIRST + ORD + (LAST)) * u0 / 3
      SA = SA + AREA
      HMAX = SA * H0
      DIFHMAX = HMAX - HMAXO
84      HMAXO = HMAX
      If Abs(DIFHMAX) < Er Then GoTo 99
      ALFA = BETA
90      ZZ = ZZ + 1
      GoTo 77

'*****
99      'OUTPUT OF RESULTS
'*****

Cells(RR, 4).Value = ZZ
Cells(RR, 2).Value = HMAX

```

```
Cells(RR, 1).Value = (R)
Cells(RR, 5).Value = ST
'*****
140
150     Next R
RR = RR + 1
End Sub
```

SUBROUTINE, 2. KOKOS_EULER_CONSTANT

```
Sub KOKOS_EULER_CONSTANT():

'EULER CONSTANT EVALUATION

  Sheets("KOKOSEULER").Activate

      HA = 10
      KR = 5
      S = 0.2
10      U1 = 1
20      Er = 0.00000000001
30      n = 1000000

*****
'OUTPUT HEADINGS
*****
Cells(1, 1).Value = " EULER CONSTANT EVALUATON"
Cells(2, 1).Value = "W(1)"
Cells(3, 1).Value = "SERIES"
Cells(4, 1).Value = "CALCULATED VALUE"
Cells(5, 1).Value = "INTERNET VALUE"
Cells(6, 1).Value = "DIFFERENCE FROM INTERNET"
H0 = QR / (4 * 3.14 * HA * KR)
'SETTING THE ACCURACY AND FINDING THE STEP ST
50  ALFA = U1
      F41 = (Exp(-ALFA) / ALFA)
      F42 = (1 + (4 / ALFA) + (12 / ALFA ^ 2) + (24 / ALFA ^ 3) + (24 / ALFA ^ 4))
      F4ALFA = F41 * F42
65  ST = (90 * Er / (F4ALFA * n)) ^ 0.2

*****
' WELL FUNCTION W(1) EVALUATION BT THE SRM
*****
70      ZZ = 1
      'ESTABLISHES THE CUMULATIVE ERROR AND MOUNT HEIGHT THAT COMES
      'FROM THE SUCCESSIVE INTEGRATION OF THE PARTS OF THE WELL FUNCTION
      'EVALUATION OF THE HMAX CORRESPONDING TO AQUIFER THICKNESS HA
      SA = 0
77      BETA = ALFA + 2 * n * ST
      ORD = 0:
      u0 = ST
      U1 = ALFA
      U2 = BETA
82      FIRST = Exp(-(U1)) / (U1)
```

```

        LAST = Exp(-(U2)) / (U2)

    For J = 2 To (2 * n - 2) Step 2:
        EV = 4 * Exp(-(U1 + ST * (J - 1))) / (U1 + ST * (J - 1))
        OD = 2 * Exp(-(U1 + ST) + ST * (J - 1)) / ((U1 + ST) + ST * (J - 1))
        ORD = ORD + (EV + OD)
    Next J

    AREA = (FIRST + ORD + (LAST)) * u0 / 3
    SA = SA + AREA
    HMAX = SA * H0
    DIFHMAX = HMAX - HMAXO
84     HMAXO = HMAX
    If Abs(DIFHMAX) < Er Then GoTo 99
    ALFA = BETA
90     ZZ = ZZ + 1
        GoTo 77

99         A0 = -1
            *****
            'SERIES EVALUATION
            ' BY RECURSION FORMULA
            *****
            For SER = 1 To (2 * n + 1)
                SU = SU + A0
                A1 = -A0 * (SER) / (SER + 1) ^ 2
                A0 = A1
            Next SER

80         EUERLCONSTANT = AREA + SU
            *****
            'INTERNET VALUE OF THE EULER COSTANT
            *****
            INTERNETEU = -0.577215664901533
            DIFFERENCE = (INTERNETEU - EUERLCONSTANT)
            *****
            'DATA OUTPUT
            *****
            Cells(2, 5).Value = SA
            Cells(3, 5).Value = SU
            Cells(4, 5).Value = EUERLCONSTANT
            Cells(5, 5).Value = INTERNETEU
            Cells(6, 5).Value = DIFFERENCE

```

End Sub

SUBROUTINE, 3. KOKOS_DIM_LINEAR

```
Sub KOKOS_DIM_LINEAR():

'SERIES SOLOUTION

Sheets("KOKOSDIMLINEAR").Activate

10           QR = 500:
20           HA = 10:
30           KR = 5:
40           S = 0.2:
50           RMIN = 2
55           RMAX = 250
60           TMIN = 5
65           TMAX = 505
70           H0 = QR / (4 * 3.14 * KR * HA):
80           n = 100

           XX = 1
           *****
           'TIME LOOP
           *****

90           For TIM = TMIN To TMAX Step 50
           TIM1 = TIM
           If TIM > 5 Then TIM1 = TIM - 5
           YY = 1
           *****
           'RADIUS LOOP
           *****

100          For R = RMIN To RMAX Step 2
           U = S * R ^ 2 / (4 * KR * HA * TIM1)
110          A0 = -U
           SU1 = 0
           *****
           'SERIES EVALUATION
           ' BY RECCURSION FORMULA
           *****

           For RS = 1 To (2 * n + 1)
           SU1 = SU1 + A0
           A1 = -A0 * U * (RS) / (RS + 1) ^ 2
           A0 = A1
120          Next RS
130          SU2 = -Log(U)
```

```

140          SU3 = -0.5772156649:
          SUT = SU2 + SU3 - SU1
150          H = SUT * H0
          SU2 = 0: SU1 = 0: SUT = 0

          '*****
          'DATA OUTPUT
          '*****
160          Cells(10, 3).Value = "DAYS"
          Cells(11, 3).Value = "RADIUS"
          Cells(10, XX + 4).Value = TIM1
          Cells(10 + YY, 4).Value = R
170          Cells(10 + YY, XX + 4).Value = H
          YY = YY + 1
          Next R
          XX = XX + 1
          Next TIM
End Sub

```


SUBROUTINE, 4. KOKOS_NONLINEAR

Sub KOKOS_NONLINEAR()

'KOKOS NONLINEAR VIA OPTIMUM LAMDA VALUES

'CORRESPONDING TO A SET TIME

Sheets("KOKOSNL").Activate

10 QR = 500:

HA = 10: HN = HA

KR = 5:

S = 0.2:

n = 1000000:

Er = 0.0001

RMIN = 2

RMAX = 250

' AUTHOR'S NON LINEAR SOLUTIONS

' BASED ON HANTUSH LAMDA=0.5

TIM = 50: LAMDA = 0.5

'TIM = 500: LAMDA = 0.5

'TIM = 5000: LAMDA = 0.5

'AUTHOR'S OPTIMUM NON LINEAR SOLUTIONS

' BASED ON hCRIT=1.584806518

'AND LAMDA OPTIMUM VALUES BELOW

'TIM = 50: LAMDA = 0.256

'TIM = 500: LAMDA = 0.204

'TIM = 5000: LAMDA = 0.170

'OUTPUT HEADINGS

Cells(1, 1).Value = "LAMDA": Cells(2, 1).Value = LAMDA

Cells(1, 2).Value = "TIME": Cells(2, 2).Value = TIM

Cells(1, 3).Value = "RADIUS"

Cells(1, 4).Value = "HMAX":

Cells(1, 5).Value = "STEP":

Cells(1, 6).Value = "ZZ":

Cells(1, 7).Value = "n": Cells(1, 8).Value = "Er"

Cells(2, 7).Value = n: Cells(2, 8).Value = Er

RR = 2

'THE RADIUS LOOP

For R = RMIN To RMAX Step 2

H0 = QR / (4 * 3.14 * (HA) * KR):

Cells(RR, 3).Value = R

'LOOP XX EVALUATES HMAX

' AT EACH RADIUS R

For XX = 1 To 10

'EVALUATES THE STEP SIZE ST FOR THE SET ACCURACY Er

H0 = QR / (4 * 3.14 * (HA) * KR):

ALFA = S * R ^ 2 / (4 * (HA) * KR * TIM):

F41 = (Exp(-ALFA) / ALFA)

F42 = (1 + (4 / ALFA) + (12 / ALFA ^ 2) + (24 / ALFA ^ 3) + (24 / ALFA ^ 4))

F4ALFA = F41 * F42

ST = (90 * Er / (F4ALFA * n)) ^ 0.2

Cells(RR, 5).Value = ST:

' THE ZZ ACCURACY LOOP

' ZZ IS THE NUMBER OF PARTS THE WELL FUNCTION INTEGRAL NEEDS

' TO AUTOMATICALLY SPLIT INTO TO ENSURE THE SET ACCURACY

'ESTABLISHES THE CUMULATIVE ERROR AND MOUNT HEIGHT THAT COMES

'FROM THE SUCCESSIVE INTEGRATION OF THE PARTS OF THE WELL FUNCTION

'EVALUATION OF THE HMAX CORRESPONDING TO AQUIFER THICKNESS HA

ZZ = 1

SA = 0

111

BETA = ALFA + 2 * n * ST

ORD = 0:

u0 = ST

```

U1 = ALFA
U2 = BETA
FIRST = Exp(-(U1)) / (U1)
LAST = Exp(-(U2)) / (U2)
  For J = 2 To (2 * n - 2) Step 2:
    EV = 4 * Exp(-(U1 + ST * (J - 1))) / (U1 + ST * (J - 1))
    OD = 2 * Exp(-((U1 + ST) + ST * (J - 1))) / ((U1 + ST) + ST * (J - 1))
    ORD = ORD + (EV + OD)
  Next J

AREA = (FIRST + ORD + (LAST)) * u0
SA = SA + AREA
HMAX = SA * H0:
DIFHMAX = Abs(HMAX - HMAXO)
If (DIFHMAX) < Er Then GoTo 222
HMAXO = HMAX:
ALFA = BETA
ZZ = ZZ + 1

140      GoTo 111
222      Cells(RR, 6).Value = ZZ

'*****
'THE FOLLOWING PART DEALS WITH THE ITERATIONS
' NEEDED TO MAKE THE MOUND HEIGHT AT h(r,t)
' TO REMAIN UNCHANGED
'*****

HA = HN + LAMDA * HMAX
DIFHA = Abs(HA - EHA)
If DIFHA < Er Then GoTo 333
EHA = HA

Next XX
333      HA = HN
          Cells(RR, 4).Value = LAMDA * HMAX

RR = RR + 1

Next R
555
End Sub

```

SUBROUTINE, 5. KOKOS_HANTUSH

Sub KOKOS_HANTUSH()

'AUTHOR'S HANTUSH

Sheets("KOKOSHANTUSH").Activate

10 QR = 500:

HA = 10: HN = 10

KR = 5:

S = 0.2:

RMIN = 2

RMAX = 250

n = 1000000:

Er = 0.0001

XMAX = 20

LAMDA = 0.5

TIM = 50

20 Cells(1, 1).Value = "EHA":

Cells(1, 2).Value = "RADIUS":

Cells(1, 3).Value = "h(r,t)":

Cells(1, 5).Value = "TIME": Cells(2, 5).Value = (TIM)

Cells(1, 6).Value = "ERROR": Cells(2, 6).Value = Er

Cells(1, 4).Value = "STEP":

Cells(1, 7).Value = "No STEPS": Cells(2, 7).Value = n

30 RR = 2

For R = RMIN To RMAX Step 2

For XX = 1 To XMAX

H0 = QR / (2 * 3.14 * KR)

'SETTING THE ACCURACY AND FINDING THE STEP ST

50 ALFA = S * R ^ 2 / (4 * HA * KR * TIM):

F41 = (Exp(-ALFA) / ALFA)

F42 = (1 + (4 / ALFA) + (12 / ALFA ^ 2) + (24 / ALFA ^ 3) + (24 /

ALFA ^ 4))

F4ALFA = F41 * F42

60 ST = (90 * Er / (F4ALFA * n)) ^ 0.2

70 ZZ = 1

'ESTABLISHES THE CUMULATIVE ERROR AND MOUNT HEIGHT

THAT COMES

```

'FROM THE SUCCESSIVE INTEGRATION OF THE PARTS OF THE
WELL FUNCTION

77      ZA = 0
        BETA = ALFA + 2 * n * ST
        ORDE = 0: ORDO = 0
        u0 = ST
        U1 = ALFA
        U2 = BETA
        FIRST = Exp(-(U1)) / (U1)
        LAST = Exp(-(U2)) / (U2)
          For JE = 2 To 2 * n - 2 Step 2:
            ORDE = ORDE + Exp(-(U1 + u0 * (JE - 1))) / (U1 + u0 * (JE
- 1))

          Next JE
          For JO = 3 To 2 * n - 1 Step 2:
            ORDO = ORDO + Exp(-(U1 + u0 * (JO - 1))) / (U1 + u0 *
(JO - 1))

          Next JO
        AREA = (FIRST + 4 * ORDE + 2 * ORDO + (LAST)) * u0 / 3
        ZA = ZA + AREA

        ZMAX = ZA * H0
        HHMAX = Sqr(ZMAX + HN ^ 2)
        HMAX = HHMAX - HN
        DIFHMAX = Abs(HMAX - HMAXO)
        If Abs(DIFHMAX) < Er Then GoTo 99
        HMAXO = HMAX
        ALFA = BETA
90      ZZ = ZZ + 1
        GoTo 77
99

'*****
'CATERS FOR THE NON LINEARITY
'SUCCESSIVE ITERATIONS UNTIL THE MOUND
'HEIGHT AT h(rMIN,t) REMAINS UNCHANGED
'AND THUS HMAX AND EHA ARE EVALUATED
'*****
HA = HN + LAMDA * HMAX
DIFHA = Abs(HA - EHA)
If DIFHA < Er Then GoTo 100
EHA = HA
Next XX
100     Cells(RR, 1).Value = EHA:
        Cells(RR, 2).Value = R
        Cells(RR, 3).Value = HMAX
        Cells(RR, 4).Value = ST
        RR = RR + 1

```

Next R

555

End Sub

SUBROUTINE, 6. KOKOS_OPTIMUM_LAMDA

Sub KOKOS_OPTIMUM_LAMDA()

```

    Sheets("KOKOSOPTLAM").Activate

10    QR = 500:
    HA = 10: HN = HA
    KR = 5:
    S = 0.2:
    *****
    n = 1000000:
    Er = 0.0001
    *****

    RMIN = 2
    TIM = 10:

20    *****
        'OUTPUT HEADINGS
    *****
        Cells(3, 4).Value = "hCRIT":
        Cells(3, 5).Value = "TIM": Cells(4, 5).Value = TIM
        Cells(3, 6).Value = "OPTLAMDA":
    *****
        'EVALUATION OF hCRIT=[H0].W[Ucrit]
    'FROM THE QR STORETIVITY VOLUME RELATIONSHIP
    'RSOT IS THE RADIUS SQUARE OVER THE TIME
    'WHICH IS A CONSTANT EQUAL TO QR/(3.14*HA*S)
    *****

30    RSOT = QR / (S * 3.14 * HA)
40        UC = S * RSOT / (4 * KR * (HA))
        H0 = QR / (4 * 3.14 * HA * KR)
        'SETTING THE ACCURACY AND FINDING THE STEP ST
50        ALFA = UC
        F41 = (Exp(-ALFA) / ALFA)
        F42 = (1 + (4 / ALFA) + (12 / ALFA ^ 2) + (24 / ALFA ^ 3) + (24 / ALFA ^ 4))
        F4ALFA = F41 * F42
60        ST = (90 * Er / (F4ALFA * n)) ^ 0.2
70        ZZ = 1

```


SUBROUTINE, 7. AQUIFER FRONT

Sub AQUIFERFRONT():

```
*****
' USING DIRECT INTEGRATION SERIES SOLOUTION
' EVALUATION OF THE AQUIFER WATER FLOW WATER FRONT
' AT A CRITICAL RADIUS rc AND ITS DISPLAY IN FIGURE 7
*****

Sheets("KOKOSFRONT").Activate

10          QR = 500:
*****
'HA INCLUDES THE CRITICAL DEPTH
*****
          HA = 11.5848
30          KR = 5:
40          S = 0.2:
          RMIN = 2
*****
          'CRITICAL RADIUS rc LOOP
          'for whichTIM = 3.14 * rc ^ 2 * HA * S / QR
          *****
          For rc = 5 To 500 Step 5
          TIM = 3.14 * rc ^ 2 * HA * S / QR
50          n = 1000

          *****
          'RADIUS R LOOP
          'corresponding to a maximum of rc
          *****
          For R = RMIN To rc

70          H0 = QR / (4 * 3.14 * KR * (HA))
99          U = S * R ^ 2 / (4 * KR * HA * TIM)
          A0 = -U
          SU1 = 0
          *****
          ' DIRECT INTEGRATION SERIES
          ' WELL FUNCTION EVALUATION
          *****
          For RS = 1 To (2 * n + 1)
          SU1 = SU1 + A0
          A1 = -A0 * U * (RS) / (RS + 1) ^ 2
          A0 = A1
120         Next RS
```

```

130         SU2 = -Log(U)
140         SU3 = -0.5772156649:
           SUT = SU2 + SU3 - SU1
150         H = SUT * H0
           Cells(10, 6).Value = "W(U)"
           Cells(11, 6).Value = SUT
           SU2 = 0: SU1 = 0: SUT = 0
160
           '*****
               'OUTPUT
           '*****
           Cells(11 + R, 4).Value = R
           Cells(11 + R, 5 + rc / 5).Value = H
           Next R
       Next rc
End Sub

```

SUBROUTINE, 8. KOKOS_VARIATIONS

Sub KOKOS_VARIATIONS()

```
*****  
      'VARIATIONS OF T& S , AT RMIN=2  
'FOR t=10,30,60,90,120,150,180,210,240,270,300,330,360,390,420,450  
*****
```

Sheets("KOKOSVARIATIONS").Activate

10

QR = 500:

HA = 10: HN = 10

KR = 5

S = 0.2

RMIN = 2

n = 1000000:

Er = 0.0001

'VT REPRESENTS $T(1-dT/T)$

VT = 1

'VS REPRESENTS $S(1+dS/S)$

VS = 1

XMAX = 10

'LAMDA FOR HANTUSH IS 0.5

'LAMDA FOR KOKOS OPTIMUM VALUES OF LAMDA

' ARE TAKEN FROM FIGURE 7 OR THE LIST BELOW

'TIME	LAMDA
'10	0.312
'30	0.272
'60	0.251
'90	0.240
'120	0.235
'150	0.230
'180	0.225
'210	0.221
'240	0.218
'270	0.216
'300	0.214
'330	0.211
'360	0.21
'390	0.209

```

          '420      0.207
          '450      0.206

LAMDA = 0.312

TIM = 10
'*****
30      'NON LINEARITY LOOP
'*****
40      For XX = 1 To XMAX
          T = (HA * KR)
          '*****
          VT = (1 + dT / T)
          '*****
          T = VT * T
          H0 = QR / (4 * 3.14 * T)

          '*****

          VS = (1 + dS / S)
          '*****

          S = VS * S
          '*****

          ' FINDING THE STEP ST FROM THE SET ACCURACY
          '*****

          ALFA = S * RMIN ^ 2 / (4 * T * TIM):
          F41 = (Exp(-ALFA) / ALFA)
          F42 = (1 + (4 / ALFA) + (12 / ALFA ^ 2) + (24 / ALFA ^ 3) + (24 / ALFA ^ 4))
          F4ALFA = F41 * F42
60      ST = (90 * Er / (F4ALFA * n)) ^ 0.2
70      ZZ = 1

'*****
'ESTABLISHES THE CUMULATIVE ERROR AND MOUNT HEIGHT SH THAT COMES
'FROM THE SUCCESSIVE INTEGRATION OF THE PARTS OF THE WELL FUNCTION
'GIVING THE HMAX CORRESPONDING TO AQUIFER THICKNESS HA

'*****

SA = 0
77      BETA = ALFA + 2 * n * ST
          ORDE = 0: ORDO = 0
          u0 = ST
          U1 = ALFA
          U2 = BETA
82      FIRST = Exp(-(U1)) / (U1)
          LAST = Exp(-(U2)) / (U2)
          For JE = 2 To 2 * n - 2 Step 2:
          ORDE = ORDE + Exp(-(U1 + u0 * (JE - 1))) / (U1 + u0 * (JE - 1))
          Next JE

```

```

For JO = 3 To 2 * n - 1 Step 2:
ORDO = ORDO + Exp(-(U1 + u0 * (JO - 1))) / (U1 + u0 * (JO - 1))
Next JO
AREA = (FIRST + 4 * ORDE + 2 * ORDO + (LAST)) * u0 / 3
SA = SA + AREA
HMAX = SA * H0
DIFHMAX = HMAX - HMAXO
84 HMAXO = HMAX
If Abs(DIFHMAX) < Er Then GoTo 95
ALFA = BETA
90 ZZ = ZZ + 1
GoTo 77
95 HA = 0
*****
'CATERS FOR THE NON LINEARITY
'SUCCESSIVE ITERATIONS UNTIL THE MOUND
'HEIGHT AT h(rMIN,t) REMAINS UNCHANGED
'AND THUS HMAX AND EHA ARE EVALUATED
*****
HA = HN + LAMDA * HMAX
DIFHA = Abs(HA - EHA)
If DIFHA < Er Then GoTo 222
EHA = HA
Next XX
222 SA = HMAX / H0
*****
'OUTPUT
*****
Cells(3, 1).Value = "W()": Cells(3, 2).Value = SA
Cells(1, 2).Value = "h(r,t)": Cells(2, 2).Value = HMAX
Cells(1, 3).Value = "TIME": Cells(2, 3).Value = (TIM)
Cells(1, 4).Value = "ERROR": Cells(2, 4).Value = Er
Cells(1, 5).Value = "STEP": Cells(2, 5).Value = ST
Cells(1, 6).Value = "No STEPS": Cells(2, 6).Value = n

```

End Sub